

SYNTHESIS AND ANTICANCER ACTION OF NITRIC OXIDE-RELEASING LIPOSOMES

Dakota J Suchyta

A dissertation submitted to the faculty at the University of North Carolina at Chapel Hill in partial fulfillment of the requirements for the degree of Doctor of Philosophy in the Department of Chemistry (Analytical Chemistry)

Chapel Hill
2017

Approved by:

Mark H. Schoenfisch

R. Mark Wightman

James W. Jorgenson

Nancy C. Fisher

William K. Kaufmann

© 2017
Dakota J Suchyta
ALL RIGHTS RESERVED

ABSTRACT

DAKOTA J SUCHYTA: Synthesis and Anticancer Action of Nitric Oxide-Releasing Liposomes
(Under the direction of Mark H. Schoenfisch)

The implementation of nitric oxide (NO)-based therapeutics has been met with formidable challenges relating to NO's gaseous, reactive nature and difficulties associated with controlled delivery. Although macromolecular vehicles have been developed for applications in NO release, a common limitation associated with these systems is exposure of the NO donor to the surrounding medium, resulting in unintended NO release. To overcome this issue, liposomes were investigated as new vehicles for NO delivery whereby the NO donor is encapsulated within the aqueous core, protected from the external solution by a lipid membrane.

Liposomes with encapsulated *N*-diazeniumdiolate NO donors were first synthesized using a reverse-phase evaporation protocol. Encapsulation efficiencies for several molecular NO donors were in the range of 33–41%. Relative to the unencapsulated (free) NO donor, NO-release half-lives at pH 7.4 were up to 7-times greater upon encapsulation, yet the NO-releasing liposomes still exhibited their unique pH-sensitive release properties. The liposomes retained ~80% of the encapsulated NO concentrations after 3 months of storage at 4°C, indicating excellent stability. In order to determine if the liposomes held merit as therapeutic agents, cytotoxicity against human pancreatic cancer cells were performed that demonstrated the liposomal NO donors required less NO to kill versus the free NO donor (183 μ M and 2.4 mM, respectively).

The ability to tune NO-release kinetics of these liposomes was further studied. It was possible to vary the NO-release kinetics by altering the encapsulated NO donor molecule or the phospholipid composing the bilayer (independently or in combination). Phospholipid headgroup surface area was determined to be a main factor in controlling NO-release half-lives. As the surface area of the lipid headgroup was decreased from 0.660 nm² to 0.420 nm², a concomitant increase in NO-release half-life was also observed. The composition of the lipid bilayer is known to affect *in vivo* properties, so NO-release kinetics were also measured in serum and whole blood. Half-lives in serum were equivalent to those measured in buffer, while those measured in blood were ~60% faster.

An investigation into the cytotoxicity of slow ($t_{1/2} > 72$ h) versus fast ($t_{1/2} \sim 2.5$ h) NO-releasing liposomes demonstrated how the biological consequences were dependent on the NO-release rate. Fast NO-releasing liposomes yielded consistently higher LD₅₀ values (>230 μM NO), relative their slow-releasing counterparts (<230 μM NO), across 9 different cancer cell lines encompassing 3 different types of cancer (breast, colorectal, and pancreatic). The fast-release system was able to eradicate 50% of the cells much quicker (~36 h vs. 72 h for slow-release system). Flow cytometry studies suggest that this faster killing is due to a more rapid intracellular build-up of NO, which was observed for both the free and encapsulated NO donors. Western blotting revealed that both the slow and fast NO-release systems could induce apoptosis, albeit to different degrees.

To my amazing parents, Richard and Shannan,
who have always supported and encouraged me to follow my passion.

ACKNOWLEDGEMENTS

I am deeply grateful for the many people who I have encountered in my life and who have given me support, advice, criticism, and friendship. The teachers who have inspired and motivated me deserve my endless gratitude. For my 8th grade teacher, Karla Morgan, who initially fueled my imagination and curiosity for science, and ultimately chemistry. Through my high school years, Sandy Schafer taught me the wonders of chemistry and pushed me to pursue my studies. Professor David Baker and Professor Ronald Sharp were my first college professors who showed me the difficulties, nuances, failures, and successes that the field of chemistry had to offer. My true introduction to research laboratory chemistry began with Professor Mark Meyerhoff who accepted me into his lab as a first-year undergraduate. He taught me how to think critically about experiments, encouraged me to pursue my own interests, and supported me throughout my first attempts at publishing scientific data. My scientific interests eventually led me to Professor Mark Schoenfisch, who I can wholeheartedly say formed me into the chemist I am today. He provided me with an opportunity to research my own desires and gave me an independence I could only hope for in graduate school. He taught me that it is not just about finishing the project, but overachieving every single part of it.

There are many colleagues that deserve my appreciation as well. Dr. Bo Peng, who mentored me as an undergraduate. Dr. Gary Jensen, Dr. Alexander Wolf, and Dr. Andrea Bell-Vlasov were some of the best colleagues and friends I could have asked for when entering the field of chemistry. They provided me with in-depth conversations about science and life that helped shape me into a better scientist. Without Dr. Chris Backlund and Dr. Rebecca Hunter I

would not have assimilated very easily into graduate school. Their entertainment, encouragement, and criticism will never be forgotten. One of my biggest friends and mentors in all of graduate school would be Dr. Robert Soto. His meticulous work ethic, tremendous writing abilities, and amiable personality inspires me to work harder and be more critical of myself every single day, both as a person and a scientist. My fellow classmates, including Nathan Whitman, Matthew Boyce, Micah Brown, and Matthew Campbell provided me with support, advice, and amusement throughout my graduate studies. Finally, the Schoenfish lab members deserve my thanks, including Evan Feura, Mona Ahonen, James Taylor, Maggie Malone-Povolny, Lei Yang, Jackson Hall, Kaitlyn Rouillard, Haibao Jin, Sara Maloney, and Pedro De Jesus Cruz for all their continuous support. I wish you all the best of luck and I am confident that you will be successful in whatever career you choose.

I must show my appreciation to friends and family who supported me during my time here in graduate school. Richie Sabias, Jake Hash, and Marc Roedel were a few of the key contributors of my personal solace throughout both life and graduate school. I cherish their friendships everyday. One of my closest friends, Mark Bokhart, has been by my side through all of my college chemistry days. Whether it came to graduate school, my scientific career, or my personal life, he always provided a listening ear, a good laugh, and sound advice. The hardest parts of graduate school were significantly less stressful because I had a remarkable woman by my side. Christelle Siohan has continuously given me hope, love, and support. She is an inspiration for me to not only be a better person, but a better father each day to our beautiful daughter, Luna Suchyta. My brother, Nicholas Suchyta, will always be a source of fuel to my work ethic and humor. I can't imagine getting through graduate school without him. And finally, my wonderful parents, Richard and Shannan Suchyta, have always supported me in each and

every one of my endeavors. I cannot write enough sentences that express my undying love and gratitude for everything that you both have sacrificed for me. Let this dissertation be a testament to how well you raised me.

TABLE OF CONTENTS

LIST OF TABLES	xiv
LIST OF FIGURES.....	xv
LIST OF ABBREVIATIONS AND SYMBOLS.....	xix
CHAPTER 1. THERAPEUTIC ACTIVITY OF NITRIC OXIDE AND METHODS OF DELIVERY FOR CANCER TREATMENT.....	1
1.1. Nitric oxide therapy	1
1.1.1. Antibacterial activity of nitric oxide	1
1.1.2. Anticancer activity of nitric oxide	3
1.2. <i>N</i> -diazoniumdiolate NO donors	5
1.2.1. Synthesis of <i>N</i> -diazoniumdiolates	6
1.2.2. Therapeutic utility of <i>N</i> -diazoniumdiolates.....	9
1.3. Macromolecular NO-releasing systems	10
1.3.1. Nitric oxide-releasing silica nanoparticles.....	10
1.3.2. Nitric oxide-releasing dendrimers.....	12
1.4. Liposomes as drug delivery vehicles	13
1.4.1. Synthesis and characterization of liposomes	15
1.4.2. Pre-clinical liposome systems.....	17
1.4.3. Commercial liposome systems.....	19
1.4.4. Intracellular uptake of liposomes.....	21
1.4.5. Ligand-bearing liposomes.....	22
1.5. Nitric oxide-releasing liposomes	23
1.5.1. NO gas-encapsulated liposomes	23
1.5.2. Metal nitrosyl complex-encapsulated liposomes	24

1.5.3. Organic nitrate-encapsulated liposomes	25
1.5.4. <i>N</i> -diazoniumdiolate-encapsulated liposomes	25
1.6. Summary of dissertation research	27
References	29
CHAPTER 2. ENCAPSULATION OF <i>N</i> -DIAZENIUMDIOLATES WITHIN LIPOSOMES FOR ENHANCED NITRIC OXIDE DONOR STABILITY AND DELIVERY	41
2.1. Introduction	41
2.2. Experimental section	43
2.2.1. Materials	43
2.2.2. Synthesis of <i>N</i> -diazoniumdiolates	44
2.2.3. Preparation of liposomes	44
2.2.4. Characterization of liposome size	45
2.2.5. Phospholipid content assay	45
2.2.6. Nitric oxide release from liposomes	45
2.2.7. Cytotoxicity assay	47
2.3. Results and Discussion	47
2.3.1. Synthesis of NO-releasing liposomes	47
2.3.2. Liposomal NO-release measurements	48
2.3.3. Stability of NO-releasing liposomes over time	55
2.3.4. Cytotoxicity of DPTA/NO-encapsulated liposomes	55
2.4. Conclusions	59
References	60
CHAPTER 3. CONTROLLED RELEASE OF NITRIC OXIDE FROM LIPOSOMES	63
3.1. Introduction	63
3.2. Experimental section	65
3.2.1. Materials	65

3.2.2	Synthesis of <i>N</i> -diazoniumdiolates	66
3.2.3.	Preparation of liposomes.....	66
3.2.4.	Characterization of liposomes size	67
3.2.5.	Nitric oxide release from liposomes	67
3.2.6.	Turbidity assay.....	68
3.2.7.	Serum protein adsorption onto liposomes.....	68
3.2.8.	Nitric oxide release from liposomes in blood and serum.....	68
3.3.	Results and Discussion.....	69
3.3.1.	Nitric oxide donor structure	69
3.3.2.	Nitric oxide-release measurements	72
3.3.3.	Effects of lipid bilayer hydrophobicity and charge.....	73
3.3.4.	Bilayer properties and NO release	76
3.3.5.	Nitric oxide-release kinetics in biological media.....	80
3.4.	Conclusions.....	85
	References.....	86
CHAPTER 4. ANTICANCER POTENCY OF NITRIC OXIDE-RELEASING LIPOSOMES.....		91
4.1.	Introduction.....	91
4.2.	Experimental section.....	93
4.2.1.	Materials.....	93
4.2.2.	Synthesis of <i>N</i> -diazoniumdiolate NO donors.....	94
4.2.3.	Liposome synthesis	94
4.2.4.	Characterization of liposomes.....	95
4.2.5.	Nitric oxide release	95
4.2.6.	Cytotoxicity assays	96
4.2.7.	Confocal fluorescence microscopy	97
4.2.8.	Flow cytometry	97

4.2.9. Western blot analysis	98
4.3. Results and Discussion.....	99
4.3.1. Cytotoxicity of the liposomes	100
4.3.2. Intracellular liposome uptake and NO delivery	106
4.3.3. Kinetics of intracellular NO accumulation	109
4.3.4. Effect of liposomes on intracellular signaling	111
4.4. Conclusions.....	113
References.....	114
CHAPTER 5. SUMMARY AND FUTURE DIRECTIONS	119
5.1. Summary of dissertation research.....	119
5.2. Future directions	121
5.2.1. Conjugation of targeting ligands to liposome surface	121
5.2.2. Dual-encapsulation to enhance anticancer action	124
5.2.3. Antibacterial properties of NO-releasing liposomes.....	125
5.3. Conclusions.....	127
5.4. References.....	129
APPENDIX A. SUPPLEMENTAL MATERIAL OF CHAPTER 2	133
APPENDIX B. SUPPLEMENTAL MATERIAL OF CHAPTER 3	136
APPENDIX C. SUPPLEMENTAL MATERIAL OF CHAPTER 4	156
APPENDIX D. SELECTIVE MONOPHOSPHORYLATION OF CHITOSAN VIA PHOSPHORUS OXYCHLORIDE.....	160
D.1. Introduction.....	160
D.2. Experimental section.....	162
D.2.1. Materials.....	162
D.2.2. Synthesis of phosphorylated chitosan	163
D.2.3. Nuclear magnetic resonance (NMR) spectroscopy.....	163
D.2.4. X-ray photoelectron spectroscopy (XPS).....	163

D.2.5. Molecular weight determination	164
D.2.6. Calcium chelation.....	164
D.3. Results and Discussion.....	165
D.3.1. Controlling phosphorylation efficiency	170
D.3.2. Molecular weight	180
D.3.3. Calcium chelation efficiency.....	180
D.4. Conclusions.....	182
References.....	184

LIST OF TABLES

Table 2.1.	Encapsulation efficiencies (EE) of various NO donor compositions.....	49
Table 2.2.	Nitric oxide-release properties of liposomes in PBS (pH = 7.4) at 37 °C	52
Table 2.3.	Nitric oxide-release properties of liposomes in acetate buffer (pH = 7.4) at 37 °C	57
Table 3.1.	Physicochemical properties of DPPC liposomes encapsulating various NO donors.....	70
Table 3.2.	Nitric oxide-release properties of DPPC liposomes as a function of NO donor in PBS (pH 7.4) at 37 °C	71
Table 3.3.	Physicochemical properties of PAPA/NO liposomes as a function of bilayer composition	74
Table 3.4.	Nitric oxide-release properties of PAPA/NO liposomes as a function of bilayer hydrophobicity and charge in PBS (pH 7.4) at 37 °C	77
Table 4.1.	Properties of NO-releasing liposomes.....	101
Table 5.1.	Ligands used for active targeting	122
Table B.1.	Nitric oxide-release properties of DPPC liposomes as a function of encapsulated <i>N</i> -diazoniumdiolate NO donor in MES (pH = 5.4) at 37 °C	144
Table B.2.	Fluorophore encapsulation efficiency for DPPC and DPPG liposome	147
Table B.3.	Nitric oxide-release properties of PAPA/NO liposomes as a function of bilayer hydrophobicity and charge in MES (pH = 5.4) at 37 °C.....	149
Table D.1.	Chitosan concentration effect on phosphorylation P/N atomic ratio.....	178
Table D.2.	Molecular weight and dispersity (\bar{M}_w) of P-chitosan as a function of POCl ₃ reaction time.....	181
Table D.3.	Calcium chelation amount of P-chitosan as a function of phosphorylation degree	183

LIST OF FIGURES

Figure 1.1.	Antibacterial mechanisms of action of nitric oxide and other nitrosative and oxidative agents	2
Figure 1.2.	The downstream effects on cancer cells after treatment with nitric oxide	4
Figure 1.3.	Mechanism of <i>N</i> -diazoniumdiolate formation via sequential NO addition and proton-initiated NO release	7
Figure 1.4.	Structures of common <i>N</i> -diazoniumdiolates with their reported half-lives in 10 mM PBS (pH 7.4, 37 °C)	8
Figure 1.5.	Representation of a liposome and its ability to encapsulate both lipophilic and hydrophilic drugs	14
Figure 1.6.	Nitric oxide-releasing liposome and mechanism of NO release	26
Figure 2.1.	Structures of the NO donors SPER/NO and DPTA/NO	46
Figure 2.2.	Nitric oxide release profiles of various encapsulated NO donors and free NO donor	50
Figure 2.3.	Fluorescence emission of pyranine-loaded liposomes in various conditions	54
Figure 2.4.	Comparison of NO remaining from SPER/NO-loaded liposomes after storage under various conditions	56
Figure 2.5.	<i>In vitro</i> efficacy of liposomal and free DPTA/NO on human PANC-1 cells after 24 h incubation	58
Figure 3.1.	Fluorescence emission of pyranine-encapsulated liposomes prepared from DMPC, DPPC, and DSPC diluted in 10 mM PBS (pH 7.4, 37 °C)	79
Figure 3.2.	Relationship between the liposomal NO-release half-life and phospholipid headgroup surface area using PAPA/NO-encapsulated liposomes	81
Figure 3.3.	Nitric oxide release in biological fluids from various PAPA/NO liposomes	83
Figure 3.4.	Neutral DPPC PAPA/NO liposome NO-release kinetics in various media	84
Figure 4.1.	Nitric oxide-release profiles from liposomal DETA/NO and PAPA/NO liposomes in 10 mM PBS (pH 7.4, 37 °C)	102

Figure 4.2.	PA14c cytotoxicity of liposomal DETA/NO and PAPA/NO and calculated LD ₅₀ values	103
Figure 4.3.	Time-course cytotoxicity study of liposomal DETA/NO and PAPA/NO at their respective LD ₅₀ values against human MCF-7 breast cancer cells	105
Figure 4.4.	Confocal fluorescence micrographs and densitometric analysis of MCF-7 cells incubated with DETA/NO and PAPA/NO liposomes	107
Figure 4.5.	Orthogonal view of MCF-7 cells after treatment with PAPA/NO liposomes	108
Figure 4.6.	Change in median fluorescence intensity over time indicating intracellular NO accumulation, as determined by flow cytometry, after treating MCF-7 cells with both free form and liposomal form of DETA/NO and PAPA/NO	110
Figure 4.7.	Western blot and densitometric analysis of MCF-7 cells after various treatments	112
Figure A.1.	Nitric oxide release profile of free DPTA/NO versus liposomal DPTA/NO in 10 mM PBS (pH 7.4, 37 °C)	133
Figure A.2.	Transmission electron micrograph of DPTA/NO loaded liposomes	134
Figure A.3.	Cytotoxicity on human PANC-1 cells after a 24 h incubation using varying concentrations of free DPTA/NO	135
Figure B.1.	Proton-initiated decomposition mechanism of <i>N</i> -diazoniumdiolates to liberate NO	136
Figure B.2.	UV-vis spectra of PROLI/NO, DEA/NO, PAPA/NO, and SPER/NO in 50 mM NaOH	137
Figure B.3.	FTIR spectra of PROLI/NO, DEA/NO, PAPA/NO, and SPER/NO	138
Figure B.4.	UV-vis spectra of PROLI/NO, DEA/NO, PAPA/NO, and SPER/NO in 10 mM PBS (pH 7.4)	140
Figure B.5.	UV-vis spectra of sodium nitrate and sodium nitrite in 10 mM PBS (pH 7.4)	141
Figure B.6.	UV-vis spectra of PROLI/NO, DEA/NO, PAPA/NO, and SPER/NO in 10 mM MES (pH 5.4)	142

Figure B.7.	<i>N</i> -diazoniumdiolate NO donors with their reported NO-release half-lives in 10 mM PBS (pH 7.4, 37 °C).	143
Figure B.8.	Structures of lipids used to make liposomes	145
Figure B.9.	Transmission electron micrographs of DMPC-, DPPC-, and DSPC-based PAPA/NO liposomes.	146
Figure B.10.	Transmission electron micrographs of DPPG- and DPTAP-based PAPA/NO liposomes.....	148
Figure B.11.	Hydrodynamic diameter and polydispersity index of various liposome compositions over time	150
Figure B.12.	Turbidity and protein adsorption measurements of various liposome compositions	151
Figure B.13.	Nitric oxide release from neutral DPPC PAPA/NO liposomes suspended in 10 mM PBS (pH 7.4, 37 °C) containing 157 mg/mL hemoglobin.	152
Figure B.14.	Hemolytic activity of various PAPA/NO-encapsulated liposome systems.....	153
Figure C.1.	Molecular structures of PAPA/NO and DETA/NO	156
Figure C.2.	Transmission electron micrographs of PAPA/NO and DETA/NO liposomes	157
Figure C.3.	Cytotoxicity plot of PAPA/NO and DETA/NO liposomes as a function of NO concentration against human HPNE epithelial pancreatic cells	158
Figure C.4.	Change in median fluorescence intensity over time, as determined by flow cytometry, after treating MCF-7 cells with various concentrations of free and liposomal PAPA/NO.....	159
Figure D.1.	¹ H NMR spectrum of phosphorylated chitosan	166
Figure D.2.	¹ H NMR spectrum in D ₂ O of P-chitosan after washing with 2 M HCl.....	167
Figure D.3.	³¹ P NMR spectra of phosphorylated chitosan prepared in neutral and basic D ₂ O	168
Figure D.4.	³¹ P NMR spectrum of D-glucosamine 6-phosphate and D-glucosamine 1-phosphate	171
Figure D.5.	³¹ P NMR spectrum of D-glucosamine 6-phosphate prepared in acidic and basic D ₂ O.....	172

Figure D.6.	³¹ P NMR spectrum of phosphorylated alginate.	173
Figure D.7.	³¹ P NMR spectrum of phosphorylated cellulose	174
Figure D.8.	³¹ P NMR spectrum of phosphorylated D-glucosamine	175
Figure D.9.	³¹ P NMR spectrum of phosphorylated <i>N</i> -acetylglucosamine	176
Figure D.10.	³¹ P NMR spectra of phosphorylated chitosan synthesized by the POCl ₃ and P ₂ O ₅ methods	177
Figure D.11.	Atomic P/N ratio as a function of reaction time for reactions with 20 mg/mL chitosan (10 molar ratio of POCl ₃)	179

LIST OF ABBREVIATION AND SYMBOLS

~	approximately
°	degree(s)
°C	degree(s) Celsius
=	equals
>	greater than
≥	greater than or equal to
<	less than
≤	less than or equal to
%	percentage(s)
× g	times the force of gravity
a.u.	arbitrary units
Ar	argon gas
As ₂ O ₃	arsenic trioxide
Ca ²⁺	calcium ion
CaCl ₂	calcium chloride
cGMP	cyclic guanosine monophosphate
Chol	cholesterol
cm	centimeter(s)
cm ⁻¹	wavenumber
CO ₂	carbon dioxide gas
d	day(s)
Đ	dispersity

DAF-FM	4-amino-5-methylamino-2',7'-difluorofluorescein diacetate
dL	deciliter(s)
D ₂ O	deuterium oxide
DEA	diethylamine
DEA/NO	<i>N</i> -diazoniumdiolate-modified diethylamine
DETA/NO	<i>N</i> -diazoniumdiolate-modified diethylenetriamine
DLS	dynamic light scattering
DMEM	Dulbecco's modified Eagle's medium
DMPCS	dimyristoylphosphatidylcholine
DMSO	dimethyl sulfoxide
DNA	deoxyribonucleic acid
DOTMA	<i>N</i> -[1-(2,3-dioleoyloxy)propyl]- <i>N,N,N</i> -trimethyl ammonium chloride
DPBS	Dulbecco's phosphate-buffered saline
DPPC	dipalmitoylphosphatidylcholine
DPPE	dipalmitoylphosphatidylethanolamine
DPPG	dipalmitoylphosphatidylglycerol
DPTAP	dipalmitoyltrimethylammoniumpropane
DPTA/NO	<i>N</i> -diazoniumdiolate-modified dipropylenetriamine
DSPC	distearoylphosphatidylcholine
DSPE	distearoylphosphatidylethanolamine
EDTA	ethylenediaminetetraacetic acid
EE	encapsulation efficiency
e.g.	exempli gratia (for example)

et al.	et alia (and others)
EtOH	ethanol
eV	electronvolt
FBS	fetal bovine serum
FTIR	Fourier transform infrared spectroscopy
g	gram(s)
GPC	gel permeation chromatography
GTP	guanosine triphosphate
h	hour(s)
H ₂ O ₂	hydrogen peroxide
HCl	hydrochloric acid
HNO ₃	nitric acid
H ₃ PO ₄	orthophosphoric acid
H ₂ SO ₄	sulfuric acid
i.e.	id est (that is)
IC ₅₀	inhibitory concentration that reduces biological function by 50%
ICP-OES	inductively coupled plasma-optical emission spectrometry
kDa	kilodalton(s)
kV	kilovolt(s)
LD ₅₀	lethal dose that kills 50% of test sample
m	meter(s)
M	molar
MΩ	Megaohm(s)

MSA	methanesulfonic acid
MES	2-(N-morpholino)ethanesulfonic acid
mg	milligram(s)
MIC	minimum inhibitory concentration
min	minute(s)
mL	milliliter(s)
mm	millimeter(s)
mM	millimolar
mmol	millimole(s)
MTS	3-(4,5-dimethylthiazol-2-yl)-5-(3-carboxymethoxy phenyl)-2-(4-sulfophen-yl)-2H-tetrazolium
mo	month(s)
mol	mole(s)
N ₂	nitrogen gas
NaOH	sodium hydroxide
NIR	near infrared
nm	nanometer(s)
nM	nanomolar
NMR	nuclear magnetic resonance spectroscopy
nmol	nanomole(s)
NO	nitric oxide
[NO] _{max}	maximum NO flux
[NO] _{total}	total amount of NO released
NO ₂	nitrogen dioxide

NO_3^-	nitrate
N_2O_3	nitrogen trioxide
N_2O_4	nitrogen tetroxide
NOS	nitric oxide synthase
O_2	oxygen
O_2^-	superoxide
ONOO^-	peroxynitrite
P_2O_5	phosphorus pentoxide
PAMAM	poly(amidoamine)
PAPA	<i>N</i> -propyl-1,3-propanediamine
PAPA/NO	<i>N</i> -diazoniumdiolate-modified <i>N</i> -propyl-1,3-propanediamine
PARP	poly adenosine diphosphate ribose polymerase
PBS	phosphate-buffered saline
PDI	polydispersity index
PEG	polyethylene glycol
pH	$-\log$ of proton concentration
pKa	$-\log$ of acid dissociation constant
PMS	phenazine methosulfate
POCl_3	phosphorus oxychloride
PPI	poly(propyleneimine)
ppb	part(s) per billion
ppm	part(s) per million
psi	pounds per square inch

PROLI	L-proline
PROLI/NO	<i>N</i> -diazoniumdiolate-modified L-proline
RBC	red blood cell
Rh-PE	1,2-dipalmitoyl- <i>sn</i> -glycero-3-phosphoethanolamine-N-(lissamine rhoadmine B sulfonyl) ammonium
RhoA	Ras homolog gene family member A
RNS	reaction nitrogen species
RPMI	Roswell Park Memorial Institute
RSNO	<i>S</i> -nitrosothiol
s	second(s)
SDS	sodium dodecyl sulfate
siRNA	small interfering ribonucleic acid
SPER	spermine
SPER/NO	<i>N</i> -diazoniumdiolate-modified spermine
$t_{1/2}$	half-life
T_c	transition temperature
t_d	total duration of NO release
TAP	trimethylammoniumpropane
TBST	tris-buffered saline with Tween 20
TEM	transmission electron microscopy
THF	tetrahydrofuran
μg	microgram(s)
μL	microliter(s)

μm	micrometer(s)
μM	micromolar
μmol	micromole(s)
UV	ultraviolet
UV-vis	ultraviolet-visible spectroscopy
v/v	volume/volume
vol%	percent by volume
vs	versus
w/v	weight/volume
XPS	X-ray photoelectron spectroscopy

CHAPTER 1: THERAPEUTIC ACTIVITY OF NITRIC OXIDE AND METHODS OF DELIVERY FOR CANCER TREATMENT

1.1 Nitric oxide therapy

Nitric oxide (NO) is an endogenously produced gasotransmitter formed by the reaction of the enzyme nitric oxide synthase (NOS) and the amino acid arginine.¹ NO is considered a potent vasodilator and cardioprotectant.² Sodium nitroprusside, a common NO donor, has been utilized in medical settings for almost 100 years due to its effective blood pressure regulation action and inexpensive production costs. In addition to cardiovascular health, NO is recognized as a vital regulator of the immune response.³ Research has heavily focused on the development of therapeutics for the treatment of NO-impaired disorders with the hope that exogenous NO will reverse the severity of certain diseases.

1.1.1. Antibacterial activity of nitric oxide

Upon bacterial invasion, the immune response is initiated and macrophages are recruited to eradicate the invaders.⁴⁻⁵ Upon stimulation by proinflammatory cytokines such as interleukins and lipopolysaccharides, macrophages release NO to inhibit bacterial reproduction and induce cell death (Figure 1.1).⁶ Nitric oxide directly impedes bacterial respiration as well as ribonucleotide reductase, thus impacting DNA synthesis and repair.⁷ Replication is further prevented by altering zinc translocation among crucial metalloproteins.⁷ While NO can directly influence the reproduction of bacteria, its indirect effects are far more common. Known NO-reactive species include hydrogen peroxide (H₂O₂), oxygen (O₂), superoxide (O₂⁻), and certain

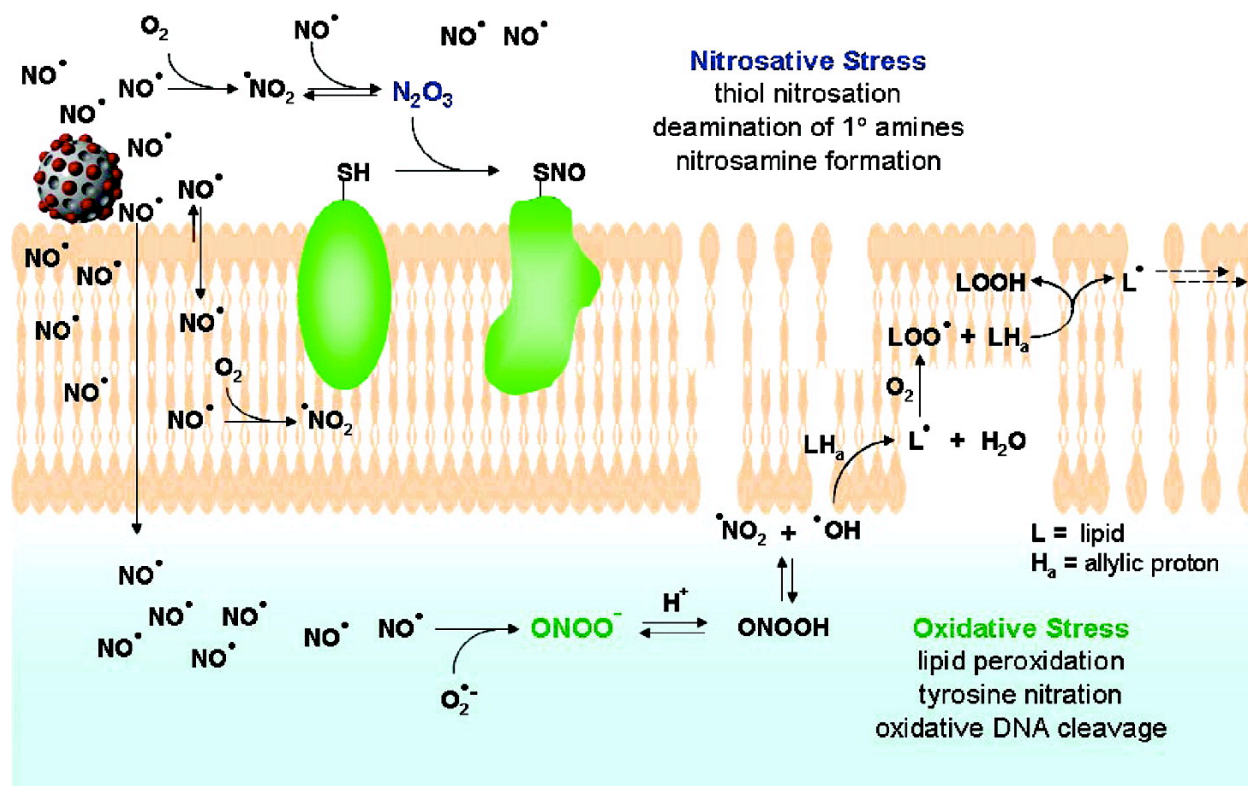


Figure 1.1. Antibacterial mechanisms of action of nitric oxide and other nitrosative and oxidative agents. Reprinted with permission from ACS Nano, 2008, 2, Hetrick, E.M.; Shin, J.H.; Stasko, N.A.; Johnson, C.B.; Wespe, D.A.; Holmuhamedov, E.; Schoenfisch, M.H. "Bactericidal efficacy of nitric oxide-releasing silica nanoparticles" pages 235–246, Copyright 2008 American Chemical Society.

biomolecules (e.g., amino acids and peptides).⁷⁻⁸ Common byproducts from the reactions of NO with these molecules, notably dinitrogen trioxide (N₂O₃), dinitrogen tetroxide (N₂O₄), nitrogen dioxide (NO₂), and peroxynitrite (ONOO⁻), are capable of inducing severe cellular damage. Peroxynitrite is a key factor for the formation of potent nitrosative agents such as N₂O₃ and NO₂ radicals. Both N₂O₃ and N₂O₄ nitrosate membrane proteins, leading to membrane fractures and holes, while NO₂ radicals are causative agents for lipid peroxidation.⁸⁻¹⁰ Additionally, NO with H₂O₂ exacerbates oxidative injury by promoting flavin reduction and Fenton chemistry (i.e., production of hydroxyl radicals from iron).⁷ This multi-mechanistic antibacterial approach hinders the ability of bacteria to foster resistance to NO.

1.1.2. Anticancer activity of nitric oxide

Cancer is known for its increased rate of replication, genomic instability, inhibited DNA repair mechanisms, and ultimately metastasis.¹¹ When used as a therapeutic, NO is able to target many of the chief promoters that accelerate metastasis (Figure 1.2). Directly damaging cancer cell DNA is a common strategy to prevent growth and metastasis. Reactive nitrogen and oxygen species, byproducts of NO scavenging, deaminate DNA bases (e.g., cytosine to uracil), nitrosate nucleophilic sites, and cause single-strand breaks.¹²⁻¹³ These alkylations and deaminations are not easily fixed in cancer cells due to the impaired DNA repair process, thus attenuating overall replication.

Aside from damaging DNA, NO is capable of interacting with major proteins involved in the cell cycle. Phosphorylation of two common proteins, p53 and c-Jun, leads to tumor cell apoptosis due to altering their native binding states. When exposed to concentrations of NO in the range of 400–800 nM, both p53 and c-Jun become phosphorylated (i.e., activated).¹²⁻¹³ p53 is

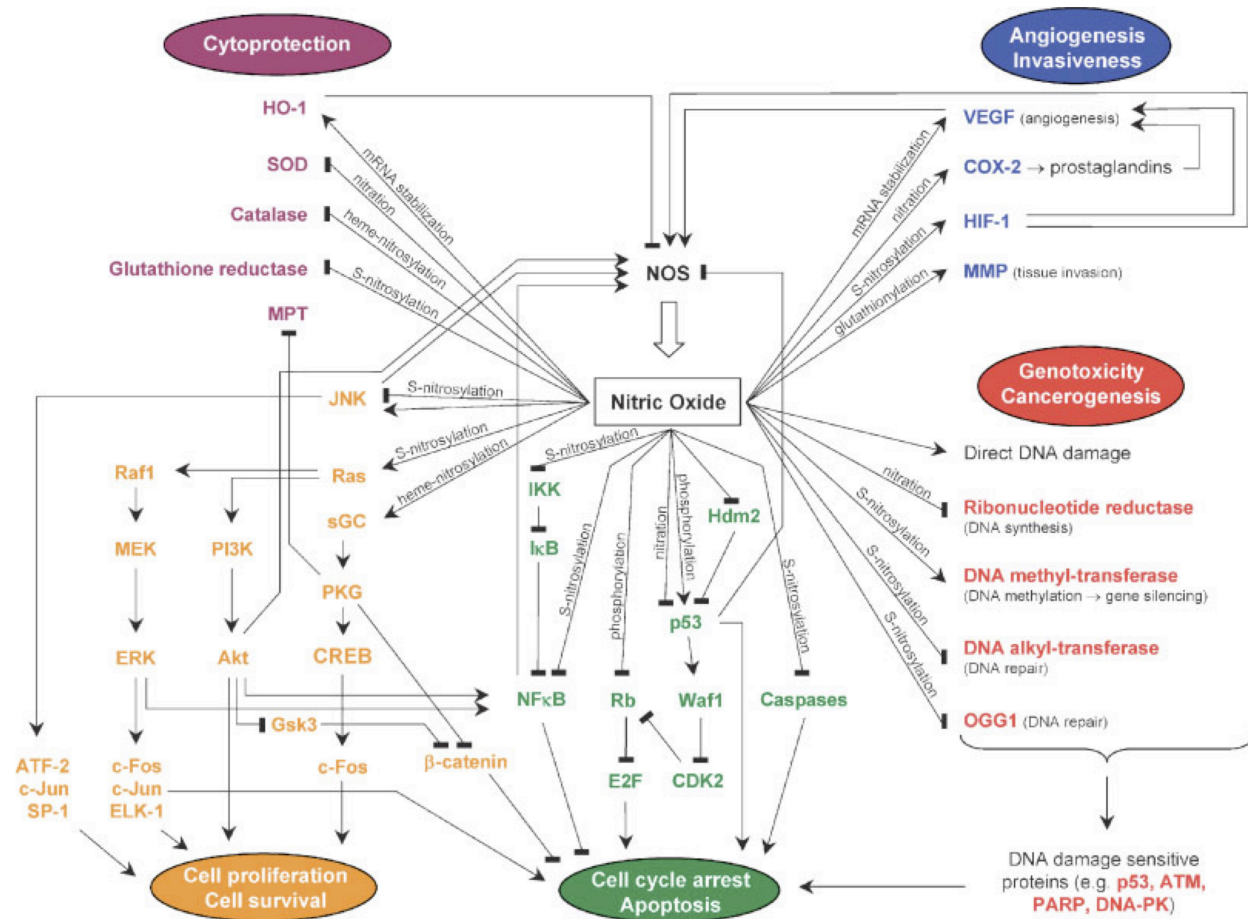


Figure 1.2. The downstream effects on cancer cells after treatment with nitric oxide. Reprinted with permission from Medicinal Research Reviews, 2007, 27, Mocellin, S.; Bronte, V.; Nitti, D. “Nitric oxide, a double edged sword in cancer biology: Searching for therapeutic opportunities” pages 317–352, Copyright 2006 John Wiley and Sons.

mutated in 50% of human malignancies, which impairs its ability to initiate programmed cell death. When wild-type p53 is phosphorylated, however, these typically closed apoptotic channels are reinitiated. For example, exposure of neuroblastoma cells to NO leads to apoptosis.¹³⁻¹⁴ In a pancreatic cancer model, NO was able to arrest all cell lines at the G1 phase, and ultimately induce apoptosis, likely from p53 activation.¹⁵ Nitrosation of DNA repair proteins (e.g., 8-oxoguanine glycosylase-1 and DNA alkyl-transferase) by RNS would inevitably reduce the ability of cancer cells to replicate, thus leading to epigenetic damage.^{13,16}

Chemosensitization, the enhancement of a chemotherapeutic with an alternative medicine, is another technique benefited by NO. Due to the vasodilatory effects of NO, patients pretreated with NO-releasing drugs (e.g., sodium nitroprusside) generally exhibit less constricted blood vessels at tumor sites.¹⁷ The increased tumor blood flow allows for greater accumulation of the chemotherapeutic at the malignant site or an increased anticancer action due to the higher oxygen levels. When NO was co-administered with doxorubicin, hypoxia-induced doxorubicin resistance was reversed in multiple human and murine prostate cancer cell models.¹⁷⁻¹⁹ Similar to chemotherapy, radiotherapy also has been shown to benefit from NO pre-treatments. The higher ensuing tumor oxygen levels were reported to enhance radical formation and oxidative damage.¹⁷

1.2 *N*-diazeniumdiolate NO donors

In normal physiological conditions, the half-life of NO ranges from 0.1 to 1 s.²⁰⁻²² The final decomposition product of NO is the innocuous nitrate (NO_3^-) anion that is formed after a series of physiological reactions (e.g., NO auto-oxidation followed by nitrite oxidation). NO's lifetime is dependent on both the concentration of NO, and the concentration (and type) of the NO scavengers present. Some of the most common scavengers in the bloodstream are oxygen, hemoglobin, thiol-rich proteins, and superoxide. To better utilize NO as a therapeutic, the

development of NO donors, which are molecules capable of storing and releasing NO, have been an active area of research.⁹⁻¹⁰ Arguably the most investigated class of NO donors is *N*-diazoniumdiolates, discussed below.

1.2.1. *Synthesis of N-diazoniumdiolates*

The general synthesis of *N*-diazoniumdiolates involves the reaction of secondary amines with high pressures of NO gas under dilute basic conditions.²³⁻²⁴ Secondary amines, as opposed to primary or tertiary amines, afford the greatest *N*-diazoniumdiolate stability post-synthesis, thus making them the most heavily studied NO storage/release system. Larry K. Keefer pioneered the synthesis, identification, characterization, and NO-release properties of *N*-diazoniumdiolates.²⁵⁻³¹ It is speculated that the *N*-diazoniumdiolate formation process occurs via the addition of one NO molecule onto the secondary amine, followed by the attachment of an additional molecule of NO to form the *N*-diazoniumdiolate (Figure 1.3a).³²⁻³³ However, others have speculated that 2 molecules of NO combine together (i.e., dimerize), with the dimer attaching to the parent secondary amine.³⁴⁻³⁵ In reality, a combination of these two processes is most likely.

Release of NO from *N*-diazoniumdiolates is highly dependent on the pH and temperature of the aqueous solution. At high pH values (>12), few protons exist to cleave the *N*-diazoniumdiolate bond, thereby making basic solutions of *N*-diazoniumdiolates very stable (i.e., weeks). However, at low pH values, the NO donor coordinating amine protonates, resulting in degradation of the *N*-diazoniumdiolate and concomitant NO release (Figure 1.3b). In addition to pH, *N*-diazoniumdiolate stability is also dependent on the molecular structure of the parent amine.²⁵ Nitric oxide-release half-lives of common *N*-diazoniumdiolates at pH 7.4 range from 2 s to 20 h (Figure 1.4).^{25,31} At elevated temperatures the NO release is accelerated even more due to

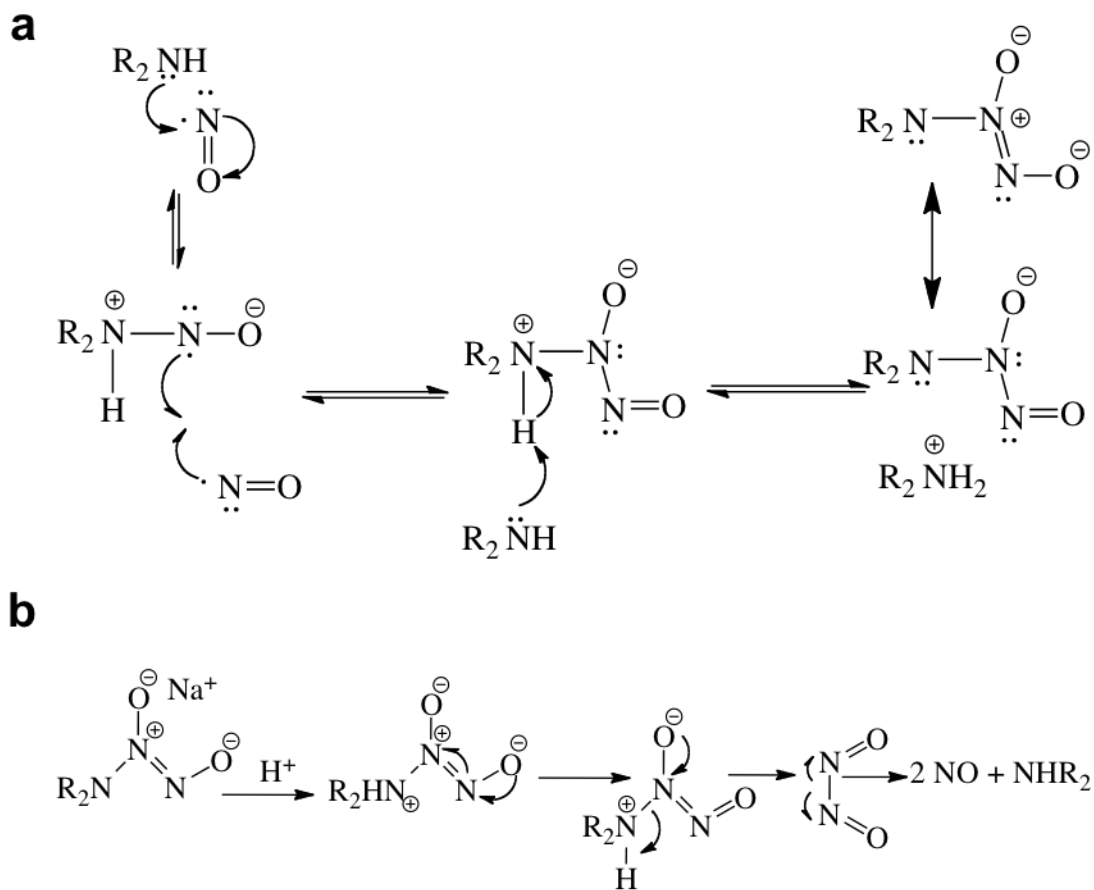
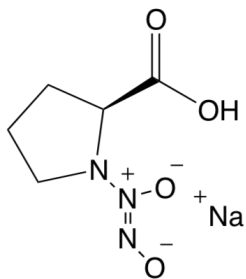
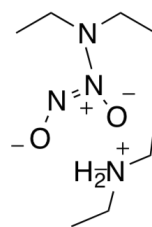


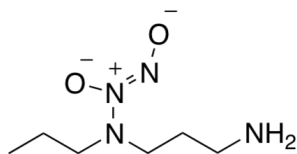
Figure 1.3. Mechanism of *N*-diazeniumdiolate (a) formation via sequential NO addition (b) and proton-initiated NO release.



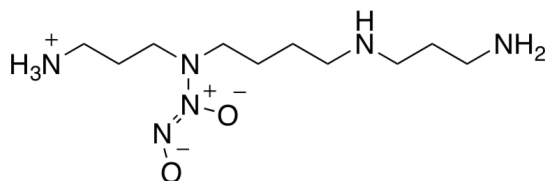
PROLI/NO ($t_{1/2} = 2$ s)



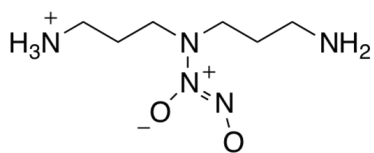
DEA/NO ($t_{1/2} = 2$ min)



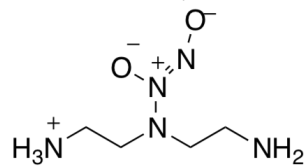
PAPA/NO ($t_{1/2} = 15$ min)



SPER/NO ($t_{1/2} = 37$ min)



DPTA/NO ($t_{1/2} = 3$ h)



DETA/NO ($t_{1/2} = 20$ h)

Figure 1.4. Structures of common *N*-diazoniumdiolates with their reported half-lives in 10 mM PBS (pH 7.4, 37 °C).

thermal energy promoting breakdown of *N*-diazoniumdiolate bond. This disparity in stability is linked to the anionic character of the diazeniumdiolate moiety. Substituents that can reduce the anionic character (i.e., ionically stabilize) often lead to greater stability of the *N*-diazoniumdiolate, with longer NO-release half-lives. For example, the stable *N*-diazoniumdiolate diethylenetriamine/NO (DETA/NO) has a reported half-life at pH 7.4 of ~20 h, the result of *N*-diazoniumdiolate stabilization by its two protonated primary amines.²⁵ Cationic charges capable of stabilizing the NO donating group are exploited to increase the NO-release half-life under physiological conditions.

1.2.2. Therapeutic utility of *N*-diazoniumdiolates

N-diazoniumdiolates are commonly used to study NO's roles in various biological applications.³⁶⁻³⁸ Studies using DETA/NO have demonstrated that MDA-MB-231 breast cancer cells are less apt to develop resistance to doxorubicin when first exposed to NO.³⁹ It was hypothesized that the chemosensitization of DETA/NO was linked to the NO donor reducing the local hypoxic environment. Spermine/NO (SPER/NO) has also been shown to aid in the eradication of MCF-7 breast cancer cells via the induction of apoptosis. At ~100 μ M SPER/NO, phosphorylation of p53 at the Ser15 site led to a signaling cascade to reopen previously closed cell cycle pathways and allow for apoptosis to occur.⁴⁰ Apoptosis may also be initiated in bone cancer F10 cells upon incubation with >20 μ M DEA/NO (LD₅₀=30 μ M).⁴¹ Further, the number of metastatic (i.e., invasive) cells was reduced by 50%, supporting the role of NO in reducing metastasis.

Promising *in vivo* studies with *N*-diazoniumdiolates have shown that *in vitro* data is replicated in animal models. Administration of a piperazine-derived *N*-diazoniumdiolate (JS-K) into rats infected with renal cell carcinoma resulted in an increase in expression of

phosphorylated p53 (Ser15), as well as a reduction in tumor volume due to apoptosis.⁴²

Moreover, rats treated with the NO donor had 75% fewer lung metastases relative to the control rats, perhaps not surprising as NO was shown to increase expression of E-cadherin, a critical transmembrane protein that is involved in cell-cell adhesion.⁴³

1.3 Macromolecular NO-releasing systems

Although low molecular weight NO donors have shown great promise as potential therapeutics, off-target cytotoxicity of small molecules is a major obstacle as a result of their size, high reactivity, and poor localization to the site of interest.⁴⁴⁻⁴⁶ As a remedy, macromolecular NO-delivery systems (e.g., gold or silica nanoparticles) have been developed to possibly promote passive localization and attenuate off-target cytotoxicity.⁴⁷⁻⁵⁴ Silica nanoparticles and dendrimers have received significant attention due to their ability to store large quantities of NO.

1.3.1 Nitric oxide-releasing silica nanoparticles

With silica being relatively non-toxic, inexpensive, and chemically modifiable, investigations into its therapeutic utility were promising. Indeed, the density of surface silanol groups affords straightforward functionalization with silanes bearing secondary amines.⁵⁵⁻⁵⁸ Upon reacting these particles with high pressures of NO gas, *N*-diazoniumdiolates are readily formed on the particle exterior. Total NO storage was shown to span 0.05 to 3.77 μmol NO per mg of particles depending on the secondary amine attached to the particle surface.⁵⁵ When the antibacterial action of the NO-releasing particles was compared to a low molecular weight NO donor (i.e., PROLI/NO), the true benefit of macromolecular chemistry is demonstrated, with 8-times less NO required to eradicate planktonic *Pseudomonas aeruginosa* (*P. aeruginosa*).⁵⁷ The localized NO release from the silica particles afforded lower NO concentrations for bacteria

eradication. At these concentrations, L929 mouse fibroblasts retained high (>80%) cellular viability. Particle size also played a pivotal role in biocidal action, with smaller 50 nm particles requiring half the amount of NO-releasing material to kill (0.8 mg/mL) relative to the larger 200 nm particles (1.5 mg/mL), which was attributed to the greater association and uptake of the smaller particles with the bacterial cell membrane.⁵⁹

Nitric oxide-releasing silica particles have also had success in killing large biofilm colonies. Biofilms are formed when planktonic bacteria form a community and collectively excrete a polysaccharide matrix. Due to the high viscosity and poor permeability of this matrix, many antibacterial agents require much larger concentrations to kill. When both *Pseudomonas aeruginosa* and *Escherichia coli* were treated with fast NO-releasing silica nanoparticles, a 5-log reduction in biofilm viability was observed.⁶⁰ As expected, a 10-times higher concentration of material was required for killing (8 mg/mL) relative to the planktonic-killing concentration (0.8 mg/mL). Unfortunately, at these larger anti-biofilm concentrations, the NO-releasing systems were also toxic to healthy mouse fibroblasts (~70% killing), demonstrating the concentration dependence on cytotoxicity for NO-releasing silica nanoparticles. Smaller system size (50 nm) continued to enhance *Pseudomonas aeruginosa* biofilm killing, requiring only 6 mg/mL versus 10 mg/mL for the 150 nm particles.⁶¹

In addition to killing bacteria, NO-releasing silica nanoparticles have shown to be potent anticancer agents. For 90 nm fast NO-releasing silica particles, the inhibitory concentrations (IC₅₀) against 11 different cell lines were in the range of 60 to 100 µg/mL.⁶² Protein expression studies revealed that apoptosis was one of the major pathways leading to cell death, as evidenced by cleaved poly adenosine diphosphate ribose polymerase (PARP) and cleaved Caspase 3 signals.⁶² Interestingly, larger (350 nm) particles showed preferential killing to Ras-transformed

ovarian cancer cells over their nontransformed counterparts (61 and 220 $\mu\text{g}/\text{mL}$, respectively). It was hypothesized that this difference in killing could be employed *in vivo* as a means to exploit the enhanced permeation and retention effect, and thus reduce off-target cytotoxicity.

1.3.2. Nitric oxide-releasing dendrimers

Dendrimers are hyperbranched nanostructures that possess a symmetrical and well-defined polymeric structure. As the generation or size of the dendrimer increases, so does the number of exterior functional groups. Dendrimers formed from poly(propyleneimine) (PPI) and poly(amidoamine) (PAMAM) were shown to possess a high density of secondary amine groups for functionalization with *N*-diazoniumdiolate NO donors.⁶³ In fact, dendrimers were shown to yield the largest NO totals per mass out of all macromolecular systems (0.91–3.80 $\mu\text{mol}/\text{mg}$).⁶⁴ Significant antibacterial action was induced upon exposing Gram-negative (*Pseudomonas aeruginosa*) and Gram-positive (*Staphylococcus aureus*) planktonic bacteria to NO-releasing PPI dendrimers.⁶⁵

Further studies on the anti-biofilm action of dendrimers revealed that killing was not only dependent on concentration, but also on generation and functional group modification.⁶⁶⁻⁶⁷ An increase in dendrimer size led to an increase in the number of secondary amines, thus increasing the amount of NO per molecule. Greater biofilm killing was therefore observed for the larger generations versus the lower generations (i.e., generation 3 vs. 1) against *Staphylococcus aureus* and *Pseudomonas aeruginosa* biofilms (concentration to kill reduced by half).⁶⁶ Additionally, as the terminal units (exterior functional groups) were altered from propyl to dodecyl groups, a significant reduction in the NO dose to kill was observed.⁶⁷ For example, NO-releasing PAMAM dendrimers bearing propyl groups required 52.5 mM NO to kill *Streptococcus mutans*, while dendrimers bearing dodecyl groups required only 1.8 mM. This disparity in concentration was

most likely the result of the long alkyl chains (i.e., dodecyl) intercalating into the bacterial cell membrane leading to cell death, which reduced the amount of NO needed for eradication.

However, more NO was required to kill for the shorter alkyl chains (i.e., propyl) as they cannot effectively damage the bacterial membrane.

1.4 Liposomes as drug delivery vehicles

The ideal NO-releasing macromolecular delivery system would protect the NO donor until the site of interest is reached. Current NO-release systems fall short in this regard as the NO donor is exposed to the aqueous environment (e.g., bloodstream) leading to *N*-diazeniumdiolate degradation and NO release. Premature NO release decreases the amount of NO available for therapeutic action, and may increase off-target cytotoxicity. Bloodstream delivery systems that confer protection to the NO donor would overcome the issue of premature NO donor degradation.

Similar to the structure of a cell, liposomes are vesicles that contain an inner aqueous core surrounded by a phospholipid bilayer (Figure 1.5). The composition of both the aqueous compartment (e.g., ionic strength) and the bilayer may be modified to achieve different vesicle properties (e.g., size and charge). Additionally, cationic lipids may be incorporated into the bilayer to produce a charged liposome surface that will ultimately affect encapsulation efficiency, liposome size, and cellular uptake. As the liposome structure is composed of only phospholipids, the delivery vehicle is non-toxic and degradable *in vivo*, unlike other particle systems (e.g., silica and gold).⁶⁸ Further, the similarity in surface between cells and liposomes suggests potential for cellular uptake through bilayer fusion, a process that cannot occur for other drug delivery vehicles.⁶⁸⁻⁶⁹

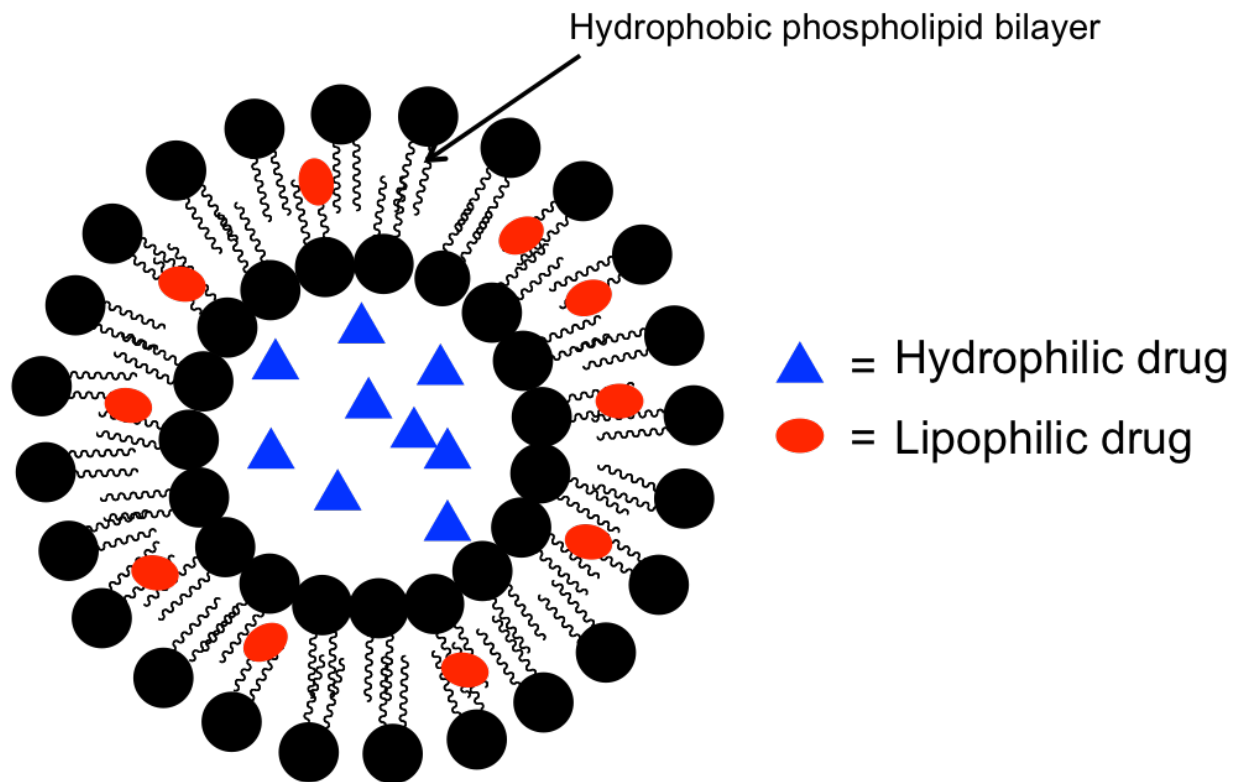


Figure 1.5. Representation of a liposome and its ability to encapsulate both lipophilic and hydrophilic drugs.

1.4.1. Synthesis and characterization of liposomes

Choosing a suitable liposome preparation method depends on the required liposome size, equipment available, and identity of the encapsulated molecule. The two most widely used protocols are thin-film hydration and the reverse phase evaporation techniques.⁶⁸ Thin-film hydration method requires the evaporation of a phospholipid solution (usually dissolved in chloroform) under a nitrogen stream or other low pressure environment.⁷⁰⁻⁷² Afterwards, a “thin film” is formed on the bottom of the flask, which is then subjected to rehydration in an aqueous phase. The molecule of interest to be encapsulated may either be added to the phospholipid solution or the aqueous phase, depending on its solubility. Sonication of the liquid causes phospholipid bilayers to form and desorb from the flask to produce liposomes. This method tends to form large, multilamellar liposomes (i.e., concentric bilayers encapsulating one another). The reproducibility of the number of lamellar phases is poor, and thus extrusion through polycarbonate membranes is ultimately required to obtain narrow distributions of liposome sizes and lamellarities.⁷³ Unfortunately, the extrusion process leads to low encapsulation efficiencies (<15%). Additionally, the thin-film hydration method is not easily scaled up like other techniques (e.g., reverse phase evaporation), further limiting its use in industrial liposome production.⁷⁴

Another popular method for synthesizing liposomes is through a reverse phase evaporation technique developed by Szoka and Papahadjopoulos.⁷⁵⁻⁷⁷ An organic phase containing the lipids and an aqueous phase are sonicated at a temperature slightly higher (~5 °C) than that of the transition temperature (where the phospholipid tails convert from an ordered, solid phase into a more fluid phase) to form an opalescent emulsion of phospholipids. Afterwards, the organic phase is evaporated at elevated temperatures, causing the hydrophobic

lipid tails to collapse onto one another in the aqueous phase and form bilayers.⁷⁶ A benefit of this technique is that liposomes are typically small (<300 nm) and have encapsulation efficiencies up to 60%. Purification by extrusion is not generally required for the reverse phase evaporation process as the resulting liposomes are unilamellar in nature and have a narrow size distribution. However, heat-sensitive molecules, such as proteins, may be degraded due to the required heating during sonication and rotoevaporation steps. To avoid this, phospholipids with low transition temperatures are preferred.

Common *ex vivo* liposome characterization techniques examine size, shape, polydispersity, drug encapsulation efficiency, drug retention, and aggregation over time. Dynamic light scattering (DLS) may be used to measure both the hydrodynamic radius of the liposomes and size distribution.⁷⁸⁻⁷⁹ Size and shape may also be examined using transmission electron microscopy (TEM).⁸⁰ TEM potentially allows for observation of the liposome interior, as well as its deformability. Freeze-fracture TEM is a specialized form of TEM where the liposome sample is fixed using liquid nitrogen, fractured, and sputtered coated with a metal.⁸¹⁻⁸² Through fracturing the liposome vesicle, the interior becomes visible and properties such as number of lamellae are observed. The efficiency of drug encapsulation is measured to determine how well the molecule of interest is encapsulated. Of note, such characterization measurements are highly dependent on the molecule encapsulated. Other tools for characterization include absorbance, fluorescence, or flow cytometry to compare the concentration of the stock solution to that of the ruptured liposomes (equal concentrations would indicate a 100% encapsulation efficiency).⁸³ Drug retention and vesicle aggregation are measured concurrently over time using a combination of DLS, TEM, and fluorescence (or whichever technique was used to identify the

encapsulant). Aggregation is minimized by lyophilizing the liposomes or by storing them at 4 °C.⁸⁴

1.4.2. *Pre-clinical liposome systems*

Many liposomal systems are being researched in the hopes of entering clinical trials for medical applications (e.g., anticancer, diagnostic) with encapsulants ranging from small molecules to large macromolecular structures. Delivery of macromolecules is a prevalent method for eradicating diseases and building immunity to foreign invaders.⁸⁵⁻⁸⁷ For example, siRNA and DNA have been encapsulated within positively charged liposomes.⁸⁸⁻⁹¹ Positive lipids such as *N*-[1-(2,3-dioleoyloxy)propyl]-*N,N,N*-trimethyl ammonium chloride (DOTMA) electrostatically bind to the negatively charged DNA molecules, causing the formation of a vesicular complex.⁹² These ionic amalgams have greater encapsulation efficiencies over liposomes bearing neutral charge. Intracellular delivery of these macromolecules is also more effective (relative to their free form) since the liposome bilayer may fuse with cell membranes.⁶⁹

Quantum dots have also been encapsulated within liposomes in order to enhance their solubility in aqueous solutions.⁹³⁻⁹⁶ The hydrophobic ligands that are usually appended to the surface of quantum dots destabilizes the particles in aqueous solutions, thereby precluding their use from efficient *in vivo* imaging. However, through the use of liposomes, the quantum dots are able to dissolve in the lipid bilayer for bloodstream delivery. After intravenous delivery of the liposomes in rats, near infrared (NIR) images show accumulation of quantum dots throughout the body, the liver and spleen in particular.⁹⁶ In addition to therapeutics, quantum dot-loaded liposomes have been used as fluorescent labels in immunoassays.⁹⁵ Sensitivities and limits of detection of assays using these liposomes were five times greater than that of assays using unencapsulated quantum dots.

Small molecule liposomal systems are by far the most utilized for research and medical applications. Chen *et al.* synthesized arsenic trioxide (As_2O_3)-loaded liposomes for use as an anticancer agent since free As_2O_3 has led to acute poisoning in patients.⁹⁷ Encapsulated As_2O_3 within a liposome prevents rapid damage to the cell membrane and promotes an extended release profile. The longer release durations mitigate undesirable off-target cytotoxicity to healthy cells. Cell viability studies verified that higher concentrations of liposomal As_2O_3 were required to kill human cells relative to unencapsulated As_2O_3 (>200 and 10 μM , respectively).

While in some cases liposomes may be used to mitigate toxicity, they are more generally employed to enhance cytotoxic action. Gemcitabine is the gold standard chemotherapeutic for treating advanced stage pancreatic cancer.⁹⁸ Gemcitabine's short plasma half-life (8–17 min) requires high doses to be administered, which can lead to adverse side effects in patients.⁹⁹ Liposomal gemcitabine was synthesized by Fresta and coworkers to increase drug pharmacokinetics.⁹⁹ Cytotoxicity studies comparing free gemcitabine to liposomal gemcitabine confirmed enhanced killing (2–3 fold decrease in IC_{50} value). Similarly, ibuprofen-loaded liposomes have been used as a treatment of lung cancer. Daily administration of ibuprofen has been shown to reduce the risk of lung cancer, but continuous exposure to ibuprofen causes gastrointestinal bleeding and renal toxicity.¹⁰⁰ Cheng *et al.* have demonstrated greater cell death against multiple lung cancer cells lines when using liposomal ibuprofen instead of free ibuprofen (<400 vs. >1,500 μM , respectively). Further *in vivo* xenograft studies verified that liposomal ibuprofen may induce oxidative stress against the cancer cells, as indicated by elevated stress marker levels in urine.

Another common drug that has benefited from liposomal encapsulation is docetaxel, a highly-utilized chemotherapeutic used to treat prostate, neck, and breast cancer.¹⁰¹ The poor

water-solubility of docetaxel requires the use of surfactants (e.g., Tween 80) and organic solvents to aid in dissolution and delivery. Unfortunately, Tween 80 elicits hypersensitivity effects *in vivo*. Formulating docetaxel-loaded liposomes has increased both its solubility and blood circulation time. Biodistribution measurements revealed that liposomal docetaxel had a 5-times longer circulation half-life than the free form (260 vs. 52 min, respectively).

The treatment of glaucoma requires continuous drug exposure to reduce intraocular pressure. As such, glaucoma patients must enroll in a daily eye drop regimen rather than a monthly dose. Latanoprost, the leading treatment of glaucoma, has been encapsulated into liposomes in an attempt to increase the release duration and eliminate the need for a daily eye drop schedule. Natarajan *et al.* were able to synthesize a liposomal system capable of continuous latanoprost release for >30 days (60% is released within 30 days).¹⁰² Evaluation of the system on a nonhuman primate model revealed that intraocular pressure was consistently lower compared to untreated and eye drop treated controls. Moreover, a single injection of the liposomes led to intraocular pressure reduction for 120 d. The authors attributed the sustained release profile to the protection of the encapsulated latanoprost conferred by the phospholipid bilayer.

1.4.3. Commercial liposome systems

A number of liposome formulations have commercially emerged for the treatment of multiple diseases.⁸⁵ One of the most well-known formulations is that of liposomal doxorubicin (Doxil), the first FDA-approved nanocarrier to be used in hospitals as a treatment for ovarian cancer and Kaposi sarcoma.¹⁰³ A unique transmembrane ammonium sulfate gradient is used to load doxorubicin at high concentrations within the liposomes.¹⁰⁴ A greater anticancer action was observed for Doxil relative to free doxorubicin.¹⁰⁵ The *in vivo* utility of the liposomes is in part due to the introduction of phospholipids bearing polyethylene glycol (PEG) headgroups into the

bilayer.¹⁰⁶ The PEGylated lipids increased the hydration of the exterior surface, helping prevent aggregation during storage (i.e., long shelf-life) and mitigating any immune response upon administration.¹⁰⁷⁻¹⁰⁸ When compared to free doxorubicin *in vivo*, Doxil had a 300-times longer clearance lifetime as a result of the liposomal encapsulation and PEGylation of the liposome surface.¹⁰³

In addition to Doxil, other liposomal drugs now include Ambisome, Marqibo, and DaunoXome. Ambisome (liposomal amphotericin B) is a therapy that utilizes the lipid bilayer to dissolve amphotericin B in order to treat fungal infections.¹⁰⁹⁻¹¹¹ Marqibo is a liposomal formulation of vincristine sulfate to treat acute lymphoblastic leukemia.¹¹² DaunoXome utilizes liposomally encapsulated daunorubicin to treat acute myeloid leukemia and non-Hodgkin lymphoma.¹¹³⁻¹¹⁴ Along these lines, liposomes loaded with morphine sulfate (DepoDur) have been used as an enhanced version of an epidural to last longer and provide extended pain relief to mothers.¹¹⁵⁻¹¹⁶ Depocyt (liposomal cytarabine) has been administered to patients who suffer from lymphomatous meningitis and has proven to be more effective than the free cytarabine.¹¹⁷⁻¹¹⁸ Drugs for photodynamic therapy have been encapsulated within liposomes to better treat individuals suffering from neovascularization ailments.¹¹⁹⁻¹²⁰ Liposomal formulations have been used to enhance the immunogenicity of vaccines.¹²¹ For example, the liposomal influenza virus vaccine (Inflexal V), first introduced onto the Swiss market in 1997, has been used over 41 million times.¹²¹⁻¹²³ Additionally, the liposomal hepatitis A vaccine (Epaxal) has been shown to be well tolerated and immunogenic in patients.¹²⁴⁻¹²⁵

While there isn't an approved liposomal cisplatin system yet, it is worth mentioning the current success of Lipoplatin, which is the liposomal form of cisplatin that is currently in clinical trials for treatment of multiple cancers (e.g., breast, ovarian, lung).¹²⁶⁻¹²⁹ Systemic administration

of cisplatin often leads to severe adverse effects such as renal tubular damage. To mitigate such issues, Lipoplatin was introduced as the liposomal formulation.¹²⁷ Preclinical trials have shown that Lipoplatin exhibits lower off-target toxicity than cisplatin, but is still able to induce apoptosis in malignant cells.¹²⁹ Further Phase I trials determined that the maximum tolerated dose was as high as 350 mg/m², over double that of the free cisplatin dose (100 mg/m²). However, hematological and gastrointestinal toxicity has been noted, albeit it to a much lower degree than free cisplatin. Many Phase II trials have been carried out and demonstrated that the combination of Lipoplatin and another chemotherapeutic (e.g., gemcitabine) is more effective than dual-administration of cisplatin and gemcitabine. Phase III clinical trials are currently underway to evaluate the potential effectiveness of Lipoplatin and gemcitabine.¹²⁹

1.4.4. Intracellular uptake of liposomes

The therapeutic efficacy of liposomes is highly dependent on its ability to be uptaken rapidly into the cell. The translocation of liposomes to the interior of a cell is a complicated process that depends on a number of factors such as liposome size and charge, type of cell, and rate of metabolic processes.¹³⁰ Clathrin-mediated endocytosis is a common pathway whereby liposomes exceeding 100 nm are able to enter cells. A less common, but still relevant pathway is that of macropinocytosis, which is reserved for vesicles larger than 1 µm.¹³¹ In this process, when external macromolecular structures are in close proximity to the cell, invagination of the cell membrane occurs along with coating the cytoplasmic face of this vesicle with the triskelion protein clathrin.¹³² After complete invagination, heat shock protein hsc70 aids in removing the external clathrin coat. The formed endosome then travels according to the pathway its on (e.g., endolysosomal pathway) and the internal contents (i.e., drug) of the liposome may either be released during this entire process or once the lysosome is reached.

Other clathrin-independent pathways exist to internalize liposomes.¹³²⁻¹³³ For example, caveolins are scaffolding proteins that can replace clathrin to aid in liposome uptake. The exact initiation of this pathway has yet to be fully understood, as even the same molecule (e.g., albumin) interacting with the same cell may not utilize caveolin pathways consistently.¹³³ Another method of entry is mediated by dynamin, a guanosine triphosphate (GTP) hydrolase enzyme that assists in the fusion of liposomes with the cell membrane. This process is actually regulated by a GTPase called Ras homolog gene family member A (RhoA).¹³³ Examples of molecules that regularly enter mammalian cells via this mechanism include receptors for interleukin-2, common γ chain cytokines, and immunoglobulin E.

1.4.5. *Ligand-bearing liposomes*

In order to increase *in vivo* blood circulation times or the binding affinity of liposomes to a particular cell, ligands are commonly attached to the vehicle's exterior surface.¹³⁴ Doxil employs PEG groups to make the liposome surface appear more endogenous and prevent an immune response that clears liposomes from the bloodstream. By increasing the water density near the liposome surface, it becomes difficult for opsonins to adhere and "mark" the liposome.¹⁰⁸ Without the opsonins on the liposomes surface, white blood cells aren't able to locate the vehicles and remove them from the bloodstream. These PEG chains may be replaced by other structures that are capable of increasing surface hydrophilicity (e.g., sugars).

Cell targeting to prevent off-target cytotoxicity is achieved by exploiting the unique receptors present (or overexpressed) on the cell of interest and attaching the receptor complement to the liposome. Folate groups at the outer surface of the liposome via covalent attachment or intercalation into the lipid bilayer represent one example. Many human tumors overexpress folate receptors on their surface because folic acid is a key vitamin required for the rapid

deoxyribonucleic acid (DNA) synthesis exhibited by malignant cells.¹³⁵ HeLa and KB cells exposed to folate-appended arsenic trioxide liposomes were shown to be 9- and 28-times, respectively, more toxic than the same liposomes without the folate groups.¹³⁶ Other non-antibody ligands (and their respective diseases) include transferrin (multiple cancers), galactosamine (hepatoma), and granulocyte macrophage colony-stimulating factor (leukemic blasts).¹³⁴ Antibodies conjugated to liposomes are continuously being discovered and produced, including anti-tenascin (breast cancer), anti-CD33 (acute myeloid leukemia), and anti-CD20 (non-Hodgkin lymphoma).¹³⁴ Difficulties associated with synthesizing liposomes bearing various markers are high cost, degradation or denaturing of the marker during liposome synthesis (e.g., organic solvents, high ionic strengths, high temperatures), and low purity (inability to remove liposomes without marker from those that have it).

1.5 Nitric oxide-releasing liposomes

Unlike current macromolecular systems (e.g., dendrimers and silica nanoparticles) where the NO donor is appended to the exterior, liposomes are able to encapsulate the NO donor behind a lipid bilayer that confers protection until subsequent localization or delivery (Figure 1.5). To date, little research has been performed on developing NO-releasing liposomes that exploit this unique characteristic of the vehicle.

1.5.1. NO gas-encapsulated liposomes

Liposomes incorporating NO gas within the aqueous core have been prepared by exposing liposomes directly to gaseous NO.¹³⁷⁻¹³⁹ These systems yield NO payloads of ~10 μL NO per mg of lipid. The kinetics of NO release are rapid upon exposure to aqueous solutions ($t_{1/2}$ =10 min). The rates of NO release may be slightly varied by encapsulating a mixture of

NO and argon. A 1:9 volumetric ratio of NO to argon was shown to yield the best system with NO totals of 0.045 $\mu\text{mol NO/mg lipid}$. Exposure of smooth muscle cells to the NO-releasing liposomes resulted in 20 and 80% cell viability at 5 $\mu\text{M NO}$ and 2 $\mu\text{M NO}$, respectively, revealing a concentration dependence on cytotoxicity. The 1:9 ratio liposomes were then injected into rabbits that had injured carotid arteries to assess the effects of NO on the vasculature healing process. After 14 days post-injection, histological studies revealed that NO induced inhibition of arterial closure by 40% relative to the untreated controls, supporting that NO release can promote healing and widening of injured arteries.

1.5.2. *Metal nitrosyl complex-encapsulated liposomes*

Metal complexes bearing nitrosyl groups, light-sensitive NO donors, have also been encapsulated within liposomes.¹⁴⁰ Ostrowski *et al.* loaded egg phosphatidylcholine-based liposomes with the NO donor *trans*-Cr(cyclam)(ONO)₂⁺. The liposomes were ~125 nm in diameter and retained their structure and NO for at least 2 weeks. After irradiation with 350 nm light, the liposomes produced up to 8 nM NO, with no detectable NO concentrations in the absence of light. The amount of NO released from the free metal complex proved dependent on the oxygen levels of the solution. The total amount of NO released in solutions purged with helium was 1.56 nmol, compared to 0.02 nmol for an air-saturated solution. The disparity in measured NO concentrations was attributed to scavenging of the liberated NO gas. However, the liposomal metal complex did not show scavenging, most likely due to differential partitioning of the NO into the bilayer or the bilayer reacting with any photoproducts.¹⁴⁰ The liposome system exhibited on/off control of NO release, as well as NO payloads ranging from 1 to 10 nM depending on the duration of irradiation (10–30 s). While this system demonstrates the utility of

liposomes for controlling NO-release kinetics, the reliance on an external light source for NO release and the low NO payloads limits their use for therapeutic applications.

1.5.3. *Organic nitrate-encapsulated liposomes*

Organic nitrates, the most common NO donor utilized in medical settings (e.g., glyceryl trinitrate and isosorbide dinitrate) have also been encapsulated within liposomes. Pedrini *et al.* reported on a doxorubicin derivative with a pendant organic nitrate group capable of releasing NO (NitDox) and dual-action therapy.¹⁴¹ To further enhance cytotoxicity towards cancer cells, NitDox was loaded into ~200 nm PEGylated liposomes. Comparing the degradation half-life of free NitDox (16 h) and liposomal NitDox (19–25 h) in human serum, it was revealed that the liposomes protected the organic nitrate from hydrolytic and enzymatic degradation. The cytotoxicity of the liposomes towards breast and ovarian cancer were then compared to free doxorubicin, free NitDox, and a liposomal form of doxorubicin. All liposome formulations resulted in greater cytotoxicity towards the cell lines relative to free drugs, which was attributed to more efficient cellular uptake. However, the NitDox-loaded liposomes proved to be more cytotoxic than the doxorubicin-loaded liposomes, indicating that dual-action release (both NO and doxorubicin) enhanced overall toxicity.

1.5.4. *N-diazeniumdiolate-encapsulated liposomes*

As mentioned above, *N*-diazeniumdiolates undergo a proton-initiated decomposition mechanism to release NO. With NO release highly dependent on pH, *N*-diazeniumdiolates represent a unique class of NO donors that can undergo spontaneous decomposition *in vivo* to liberate their stored NO, unlike the previously mentioned NO donors that rely on enzymes (organic nitrates) or light (nitrosyl metal complexes) to initiate NO release. With respect to cancer, the low pH of malignant sites could act as a trigger to increase the rate of NO liberation,

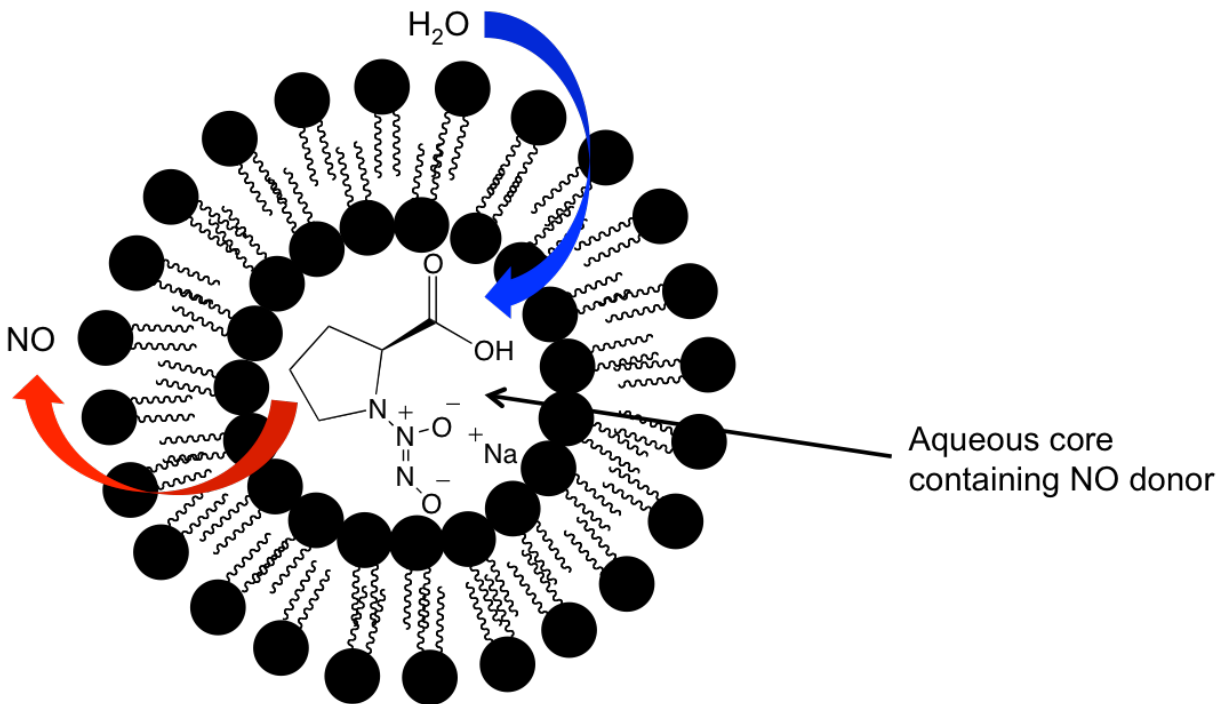


Figure 1.6. Nitric oxide-releasing liposome and mechanism of NO release.

thus leading to high, local concentrations of NO at the tumor site. A single, prior study demonstrated the feasibility of encapsulating *N*-diazoniumdiolates within liposomes, although the liposomes were not extensively characterized (e.g., encapsulation efficiency and NO totals) or studied further (e.g., stability or cytotoxicity).¹⁴² Nevertheless, an important conclusion of this one report was that the NO release at pH 7.4 could be prolonged (up to a half-life of 449 min) through the use of thermally stable lipids. The researchers hypothesized that the enhanced rigidity of the bilayer provided better protection of the NO donor from the external solution (Figure 1.6). Collectively, the data suggested further *N*-diazoniumdiolate protection *in vivo*, while still maintaining their unique pH-sensitive NO release capabilities.

1.6 Summary of dissertation research

The focus of my dissertation research was to synthesize a macromolecular liposome system capable of delivering NO to eradicate cancer cells. Initially, I studied the encapsulation of *N*-diazoniumdiolate NO donors within liposomes and their ensuing stability. Preliminary cytotoxicity assays were carried out to examine if the NO-releasing liposomes exerted any anticancer action against pancreatic cancer cells. Upon proving that a stable liposomal formulation could be synthesized, the liposomal formulation was optimized in order to better understand the release mechanism. Lastly, the kinetic-dependent killing of the NO-releasing liposomes against 9 human cancer lines, encompassing three different cancers was investigated. To summarize, my research aims were to:

- (1) synthesize *N*-diazoniumdiolate-encapsulated liposomes and determine their stability and cytotoxicity towards human cancer cells;

- (2) tune both NO-release properties (e.g., NO totals and half-life) and liposomal properties (e.g., surface charge) while understanding how these affect NO release in biological media; and,
- (3) evaluate the role of liposomal NO-release kinetics with respect to cytotoxicity against human breast, pancreatic, and colorectal cancer cells.

The goal of this introductory chapter was to set the stage for using NO as a chemotherapeutic, review current NO-release materials, and demonstrate that liposomes provide advantages over other NO delivery systems. In Chapter 2, the formulation of NO-releasing liposomes is discussed with evaluation of size, NO totals, stability, and cytotoxicity. Chapter 3 describes the effects of the encapsulated NO donor and composition of the lipid bilayer on NO-release properties, and role of media on stability and NO release. The cytotoxicity of two liposome systems with distinct NO-release profiles (e.g., slow and fast) is described in Chapter 4 to better understand the effect of killing and intracellular NO delivery with respect to liposomal NO-release kinetics. Finally, Chapter 5 provides a summary of my work with suggested future studies involving NO-releasing liposomes.

REFERENCES

- (1) Moncada, S.; Palmer, R.; Higgs, E. "Nitric oxide: Physiology, pathophysiology, and pharmacology" *Pharmacological Reviews* **1991**, *43*, 109-142.
- (2) Jones, S.P.; Bolli, R. "The ubiquitous role of nitric oxide in cardioprotection" *Journal of Molecular and Cellular Cardiology* **2006**, *40*, 16-23.
- (3) Sharma, J.N.; Al-Omran, A.; Parvathy, S.S. "Role of nitric oxide in inflammatory diseases" *Inflammopharmacology* **2007**, *15*, 252-259.
- (4) Wink, D.A.; Hines, H.B.; Cheng, R.S.; Switzer, C.H.; Flores-Santana, W.; Vitek, M.P.; Ridnour, L.A.; Colton, C.A. "Nitric oxide and redox mechanisms in the immune response" *Journal of Leukocyte Biology* **2011**, *89*, 873-891.
- (5) MacMicking, J.; Xie, Q.; Nathan, C. "Nitric oxide and macrophage function" *Annual Review of Immunology* **1997**, *15*, 323-350.
- (6) Fang, F.C. "Perspective series: Host/pathogen interactions. Mechanisms of nitric oxide-related antimicrobial activity" *Journal of Clinical Investigation* **1997**, *99*, 2818-2825.
- (7) Fang, F.C. "Antimicrobial reactive oxygen and nitrogen species: Concepts and controversies" *Nature Reviews Microbiology* **2004**, *2*, 820-832.
- (8) Hetrick, E.M.; Shin, J.H.; Stasko, N.A.; Johnson, C.B.; Wespe, D.A.; Holmuhamedov, E.; Schoenfish, M.H. "Bactericidal efficacy of nitric oxide-releasing silica nanoparticles" *ACS Nano* **2008**, *2*, 235-246.
- (9) Carpenter, A.W.; Schoenfish, M.H. "Nitric oxide release: Part II. Therapeutic applications" *Chemical Society Reviews* **2011**, *41*, 3742-3752.
- (10) Schairer, D.O.; Chouake, J.S.; Nosanchuk, J.D.; Friedman, A.J. "The potential of nitric oxide releasing therapies as antimicrobial agents" *Virulence* **2012**, *3*, 271-279.
- (11) Hanahan, D.; Weinberg, R.A. "Hallmarks of cancer: The next generation" *Cell* **2011**, *144*, 646-674.
- (12) Hickok, J.R.; Thomas, D.D. "Nitric oxide and cancer therapy: The emperor has NO clothes" *Current Pharmaceutical Design* **2010**, *16*, 381-391.
- (13) Mocellin, S.; Bronte, V.; Nitti, D. "Nitric oxide, a double edged sword in cancer biology: Searching for therapeutic opportunities" *Medicinal Research Reviews* **2007**, *27*, 317-352.
- (14) Wang, X.; Zalcenstein, A.; Oren, M. "Nitric oxide promotes p53 nuclear retention and sensitizes neuroblastoma cells to apoptosis by ionizing radiation" *Cell Death and Differentiation* **2003**, *10*, 468-476.

- (15) Wang, L.; Xie, K. "Nitric oxide and pancreatic cancer pathogenesis, prevention, and treatment" *Current Pharmaceutical Design* **2010**, *16*, 421-427.
- (16) Wink, D.A.; Vodovotz, Y.; Laval, J.; Laval, F.; Dewhirst, M.W.; Mitchell, J.B. "The multifaceted roles of nitric oxide in cancer" *Carcinogenesis* **1998**, *19*, 711-721.
- (17) Sullivan, R.; Graham, C.H. "Chemosensitization of cancer by nitric oxide" *Current Pharmaceutical Design* **2008**, *14*, 1113-1123.
- (18) Matthews, N.E.; Adams, M.A.; Maxwell, L.R.; Gofton, T.E.; Graham, C.H. "Nitric oxide-mediated regulation of chemosensitivity in cancer cells" *Journal of the National Cancer Institute* **2001**, *93*, 1879-1885.
- (19) Frederiske, L.J.; Siemens, D.R.; Heaton, J.P.; Maxwell, L.R.; Adams, M.A.; Graham, C.H. "Hypoxia induced resistance to doxorubicin in prostate cancer cells is inhibited by low concentrations of glyceryl trinitrate" *Journal of Urology* **2003**, *170*, 1003-1007.
- (20) Thomas, D.D.; Ridnour, L.A.; Isenberg, J.S.; Flores-Santana, W.; Switzer, C.H.; Donzelli, S.; Hussain, P.; Vecoli, C.; Paolocci, N.; Ambs, S.; Colton, C.A.; Harris, C.C.; Roberts, D.D.; Wink, D.A. "The chemical biology of nitric oxide: Implications in cellular signaling" *Free Radical Biology & Medicine* **2008**, *45*, 18-31.
- (21) Thomas, D.D.; Liu, X.; Kantrow, S.P.; Lancaster J.R. Jr. "The biological lifetime of nitric oxide: Implications for the perivascular dynamics of NO and O₂" *Proceedings of the National Academy of Sciences* **2001**, *98*, 355-360.
- (22) Beckman, J.S.; Koppenol, W.H. "Nitric oxide, superoxide, and peroxynitrite: The good, bad, and the ugly" *American Journal of Physiology* **1996**, *271*, C1424-C1437.
- (23) Drago, R.S.; Paulik, F.E. "The reaction of nitrogen(II) oxide with diethylamine" *Journal of the American Chemical Society* **1960**, *82*, 96-98.
- (24) Drago, R.S.; Karstetter, B.R. "The reaction of nitrogen(II) oxide with various primary and secondary amines" *Journal of the American Chemical Society* **1961**, *83*, 1819-1822.
- (25) Hrabie, J.A.; Klose, J.R.; Wink, D.A.; Keefer, L.K. "New nitric oxide-releasing zwitterions derived from polyamines" *Journal of Organic Chemistry* **1993**, *58*, 1472-1476.
- (26) Keefer, L.K.; Nims, R.W.; Davies, K.M.; Wink, D.A. "NONOates (1-substituted diazenium-1,2-diolates) as nitric oxide donors: Convenient nitric oxide dosage forms" *Methods in Enzymology* **1996**, *268*, 281-293.
- (27) Davies, K.M.; Wink, D.A.; Saavedra, J.E.; Keefer, L.K. "Chemistry of diazeniumdiolates. 2. Kinetics and mechanism of dissociation to nitric oxide in aqueous solution" *Journal of the American Chemical Society* **2001**, *123*, 5473-5481.

- (28) Hrabie, J.A.; Keefer, L.K. "Chemistry of the nitric oxide-releasing diazeniumdiolate ("Nitrosohydroxylamine") functional group and its oxygen-substituted derivatives" *Chemical Reviews* **2002**, *102*, 1135-1154.
- (29) Saavedra, J.E.; Keefer, L.K. "Nitrogen-based diazeniumdiolates: Versatile nitric oxide-releasing compounds in biomedical research and potential clinical applications" *Journal of Chemical Education* **2002**, *79*, 1427-1434.
- (30) Keefer, L.K. "Progress toward clinical application of the nitric oxide-releasing diazeniumdiolates" *Annual Review of Pharmacology and Toxicology* **2003**, *43*, 585-607.
- (31) Keefer, L.K. "Fifty years of diazeniumdiolate research. From laboratory curiosity to broad-spectrum biomedical advances" *ACS Chemical Biology* **2011**, *6*, 1147-1155.
- (32) Zhang, H.; Annich, G.M.; Miskulin, J.; Stankiewicz, K.; Osterholzer, K.; Merz, S.I.; Bartlett, R.H.; Meyerhoff, M.E. "Nitric oxide-releasing fumed silica particles: Synthesis, characterization, and biomedical applications" *Journal of the American Chemical Society* **2003**, *125*, 5015-5024.
- (33) Drago, R.S.; Ragsdale, R.O.; Eyman, D.P. "A mechanism for the reaction of diethylamine with nitric oxide" *Journal of the American Chemical Society*, **1961**, *83*, 4337-4339.
- (34) Coneski, P.N.; Schoenfish, M.H. "Competitive formation of *N*-diazeniumdiolates and *N*-nitrosamines via anaerobic reactions of polyamines with nitric oxide" *Organic Letters* **2009**, *11*, 5462-5465.
- (35) Bohle, D.S.; Smith, K.N. "Kinetics and mechanism of nucleophilic addition to nitric oxide: Secondary amine diazeniumdiolation" *Inorganic Chemistry* **2008**, *47*, 3925-3927.
- (36) Miller, M.R.; Megson, I.L. "Recent developments in nitric oxide donor drugs" *British Journal of Pharmacology* **2007**, *151*, 305-321.
- (37) Feelisch, M. "The use of nitric oxide donors in pharmacological studies" *Naunyn-Schmiedeberg's Archives of Pharmacology* **1998**, *358*, 113-122.
- (38) Huerta, S.; Chilka, S.; Bonavida, B. "Nitric oxide donors: Novel cancer therapeutics (review)" *International Journal of Oncology* **2008**, *33*, 909-927.
- (39) Matthews, N.E.; Adams, M.A.; Maxwell, L.R.; Gofton, T.E.; Graham, C.H. "Nitric oxide-mediated regulation of chemosensitivity in cancer cells" *Journal of the National Cancer Institute* **2001**, *93*, 1879-1885.
- (40) Thomas, D.D.; Espey, M.G.; Ridnour, L.A.; Hofseth, L.J.; Mancardi, D.; Harris, C.C.; Wink, D.A. "Hypoxic inducible factor 1 α , extracellular signal-regulated kinase, and p53 are regulated by distinct threshold concentrations of nitric oxide" *Proceedings of the National Academy of Sciences* **2004**, *101*, 8894-8899.

- (41) Simeone, A.; Colella, S.; Krahe, R.; Johnson, M.M.; Mora, E.; Tari, A.M. "N-(4-Hydroxyphenyl)retinamide and nitric oxide pro-drugs exhibit apoptotic and anti-invasive effects against bone metastatic breast cancer cells" *Carcinogenesis* **2006**, *27*, 568-577.
- (42) Weiss, J.M.; Ridnour, L.A.; Back, T.; Hussain, S.P.; He, P.; Maciag, A.E.; Keefer, L.K.; Murphy, W.J.; Harris, C.C.; Wink, D.A.; Wiltout, R.H. "Macrophage-dependent nitric oxide expression regulates tumor cell detachment and metastasis after IL-2/anti-CD40 immunotherapy" *The Journal of Experimental Medicine* **2007**, *11*, 2455-2467.
- (43) van Roy, F.; Berx, G. "The cell-cell adhesion molecule E-cadherin" *Cellular and Molecular Life Sciences* **2008**, *65* 3756-3788.
- (44) Bender, A.; Schieber, J.; Glick, M.; Davies, J.W.; Azzaoui, K.; Hamon, J.; Urban, L.; Whitebread, S.; Jenkins, J.L. "Analysis of pharmacology data and the prediction of adverse drug reactions and off-target effects from chemical structure" *ChemMedChem* **2007**, *2*, 861-873.
- (45) Park, B.K.; Boobis, A.; Clarke, S.; Goldring, C.; Jones, D.; Kenna, J.G.; Lambert, C.; Lavery, H.G.; Naisbitt, D.J.; Nelson, S.; Nicoll-Griffith, D.A.; Obach, R.S.; Routledge, P.; Smith, D.A.; Tweedie, D.J.; Vermeulen, N.; Williams, D.P.; Wilson, I.D.; Baillie, T.A. "Managing the challenge of chemically reactive metabolites in drug development" *Nature Reviews Drug Discovery* **2011**, *10*, 292-306.
- (46) Muller, P.Y.; Milton, M.N. "The determination and interpretation of the therapeutic index in drug development" *Nature Reviews Drug Discovery* **2012**, *11*, 751-761.
- (47) Batchelor, M.M.; Reoma, S.L.; Fleser, P.S.; Nuthakki, V.K.; Callahan, R.E.; Shanley, C.J.; Politis, J.K.; Elmore, J.; Merz, S.I.; Meyerhoff, M.E. "More lipophilic dialkyldiamine-based diazeniumdiolates: Synthesis, characterization, and application in preparing thromboresistant nitric oxide release polymeric coatings" *Journal of Medicinal Chemistry* **2003**, *46*, 5153-5161.
- (48) Frost, M.C.; Reynolds, M.M.; Meyerhoff, M.E. "Polymers incorporating nitric oxide releasing/generating substances for improved biocompatibility of blood-contacting medical devices" *Biomaterials* **2005**, *26*, 1685-1693.
- (49) Hetrick, E.M.; Schoenfisch, M.H. "Reducing implant-related infections: Active release strategies" *Chemical Society Reviews* **2006**, *35*, 780-789.
- (50) Sortino, S. "Light-controlled nitric oxide delivering molecular assemblies" *Chemical Society Reviews* **2010**, *39*, 2903-2913.
- (51) Seabra, A.B.; Duran, N. "Nitric oxide-releasing vehicles for biomedical applications" *Journal of Materials Chemistry* **2010**, *20*, 1624-1637.
- (52) Riccio, D.A.; Schoenfisch, M.H. "Nitric oxide release: Part I. Macromolecular scaffolds" *Chemical Society Reviews* **2012**, *41*, 3731-3741.

- (53) Rothrock, A.R.; Donkers, R.L.; Schoenfish, M.H. "Synthesis of nitric oxide-releasing gold nanoparticles" *Journal of the American Chemical Society* **2005**, *127*, 9362-9363.
- (54) Polizzi, M.A.; Stasko, N.A.; Schoenfish, M.H. "Water-soluble nitric oxide-releasing gold nanoparticles" *Langmuir* **2007**, *23*, 4938-4943.
- (55) Shin, J.H.; Metzger, S.K.; Schoenfish, M.H. "Synthesis of nitric oxide-releasing silica nanoparticles" *Journal of the American Chemical Society* **2007**, *129*, 4612-4619.
- (56) Shin, J.H.; Schoenfish, M.H. "Inorganic/organic hybrid silica nanoparticles as a nitric oxide delivery scaffold" *Chemistry of Materials* **2008**, *20*, 239-249.
- (57) Hetrick, E.M.; Shin, J.H.; Stasko, N.A.; Johnson, C.B.; Wespe, D.A.; Holmuhamedov, E.; Schoenfish, M.H. "Bactericidal efficacy of nitric oxide-releasing silica nanoparticles" *ACS Nano* **2008**, *2*, 235-246.
- (58) Soto, R.J.; Yang, L.; Schoenfish, M.H. "Functionalized mesoporous silica via an aminosilane surfactant ion exchange reaction: Controlled scaffold design and nitric oxide release" *ACS Applied Materials & Interfaces* **2016**, *8*, 2220-2231.
- (59) Carpenter, A.W.; Slomberg, D.L.; Rao, K.S.; Schoenfish, M.H. "Influence of scaffold size on bactericidal activity of nitric oxide-releasing silica nanoparticles" *ACS Nano* **2011**, *5*, 7235-7244.
- (60) Hetrick, E.M.; Shin, J.H.; Paul, H.S.; Schoenfish, M.H. "Anti-biofilm efficacy of nitric oxide-releasing silica nanoparticles" *Biomaterials* **2009**, *30*, 2782-2789.
- (61) Slomberg, D.L.; Lu, Y.; Broadnax, A.D.; Hunter, R.A.; Carpenter, A.W.; Schoenfish, M.H. "Role of size and shape on biofilm eradication for nitric oxide-releasing silica nanoparticles" *ACS Applied Materials & Interfaces* **2013**, *5*, 9322-9329.
- (62) Stevens, E.V.; Carpenter, A.W.; Shin, J.H.; Liu, J.; Der, C.J.; Schoenfish, M.H. "Nitric oxide-releasing silica nanoparticle inhibition of ovarian cancer cell growth" *Molecular Pharmaceutics* **2010**, *7*, 775-785.
- (63) Stasko, N.A.; Schoenfish, M.H. "Dendrimers as a scaffold for nitric oxide release" *Journal of the American Chemical Society* **2006**, *128*, 8265-8271.
- (64) Lu, Y.; Sun, B.; Li, C.; Schoenfish, M.H. "Structurally diverse nitric oxide-releasing poly(propylene imine) dendrimers" *Chemistry of Materials* **2011**, *23*, 4227-4233.
- (65) Sun, B.; Slomberg, D.L.; Chudasama, S.L.; Lu, Y.; Schoenfish, M.H. "Nitric oxide-releasing dendrimers as antibacterial agents" *Biomacromolecules* **2012**, *13*, 3343-3354.

- (66) Worley, B.V.; Schilly, K.M.; Schoenfisch, M.H. "Anti-biofilm efficacy of dual-action nitric oxide-releasing alkyl chain modified poly(amidoamine) dendrimers" *Molecular Pharmaceutics* **2015**, *12*, 1573-1583.
- (67) Backlund, C.J.; Worley, B.V.; Schoenfisch, M.H. "Anti-biofilm action of nitric oxide-releasing alkyl-modified poly(amidoamine) dendrimers against *Streptococcus mutans*" *Acta Biomaterialia* **2016**, *29*, 198-205.
- (68) Pattni, B.S.; Chupin, V.V.; Torchilin, V.P. "New developments in liposomal drug delivery" *Chemical Reviews* **2015**, *115*, 10938-10966.
- (69) Torchilin, V.P. "Recent advances with liposomes as pharmaceutical carriers" *Nature Reviews Drug Discovery* **2005**, *4*, 145-160.
- (70) Varona, S.; Martín, A.; Cocero, M.J. "Liposomal incorporation of lavandin essential oils by a thin-film hydration method and particles from gas-saturated solutions" *Industrial and Engineering Chemistry Research* **2011**, *50*, 2088-2097.
- (71) Liu, X.; Yang, B.; Wang, Y.; Wang, J. "Photoisomerisable cholesterol derivatives as photo-trigger of liposomes: Effect of lipid polarity, temperature, incorporation ratio, and cholesterol" *Biochimica et Biophysica Acta* **2005**, *1720*, 28-34.
- (72) Johnson, S.M. "The effect of charge and cholesterol on the size and thickness of sonicated phospholipid vesicles" *Biochimica et Biophysica Acta* **1973**, *307*, 27-41.
- (73) Lapinski, M.M.; Castro-Forero, A.; Greiner, A.J.; Ofoli, R.Y.; Blanchard, G.J. "Comparison of liposomes formed by sonication and extrusion: Rotational and translational diffusion of an embedded chromophore" *Langmuir* **2007**, *23*, 11677-11683.
- (74) Meure, L.A.; Foster, N.R.; Dehghani, F. "Conventional and dense gas techniques for the production of liposomes: A review" *AAPS PharmSciTech* **2008**, *9*, 798-809.
- (75) Szoka, F. Jr. Papahadjopoulos, D. "Comparative properties and methods of preparation of lipid vesicles (liposomes)" *Annual Review of Biophysics and Bioengineering* **1980**, *9*, 467-508.
- (76) Szoka, F. Jr. Papahadjopoulos, D. "Procedure for preparation of liposomes with large internal aqueous space and high capture by reverse-phase evaporation" *Proceedings of the National Academy of Sciences* **1978**, *75*, 4194-4198.
- (77) Giulio, A.D.; Maurizi, G.; Odoardi, P.; Saletti, M.A.; Amicosante, G.; Oratore, A. "Encapsulation of ampicillin in reverse-phase evaporation liposomes: A direct evaluation by derivative spectrophotometry" *International Journal of Pharmaceutics* **1991**, *74*, 183-188.
- (78) Lichtenberg, D. "Liposomes: Preparation, characterization, and preservation" *Methods of Biochemical Analysis* **1988**, *33*, 337-462.

- (79) Ostrowsky, N. "Liposome size measurements by photon correlation spectroscopy" *Chemistry and Physics of Lipids* **1993**, *64*, 45-56.
- (80) Ruozi, B.; Belletti, D.; Tombes, A.; Tosi, G.; Bondioli, L.; Forni, F.; Vandelli, M.A. "AFM, ESEM, TEM, and CLSM in liposomal characterization: A comparative study" *International Journal of Nanomedicine* **2011**, *6*, 557-563.
- (81) Guiot, P.; Baudhuin, P.; Gotfredsen, C. "Morphological characterization of liposome suspensions by stereological analysis of freeze-fracture replicas from spray-frozen samples" *Journal of Microscopy* **1980**, *120*, 159-174.
- (82) Papahadjopoulos, D.; Vail, W.J.; Poste, G. "Cochleate lipid cylinders: Formation by fusion of unilamellar lipid vesicles" *Biochimica et Biophysica Acta* **1975**, *394*, 483-491.
- (83) Chen, C.; Zhu, S.; Huang, T.; Wang, S.; Yan, X. "Analytical techniques for single-liposome characterization" *Analytical Methods* **2013**, *5*, 2150-2157.
- (84) Crommelin, D.J.A.; van Bommel, E.M.G. "Stability of liposomes on storage: Freeze dried, frozen, or as an aqueous dispersion" *Pharmaceutical Research* **1984**, *1*, 159-163.
- (85) Allen, T.M.; Cullis, P.R. "Liposomal drug delivery systems: From concept to clinical applications" *Advanced Drug Delivery Reviews* **2013**, *65*, 36-48.
- (86) Tan, M.L.; Choong, P.F.; Dass, C.R. "Recent developments in liposomes, microparticles and nanoparticles for protein and peptide drug delivery" *Peptides* **2010**, *31*, 184-193.
- (87) Al-Jamal, W.T.; Kostarelos, K. "Liposomes: From a clinically established drug delivery system to a nanoparticles platform for theranostic nanomedicine" *Accounts of Chemical Research* **2011**, *44*, 1094-1104.
- (88) Wan, C.; Allen, T.M.; Cullis, P.R. "Lipid nanoparticles delivery systems for siRNA-based therapeutics" *Drug Delivery and Translational Research* **2014**, *4*, 74-83.
- (89) Buyens, K.; De Smedt, S.C.; Braeckmans, K.; Demeester, J.; Peeters, L.; van Grunsven, L.A.; de Mollerat du Jeu, X.; Sawant, R.; Torchilin, V.; Farkasova, K.; Ogris, M.; Sanders, N.N. "Liposome based systems for systemic siRNA delivery: Stability in blood sets the requirements for optimal carrier design" *Journal of Controlled Release* **2012**, *158*, 362-370.
- (90) Gonçalves, E.; Debs, R.J.; Heath, T.D. "The effect of liposome size on the final lipid/DNA ratio of cationic lipoplexes" *Biophysical Journal* **2004**, *86*, 1554-1563.
- (91) Ito, I.; Began, G.; Mohiuddin, I.; Saeki, T.; Saito, Y.; Branch, C.D.; Vaporciyan, A.; Stephens, L.C.; Yen, N.; Roth, J.A.; Ramesh, R. "Increased uptake of liposomal-DNA complexes by lung metastases following intravenous administration" *Molecular Therapy* **2003**, *7*, 409-418.

- (92) Felgner, P.L.; Gadek, T.R.; Holm, M.; Roman, R.; Chan, H.W.; Wenz, M.; Northrop, J.P.; Ringold, G.M.; Danielsen, M. "Lipofection: A highly efficient, lipid-mediated DNA-transfection procedure" *Proceedings of the National Academy of Sciences* **1987**, *84*, 7413-7417.
- (93) Zheng, W.; Liu, Y.; West, A.; Schuler, E.E.; Yehl, K.; Dyer, R.B.; Kindt, J.T.; Salaita, K. "Quantum dots encapsulated within phospholipid membranes: Phase-dependent structure, photostability, and site-selective functionalization" *Journal of the American Chemical Society* **2014**, *136*, 1992-1999.
- (94) Batalla, J.; Cabrera, H.; Martín-Martínez, E.S.; Korte, D.; Calderón, A.; Marín, E. "Encapsulation efficiency of CdSe/ZnS quantum dots by liposomes determined by thermal lens microscopy" *Biomedical Optics Express* **2015**, *6*, 3898-3906.
- (95) Beloglazova, N.V.; Shmelin, P.S.; Speranskaya, E.S.; Lucas, B.; Helmbrecht, C.; Knopp, D.; Niessner, R.; Saeger, S.D.; Goryacheva, I.Y. "Quantum dot loaded liposomes as fluorescent labels for immunoassay" *Analytical Chemistry* **2013**, *85*, 7197-7204.
- (96) Ye, C.; Wang, Y.; Li, C.; Yu, J.; Hu, Y. "Preparation of liposomes loaded with quantum dots, fluorescence resonance energy transfer studies, and near-infrared in-vivo imaging of mouse tissue" *Microchim Acta* **2013**, *180*, 117-125.
- (97) Chen, H.; MacDonald, R.C.; Li, S.; Krett, N.L.; Rosen, S.T.; O'Halloran, T.V. "Lipid encapsulation of arsenic trioxide attenuates cytotoxicity and allows for controlled anticancer drug release" *Journal of the American Chemical Society* **2006**, *128*, 13348-13349.
- (98) Yang, F.; Jin, C.; Jiang, Y.; Li, J.; Di, Y.; Ni, Q.; Fu, D. "Liposome based delivery systems in pancreatic cancer treatment: From bench to bedside" *Cancer Treatment Reviews* **2011**, *37*, 633-642.
- (99) Cosco, D.; Bulotta, A.; Ventura, M.; Celia, C.; Calimeri, T.; Perri, G.; Paolino, D.; Costa, N.; Neri, P.; Tagliaferri, P.; Tassone, P.; Fresta, M. "In vivo activity of gemcitabine-loaded PEGylated small unilamellar liposomes against pancreatic cancer" *Cancer Chemotherapy and Pharmacology* **2009**, *64*, 1009-1020.
- (100) Cheng, K.W.; Nie, T.; Ouyang, N.; Alston, N.; Wong, C.C.; Mattheolabakis, G.; Papayannis, I.; Huang, L.; Rigas, B. "A novel ibuprofen derivative with anti-lung cancer properties: Synthesis, formulation, pharmacokinetic and efficacy studies" *International Journal of Pharmaceutics* **2014**, *477*, 236-243.
- (101) Immordino, M.L.; Brusa, P.; Arpicco, S.; Stella, B.; Dosio, F.; Cattel, L. "Preparation, characterization, cytotoxicity and pharmacokinetics of liposomes containing docetaxel" *Journal of Controlled Release* **2003**, *91*, 417-429.
- (102) Natarajan, J.; Darwitan, A.; Barathi, V.A.; Ang, M.; Htoon, H.M.; Boey, F.; Tam, K.C.; Wong, T.T.; Venkatraman, S.S. "Sustained drug release in nanomedicine: A long-acting nanocarrier-based formulation for glaucoma" *ACS Nano* **2014**, *8*, 419-429.

- (103) Barenholz, Y.C. “Doxil – The first FDA-approved nano-drug: Lessons learned” *Journal of Controlled Release* **2012**, *160*, 117-134.
- (104) Haran, G.; Cohen, R.; Bar, L.K.; Barenholz, Y. “Transmembrane ammonium sulfate gradients in liposomes produce efficient and stable entrapment of amphipathic weak bases” *Biochimica et Biophysica Acta* **1993**, *1151*, 201-215.
- (105) Amselem, S.; Gabizon, A.; Barenholz, Y. “Optimization and upscaling of doxorubicin-containing liposomes for clinical use” *Journal of Pharmaceutical Sciences* **1990**, *79*, 1045-1052.
- (106) Emanuel, N.; Kedar, E.; Bolotin, E.M.; Smorodinsky, N.I.; Barenholz, Y. “Preparation and characterization of doxorubicin-loaded sterically stabilized immunoliposomes” *Pharmaceutical Research* **1996**, *13*, 352-359.
- (107) Rand, R.P. “Interacting phospholipid bilayers: Measured forces and induced structural changes” *Annual Review of Biophysics and Bioengineering* **1981**, *10*, 277-314.
- (108) Immordino, M.L.; Dosio, F.; Cattel, L. “Stealth liposomes: Review of the basic science, rationale, and clinical applications, existing and potential” *International Journal of Nanomedicine* **2006**, *3*, 297-315.
- (109) Adler-Moore, J.; Proffitt, R.T. “AmBisome: Liposomal formulation, structure, mechanism of action and pre-clinical experience” *Journal of Antimicrobial Chemotherapy* **2002**, *49*, 21-30.
- (110) Larabi, M.; Pages, N.; Pons, F.; Appel, M.; Gulik, A.; Schlatter, J.; Bouvet, S.; Barratt, G. “Study of the toxicity of a new lipid complex formulation of amphotericin B” *Journal of Antimicrobial Chemotherapy* **2004**, *53*, 81-88.
- (111) Khan, M.A.; Owais, M. “Toxicity, stability, and pharmacokinetics of amphotericin B in immunomodulator tuftsin-bearing liposomes in a murine model” *Journal of Antimicrobial Chemotherapy* **2006**, *58*, 125-132.
- (112) Silverman, J.A.; Deitcher, S.R. “Marqibo (vincristine sulfate liposome injection) improves the pharmacokinetics and pharmacodynamics of vincristine” *Cancer Chemotherapy and Pharmacology* **2013**, *71*, 555-564.
- (113) Tulpule, A. “Liposomally encapsulated daunorubicin (daunoXome) in the treatment of non-Hodgkin’s lymphoma” *The Oncologist* **1997**, *2*, 181-195.
- (114) Piccaluga, P.P.; Visani, G.; Martinelli, G.; Isidori, A.; Malagola, M.; Rondoni, M.; Baccarani, M.; Tura, S. “Liposomal daunorubicin (daunoXome) for treatment of relapsed meningeal acute myeloid leukemia” *Leukemia* **2002**, *16*, 1880-1881.
- (115) Carvalho, B.; Roland, L.M.; Chu, L.F.; Campitelli, V.A.; Riley, E.T. “Single-dose, extended-release epidural morphine (DepoDur) compared to conventional epidural morphine for post-cesarean pain” *Anesthesia and Analgesia* **2007**, *105*, 176-183.

- (116) Ford, S.R.; Swanevelder, C.S.; Mills, P.M. “Extended-release epidural morphine (DepoDur) as analgesia for rib fractures” *British Journal of Anaesthesia* **2012**, *108*, 883-884.
- (117) Beauchesne, P.; Blonski, M.; Brissart, H. “Response to intrathecal infusions of Depocyt in secondary diffuse leptomeningeal gliomatosis. A case report” *In Vivo* **2011**, *25*, 991-993.
- (118) McClune, B.; Buadi, F.; Aslam, N.; Przepiorka, D. “Intrathecal liposomal cytarabine (Depocyt) is safe and effective for prevention of meningeal disease in patients with acute lymphoblastic leukemia and high-grade lymphoma treated with the HyperCVAD regimen” *Blood* **2005**, *106*, 4594.
- (119) Bressler, N.M.; Bressler, S.B. “Photodynamic therapy with verteporfin (Visudyne): Impact on ophthalmology and visual sciences” *Investigative Ophthalmology and Visual Science* **2000**, *41*, 624-628.
- (120) Verteporfin Roundtable Participants “Guidelines for using verteporfin (Visudyne) in photodynamic therapy for choroidal neovascularization due to age-related macular degeneration and other causes: Update” *Retina* **2005**, *25*, 119-134.
- (121) Herzog, C.; Hartmann, K.; Künzi, V.; Kürsteiner, O.; Mischler, R.; Lazar, H.; Glück, R. “Eleven years of Inflexal V—a virosomal adjuvanted influenza vaccine” *Vaccine* **2009**, *27*, 4381-4387.
- (122) Mischler, R.; Metcalfe, I.C. “Inflexal V a trivalent virosome subunit influenza vaccine: Production” *Vaccine* **2002**, *20*, B17-B23.
- (123) Gasparini, R.; Amicizia, D.; Lai, P.L.; Rossi, S.; Panatto, D. “Effectiveness of adjuvanted seasonal influenza vaccines (Inflexal V and Fluad) in preventing hospitalization for influenza and pneumonia in the elderly” *Human Vaccines and Immunotherapeutics* **2013**, *9*, 144-152.
- (124) D’Acremont, V.; Herzog, C.; Genton, B. “Immunogenicity and safety of a virosomal hepatitis A vaccine (Epaxal) in the elderly” *Journal of Travel Medicine* **2006**, *13*, 78-83.
- (125) Bovier, P.A. “Epaxal: A virosomal vaccine to prevent hepatitis A infection” *Expert Reviews Vaccines* **2008**, *7*, 1141-1150.
- (126) Casagrande, N.; Celegato, M.; Borghese, C.; Mongiat, M.; Colombatti, A.; Aldinucci, D. “Preclinical activity of the liposomal cisplatin lipoplatin in ovarian cancer” *Clinical Cancer Research* **2014**, *20*, 5496-5506.
- (127) Stathopoulos, G.P.; Boulikas, T. “Lipoplatin formulation review article” *Journal of Drug Delivery* **2012**, *2012*, 1-10.
- (128) Fantini, M.; Gianni, L.; Santelmo, C.; Drudi, F.; Castellani, C.; Affatato, A.; Nicolini, M.; Ravaioli, A. “Lipoplatin treatment in lung and breast cancer” *Chemotherapy Research and Practice* **2011**, *2011*, 1-7.

- (129) Boulikas, T. "Clinical overview on Lipoplatin: A successful liposomal formulation of cisplatin" *Expert Opinion on Investigational Drugs* **2009**, *18*, 1197-1218.
- (130) Senior, J.H. "Fate and behavior of liposomes in vivo: A review of controlling factors" *Critical Reviews in Therapeutic Drug Carrier Systems* **1987**, *3*, 123-193.
- (131) Soriano, J.; Stockert, J.C.; Villanueva, A.; Canete, M. "Cell uptake of Zn(II)-phthalocyanine-containing liposomes by clathrin-mediated endocytosis" *Histochemistry and Cell Biology* **2010**, *133*, 449-454.
- (132) Bareford, L.M.; Swaan, P.W. "Endocytic mechanisms for targeted drug delivery" *Advanced Drug Delivery Reviews* **2007**, *59*, 748-758.
- (133) Mayor, S.; Pagano, R.E. "Pathways of clathrin-independent endocytosis" *Nature Reviews Molecular Cell Biology* **2007**, *8*, 603-612.
- (134) Allen, T.M. "Ligand-targeted therapeutics in anticancer therapy" *Nature Reviews Cancer* **2002**, *2*, 750-763.
- (135) Zwicke, G.L.; Mansoori, G.A.; Jeffery, C.J. "Utilizing the folate receptor for active targeting of cancer nanotherapeutics" *Nano Reviews* **2012**, *3*, 18496.
- (136) Chen, H.; Ahn, R.; Van der Bossche, J.; Thompson, D.H.; O'Halloran, T.V. "Folate-mediated intracellular drug delivery increases the anticancer efficacy of nanoparticulate formulation of arsenic trioxide" *Molecular Cancer Therapeutics* **2009**, *8*, 1955-1963.
- (137) Huang, S.L.; McPherson, D.D.; Macdonald, R.C. "A method to co-encapsulate gas and drugs in liposomes for ultrasound-controlled drug delivery" *Ultrasound in Medicine and Biology* **2008**, *34*, 1272-1280.
- (138) Huang, S.; Kee, P.H.; Kim, H.; Moody, M.R.; Chrzanowski, S.M.; MacDonald, R.C.; McPherson, D.D. "Nitric oxide-loaded echogenic liposomes for nitric oxide delivery and inhibition of intimal hyperplasia" *Journal of the American College of Cardiology* **2009**, *54*, 652-659.
- (139) Klegerman, M.E.; Wassler, M.; Huang, S.; Zou, Y.; Kim, H.; Shelat, H.S.; Holland, C.K.; Geng, Y.; McPherson, D.D. "Liposomal modular complexes for simultaneous targeted delivery of bioactive gases and therapeutics" *Journal of Controlled Release* **2010**, *142*, 326-331.
- (140) Ostrowski, A.D.; Lin, B.F.; Tirrell, M.V.; Ford, P.C. "Liposome encapsulation of a photochemical NO precursor for controlled nitric oxide release and simultaneous fluorescence imaging" *Molecular Pharmaceutics* **2012**, *9*, 2950-2955.
- (141) Pedrini, I.; Gazzano, E.; Chegaev, K.; Rolando, B.; Marengo, A.; Kopecka, J.; Fruttero, R.; Ghigo, D.; Arpicco, S.; Riganti, C. "Liposomal nitrooxy-doxorubicin: One step over caelyx in drug-resistant human cancer cells" *Molecular Pharmaceutics* **2014**, *11*, 3068-3079.

(142) Tai, L.; Wang, Y.; Yang, C. “Heat-activated sustaining nitric oxide release from zwitterionic diazeniumdiolate loaded in thermo-sensitive liposomes” *Nitric Oxide* **2010**, *23*, 60-64.

CHAPTER 2: ENCAPSULATION OF *N*-DIAZENIUMDIOLATES WITHIN LIPOSOMES FOR ENHANCED NITRIC OXIDE DONOR STABILITY AND DELIVERY¹

2.1 Introduction

Nitric oxide (NO) is often proposed as a potential therapeutic due to the many roles it plays in human physiology.¹⁻⁴ For example, NO functions as an antiplatelet agent because it helps regulate the production of cyclic guanosine monophosphate (cGMP) and concentration of calcium ions (Ca^{2+}) within platelets required for platelet activation.⁵ In addition to its antithrombotic properties, NO exhibits broad-spectrum antibacterial activity and is central to the innate immune response.⁶ Nitric oxide exerts antibacterial action through the reaction with other oxidants and production of cytotoxic byproducts (e.g., dinitrogen trioxide, peroxy nitrite) that subsequently induce DNA deamination and cell membrane damage.⁷⁻⁸ Nitric oxide has been shown to kill cancer cells through similar nitrosative and oxidative stresses.⁹ Another potential mechanism of NO's anticancer action is through the regulation of intracellular protein expression. For example, Hofseth et. al. reported the effects of NO on the reactivation of the p53 tumor suppressor protein.¹⁰ In this manner, cell death may be reinitiated to control cellular proliferation since p53 controls cell cycle entry/exit and apoptosis.¹¹ A major advantage of

¹ This chapter was adapted from an article that previously appeared in *Molecular Pharmaceutics*. The original citation is as follows: Suchyta, D.J.; Schoenfisch, M.H. "Encapsulation of *N*-diazoniumdiolates within liposomes for enhanced nitric oxide donor stability and delivery" *Molecular Pharmaceutics* **2015**, *12*, 3569-3574.

exogenous NO over current chemotherapeutics would be the limited off-target cytotoxicity as NO has a relatively short lifetime in physiological milieu.¹

The reactivity and short half-life of NO in biological media necessitates the use of NO donors as sources of NO. *N*-diazoniumdiolate NO donors have received considerable attention due to their ability to spontaneously (i.e., non-enzymatically) produce NO under physiological conditions, as a result of donor breakdown by water (protons).¹² This NO release mechanism gives rise to controllable NO-release kinetics that are dependent on both NO donor and pH.¹³⁻¹⁴ Unfortunately, the use of free NO donors often results in insufficient control over targeting the delivery and insufficient NO payloads for therapeutic applications.¹⁵ Macromolecular NO-release scaffolds (e.g., dendrimers, nanoparticles) consisting of multiple NO donors have been developed to achieve greater NO payloads and delivery.¹⁶ Nanoparticle-based delivery vehicles have shown a broad range of NO-release kinetics that are highly dependent on the NO donor utilized (e.g., *S*-nitrosothiol, *N*-diazoniumdiolate).¹⁷ The therapeutic action of these NO-release systems has been demonstrated against both bacteria and cancer cells with directed cell membrane and DNA damage.¹⁸ While the NO payloads of these scaffolds are substantial (>1 $\mu\text{mol NO/mg}$), the majority of the NO can be released too rapidly depending on their structure.^{8,18-19} Ideally, next generation NO-release scaffolds would be stable or only minimally breakdown at pH 7.4 and 37 °C until certain physiology (e.g., a change in pH) would trigger a burst of NO release. Such pH-triggered NO delivery might prove useful in the development of new anticancer agents, exploiting the acidic (pH 5.4–7.6) microenvironments inside tumors.²⁰⁻²¹ In this respect, the majority of NO would be released at the tumor site avoiding potential off-target cytotoxicity.

Liposomes are nanostructures composed of an inner aqueous core surrounded by a bilayer of phospholipids that have been used to enhance drug delivery against many diseases (e.g., cancer).²² Encapsulation of a NO-releasing chromium complex within liposomes proved that the lipid bilayer can confer protection to the NO donor.²³ Tai et al. previously reported the encapsulation of spermine/NO within a phosphatidylcholine-based liposome utilizing a thin-film hydration method to achieve NO release.²⁴ Unfortunately, their resulting liposomes yielded low NO totals and their stability was unknown. Herein, we describe an alternative approach for preparing NO-releasing liposomes containing *N*-diazoniumdiolate NO donors with attention to vehicle formation, stability, and pH-triggered delivery. In contrast to other macromolecular NO-release systems (e.g., nanoparticles), the *N*-diazoniumdiolate NO donor is encapsulated within an aqueous core whereby a high interior pH limits undesirable NO donor decomposition.

2.2 Experimental section

2.2.1. Materials

Dipalmitoylphosphatidylcholine (DPPC) was purchased from Avanti Polar Lipids (Alabaster, AL). Cholesterol (Chol), iron (III) chloride hexahydrate, ammonium thiocyanate, bis(3-aminopropyl)amine, fetal bovine serum (FBS), penicillin streptomycin, Dulbecco's modified Eagle's medium (DMEM), phosphate-buffered saline (PBS) for cell culture, and dipropylentriamine were obtained from Sigma (St. Louis, MO). Phenazine methosulfate (PMS), chloroform, anhydrous acetonitrile, sulfuric acid, and isopropyl ether were purchased from Fisher Scientific (Fair Lawn, NJ). 3-(4,5-dimethylthiazol-2-yl)-5-(3-carboxymethoxyphenyl)-2-(4-sulfophen-yl)-2H-tetrazolium inner salt (MTS) was from Promega (Madison, WI). Sephadex G-25 was from GE Healthcare (Pittsburgh, PA). Spermine was purchased from Alfa Aesar (Ward Hill, MA). Pure nitric oxide (NO) gas (99.5%) was obtained from Praxair (Sanford, NC).

Argon, nitrogen (N₂), nitric oxide (NO) calibration gas (26.80 ppm, balance N₂), and carbon dioxide (CO₂) gas cylinders were from Airgas National Welders (Durham, NC). A Millipore Milli-Q UV Gradient A10 System (Bedford, MA) was used to purify distilled water to a resistivity of 10.2 MΩ·cm and a total organic content ≤6 ppb. PANC-1 cells (ATCC number CRL 1469) were a gift from Dr. Channing Der of the Department of Pharmacology at the University of North Carolina (Chapel Hill, NC).

2.2.2. *Synthesis of N-diazeniumdiolates*

Previously reported methods were employed to synthesize the NO donors (Figure 2.1).¹²⁻¹³ Briefly, the precursor molecule was dissolved in anhydrous acetonitrile (typically 33.3 mg/mL). The solution was subsequently purged with argon at 100 psi inside a stainless steel Parr bomb. Six sequential purges removed any residual oxygen in the solution. The solution was then charged with 10 bar NO for 3 d. After 3 d, the solution was purged six times with argon to 100 psi to remove any residual NO. The final solutions, containing the precipitated product, were poured over a Hirsch funnel, washed twice with diethyl ether, and dried under vacuum overnight. The final product was stored at -20 °C until use.

2.2.3. *Preparation of liposomes*

Liposomes were made using a 1:1 molar ratio of DPPC to Chol (typically 33 μmol DPPC to 33 μmol Chol) using the method of Szoka and Papahadjopoulos.²⁵ Lipids were dissolved in a 1:1 volumetric ratio of chloroform to isopropyl ether and added to a round-bottom flask with a septum under a nitrogen atmosphere. Subsequently, the *N*-diazeniumdiolate was dissolved in 50 mM NaOH to make a 14 mM stock NO donor solution and injected into the flask, which was sonicated for 4 min at 45 °C. The organic phase was removed using rotoevaporation, and the resulting liposomes were allowed to sit at 45 °C for 30 min. The unencapsulated material was

removed using four Sephadex G-25 spin columns packed in 10-mL syringes to minimize dilution of the liposomes. The final liposome solution was stored at 4 °C protected from light.

2.2.4. Characterization of liposome size

For dynamic light scattering measurements, the liposomes were diluted with water and analyzed with a Zetasizer Nano (Malvern Instruments, UK). Transmission electron microscopy (TEM) images were taken using liposomes diluted 1:1 with Milli-Q water. The liposomes were cast Formvar coated, square mesh copper TEM grids (Electron Microscopy Sciences, Hatfield, PA). After 45 minutes to allow evaporation of the solvent, a negative-stain was performed using 2% uranyl acetate. A drop of the stain was left on the grid for 1 min and subsequently removed using filter paper, followed by a 15 min dry time. The liposomes were imaged using a JEOL 100CX II transmission electron microscope at an accelerating voltage of 100 kV.

2.2.5. Phospholipid content assay

Total phospholipid content of the final liposome solution was determined using the Stewart assay.²⁶ Briefly, a 0.1 M ammonium ferrothiocyanate solution was made by dissolving 27.03 g iron (III) chloride hexahydrate and 30.4 g of ammonium thiocyanate in 1 liter of Milli-Q water. One microliter of the liposomes was mixed with 1.999 mL of the ammonium ferrothiocyanate solution. Subsequently, 2 mL of chloroform was added and the solution was vortexed for 15 s. Centrifugation ensued at $116 \times g$ for 5 min and the lower layer was analyzed at 485 nm using a UV-Vis Lambda 40 Spectrophotometer (Perkin Elmer, Waltham, MA).

2.2.6. Nitric oxide release from liposomes

Analysis of liposomal NO totals and release kinetics were evaluated using a Sievers (Boulder, CO) chemiluminescence nitric oxide analyzer (NOA).²⁷⁻²⁸ The instrument was calibrated using a NO zero filter (0 ppm NO) and a 26.80 ppm NO standard (balance N₂). Before

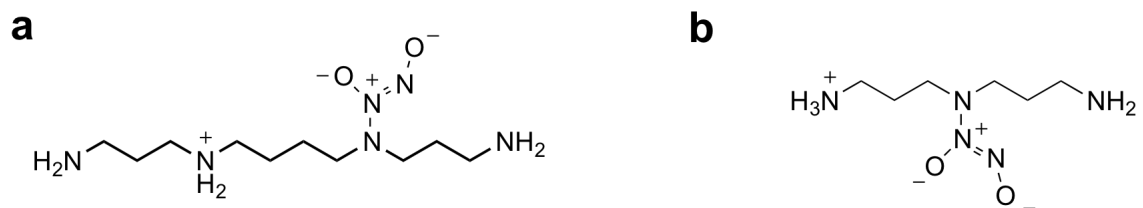


Figure 2.1. Structures of the NO donors synthesized (a) SPER/NO, (b) and DPTA/NO

NO analysis, the liposomes were passed through a Sephadex G-25 spin column to remove any material that may have permeated the liposomal bilayer during storage. After passage through the column, an aliquot of the liposomes was injected into a 2:1 volumetric ratio of ethanol to 0.183 M sulfuric acid (30 mL total volume) at 37 °C for encapsulation efficiency determination. Kinetic studies were performed in 10 mM acetate buffer (pH 5.4) and 10 mM PBS (pH 7.4) at 37 °C.

2.2.7. Cytotoxicity assay

PANC-1 cells were cultured in DMEM supplemented with 10 vol% FBS and 1 wt% penicillin/streptomycin. Cells were maintained at 37 °C in a humidified incubator with 5% CO₂. For cell viability evaluations, the MTS assay was used as previously described.²⁹ Briefly, cells (2×10^4 cells/mL) were treated with various volumes of drug and plated in triplicate (200 μ L total volume per well). Following a 24 h incubation period at 37 °C, the supernatant of each well was removed, rinsed with PBS (100 μ L) to remove any liposomes, and DMEM was added (100 μ L). The cells were further incubated with 20 μ L of MTS reagent (20:1 v/v MTS to PMS) at 37 °C for 90 minutes. Subsequently, the supernatant was removed and added to a new 96-well plate. The absorbance of the resulting solutions was measured at 490 nm using a ThermoScientific Multiskan EX plate reader (Waltham, MA). The ratio of absorbance values between the samples and the controls multiplied by 100 was determined to be the percent cell viability.

2.3 Results and discussion

2.3.1. Synthesis of NO-releasing liposomes

Nitric oxide-releasing liposomes were synthesized by dissolving the *N*-diazoniumdiolate NO donor (spermine/NO [SPER/NO] and/or dipropylentriamine/NO [DPTA/NO]) in 50 mM NaOH. This solution was added to a dipalmitoylphosphatidylcholine (DPPC)/cholesterol organic

mixture and briefly sonicated to form an emulsion. Subsequent removal of the organic phase by rotoevaporation resulted in the formation of 275 ± 21 nm liposomes (diameter; dynamic light scattering). Transmission electron microscopy further confirmed the formation of liposomes (Appendix A). Unencapsulated solute was removed by passing the liposomal solution through a Sephadex G-25 centrifuge column.³⁰ Liposomes were stored at 4 °C to ensure vesicle stability and minimize NO donor decomposition.

2.3.2. Liposomal NO-release measurements

Real-time NO release was measured from the NO donor-containing liposomes using a Sievers chemiluminescence nitric oxide analyzer (Boulder, CO).²⁷⁻²⁸ Prior to NO analysis, the liposomal solution was passed through a Sephadex G-25 mini centrifuge column to remove solute that may have permeated the bilayer during storage. Total NO release was determined by adding the liposomes to a 1:2 sulfuric acid/ethanol solution, which in turn compromised the stability of the liposomes and decomposed the *N*-diazoniumdiolates to NO. The same procedure was used to breakdown the free NO donor. The encapsulation efficiency (EE) for the NO-releasing liposomes was calculated based on total NO release for both the free and encapsulated NO donor (Table 2.1). Of note, the EE increased with increasing DPTA/NO to SPER/NO molar ratios. This phenomenon is attributed to the lower molecular weight of DPTA/NO.

Nitric oxide release from the liposomes was monitored under physiological conditions (pH 7.4, 37 °C) to understand how NO donor encapsulation influenced breakdown of the *N*-diazoniumdiolates. As shown in Figure 2.2, the initial burst associated with NO donor decomposition for free SPER/NO was more rapid than for liposome encapsulated SPER/NO ($t_{1/2}$ =35 vs. 162 min, respectively). Additionally, the initial rate of release was slowed further

Table 2.1. Encapsulation efficiencies (EE) of various NO donor compositions.^a

NO donor	EE (%)^b
SPER/NO	33.7 ± 1.5
DPTA/NO:SPER/NO (50:50)	36.8 ± 2.1
DPTA/NO	41.3 ± 3.5

^aFrom n≥3 separate preparations. ^bRatio of μmol of NO inside liposomes to μmol used for synthesis multiplied by 100.

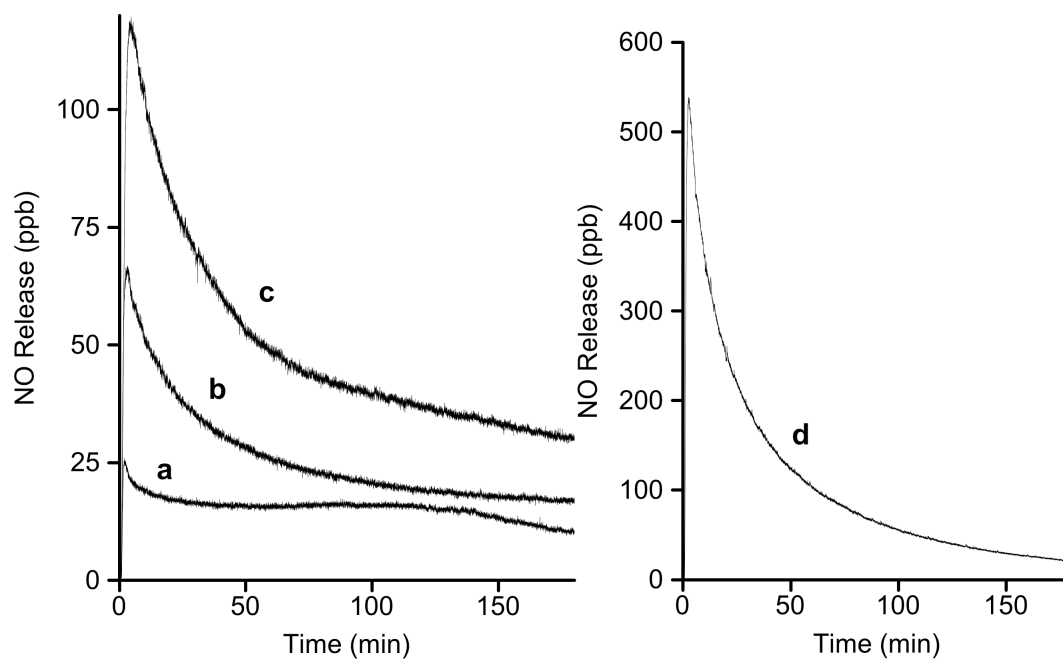


Figure 2.2. Nitric oxide release profiles of various encapsulated NO donors and free NO donor. Release profile from liposomal (a) DPTA/NO, (b) DPTA/NO:SPER/NO (50:50 molar ratio), (c) SPER/NO, (d) and free SPER/NO for the first 3 hours in 10 mM PBS (pH 7.4, 37 °C). Same amount of lipid was injected (0.70 mg) for profiles a-c. NO release was measured in real-time.

(Table 2.2) by employing a more stable NO-releasing molecule (i.e., DPTA/NO; $t_{1/2}$ =3 h). For the encapsulated DPTA/NO, the duration of NO release is dramatically extended versus the free NO donor (Appendix A). In this manner, tunable NO release was achieved under physiological conditions by altering the low molecular weight NO donor selected for encapsulation. We hypothesize the NO release can also be attributed to slower decomposition of the donor within the liposomes rather than slow diffusion of the NO donor out of the liposome. Since the liposomes are below their 42 °C transition temperature (T_c), the liposome bilayer remains rigid and impermeable to molecules, especially charged molecules (i.e., our NO donors). Relative to free NO donors, SPER/NO and DPTA/NO-containing liposomes exhibited increased NO-release half-lives (~4 and 7 times greater, respectively). Moreover, increasing the molar ratio of DPTA/NO to SPER/NO inside the vesicles (i.e., 0, 50, 100 mol% DPTA/NO) enhanced both the half-life and duration of NO release. In fact, DPTA/NO-based liposomes released NO continuously for ~3 d. The ability to tune the NO-release kinetics by simply varying the ratio and/or type of encapsulated NO donor represents a unique property of liposomes over previously reported macromolecular scaffolds.

Liposomal NO release was also monitored under acidic conditions (pH 5.4) to ascertain NO production relevant to the microenvironment of tumors.²¹⁻²² While the lipid bilayer provides both NO donor protection and tunable release kinetics at pH 7.4, the NO release in acidic solution was rapid, regardless of the *N*-diazeniumdiolate NO donor utilized (Table 2.3). The NO-release kinetics of the liposomal systems were essentially equivalent to the free NO donors under the same conditions (i.e., DPTA/NO: $t_{1/2}$ =5.3±0.2 min; SPER/NO $t_{1/2}$ =3.4±0.8 min) as a result of the rapid NO donor decomposition by protons. Indeed, the duration of NO release for DPTA/NO-containing liposomes was only slightly longer than those with SPER/NO.

Table 2.2. Nitric oxide-release properties of liposomes in PBS (pH = 7.4) at 37 °C.^a

NO donor	t_{1/2}^b (h)	[NO]_{max}^c (ppb/mg)	t_d^d (h)	[NO]_{total}^e (μmol/mg)
SPER/NO	2.7 ± 0.7	217 ± 98	18.4 ± 0.5	0.19 ± 0.02
DPTA/NO:SPER/NO ^f	16.6 ± 2.1	114 ± 17	51.2 ± 2.1	0.29 ± 0.03
DPTA/NO	20.4 ± 2.7	29 ± 8	65.9 ± 1.8	0.26 ± 0.05

^aError bars indicate standard deviation from n≥3 separate preparations. ^bHalf-life of NO release.

^cThe highest instantaneous amount of NO generated. ^dDuration of NO release until the measured NO reached 10 ppb per 300 μL of liposomes (three-times the detection limit of the instrument).

^eLipid concentration was 23.3 ± 5.4 mg phospholipid per mL of aqueous phase. ^fMolar ratio of 50:50.

Further studies were performed to determine the cause of the faster NO-release kinetics under pH 5.4 conditions. We rationalized that the rapid NO release stemmed from either compromised lipid structure, which would result in leaching of the NO donor into the acidic media, or increased proton influx through the liposome bilayer. The first explanation was dismissed as dynamic light scattering analysis of the liposomes in pH 5.4 acetate buffer indicated that liposome size/shape was preserved, suggesting the faster NO-release kinetics must be the result of a greater influx of protons. To verify this hypothesis, the interior pH of the liposomes was monitored using the bilayer-impermeable pH-sensitive dye pyranine.³¹ Under basic conditions pyranine fluoresces strongly, whereas protonation of the 8-hydroxyl group ($pK_a=7.2$) yields a decrease in fluorescence, thus allowing for suitable analysis of the intraliposomal pH. After formation of pyranine-loaded liposomes, the fluorescence emission was analyzed after being diluted 100-fold (same as the NOA experiments) in NaOH, PBS, and acetate buffer (Figure 2.3). A small change in fluorescence intensity between the NaOH-diluted (2.3a) and PBS-diluted (2.3c) liposomes indicates that the intraliposomal pH remains relatively basic, supporting the observed extended NO-release kinetics in PBS. Upon bursting of the liposomes with a surfactant, the 512 nm emission peak almost completely disappears (2.3d). The large drop in fluorescence after liposome destruction confirms that the lipid bilayer confers protection to the NO donor by maintaining a basic interior (i.e., hindering proton permeation). However, upon exposure of the liposomes to acetate buffer (2.3e), the fluorescence decreases dramatically, and was similar to free pyranine in acetate buffer, indicating a drop in intraliposomal pH (2.3f). In fact, this behavior was expected as the number of ion channels in lipid bilayers have been

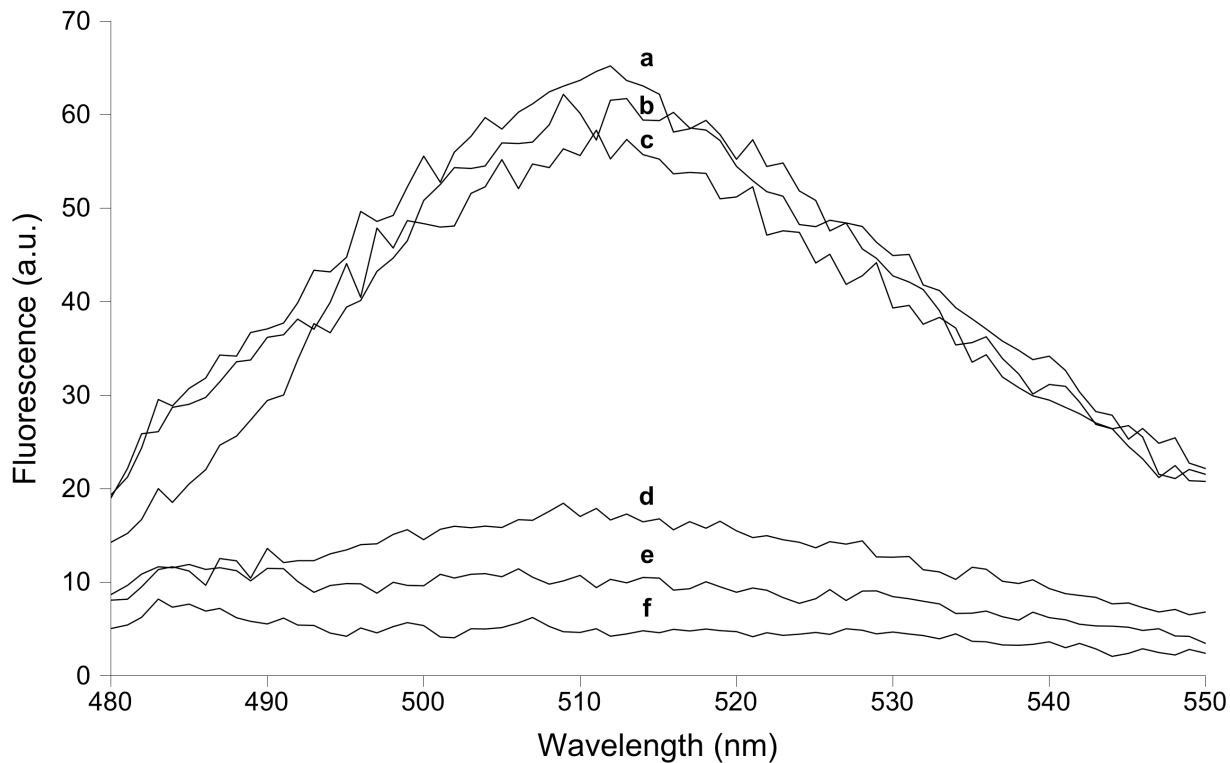


Figure 2.3. Fluorescence emission of pyranine-loaded liposomes (0.47 mg) made in 50 mM NaOH diluted 100-fold in (a) 50 mM NaOH, (c) 10 mM PBS (pH 7.4), (e) and 10 mM acetate buffer (pH 5.4). Free pyranine fluorescence after bursting of liposomes suspended in (b) 50 mM NaOH, (d) 10 mM PBS, (f) and 10 mM acetate buffer using 5 μ L of Triton X-100. Spectra were measured at 37 $^{\circ}$ C using a 450 nm excitation wavelength.

reported to increase under acidic conditions.³² Such channels are obviously well suited to accommodate bilayer translocation of motile hydrogen ions. Thus, the faster NO release can be attributed to increased donor degradation and not a compromised bilayer.

2.3.3. *Stability of NO-releasing liposomes over time*

The stability of the NO-releasing liposomes was evaluated in a series of solutions as a function of pH. For these studies, the NO remaining within liposomes prepared in PBS (pH 7.4), borate buffer (pH 9.0) or NaOH (pH >12) was monitored over time. As expected, liposomes synthesized and stored in NaOH were characterized as having larger NO payloads (0.23 μmol NO/mg) relative to those made (and stored) in PBS or borate buffer (Figure 2.4). Substantial NO loss occurred for systems synthesized in PBS/borate solutions due to poor *N*-diazeniumdiolate stability in the non-alkaline media. After 3 months of storage at 4 °C, the liposomes in PBS and borate buffer lost 99 and 65% of their total stored NO. Clearly, the stability of the NO donor is maximized under basic conditions.

2.3.4. *Cytotoxicity of DPTA/NO-encapsulated liposomes*

Cytotoxicity was assessed against human PANC-1 pancreatic cancer cells over 24 h to investigate the anticancer action of both free DPTA/NO and liposomal DPTA/NO (Figure 2.5). We hypothesized that cancer cell killing would be greater for liposomes containing larger payloads of NO. DPTA/NO-based liposomes were thus chosen for the cytotoxicity study over the SPER/NO system. The encapsulated NO donor reduced cell viability by 50% (the LD₅₀) at only 183 μM NO, whereas free DPTA/NO elicited cytotoxic effects (Appendix A) at much higher NO concentrations (2.4 mM). The increased cytotoxic effect elicited by liposomal DPTA/NO is greater because of the larger payload of NO that can be delivered, since less of the

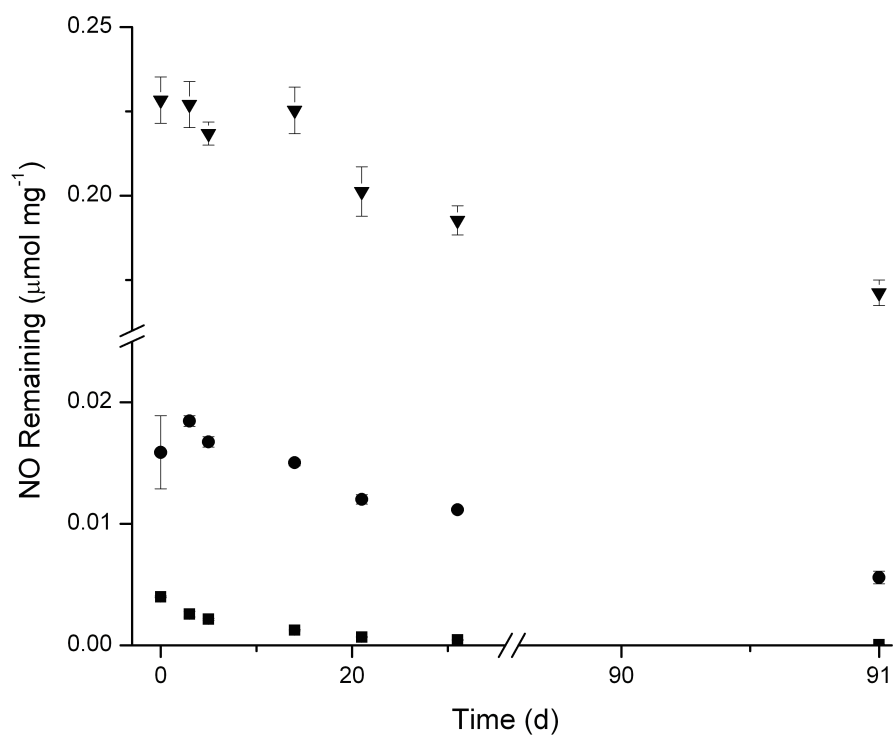


Figure 2.4. Comparison of NO remaining from SPER/NO-loaded liposomes. Liposomes made in (■) 50 mM PBS, (●) 50 mM borate buffer, (▼) and 50 mM NaOH. The amount of NO remaining within the liposomes was determined by injecting the liposomes into an acidic solution at discrete timepoints.

Table 2.3. Nitric oxide-release properties of liposomes in acetate buffer (pH = 5.4) at 37 °C.^a

NO donor	t_{1/2}^b (min)	[NO]_{max}^c (ppb/mg)	t_d^d (h)	[NO]_{total}^e (μmol/mg)
SPER/NO	3.9 ± 0.5	8154 ± 859	1.0 ± 0.1	0.29 ± 0.03
DPTA/NO:SPER/NO ^f	4.9 ± 0.7	5857 ± 990	1.3 ± 0.1	0.34 ± 0.08
DPTA/NO	5.4 ± 0.3	6389 ± 1360	1.3 ± 0.1	0.39 ± 0.09

^aError bars indicate standard deviation from n≥3 separate preparations. ^bHalf-life of NO release.

^cThe highest instantaneous amount of NO generated. ^dDuration of NO release. ^eLipid concentration was 23.3 ± 5.4 mg phospholipid per mL of aqueous phase. ^fMolar ratio of 50:50.

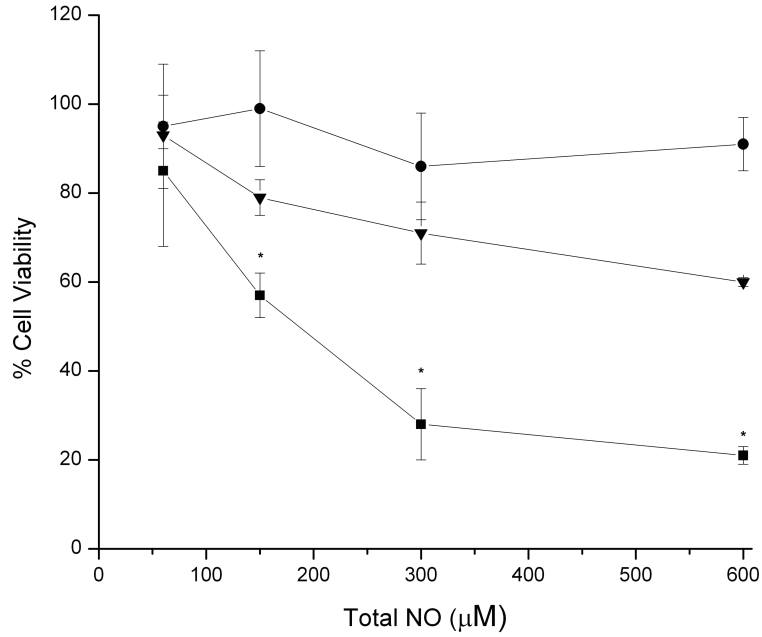


Figure 2.5. *In vitro* efficacy of liposomal and free DPTA/NO on human PANC-1 cells after 24 h incubation. Liposomal DPTA/NO (■), liposomal DPTA (▼), and free DPTA/NO donor (●). Error bars indicate standard deviation from $n \geq 3$ separate experiments. Asterisk denotes $p < 0.05$ between DPTA/NO liposomes and both the free donor and DPTA-containing liposomes.

total NO is released prior to reaching the cell. Furthermore, an increase in intracellular uptake of the NO donor afforded by the liposomes, relative to the unencapsulated donor, would potentially allow for a more efficacious delivery of NO into the cell. Such trends have been reported previously for other liposomally encapsulated chemotherapeutic drugs (e.g., gemcitabine).³³ Liposomes loaded with only DPTA (i.e., no NO release capabilities) were mildly cytotoxic at larger concentrations (>300 μ M) due to the anticancer properties of DPTA alone.³⁴ However, these systems still exhibited significantly lower anticancer action compared to their NO-releasing counterpart. The reduced dose of liposomally-derived NO required (0.23 mg liposomes) to induce cytotoxic effects to pancreatic cancer cells demonstrates their promising therapeutic potential over free NO donor systems that require mM concentrations.³⁵

2.4 Conclusions

The preparation of NO-releasing liposomes utilizing an alkaline interior aqueous phase enables the encapsulation of varying concentrations of NO with long shelf-lives (>3 mo). A preliminary investigation into the utility of these liposomal NO donors as anticancer agents demonstrates their therapeutic potential over small molecule NO donors. As the understanding of NO and its biological effects continues to expand, so does the need for diverse NO-releasing platforms that are robust, facilitate targeting, and possess tunable biological action. Nitric oxide-releasing liposomes represent a unique strategy for cancer treatment in particular due to their pH-triggered release. Varying the lipid bilayer content (e.g., phospholipid composition, charge) should further enhance the stability of this NO-delivery system and influence NO-release payloads. Future studies utilizing a more thermally stable lipid (e.g., 1,2-distearoyl-sn-glycero-3-phosphocholine), could potentially prolong the NO-release duration even further due to greater bilayer rigidity. Such experiments are currently underway in our laboratory.

REFERENCES

- (1) Thomas, D.D.; Ridnour, L.A.; Isenberg, J.S.; Flores-Santana, W.; Switzer, C.H.; Donzelli, S.; Hussain, P.; Vecoli, C.; Paolucci, N.; Ambs, S.; Colton, C.A.; Harris, C.C.; Roberts, D.D.; Wink, D.A. "The chemical biology of nitric oxide: Implications in cellular signaling." *Free Radical Biology and Medicine* **2008**, *45*, 18-31.
- (2) Moncada, S.; Palmer, R.M.J.; Higgs, E.A. "Nitric oxide: Physiology, pathophysiology, and pharmacology." *Pharmacological Reviews* **1991**, *43*, 109-142.
- (3) Gross, S.S.; Wolin, M.S. "Nitric oxide: Pathophysiological Mechanisms." *Annual Review of Physiology* **1995**, *57*, 737-769.
- (4) Rosselli, M.; Keller, P.J.; Dubey, R.K. "Role of nitric oxide in the biology, physiology and pathophysiology of reproduction." *Human Reproduction Update* **1998**, *4*, 3-24.
- (5) Radomski, M.W.; Palmer, R.; Moncada, S. "An L-arginine/nitric oxide pathway present in human platelets regulates aggregation." *Proceedings of the National Academy of Sciences* **1990**, *87*, 5193-5197.
- (6) Bogdan, C. "Nitric oxide and the immune response." *Nature Immunology* **2001**, *2*, 907-916.
- (7) Carpenter, A.W.; Schoenfisch, M.H. "Nitric oxide release: Part II. Therapeutic applications." *Chemical Society Reviews* **2012**, *41*, 3742-3752.
- (8) Sun, B.; Slomberg, D.L.; Chudasama, S.L.; Lu, Y.; Schoenfisch, M.H. "Nitric oxide-releasing dendrimers as antibacterial agents." *Biomacromolecules* **2012**, *13*, 3343-3354.
- (9) Huerta, S.; Chilka, S.; Bonavida, B. "Nitric oxide donors: novel cancer therapeutics." *International Journal of Oncology* **2008**, *33*, 909-927.
- (10) Hofseth, L.J.; Saito, S.; Hussain, S.P.; Espey, M.G.; Miranda, K.M.; Araki, Y.; Jhappan, C.; Higashimoto, Y.; He, P.; Linke, S.P.; Quezado, M.M.; Zurer, I.; Rotter, V.; Wink, D.A.; Appella, E.; Harris, C.C. "Nitric oxide-induced cellular stress and p53 activation in chronic inflammation." *Proceedings of the National Academy of Sciences* **2003**, *100*, 143-148.
- (11) Fridman, J.S.; Lowe, S.W. "Control of apoptosis by p53." *Oncogene*, **2003**, *22*, 9030-9040.
- (12) Hrabie, J.A.; Keefer, L.K. "Chemistry of the nitric-oxide releasing diazeniumdiolate ("Nitrosohydroxylamine") functional group and its oxygen-substituted derivatives." *Chemical Reviews* **2002**, *102*, 1135-1154.
- (13) Hrabie, J.A.; Klose, J.R.; Wink, D.A.; Keefer, L.K. "New nitric oxide-releasing zwitterions derived from polyamines." *Journal of Organic Chemistry* **1993**, *58*, 1472-1476.
- (14) Keefer, L.K. "Fifty years of diazeniumdiolate research. From laboratory to broad-spectrum biomedical advances." *ACS Chemical Biology* **2011**, *6*, 1147-1155.

- (15) Nichols, S.P.; Storm, W.L.; Koh, A.; Schoenfisch, M.H. "Local delivery of nitric oxide: Targeted delivery of therapeutics to bone and connective tissues." *Advanced Drug Delivery Reviews* **2012**, *64*, 1177-1188.
- (16) Riccio, D.A.; Schoenfisch, M.H.; "Nitric oxide release: Part I. Macromolecular scaffolds." *Chemical Society Reviews* **2012**, *41*, 3731-3741.
- (17) Quinn, J.F.; Whittaker, M.R.; Davis, T.P. "Delivering nitric oxide with nanoparticles." *Journal of Controlled Release* **2015**, *205*, 190-205.
- (18) Carpenter, A.W.; Worley, B.V.; Slomberg, D.L.; Schoenfisch, M.H. "Dual action antimicrobials: nitric oxide release from quaternary ammonium-functionalized silica nanoparticles." *Biomacromolecules* **2012**, *13*, 3334-3342.
- (19) Rothrock, A.R.; Donkers, R.L.; Schoenfisch, M.H. "Synthesis of nitric oxide-releasing gold nanoparticles." *Journal of the American Chemical Society* **2005**, *127*, 9362-9363.
- (20) Shamim, U.; Hanif, S.; Albanyan, A.; Beck, F.; Bao, B.; Wang, Z.; Banerjee, S.; Sarkar, F.H.; Mohammad, R.M.; Hadi, S.M.; Azmi, A.S. "Resveratrol-induced apoptosis is enhanced in low pH environments associated with cancer." *Journal of Cellular Physiology* **2012**, *227*, 1493-1500.
- (21) Torchilin, V.P. "Recent advances with liposomes as pharmaceutical carriers." *Nature Reviews Drug Discovery* **2005**, *4*, 145-160.
- (22) Tannock, I.F.; Rotin, D. "Acid pH in tumors and its potential for therapeutic exploitation." *Cancer Research* **1989**, *49*, 4373-4384.
- (23) Ostrowski, A.D.; Lin, B.F.; Tirrell, M.V.; Ford, P.C. "Liposome encapsulation of a photochemical NO precursor for controlled nitric oxide release and simultaneous fluorescence imaging." *Molecular Pharmaceutics* **2012**, *9*, 2950-2955.
- (24) Tai, L.-A.; Wang, Y.-C.; Yang, C.-S. "Heat-activated sustaining nitric oxide release from zwitterionic diazeniumdiolate loaded into thermo-sensitive liposomes." *Nitric Oxide* **2010**, *23*, 60-64.
- (25) Szoka, F. Jr.; Papahadjopoulos, D. "Procedure for preparation of liposomes with large internal aqueous space and high capture by reverse-phase evaporation." *Proceedings of the National Academy of Sciences* **1978**, *75*, 4194-4198.
- (26) Stewart, J. "Colorimetric determination of phospholipids with ammonium ferrothiocyanate." *Analytical Biochemistry* **1980**, *104*, 10-14.
- (27) Hetrick, E.M.; Schoenfisch, M.H. "Analytical chemistry of nitric oxide." *Annual Review of Analytical Chemistry* **2009**, *2*, 409-433.
- (28) Coneski, P.N.; Schoenfisch, M.H. "Nitric oxide release: Part III. Measurement and reporting" *Chemical Society Reviews* **2012**, *41*, 3753-3758.

- (29) Ganguly, S.; Bandyopadhyay, S.; Sarkar, A.; Chatterjee, M. "Development of a semi-automated colorimetric assay for screening of anti-leishmanial agents." *Journal of Microbiological Methods* **2006**, *66*, 79-86.
- (30) Fry, D.W.; White, J.C.; Goldman, I.D. "Rapid separation of low molecular weight solutes from liposomes without dilution." *Analytical Biochemistry* **1978**, *90*, 809-815.
- (31) Clement, N.R.; Gould, J.M. "Pyranine (8-hydroxy-1,3,6-pyrenetrisulfonate) as a probe of internal aqueous hydrogen ion concentration in phospholipid vesicles." *Biochemistry* **1981**, *20*, 1534-1538.
- (32) Kaufmann, K.; Silman, I. "The induction by protons of ion channels through lipid bilayer membranes." *Biophysical Chemistry* **1983**, *18*, 89-99.
- (33) Celia, C.; Calvagno, M.G.; Paolino, D.; Bulotta, S.; Ventura, C.A.; Russo, D.; Fresta, M. "Improved in vitro anti-tumoral activity, intracellular uptake and apoptotic induction of gemcitabine-loaded pegylated unilamellar liposomes." *Journal of Nanoscience and Nanotechnology* **2008**, *8*, 2102-2113.
- (34) Prakash, N.J.; Bowlin, T.L.; Davis, G.F.; Sunkara, P.S.; Sjoerdsma, A. "Antitumor activity of norspermidine, a structural homologue of the natural polyamine spermidine." *Anticancer Research* **1988**, *8*, 563-568.
- (35) Reiter, T.A.; Demple, B. "Carbon monoxide mediates protection against nitric oxide toxicity in HeLa cells." *Free Radical Biology and Medicine* **2005**, *39*, 1075-1088.

CHAPTER 3: CONTROLLED RELEASE OF NITRIC OXIDE FROM LIPOSOMES²

3.1 Introduction

The drug delivery field has demonstrated that the encapsulation of therapeutics (e.g., antifungals, biocides, chemotherapeutics, and virucides) within liposomes is an effective strategy for controlled delivery to select targets of interest.¹⁻⁴ Using liposomes as drug delivery vehicles affords many benefits, including reduced immune response, increased cellular uptake, and protection of drug payload from premature action or breakdown.⁵ Although liposomes passively localize themselves at the site of interest,⁵ post-delivery accumulation of the encapsulated therapeutic (e.g., cisplatin and doxorubicin) has been shown to negatively impact surrounding healthy tissue.⁶⁻⁷ The need to develop therapeutics with limited off-target cytotoxicity remains highly desirable.

Nitric oxide (NO) is an endogenously produced free radical involved in multiple physiological processes, including blood pressure regulation, the immune response to pathogens, neurotransmission, and cellular proliferation.⁸⁻¹¹ Unlike current chemotherapeutics, NO is rapidly converted to a harmless metabolite (i.e., nitrite) and cleared in biological media, mitigating the toxic accumulation common to most drugs. Based on NO's promise as a potential therapeutic, a significant body of research has focused on strategies to exogenously deliver NO using synthetic

² This chapter was adapted from an article that previously appeared in *ACS Biomaterials Science & Engineering*. The original citation is as follows: Suchyta, D.J.; Schoenfisch, M.H. "Controlled release of nitric oxide from liposomes" *ACS Biomaterials Science & Engineering* **2017**, *3*, 2136-2143.

NO donors, such as metal-NO complexes, *S*-nitrosothiols (RSNOs), and *N*-diazoniumdiolates.¹²⁻¹⁶ *N*-Diazoniumdiolates are a particularly attractive vehicle for NO storage and delivery because they undergo pH-dependent decomposition (faster release as the pH is lowered) to liberate NO (Appendix B). Furthermore, the breakdown and release of NO is a direct function of the molecular structure of the donor, enabling exquisite control over the rate of release.¹⁶ Structures bearing cationic primary amines can electrostatically stabilize their anionic diazoniumdiolate group, thus yielding longer NO-release half-lives. For example, spermine/NO (SPER/NO) exhibits a much longer half-life than proline/NO (PROLI/NO) at pH 7.4 ($t_{1/2}$ = 37 min and 2 s, respectively).¹⁷ This breakdown of *N*-diazoniumdiolates to NO can be used therapeutically by exploiting the microenvironment of certain disease sites (e.g., cancer, dental caries, and ulcerative colitis) that exhibit a lowered pH due to altered cellular metabolisms. In contrast to healthy tissue, where pH homeostasis is maintained near pH 7.4, these diseased tissues should promote more rapid NO release at the site of interest, thereby mitigating off-target cytotoxicity.¹⁸⁻²⁰

Others have previously demonstrated that liposomes can encapsulate NO donors in order to enhance delivery and prolong NO release.²¹⁻²⁴ In contrast to these studies that used gaseous NO and NO photodors, our lab has utilized encapsulated *N*-diazoniumdiolates to deliver NO. The liposomes exhibited enhanced NO donor stability (>3 mo shelf-life) along with greater *in vitro* cytotoxicity toward pancreatic cancer cells compared to the free, unencapsulated NO donor.²⁵ However, the kinetic tunability of this system was rather limited (i.e., controlled only by pH) with the relationship between liposomal characteristics (e.g., composition and size) and NO-release properties remaining unclear. As such, the focus of this research is developing strategies for altering the properties of NO release (e.g., half-life and total storage) by modifying the *N*-

diazoniumdiolate and phospholipid structures. The utility of these changes on protein surface adsorption in serum (important for determining scaffold clearance in the bloodstream) is also investigated, with attention to NO-release properties as a function of solution media.²⁶⁻²⁷

3.2 Experimental section

3.2.1. Materials

Dimyristoylphosphatidylcholine (DMPC), dipalmitoylphosphatidylcholine (DPPC), distearoylphosphatidylcholine (DSPC), dipalmitoylphosphatidylglycerol (DPPG), dipalmitoyltrimethylammoniumpropane chloride salt (DPTAP), dipalmitoylphosphatidylethanolamine-*N*-[methoxy(polyethyleneglycol)-2000] (DPPE-PEG2000), dipalmitoylphosphatidylethanolamine (DPPE), and distearoylphosphatidylethanolamine (DSPE) were purchased from Avanti Polar Lipids (Alabaster, AL). Cholesterol (Chol), *N*-propyl-1,3-propanediamine (PAPA), L-proline (PROLI), diethylamine (DEA), spermine (SPER), pyranine, coumarin, 5(6)-carboxyfluorescein, Dowex 1X2 chloride (200-400 mesh) anion exchange resin, hemoglobin from bovine, and fetal bovine serum (FBS) were obtained from Sigma (St. Louis, MO). Chloroform, anhydrous acetonitrile, sulfuric acid, diethyl ether, sodium hydroxide, and the Bradford assay kit were purchased from Fisher Scientific (Fair Lawn, NJ). The source of Sephadex G-25 was GE Healthcare (Pittsburgh, PA). Pure nitric oxide (NO) gas (99.5%) was obtained from Praxair (Sanford, NC). Nitrogen (N₂), argon (Ar), and nitric oxide (NO) calibration gas cylinders (26.80 ppm, balance N₂) were obtained from Airgas National Welders (Durham, NC). A Millipore Milli-Q UV Gradient A10 System (Bedford, MA) was used to purify distilled water to a resistivity of 18.2 MΩ·cm and a total organic content of ≤6 ppb. Canine blood was freshly collected into EDTA-coated

vacutainers by the Francis Owen Blood Lab (Carrboro, NC). Serum was isolated from the blood samples within 15 min of initial collection.

3.2.2. *Synthesis of N-diazeniumdiolates*

A previously reported method was used to synthesize the NO donors.¹⁷ Briefly, the precursor amine (i.e., PROLI, DEA, PAPA, or SPER) was dissolved in anhydrous acetonitrile at a concentration of 33.3 mg/mL. The solution was then purged with argon to 100 psi inside a stainless steel Parr bomb. Six sequential purges (three quick purges of 10 s each, followed by three slow purges of 10 min each) was used to remove residual oxygen. The solution was subsequently charged with 145 psi NO for 3 d. After 3 d, the solution was purged six times with argon to 100 psi to remove residual NO. The precipitated product was poured over a Hirsch funnel, washed twice with diethyl ether, and dried under vacuum overnight. The final NO-releasing product (i.e., PROLI/NO, DEA/NO, PAPA/NO, or SPER/NO) was stored at -20 °C until further use. Spectroscopic characterization was performed on the NO donors, including their decomposition products at pH 5.4 and 7.4 (Appendix B).

3.2.3. *Preparation of liposomes*

Liposomes were synthesized using a 1:1 molar ratio of lipid to Chol (49.5 μ mol lipid:49.5 μ mol Chol) following the report by Szoka and Papahadjopoulos.²⁸ Chloroform and diethyl ether (5 mL each) were used to dissolve the lipids in a round-bottomed flask under a N₂ atmosphere. The *N*-diazeniumdiolate donor (i.e., PROLI/NO, DEA/NO, PAPA/NO, or SPER/NO) was dissolved in 50 mM NaOH to make a 14 mM stock NO donor solution and subsequently injected (1.5 mL) into the flask, which was sonicated for 4 min at a temperature 5 °C higher than the transition temperature of the phospholipid. The organic phase was removed by rotoevaporation and the resulting liposomes incubated above their respective transition

temperature for 30 min. The unencapsulated donor was removed using four Sephadex G-25 spin columns packed in 10-mL syringes. The final volume of purified liposomes collected from the column was stored at 4 °C. Fluorophore-encapsulated liposomes were prepared in the same manner as NO-releasing liposomes.

3.2.4. Characterization of liposome size

Dynamic light scattering (DLS) measurements were performed to determine liposome size and polydispersity. The liposomes were diluted with water and their size characterized using a Zetasizer Nano (Malvern Instruments, UK). Transmission electron micrographs (TEM) were also collected to confirm liposome formation. Liposome samples for TEM analysis were prepared by diluting the stock solution with Milli-Q water (1:1 volumetric ratio) and casting the suspension onto Formvar-coated, square mesh copper TEM grids (Electron Microscopy Sciences, Hatfield, PA). The solvent was allowed to evaporate for 45 min prior to applying a negative-stain using 2% (w/v) uranyl acetate. A drop of the stain was left on the grid for 30 s after which the droplet was removed using filter paper. The sample was then allowed to dry for 5 min. The liposomes were imaged using a JEOL 100CX II transmission electron microscope at an accelerating voltage of 100 kV.

3.2.5. Nitric oxide release from liposomes

Nitric oxide totals and the overall release kinetics were evaluated using a Sievers chemiluminescence Nitric Oxide Analyzer (NOA; Boulder, CO).²⁹⁻³⁰ The instrument was calibrated using a NO zero filter (0 ppm NO) and a 26.80 ppm NO standard (balance N₂). An aliquot of the liposomes was injected into a 2:1 volumetric ratio of ethanol to 0.183 M sulfuric acid (30 mL total volume) at 37 °C to determine the NO donor encapsulation efficiency. The encapsulation efficiency, or the extent to which the NO donor is entrapped within the liposomal

aqueous core, was calculated by comparing the liposome NO payload to the amount of NO in the free donor solution used during preparation of the liposomes. Studies to evaluate NO-release kinetics were performed in 10 mM MES buffer (pH 5.4) and 10 mM PBS (pH 7.4) at 37 °C. The presented data and error are from at least 3 separate liposome preparations. Nitric oxide release was terminated when the NO concentration dropped below 10 ppb per 300 μ L liposomes.

3.2.6. *Turbidity assay*

Liposomes (30 μ L) were mixed with 600 μ L FBS and incubated at 37 °C with slight agitation. After 1 h, 100 μ L was removed, placed into a 96-well plate, and then the absorbance at 450 nm measured using a ThermoScientific Multiskan EX plate reader (Waltham, MA). The relative turbidity increase was compared against that of a control solution (30 μ L of 50 mM NaOH mixed with 600 μ L FBS). Of note, no further changes in turbidity were observed after 1 h incubation with FBS.

3.2.7. *Serum protein adsorption onto liposomes*

Quantification of proteins adsorbed onto the liposome surface was measured using the Bradford assay.³¹ Briefly, liposomes (20 μ L) were mixed with 400 μ L of a 10% (v/v in 10 mM PBS) FBS solution and incubated for 1 h at 37 °C with slight agitation. Afterwards, the liposomes were centrifuged (13,000 \times g for 3 min) and washed twice with 10 mM PBS. The resulting lipid pellet was then dissolved in 100 μ L of a 1:2 volumetric ratio of 10 mM PBS to ethanol. This dissolved pellet (30 μ L) was added to a 96-well plate and mixed with 300 μ L dye solution. After 10 min, the absorbance from the solution was measured at 595 nm. Bovine serum albumin standards (330 μ L total volume) were used to generate linear calibration curves.

3.2.8. *Nitric oxide release from liposomes in blood and serum*

Nitric oxide release from liposomes was measured in both animal blood and serum. Briefly, liposomes (30 μ L) were mixed with 600 μ L freshly-obtained citrated whole blood or serum (pre-incubated at 37 $^{\circ}$ C). The solution was stored in a 37 $^{\circ}$ C incubator for a pre-determined period of time, after which an 80 μ L aliquot was injected into a 2:1 volumetric ratio of ethanol to 0.183 M sulfuric acid (30 mL total volume) at 37 $^{\circ}$ C. The % NO remaining was determined by dividing the total NO released at each timepoint by the total NO released at the initial timepoint (\sim 10 s after mixing liposomes with blood/serum) and multiplying by 100.

3.3 Results and discussion

3.3.1. Nitric oxide donor structure

An important aspect in choosing an appropriate delivery system is the ability to easily modify drug-release kinetics. Altering the release rates of most liposome systems requires varying the lipid bilayer composition (e.g., cholesterol content, phospholipid property). Such an approach is not ideal since other aspects of the scaffold (i.e., hydrophobicity, aggregation, and the potential immune response) will be inevitably altered as well. One unique advantage of *N*-diazoniumdiolate NO donors is the ability to independently manipulate liposomal NO-release kinetics at the molecular level using discrete NO donors. In this study, four different NO donors (Appendix B) were encapsulated within liposomes composed of DPPC.

The size, polydispersity, and encapsulation efficiency (EE) of each NO donor-containing liposome was measured to determine how varying the NO donor affected the resulting liposome (Table 3.1). As expected, sizes of the liposomes remained consistent (\sim 200 nm) regardless of the encapsulated NO donor, likely the result of the donors' similar molecular weights. Low polydispersity index (PDI) values (\sim 0.2) indicated that the liposomes were monodisperse and did not form aggregates. Both the size and monodispersity of the PAPA/NO liposomes were

Table 3.1. Physicochemical properties of DPPC liposomes encapsulating various NO donors.

NO donor	Size^a (nm)	Polydispersity index	Encapsulation efficiency^b (%)
PROLI/NO	174 ± 18	0.166 ± 0.018	30.6 ± 1.9
DEA/NO	234 ± 20	0.185 ± 0.024	33.7 ± 4.2
PAPA/NO	203 ± 33	0.167 ± 0.070	33.4 ± 3.1
SPER/NO	248 ± 54	0.251 ± 0.020	38.3 ± 3.9

^aZ-average size measured using DLS. ^bRatio of μmol of NO inside liposomes to μmol used for synthesis multiplied by 100.

Table 3.2. Nitric oxide-release properties of DPPC liposomes as a function of NO donor in PBS (pH 7.4) at 37 °C.

NO donor	$t_{1/2}^a$ (h)	t_d^b (h)	[NO] _{total} ^c (μmol/mL)
PROLI/NO	0.16 ± 0.05	2.8 ± 0.1	5.10 ± 0.51
DEA/NO	0.31 ± 0.02	4.6 ± 2.3	9.16 ± 0.33
PAPA/NO	2.60 ± 0.40	43.4 ± 3.9	8.83 ± 0.64
SPER/NO	45.30 ± 4.60	168.2 ± 17.0	7.73 ± 0.71

^aHalf-life of NO release. ^bDuration of NO release until the measured NO reached 10 ppb per 300 μL of liposomes (three-times the detection limit of the instrument). ^cTotal amount of NO released normalized to the injected volume from the liposome stock solution. Respective pH 7.4 half-lives of free (i.e., unencapsulated) PROLI/NO, DEA/NO, PAPA/NO, SPER/NO at 37 °C : 2 s, 2 min, 15 min, and 37 min.

preserved even after a 3-month storage period at 4 °C (193 nm and 0.211, respectively). The average EE was approximately 35%, regardless of the NO donor, a value similar to reported values for other solutes encapsulated by reverse-phase evaporation methods.^{24,28} The slightly lower EE observed for PROLI/NO liposomes (30%) is attributed to the unavoidable loss of NO during preparation. Indeed, this NO donor has a short NO-release half-life in its free form ($t_{1/2}$ = 2 s).

3.3.2. Nitric oxide-release measurements

Nitric oxide release was measured in 10 mM PBS (pH 7.4, 37 °C) to evaluate the effect of NO donor identity on the liposomal NO-release rates under physiological conditions. Each of the encapsulated NO donors exhibited extended NO-release kinetics relative to the free NO donor (Table 3.2). For example, the half-life of SPER/NO increased from 37 min in its free form to ~2 d when encapsulated within the liposome. The prolonged NO release for all systems is attributed to the lipid bilayer providing a physical barrier against proton diffusion/exchange into or with the aqueous core.²⁴ As the molar amount of the lipid was held constant for all liposomal preparations, the total NO payload was normalized to the volume of each liposome system injected during analysis. Relative to the average NO payloads reported previously for NO-releasing liposomes (~6 μ mol NO/mL liposomes or ~0.25 μ mol NO/mg lipid),²⁴ we measured payloads that were significantly larger (~8-9 μ mol NO/mL) for DEA/NO, PAPA/NO, and SPER/NO containing liposomes. In contrast, the NO totals for the PROLI/NO liposomes were lower than other systems, which we again attributed to the rapid breakdown of the NO donor.

Nitric oxide release from the liposomes was also evaluated in 10 mM MES buffer (pH 5.4, 37 °C) to mimic NO release at more acidic disease sites (e.g., tumor microenvironments). A pH gradient is thus created across the lipid bilayer, causing a large influx of protons into the

liposomal core that reduced the internal pH.²⁴ As expected, the lower intraliposomal pH resulted in rapid *N*-diazoniumdiolate decomposition, large levels of NO, and reduced NO-release half-lives for the four liposome systems (Appendix B) relative to pH 7.4. The system with the most prolonged NO release (SPER/NO liposomes) exhibited a decrease in overall NO-release duration from >1 week (pH 7.4) to <48 h (pH 5.4). Dynamic light scattering measurements confirmed preservation of the liposome size (i.e., rupturing did not occur). Despite the significantly more rapid release, the NO-release kinetics were still tunable, even at low pH, with half-lives ranging from 4 min to 10 h depending on the *N*-diazoniumdiolate identity.

3.3.3. *Effects of lipid bilayer hydrophobicity and charge*

The liposome structure and NO-release rates of PAPA/NO liposomes were studied as a function of the lipid bilayer composition and associated properties (lipid structures are provided in Appendix B). PAPA/NO was selected as the model NO donor for this work due to its moderate NO-release characteristics under the tested conditions. By preparing different liposomes using electrically neutral lipids of varying alkyl chain length (DMPC, C₁₄, DPPC, C₁₆, and DSPC, C₁₈), liposome size and the NO-release characteristics could be studied as a function of bilayer hydrophobicity. In addition, parallel studies were performed using C₁₆ cationic (DPTAP) and anionic (DPPG) lipids to investigate the effects of charge on these same properties. Charged lipids are typically used to encapsulate larger macromolecules (e.g., DNA) more effectively or to localize the vesicle at an area of interest due to coulombic attraction.³²⁻³³ As the *N*-diazoniumdiolate NO donors are anionic, studying coulombic interactions using charged lipids, such as DPPG (negative) and DPTAP (positive), may elucidate unique effects on both EE and NO-release properties (i.e., NO payloads and release kinetics).

Table 3.3. Physicochemical properties of PAPA/NO liposomes as a function of bilayer composition.

Lipid^a	Size^b (nm)	Polydispersity index	Encapsulation efficiency^c (%)
DMPC (C ₁₄)	236 ± 44	0.215 ± 0.050	30.3 ± 1.5
DPPC (C ₁₆)	203 ± 33	0.167 ± 0.070	33.4 ± 3.1
DSPC (C ₁₈)	340 ± 77	0.328 ± 0.080	32.2 ± 2.7
DPPG (- C ₁₆)	161 ± 11	0.203 ± 0.030	22.0 ± 3.2
DPTAP (+ C ₁₆)	446 ± 63	0.497 ± 0.120	29.4 ± 0.6

^aCharge and alkyl chain length of the lipid is denoted in parentheses. ^bZ-average size measured using DLS. ^cRatio of the μmol of NO inside the liposomes to the μmol used for the synthesis, multiplied by 100.

Varying the phospholipid's carbon chain length caused only slight deviations in the liposome size for the longest chain length (C_{18}), as indicated by DLS (Table 3.3) and TEM analysis (Appendix B). Liposomes made from DMPC (C_{14}) and DPPC (C_{16}) remained similar in size (~200 nm) with comparable PDI and EE values (~30%). In contrast, liposomes prepared using DSPC (C_{18}) were significantly larger (340 nm) and more polydisperse, likely due to the longer alkyl chains disrupting bilayer formation.³⁴ Anionic DPPG liposomes exhibited size and monodispersity similar to that of neutral DPPC liposomes (Table 3.3 and Appendix B), but demonstrated an 11% decrease in EE. We hypothesize that the repulsive interactions between the negatively charged phospholipid and anionic *N*-diazoniumdiolate prevented efficient encapsulation within the liposomal core. The effects of coulombic charge were probed further by comparing the EE values of DPPC and DPPG liposomes encapsulating either neutral (coumarin) or negatively charged (carboxyfluorescein) fluorophores. While similar coumarin EE values were observed for both liposome systems, neutral DPPC liposomes exhibited greater encapsulation of carboxyfluorescein relative to anionic DPPG (Appendix B). Therefore, charge interactions between the encapsulated molecule and the phospholipid may significantly affect the efficiency of drug encapsulation.

Liposomes prepared using cationic DPTAP lipids had comparable EE values to the neutral liposomes. However, DLS measurements revealed substantially larger and more polydisperse sizes relative to liposomes prepared using the other lipids (Table 3.3). Large PDI values have been previously reported for liposomes synthesized utilizing TAP-based lipids in high ionic strength solutions as a result of aggregation.³⁵⁻³⁷ Indeed, we found that we were able to obtain better size (308 nm) and PDI values (0.316) after preparing DPTAP liposome solutions of a lower ionic strength (1 mM), corroborating the correlation between ionic strength and vesicle

aggregation. As an alternative to changing the ionic strength, DPPC was employed as a co-lipid for DPTAP liposome preparation. Positively charged liposomes with a 50:50 DPPC:DPTAP molar ratio were characterized as having similar size, PDI, and EE (227 nm, 0.168, and 31%, respectively) compared to pure DPPC liposomes. By utilizing this method, cationic liposomes with sizes and PDI values mirroring those of neutral and anionic liposomal systems were readily achieved.

3.3.4. *Bilayer properties and NO release*

Nitric oxide-release properties of the liposome systems were determined at pH 7.4 and 37 °C (Table 3.4). With the exception of the liposomes composed of negatively charged DPPG lipids, each liposome system studied exhibited similar NO payloads (~8.5 $\mu\text{mol/mL}$). Although the repulsive ionic forces lowered the NO totals of the DPPG liposomes, the release kinetics remained similar to that from neutral liposomes, indicating that bilayer water permeability was not appreciably influenced by the bilayer's negative charge. Conversely, aggregation of the positively charged DPTAP liposomes may likely have caused a greater proton influx to the liposome center with concomitantly more rapid NO release (i.e., shorter half-life) compared to the neutral liposome systems. To rule out the influence of electrostatically surface-bound NO donor on rapid NO release, DPTAP liposomes were incubated with an anion exchange resin. After filtering the liposomes from the resin, the measured NO-release kinetics were nearly identical to the liposomes prior to resin incubation, suggesting that DPTAP bilayer defects represent the only factor impacting the rapid NO release.

We initially hypothesized that the liposome NO-release kinetics would be prolonged as the hydrophobicity (i.e., carbon chain length) of the phospholipid was increased. While the C₁₈-containing DSPC liposomes exhibited significantly longer NO-release kinetics, the DMPC and

Table 3.4. Nitric oxide-release properties of PAPA/NO liposomes as a function of bilayer hydrophobicity and charge in PBS (pH 7.4) at 37 °C.

Lipid	$t_{1/2}^a$ (h)	t_d^b (h)	[NO]_{total}^c (μmol/mL)
DMPC (C ₁₄)	2.6 ± 0.5	42.9 ± 5.1	8.26 ± 0.29
DPPC (C ₁₆)	2.6 ± 0.4	43.4 ± 3.9	8.83 ± 0.64
DSPC (C ₁₈)	16.7 ± 1.2	85.6 ± 7.6	9.00 ± 0.74
DPPG (- C ₁₆)	2.6 ± 1.0	38.1 ± 1.8	6.33 ± 1.17
DPTAP (+ C ₁₆)	0.9 ± 0.4	18.4 ± 1.9	8.63 ± 0.43

^aHalf-life of NO release. ^bDuration of NO release until the measured NO reached 10 ppb per 300 μL of liposomes (three-times the detection limit of the instrument). ^cTotal amount of NO released normalized to the injected volume from the liposome stock solution.

DPPC systems demonstrated similar NO-release half-lives. As such, it seemed unlikely that the extended NO-release kinetics observed for the DSPC liposomes was a result of greater alkyl character or hydrophobicity. Further, differential release kinetics due to varying transition phase temperatures between the phospholipids should not occur as cholesterol was included in all liposome formulations, which homogenizes the bilayer and attenuates the effects of temperature on ordering of the lipid phase.³⁸

In lieu of hydrophobicity alone, the NO-release kinetics proved dependent on the compactness of the lipid chains upon liposome formation. Indeed, tighter packing of the lipid chains has been shown to occur as the headgroup surface area of the lipid decreases, resulting in reduced water permeability of the lipid bilayer.³⁹ Given the area per lipid headgroup being nearly identical for DMPC and DPPC ($\sim 0.655 \text{ nm}^2$) and distinct from DSPC ($\sim 0.430 \text{ nm}^2$),⁴⁰⁻⁴¹ the tighter lipid packing for the DSPC liposomes would slow the decrease in intraliposomal pH and *N*-diazeniumdiolate NO donor decomposition to NO.

Proton permeation into the liposome core was characterized by examining intraliposomal pH changes using a fluorescent dye. Pyranine ($10 \mu\text{M}$), a bilayer-impermeable pH-sensitive dye, was encapsulated within the liposomes to probe internal pH changes over time. Under basic conditions, pyranine produces a strong fluorescent signal ($\lambda = 520 \text{ nm}$) that reduces in intensity upon becoming protonated (i.e., as pH decreases).⁴² After immersion into pH 7.4 buffer, the fluorescence from DMPC and DPPC liposomes would be expected to decrease at similar rates over time, whereas that from the DSPC liposomes would be more gradual due to the restricted water permeability. As shown in Figure 3.1, this behavior was followed exactly. Over 24 h, the fluorescence measured from DSPC liposomes approached that from the DMPC and DPPC vesicles. The smaller initial change in intraliposomal pH combined with the gradual fluorescence

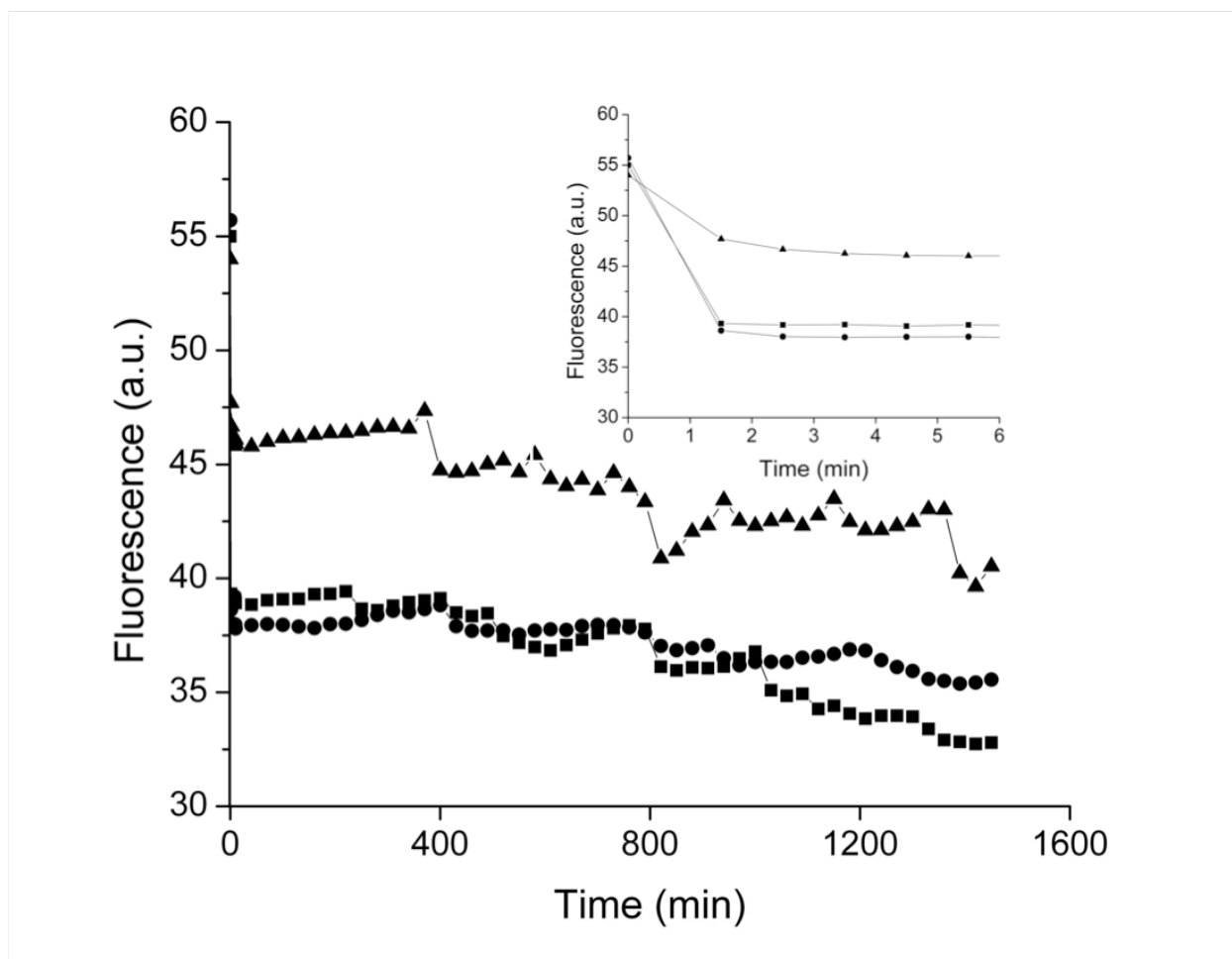


Figure 3.1. Fluorescence emission at 520 nm from pyranine-encapsulated (■) DMPC, (●) DPPC, and (▲) DSPC liposomes diluted 100-fold in 10 mM PBS (pH 7.4, 37 °C) as a function of time. The spectra were collected using a 450 nm excitation wavelength. Inset depicts fluorescence from the first 5 min of data collection.

drop over time for DSPC liposomes clearly confirms the influence of headgroup-mediated water/proton permeation on NO release. Of note, DLS measurements confirmed typical size values, indicating that bursting of the liposomes did not occur during the experiment.

As shown in Figure 3.2, lipids with similar packing (i.e., headgroup surface area) exhibited nearly identical water/proton permeation with similar NO-release kinetics regardless of charge or headgroup moiety.³⁹ These results explain why the anionic (and lower EE) DPPG liposomes maintain identical NO-release properties as neutral DPPC liposomes. A range of NO-release kinetics is therefore possible by varying the lipid bilayer composition (both partially or completely). For example, we used a 10:90 DPPE:DPPC molar mixture to produce PAPA/NO liposomes with intermediate NO-release half-lives ($t_{1/2} = 3.7$ h) relative to analogous single-lipid systems (DPPC $t_{1/2} = 2.5$ h; DPPE $t_{1/2} = 6.6$ h). Identical trends in NO release were observed at pH 5.4 (Appendix B), indicating that the bilayer composition-mediated control over NO release was maintained at lower pH as well.

3.3.5. Nitric oxide-release kinetics in biological media

Bilayer composition has been shown to influence the *in vivo* fate of liposomes.⁴⁶ For example, cationic liposomes are efficiently uptaken or internalized by cells, which is attributed to the electrostatic interactions with negatively charged cell membranes.⁴⁷ Charged liposomes also promote protein binding and opsonization, facilitating rapid clearance from the bloodstream.⁴⁸ We thus investigated if the liposomal surface properties (e.g., charge and PEGylation) affected the NO-release kinetics in biological fluids where protein adsorption may occur. DPPC (neutral), DPPG (negative), 50:50 DPTAP:DPPC (positive), and 10:90 DPPE-PEG/DPPC (PEGylated) liposomes were selected due to their similar NO release ($t_{1/2} \sim 2.5$ h) and long-term structural stability (Appendix B).

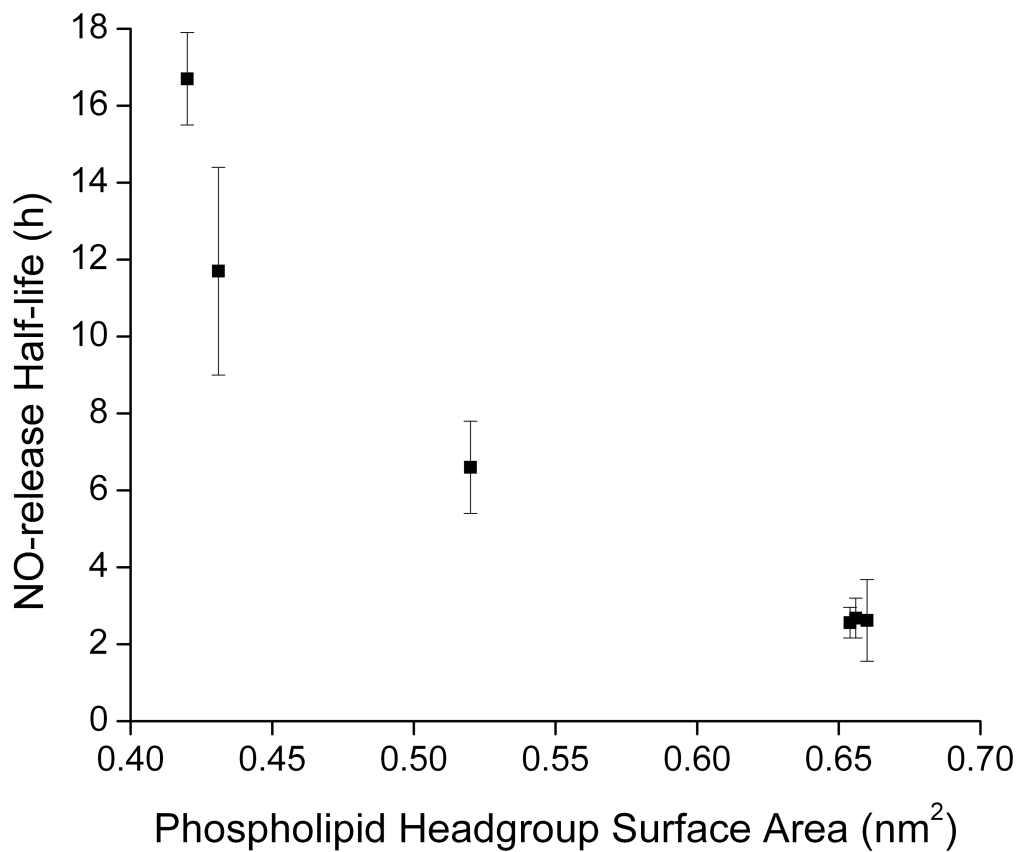


Figure 3.2. Relationship between the liposomal NO-release half-life and phospholipid headgroup surface area using PAPA/NO-encapsulated liposomes. Each point represents a different phospholipid (see Materials section for list of lipids).^{40-41,43-45}

NO-release kinetics were first measured in serum to determine if permanent or transient defects form in the liposome bilayer upon protein fouling, perhaps altering the NO release. Surprisingly, the NO release did not change appreciably (Figure 3.3a). Indeed, the liposomes exhibited similar half-lives ($t_{1/2} \sim 2.5$ h) to those measured in PBS, which agrees with the minimal protein adsorption that had occurred on the liposome surface in serum (Appendix B).⁴⁹⁻⁵²

While measuring NO release in serum elucidated the effects of proteins on liposomal NO-release kinetics, serum lacks a number of complex cellular components and molecules (e.g., hemoglobin) that are capable of scavenging NO. Nevertheless, nearly analogous NO release was measured in whole blood between the different liposome compositions (Figure 3.3b). Even the PEG-stabilized liposomes exhibited only slight initial differences in NO-release rates. These results indicate that the surface properties of PAPA/NO-containing liposomes (e.g., charge) can be controlled independently of NO-release kinetics in blood, to achieve potential targeting and/or adjust bloodstream clearance.

A notable decrease in the NO-release half-life in blood was observed relative to PBS and serum. For example, neutral DPPC PAPA/NO liposomes having similar PBS and serum NO release ($t_{1/2} = 2.6 \pm 0.4$ and 2.9 ± 1.0 h, respectively), exhibited 60% faster NO release ($t_{1/2} = 1.0 \pm 0.2$ h) in whole blood (Figure 3.4). We hypothesize that these results are caused by the high concentration of NO scavengers in blood.⁵³ At concentrations from 129–177 mg/mL (12.9–17.7 g/dL) in humans, hemoglobin is among the most active NO scavengers in the bloodstream due to iron-NO radical complexation.⁵³⁻⁵⁸ As such, scavenging would lead to an increase in the measured real time NO-release kinetics due to the consumption of detectable NO. To explore this, NO release from neutral DPPC PAPA/NO liposomes was measured in 10 mM PBS (pH 7.4,

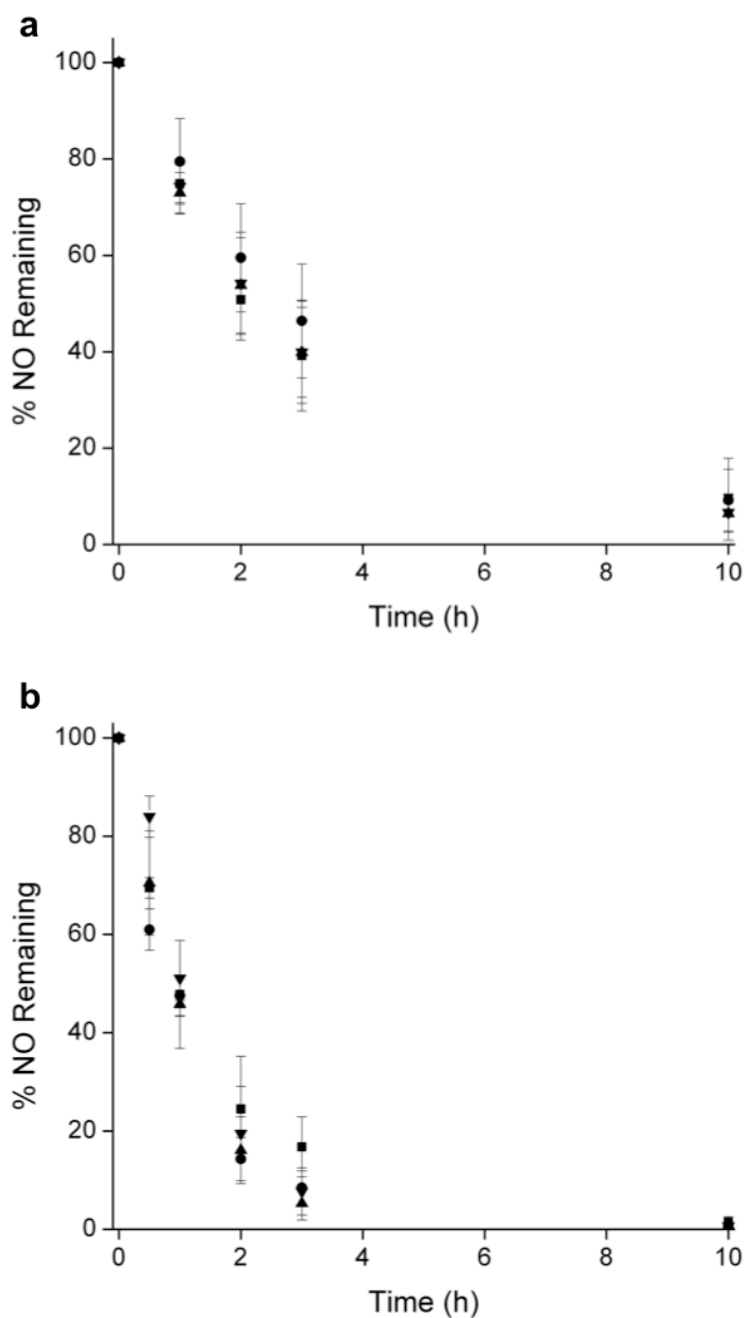


Figure 3.3. Nitric oxide release in (a) serum and (b) blood from (■) neutral DPPC, (▲) anionic DPPG, (●) cationic DPTAP, and (▼) PEGylated PAPA/NO liposomes. The amount of NO remaining within the liposomes was determined by injecting the liposomes into an acidic solution at discrete timepoints.

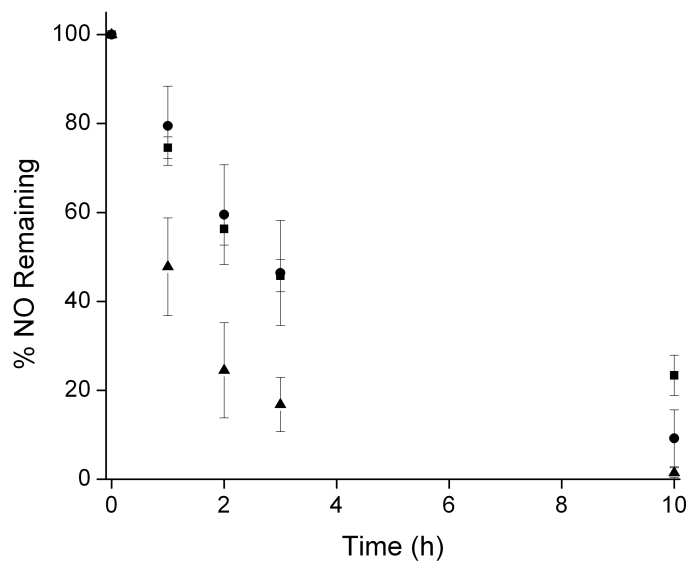


Figure 3.4. Neutral DPPC PAPA/NO liposome NO-release kinetics in (■) PBS, (●) serum, and (▲) blood. Statistical analysis yielded $p < 0.02$ between all PBS and blood values. The amount of NO remaining within the liposomes was determined by injecting the liposomes into an acidic solution at discrete timepoints.

37 °C) containing 157 mg/mL hemoglobin (Appendix B). The measured NO-release half-life indeed decreased ($t_{1/2} = 0.5$ h) relative to in pure PBS ($t_{1/2} = 2.6$ h), supporting blood hemoglobin being at least partially responsible for the observed differences in the NO-release kinetics for blood versus PBS/serum. The disparity between blood and PBS containing hemoglobin is likely due to compartmentalization of hemoglobin within erythrocytes (not free, as in the PBS solution), leading to less overall NO scavenging and longer measured NO-release durations.⁵⁴ Of note, negligible hemolytic activity of the NO-releasing liposome systems (Appendix B) indicates that the liposomes do not enhance liberation of intracellular hemoglobin.

3.4 Conclusions

Herein, the ability to precisely control NO-release half-lives was demonstrated by selection of an appropriate NO donor and varying the composition of the lipid bilayer. We found that the lipid headgroup surface area was the defining factor that controlled NO-release kinetics due to the dependence of bilayer proton permeability on lipid packing density. Liposomes prepared using different ionic charges and PEG-modified lipids exhibited low protein adsorption (≤ 5 g protein/mol lipid) and similar NO release in PBS and serum, regardless of the lipid identity. However, the overall NO-release flux in whole blood compared to PBS and serum was less, and thus the NO-release kinetics appeared shorter. These results were attributed to the large concentrations of hemoglobin in blood, a known NO scavenger. Our study may provide guidance for the development of other macromolecular scaffolds with respect to how charge may affect protein adsorption and the influence of complex cellular components of blood on *in vivo* NO-release kinetics.

REFERENCES

- (1) Lopez-Berestein, G. "Liposomes as carriers of antifungal drugs." *Annals of the New York Academy of Sciences* **1988**, *544*, 590-597.
- (2) Jones, M.N. "Use of liposomes to deliver bactericides to bacterial biofilms." *Methods in Enzymology* **2005**, *391*, 211-228.
- (3) Lammers, T.; Kiessling, F.; Hennink, W.E.; Storm, G. "Drug targeting to tumors: Principles, pitfalls, and (pre-) clinical progress." *Journal of Controlled Release* **2012**, *161*, 175-187.
- (4) Wutzler, P.; Sauerbrei, A.; Klöcking, R.; Brögman, B.; Reimer, K. "Virucidal activity and cytotoxicity of the liposomal formulation of povidone-iodine." *Antiviral Research* **2002**, *54*, 89-97.
- (5) Torchilin, V.P. "Recent advances with liposomes as pharmaceutical carriers." *Nature Reviews Drug Discovery* **2005**, *4*, 145-160.
- (6) De Angelis, A.; Urbanek, K.; Cappetta, D.; Piegari, E.; Ciuffreda, L.; Rivellino, A.; Russo, R.; Esposito, G.; Rossi, F.; Berrino, L. "Doxorubicin cardiotoxicity and target cells: A broader perspective." *Cardio-Oncology* **2016**, *2*, 1-8.
- (7) Galluzzi, L.; Vitale, I.; Michels, J.; Brenner, C.; Szabadkai, G.; Harel-Bellan, A.; Castedo, M.; Kroemer, G. "Systems biology of cisplatin resistance: Past, present, and future." *Cell Death & Disease* **2014**, *5*, 1-18.
- (8) Moncada, S.; Palmer, R.; Higgs, E. "Nitric oxide: Physiology, pathophysiology, and pharmacology." *Pharmacological Reviews* **1991**, *43*, 109-142.
- (9) Thomas, D.D.; Ridnour, L.A.; Isenberg, J.S.; Flores-Santana, W.; Switzer, C.H.; Donzelli, S.; Hussain, P.; Vecoli, C.; Paolocci, N.; Ambs, S.; Colton, C.A.; Harris, C.C.; Roberts, D.D.; Wink, D.A. "The chemical biology of nitric oxide: Implications in cellular signaling." *Free Radical Biology & Medicine* **2008**, *45*, 18-31.
- (10) Gross, S.S.; Wolin, M.S.; "Nitric oxide: Pathophysiological mechanisms." *Annual Review of Physiology* **1995**, *57*, 737-769.
- (11) Rosselli, M.; Keller, P.J.; Dubey, R.K. "Role of nitric oxide in the biology, physiology, and pathophysiology of reproduction." *Human Reproduction Update* **1998**, *4*, 3-24.
- (12) Carpenter, A.W.; Schoenfisch, M.H. "Nitric oxide release: part II. Therapeutic applications." *Chemical Society Reviews* **2012**, *41*, 3742-3752.
- (13) Nichols, S.P.; Storm, W.L.; Koh, A.; Schoenfisch, M.H. "Local delivery of nitric oxide: targeted delivery of therapeutics to bone and connective tissues." *Advanced Drug Delivery Reviews* **2012**, *64*, 1177-1188.
- (14) Huerta, S.; Chilka, S.; Bonavida, B. "Nitric oxide donors: novel cancer therapeutic (review)." *International Journal of Oncology* **2008**, *33*, 909-927.

- (15) Wang, P.G.; Xian, M.; Tang, X.; Wu, X.; Wen, Z.; Cai, T.; Janczuk, A.J. "Nitric oxide donors: Chemical activities and biological applications." *Chemical Reviews* **2002**, *102*, 1091-1134.
- (16) Hrabie, J.A.; Keefer, L.K. "Chemistry of the nitric oxide-releasing diazeniumdiolate ("nitrosohydroxylamine") functional group and its oxygen-substituted derivatives." *Chemical Reviews* **2002**, *102*, 1135-1154.
- (17) Hrabie, J.A.; Klose, J.R.; Wink, D.A.; Keefer, L.K. "New nitric oxide-releasing zwitterions derived from polyamines." *Journal of Organic Chemistry* **1993**, *58*, 1472-1476.
- (18) Tannock, I.F.; Rotin, D. "Acid pH in tumors and its potential for therapeutic exploitation." *Cancer Research* **1989**, *49*, 4373-4384.
- (19) Loesche, W.J. "Role of *streptococcus mutans* in human dental decay." *Microbiological Reviews* **1986**, *50*, 353-380.
- (20) Fallingborg, J.; Christensen, A.; Jacobsen, B.; Rasmussen, S. "Very low intraluminal colonic pH in patients with active ulcerative colitis." *Digestive Diseases and Sciences* **1993**, *38*, 1989-1993.
- (21) Ostrowski, A.D.; Lin, B.F.; Tirrell, M.V.; Ford, P.C. "Liposome encapsulation of a photochemical NO precursor for controlled nitric oxide release and simultaneous fluorescence imaging." *Molecular Pharmaceutics* **2012**, *9*, 2950-2955.
- (22) Giancane, G.; Valli, L.; Sortino, S. "Dual-function multilayers for the photodelivery of nitric oxide and singlet oxygen." *ChemPhysChem* **2009**, *10*, 3077-3082.
- (23) Huang, S.; Kee, P.H.; Kim, H.; Moody, M.R.; Chrzanowski, S.M.; MacDonald, R.C.; McPherson, D.D. "Nitric oxide loaded echogenic liposomes for nitric oxide delivery and inhibition of intimal hyperplasia." *Journal of the American College of Cardiology* **2009**, *54*, 652-659.
- (24) Klegerman, M.E.; Wassler, M.; Huang, S.; Zou, Y.; Kim, H.; Shelat, H.S.; Holland, C.K.; Geng, Y.; McPherson, D.D. "Liposomal modular complexes for simultaneous targeted delivery of bioactive gases and therapeutics." *Journal of Controlled Release* **2010**, *142*, 326-331.
- (25) Suchyta, D.J.; Schoenfisch, M.H. "Encapsulation of *N*-diazeniumdiolates within liposomes for enhanced nitric oxide donor stability and delivery." *Molecular Pharmaceutics* **2015**, *12*, 3569-3574.
- (26) Mahon, E.; Salvati, A.; Bombelli, F.B.; Lynch, I.; Dawson, K.A. "Designing the nanoparticle-biomolecule interface for "targeting and therapeutic delivery"." *Journal of Controlled Release* **2012**, *161*, 164-174.
- (27) Göppert, T.M.; Müller, R.H. "Adsorption kinetics of plasma proteins on solid lipid nanoparticles for drug targeting." *International Journal of Pharmaceutics* **2005**, *302*, 172-186.

- (28) Szoka, F. Jr.; Papahadjopoulos, D. "Procedure for preparation of liposomes with large internal aqueous space and high capture by reverse-phase evaporation." *Proceedings of the National Academy of Sciences* **1978**, *75*, 4194-4198.
- (29) Soto, R.J.; Yang, L.; Schoenfish, M.H. "Functionalized mesoporous silica via an aminosilane surfactant ion exchange reaction: Controlled scaffold design and nitric oxide release." *ACS Applied Materials & Interfaces* **2016**, *8*, 2220-2231.
- (30) Worley, B.V.; Schilly, K.M.; Schoenfish, M.H. "Anti-biofilm efficacy of dual-action nitric oxide-releasing alkyl chain modified poly(amidoamine) dendrimers." *Molecular Pharmaceutics* **2015**, *12*, 1573-1583.
- (31) Bradford, M.M. "A rapid and sensitive method for the quantitation of microgram quantities of protein utilizing the principle of protein-dye binding." *Analytical Biochemistry* **1976**, *72*, 248-254.
- (32) Felgner, P.L.; Gadek, T.R.; Holm, M.; Roman, R.; Chan, H.W.; Wenz, M.; Northrop, J.P.; Ringold, G.M.; Danielsen, M. "Lipofection: A highly efficient, lipid-mediated DNA-transfection procedure." *Proceedings of the National Academy of Sciences* **1987**, *84*, 7413-7417.
- (33) Campbell, R.B.; Fukumura, D.; Brown, E.B. "Cationic charge determines the distribution of liposomes between the vascular and extravascular compartments of tumors." *Cancer Research* **2002**, *62*, 6831-6836.
- (34) Nyren-Erickson, E.K.; Haldar, M.K.; Totzauer, J.R.; Ceglowski, R.; Patel, D.S.; Friesner, D.L.; Srivastava, D.K.; Mallik, S. "Glycosaminoglycan-mediated selective changes in the aggregation states, zeta potentials, and intrinsic stability of liposomes." *Langmuir* **2012**, *28*, 16115-16125.
- (35) Wieber, A.; Selzer, T.; Kreuter, J. "Physico-chemical characterisation of cationic DOTAP liposomes as drug delivery system for a hydrophilic decapeptide before and after freeze-drying." *European Journal of Pharmaceutics and Biopharmaceutics* **2012**, *80*, 358-367.
- (36) Tavakoli, S.; Tamaddon, A.; Golkar, N.; Samani, S. "Microencapsulation of (deoxythymidine)₂₀-DOTAP complexes in stealth liposomes optimized by Taguchi design." *Journal of Liposome Research* **2015**, *25*, 67-77.
- (37) Wasan, E.K.; Harvie, P.; Edwards, K.; Karlsson, G.; Bally, M.B. "A multi-step lipid mixing assay to model structural changes in cationic lipoplexes used for in vitro transfection." *Biochimica et Biophysica Acta*, **1999**, *1461*, 27-46.
- (38) Redondo-Morata, L.; Giannotti, M.L.; Sanz, F. "Influence of cholesterol on the phase transition of lipid bilayers: A temperature-controlled force spectroscopy study." *Langmuir* **2012**, *28*, 12851-12860.
- (39) Mathai, J.C.; Tristram-Nagle, S.; Nagle, J.F.; Zeidel, M.L. "Structural determinants of water permeability through the lipid membrane." *Journal of General Physiology* **2008**, *131*, 69-76.

- (40) Magarkar, A.; Dhawan, V.; Kallinteri, P.; Viitala, T.; Elmowafy, M.; Róg, T.; Bunker, A. "Cholesterol level affects surface charge of lipid membranes in saline solution." *Scientific Reports* **2014**, *21*, 5005.
- (41) Kupiainen, M.; Falck, E.; Ollila, S.; Niemelä, P.; Gurtovenko, A. "Free volume properties of sphingomyelin, DMPC, DPPC, and PLPC bilayers." *Journal of Computational and Theoretical Nanoscience* **2005**, *2*, 401-413.
- (42) Clement, N.R.; Gould, J.M. "Pyranine (8-hydroxy-1,3,6-pyrenetrisulfonate) as a probe of internal aqueous hydrogen ion concentration in phospholipid vesicles." *Biochemistry* **1981**, *20*, 1534-1538.
- (43) Bensikaddour, H.; Snoussi, K.; Lins, L.; Bambeke, F.; Tulkens, P.M.; Brassaru, R.; Goormaghtigh, E.; Mingeot-Leclercq, M. "Interaction of ciprofloxacin with DPPC and DPPG: Fluorescence anisotropy, ATR-FTIR and ³¹P NMR spectroscopies and conformational analysis." *Biochimica et Biophysica Acta* **2008**, *1778*, 2535-2543.
- (44) Leekumjorn, S.; Sum, A.K. "Molecular simulation study of structural and dynamic properties of mixed DPPC/DPPE bilayers." *Biophysical Journal* **2006**, *90*, 3951-3965.
- (45) Kuhl, T.L.; Majewski, J.; Wong, J.Y.; Steinberg, S.; Leckband, D.E.; Israelachvili, J.N.; Smith, G.S. "A neutron reflectivity study of polymer-modified phospholipid monolayers at the solid-solution interface: Polyethylene glycol-lipids on the silane-modified substrates." *Biophysical Journal* **1998**, *75*, 2352-2362.
- (46) Pattni, B.S.; Chupin, V.V.; Torchilin, V.P. "New developments in liposomal drug delivery." *Chemical Reviews* **2015**, *115*, 10938-10966.
- (47) Campbell, R.B.; Fukumura, D.; Brown, E.B.; Mazzola, L.M.; Izumi, Y.; Jain, R.K.; Torchilin, V.P.; Munn, L.L. "Cationic charge determines the distribution of liposomes between the vascular and extravascular compartments of tumors." *Cancer Research* **2002**, *62*, 6831-6836.
- (48) Gregoriadis, G. "Overview of liposomes." *Journal of Antimicrobial Chemotherapy* **1991**, *28*, 39-48.
- (49) Oku, N.; Tokudome, Y.; Namba, Y.; Saito, N.; Endo, M.; Hasegawa, Y.; Kawai, M.; Tsukada, H.; Okada, S. "Effect of serum protein binding on real-time trafficking of liposomes with different charges analyzed by positron emission tomography." *Biochimica et Biophysica Acta* **1996**, *1280*, 149-154.
- (50) Price, M.E.; Cornelius, R.M.; Brash, J.L. "Protein adsorption to polyethylene glycol modified liposomes from fibrinogen solution and from plasma." *Biochimica et Biophysica Acta* **2001**, *1512*, 191-205.
- (51) Kuznetsova, R.R.; Vodovozova, E.L. "Differential binding of plasma proteins by liposomes loaded with lipophilic prodrugs of methotrexate and melphalan in the bilayer." *Biochemistry (Moscow)* **2014**, *79*, 797-804.

- (52) Chonn, A.; Semple, S.C.; Cullis, P.R. "Association of blood proteins with large unilamellar liposomes *in vivo*." *Journal of Biological Chemistry* **1992**, *267*, 18759-18765.
- (53) Butler, A.R.; Megson, I.L.; Wright, P.G. "Diffusion of nitric oxide and scavenging by blood in the vasculature." *Biochimica et Biophysica Acta* **1998**, *1425*, 168-176.
- (54) Azarov, I.; Huang, K.T.; Basu, S.; Gladwin, M.T.; Hogg, N.; Kim-Shapiro, D.B. "Nitric oxide scavenging by red blood cells as a function of hematocrit and oxygenation." *Journal of Biological Chemistry* **2005**, *280*, 39024-39032.
- (55) Kim-Shapiro, D.B.; Schechter, A.N.; Gladwin, M.T. "Unraveling the reactions of nitric oxide, nitrite, and hemoglobin in physiology and therapeutics." *Arteriosclerosis, Thrombosis, and Vascular Biology* **2006**, *26*, 697-705.
- (56) Van Slyke, D.D.; Philips, R.A.; Dole, V.P.; Hamilton, P.B.; Archibald, R.M.; Plazin, J. "Calculation of hemoglobin from blood specific gravities." *Journal of Biological Chemistry* **1950**, *183*, 349-360.
- (57) Beutler, E.; Waalen, J. "The definition of anemia: What *is* the lower limit of normal of the blood hemoglobin concentration." *Blood* **2006**, *107*, 1747-1750.
- (58) Hunter, R.A.; Storm, W.L.; Coneski, P.N.; Schoenfisch, M.H. "Inaccuracies of nitric oxide measurement methods in biological media." *Analytical Chemistry* **2013**, *85*, 1957-1963.

CHAPTER 4: ANTICANCER POTENCY OF NITRIC OXIDE-RELEASING LIPOSOMES³

4.1 Introduction

Small molecule chemotherapeutics (e.g., doxorubicin and cisplatin) often exhibit off-target cytotoxicity due to poor localization.¹⁻⁵ The use of a large macromolecular (e.g., polymer, nanoparticle) carrier to deliver the therapeutic to the targeted site represents one method for mitigating the adverse side effects of small molecules. The leaky vasculature of tumors allows macromolecules to extravasate at the malignant site, with the delivery of the therapeutic payload via cellular uptake or triggered release (e.g., pH and temperature).⁶ Liposomes are among the most widely-investigated delivery systems available for drug delivery. Traditionally, liposomes are composed of an aqueous inner core separated from the external solution by a phospholipid bilayer. This unique architecture allows for the confinement of compounds with a wide range of molecular weights, hydrophobicities, and charges until delivery at a location of interest. The ability of liposomes to absorb and fuse with cell membranes enhances the intracellular uptake of the therapeutic payload, a process that is not typically observed for other macromolecular vehicles (e.g., nanoparticles). Liposomes have thus been developed for a number of therapeutic agents, such as gemcitabine and DNA.⁶⁻⁷ The exterior surface properties of the liposome (e.g., charge) may be tuned independently of the encapsulant, a critical feature for impacting targeting

³ This chapter was adapted from an article that previously appeared in *RSC Advances*. The original citation is as follows: Suchyta, D.J.; Schoenfisch, M.H. “Anticancer potency of nitric oxide-releasing liposomes” *RSC Advances* **2017**.

capabilities and/or reducing aggregation in the bloodstream. In this manner, liposomes have improved the anticancer delivery of many chemotherapeutics, including doxorubicin, arsenic trioxide, and daunorubicin.⁸⁻¹⁰

Nitric oxide (NO), an endogenous diatomic free radical, is an important mediator of inflammation,¹¹⁻¹³ vasodilation,¹⁴⁻¹⁵ biocidal action,¹⁶⁻¹⁸ cardio- and neuroprotection,¹⁹⁻²⁰ and cancer cell proliferation/killing.²¹⁻²³ Off-target toxicity of NO is mitigated by scavenging and/or reaction to nitrite/nitrate.¹⁴ Nitric oxide donors have been developed as a strategy for delivering NO to biological systems as dissolved NO rather than a gas. Examples of currently approved NO donors are sodium nitroprusside, isosorbide mononitrate, glyceryl trinitrate, and pentaerythryl tetranitrate.²⁴ *N*-diazoniumdiolates are a class of NO donors that spontaneously release NO under physiological conditions. The rate of NO release depends on the molecular structure of the amine precursor, facilitating diverse and tunable NO-release kinetics.²⁵⁻²⁶ With respect to chemotherapy, the pH-dependent release of *N*-diazoniumdiolates is advantageous because tumor microenvironments are generally more acidic (pH ~6) than healthy tissue (pH 7.4).²⁷⁻²⁸ The lower pH promotes accelerated NO release at the tumor. A vast literature has proven that small molecule *N*-diazoniumdiolates are capable of eliciting potent anticancer action.²⁹⁻³⁵ Clinical utility has not been achieved because of the excessive loss of NO, prematurely, prior to reaching the tumor site.

In this study, two *N*-diazoniumdiolate-encapsulated liposome systems were prepared with distinct NO-release kinetics (fast and slow). The anticancer activity of these liposomes was evaluated against pancreatic, colorectal, and breast cancer cell lines. Confocal fluorescence and flow cytometry were used to measure both cellular uptake of the liposomes and intracellular NO delivery. The effect of the NO release on protein expression, specifically cleaved PARP, cyclin

B1, and cyclin D1, was also examined via Western blot analysis to assess apoptosis and cell cycle arrest/ejection.

4.2 Experimental section

4.2.1. Materials

Dipalmitoylphosphatidylcholine (DPPC) and 1,2-dipalmitoyl-*sn*-glycero-3-phosphoethanolamine-N-(lissamine rhoadmine B sulfonyl) ammonium salt (Rh-PE) were purchased from Avanti Polar Lipids (Alabaster, AL). Cholesterol (Chol), paraformaldehyde, fetal bovine serum (FBS), penicillin streptomycin, 1x Dulbecco's modified Eagle's medium (DMEM), McCoy's 5A medium, RPMI 1640 medium, Dulbecco's phosphate-buffered saline (DPBS) for cell culture, *N*-propyl-1,3-propanediamine (PAPA), and diethylenetriamine (DETA) were obtained from Sigma (St. Louis, MO). Prolong diamond antifade mountant, 4-amino-5-methylamino-2',7'-difluorofluorescein diacetate (DAF-FM), trypsin, Accutase, 1% (v/v) NP40 lysis buffer, chloroform, phenazine methosulfate (PMS), anhydrous acetonitrile, anhydrous diethyl ether, dimethyl sulfoxide (DMSO), anhydrous ethanol (EtOH), sulfuric acid (H₂SO₄), protein stripping buffer, sodium hydroxide (NaOH), calcium chloride (CaCl₂), PageRuler Plus prestained protein ladder, and secondary antibodies (both mouse and rabbit) for Western blotting were purchased from Fisher Scientific (Fair Lawn, NJ). Sephadex G-25 was obtained from GE Healthcare (Pittsburgh, PA). 3-(4,5-dimethylthiazol-2-yl)-5-(3-carboxymethoxyphenyl)-2-(4-sulfophen-yl)-2H-tetrazolium inner salt (MTS) was purchased from Promega (Madison, WI). Primary antibodies for total and cleaved PARP (rabbit), cyclin B1 (rabbit), cyclin D1 (rabbit), and vinculin (mouse) used in Western blotting were obtained from Cell Signaling (Danvers, MA). Western lightning ECL pro substrate for Western blot detection was from PerkinElmer (Waltham, MA). Phosphatase and protease inhibitors were purchased from Roche (Basel,

Switzerland). Criterion TGX Gel, tris/glycine transfer buffer with sodium dodecyl sulfate (SDS), tris-buffered saline with Tween 20 (TBST), and polyvinylidene fluoride (PVDF) transfer membrane were obtained from Bio-Rad (Hercules, CA). Nitric oxide (NO; 99.5%), nitrogen (N₂; 99.998%), argon (Ar; 99.995%), and NO calibration (26.80 ppm, balance N₂) gases were obtained from Airgas National Welders (Durham, NC). A Millipore Milli-Q UV Gradient A10 System (Bedford, MA) was used to purify distilled water to a resistivity of 18.2 MΩ·cm and a total organic content ≤6 ppb. MIA PaCa-2, AsPc1, and Pa14c pancreatic cancer cells were a gift from Dr. Channing Der of the Department of Pharmacology at the University of North Carolina (Chapel Hill, NC). MDA-MB-231, MCF-7, MDA-MB-468, HCT116, HT-29, and SW480 breast and colorectal cancer cells were a gift from Dr. Matthew Lockett of the Department of Chemistry at the University of North Carolina (Chapel Hill, NC).

4.2.2. *Synthesis of N-diazeniumdiolate NO donors*

A previously reported method was used to synthesize small molecule *N*-diazeniumdiolate NO donors.²⁷ Briefly, DETA and PAPA were dissolved in anhydrous acetonitrile at a concentration of 33.3 mg/mL. The solution was then purged with Ar to 100 psi inside a stainless steel Parr bomb. Six consecutive purges with Ar (three quick purges of 10 s each, followed by three slow purges of 10 min each) were carried out to remove dissolved oxygen. The solution was subsequently pressurized to 145 psi with NO for 3 d, after which the solution was purged again with Ar (100 psi) at least six times to remove residual NO. The precipitated product was filtered over a Hirsch funnel, washed three times with diethyl ether, and dried under vacuum overnight. The final NO donor product was stored at -20 °C until use.

4.2.3. *Liposome synthesis*

The liposomes were prepared using a reverse phase evaporation method.³⁷ A 1:1 molar ratio of lipid to Chol (49.5 μ mol lipid:49.5 μ mol Chol) was dissolved in a mixture of diethyl ether (5.0 mL) and chloroform (5.0 mL) in a round-bottom flask under N₂ atmosphere. Fluorescent liposomes were prepared using the above protocol, but with 1 mol% lipid of Rh-PE. The *N*-diazoniumdiolate was dissolved in 10 mM NaOH to make a 14 mM stock NO donor solution. This solution was injected into the flask, and then sonicated for 4 min at 45 °C. The organic phase was removed by rotoevaporation to yield the aqueous liposome suspension. Liposomes were incubated at 45 °C for an additional 30 min, after which the unencapsulated material was removed using four Sephadex G-25 spin columns packed in 10-mL syringes. The liposomes collected from the column were stored at 4 °C.

4.2.4. Characterization of liposomes

Dynamic light scattering (DLS; Malvern Zetasizer Nano; UK) was used to determine liposome size distribution in water. Transmission electron microscopy (TEM) was used to confirm liposome formation. Liposome samples for TEM analysis were prepared by diluting the stock solution with Milli-Q water (1:1 volumetric ratio) and casting the suspension onto Formvar-coated, square mesh copper TEM grids (Electron Microscopy Sciences, Hatfield, PA). The solvent was allowed to evaporate for 45 min prior to applying a negative-stain using a 2% (w/v) uranyl acetate solution. A drop of the stain was left on the grid for 30 s and then removed using filter paper. The grid was dried for 5 min prior to imaging using a JEOL 100CX II transmission electron microscope (100 kV accelerating voltage).

4.2.5. Nitric oxide release

Nitric oxide storage and NO-release kinetics from the liposomes were measured using a Sievers Chemiluminescence Nitric Oxide Analyzer (NOA; Boulder, CO).³⁸⁻³⁹ Studies to evaluate

NO-release kinetics were performed in 10 mM PBS (pH 7.4) at 37 °C. The instrument was calibrated using air passed through a NO zero filter (0 ppm NO) and a 26.80 ppm NO standard (balance N₂). Nitric oxide storage for encapsulation efficiency (i.e., the extent to which the NO donor is entrapped within the liposomal aqueous core) was performed in a 2:1 volumetric ratio of ethanol to 0.183 M sulfuric acid (30 mL total volume) at 37 °C. The encapsulation efficiency was calculated by comparing the liposome NO storage to the amount of NO in the free donor solution used during liposome preparation. All presented data is from $n \geq 3$ separate liposome preparations. Nitric oxide release measurements were terminated when the NO concentration dropped below 10 ppb per 300 μ L liposomes.

4.2.6. Cytotoxicity assays

Pa14c and MIA PaCa-2 cells were cultured in DMEM. HCT116 and HT-29 cells were cultured in McCoy's 5A medium. MDA-MB-231, MCF-7, MDA-MB-468, SW480, and AsPc1 cells were cultured in RPMI medium. All media were supplemented with 10 vol% FBS and 1 wt% penicillin/streptomycin. Cells were maintained at 37 °C in a humidified incubator with 5 vol% CO₂. For cell viability evaluations, the MTS assay was used as previously described with cells plated in triplicate.⁴⁰ Briefly, cells (2×10^3 cells/well) in DMEM were treated with various volumes of liposomes in a 96-well plate (100 μ L total volume per well). Following a 72 h incubation period at 37 °C, the supernatant of each well was removed, rinsed with PBS (100 μ L), and replaced with fresh DMEM (100 μ L). The cells were further incubated with 20 μ L of MTS/PMS reagent (20:1 v/v MTS to PMS) at 37 °C for ~90 min. The absorbances of the resulting solutions at 490 nm were measured using a ThermoScientific Multiskan EX plate reader (Waltham, MA). The ratio of absorbance values between the samples and the controls was represented as the percent cell viability. Dose response curves and LD₅₀ values were plotted and

tabulated using GraphPad Prism 6 software (La Jolla, CA) and non-linear regression (three-parametric Hill function), respectively. All presented data are from $n \geq 3$ separate experiments.

4.2.7. *Confocal fluorescence microscopy*

Cells were plated in 10×10 mm cloning cylinders (VWR, Atlanta, GA) secured to No 1.5 glass cover slips (VWR, Atlanta, GA) using silicone grease. The slip was placed in a Petri dish prior to the addition of cell media. After 24 h, the medium within the cylinders was replaced with a 10 μM DAF-FM solution. An additional 30 min incubation period at 37 °C was then carried out before removing the DAF-FM solution. Fresh cell media was subsequently added and allowed to incubate for another 15 min at 37 °C to allow for saponification of the probe. Liposomes were added to the cells and incubated for 2 h, followed by rinsing twice with 100 μL DPBS. A 100-μL aliquot of 4 vol% paraformaldehyde solution (diluted with DPBS) was injected into the wells and incubated for 15 min at room temperature. The cover slips were then mounted on glass slides using a droplet of mounting media, sealed with nail polish (Electron Microscopy Sciences; Hatfield, PA), and imaged after 1 h using a Zeiss LSM 700 laser scanning confocal microscope. The excitation/emission wavelengths for DAF-FM and Rh-PE were 495/515 and 560/583 nm, respectively. Fiji software was used for image processing and densitometry calculations. Autoquant X3 software (Media Cybernetics; Warrendale, PA) generated orthogonal views of the z-stacked images. All images were collected under constant exposure times. The images were also processed equivalently and normalized to a single brightness level.

4.2.8. *Flow cytometry*

Cells were plated (1×10^4 cells/well) in 96-well plates and allowed to adhere for 24 h in RPMI media (100 μL). The media was then removed and cells were incubated with fresh media containing 5 μM DAF-FM for 1 h. The media containing the DAF-FM was subsequently

removed and free or liposomal *N*-diazeniumdiolate NO donors were added to the wells (dissolved in fresh media) and allowed to incubate for specified times. Cells were then washed with DPBS and detached by exposure to Accutase (30 μ L) for 5 min at room temperature. Media containing 5 mM CaCl₂ was added (30 μ L) to the wells while maintaining the plate at 0 °C for 20 min. The plate was placed on a shaker for 30 s (2000 rpm) to resuspend cells prior to analysis with an iQue Screener Plus flow cytometer (IntelliCyt, Albuquerque, NM). A 33 s sampling (sip) time was used with a 0.5 s up time between wells. The plate was shaken (and the probe cleaned) for 20 s at 2000 rpm every 4 wells. Data acquisition and processing were carried out with ForeCyt software (IntelliCyt; Albuquerque, NM). Single color compensation controls were performed to minimize spectral overlap. Gates were placed around singlet cells to exclude data from aggregated cells. Fluorescence intensities were calculated and plotted versus number of events.

4.2.9. *Western blot analysis*

Cells were added to a 6-well plate (3×10^5 cells/well) and incubated for 24 h. Media was then removed and replaced with fresh media containing liposomes. At specified timepoints, the plates were placed on ice, washed once with cold DPBS, and incubated for 15 min with 1 vol% NP40 lysis buffer (50 μ L) containing protease and phosphatase inhibitors. The wells were then scraped and the solution added to cold microcentrifuge tubes. Cellular debris was removed by centrifugation (4 °C, 5 min). Protein concentrations in samples were determined using the Bradford assay. Equal total protein amounts (~30 μ g) were added to each lane of the gel (4–20% gradient). After electrophoresis, the proteins were transferred onto PVDF membranes, blocked with 5% (w/v) milk, and stained with primary antibody overnight. After incubation with the secondary antibody for 1 h, the membrane was incubated with the Western lightning ECL pro

substrate (10 min) and then imaged using a ChemiDoc chemiluminescence imaging system (Bio-Rad; Hercules, CA). Western blot images were processed using Image Lab software (Bio-Rad; Hercules, CA). Fiji software was used for densitometry calculations. Loading controls were used as a normalization factor for densitometric calculations.

4.3 Results and discussion

The *N*-diazoniumdiolates used in this study (PAPA/NO and DETA/NO; Appendix C) were selected because of their dissimilar NO-release half-lives in PBS at pH 7.4 (0.25 h and 20 h, respectively). On the basis of our previous work and others,^{28,41} we anticipated that the resulting NO-releasing liposomes would have different NO-release kinetics. Liposome formation was confirmed by dynamic light scattering (DLS) measurements. As shown in Figure 1, DETA/NO and PAPA/NO liposomes exhibited hydrodynamic sizes typical of liposomes synthesized via reverse-phase evaporation (Table 1).³⁷ The slight difference in size between the systems should not appreciably affect their anticancer activity as liposomes with sizes of approximately 150 to 400 nm exhibit similar cellular uptake.⁴² Transmission electron microscopy (TEM) corroborated the DLS measurements and indicated negligible liposome-liposome fusion (Appendix C). Real-time NO release measurements demonstrated that the NO donor encapsulation efficiency was similar to efficiencies of other reverse-phase evaporated liposomes and consistent between the two liposome formulations (Table 1), likely the result of similar size of the NO donors.³⁷ As expected, the liposomes released NO more slowly at physiological pH (7.4) than the corresponding small molecule NO donor alone (Figure 1). The PAPA/NO liposomes released ~50% of their total NO in 2.5 h, a ten-fold longer NO-release half-life than the free NO donor. As the rate of NO release impacts NO's toxicity,²⁹⁻³⁵ the use of two distinct

N-diazoniumdiolates as encapsulants allows for the study of the anticancer therapeutic potential of the liposomes as a function of NO-release kinetics.

4.3.1. *Cytotoxicity of the liposomes*

The potential anticancer activity of the NO-releasing liposomes was initially tested against Pa14c pancreatic cancer cells, an aggressive pancreatic cancer cell line. The PAPA/NO and DETA/NO liposome systems showed a pronounced toxicity difference, attributable to the NO release (Figure 2A). At low NO payloads (~0.9 µg/mL), the viability was slightly enhanced for each liposomal system. Previous research has reported that low levels of NO induces EGF-dependent cell proliferation.^{14,43} At NO payloads >1.5 µg/mL, the slower NO-release system (DETA/NO liposomes) was markedly more toxic towards the Pa14c cells. The less effective PAPA/NO liposomes required larger NO payloads to induce toxicity likely because of the faster release rate, resulting in the release of the majority of the NO payload before reaching the cell and/or cellular uptake. Significantly less toxicity (killing) was observed (Appendix C) when using a noncancerous epithelial cell line (HPNE), indicating that NO may elicit preferential cytotoxicity towards cancer cells due to its ability to further increase the oxidative/nitrosative stress that cancer cells are already under.⁴⁴

The cytotoxicity of the liposomes was next evaluated against a number of malignant lines from pancreatic, breast, and colorectal cancers to ascertain if the observed dependence on NO-release kinetics applied to other cell lines. The slow NO-releasing liposomes (DETA/NO) consistently required lower NO payloads to elicit cytotoxic effects, regardless of cancer type or cell line (Figure 2B). In fact, the LD₅₀ was <3 µg/mL NO for the DETA/NO liposomes against all cancer cell lines investigated, while the faster-releasing PAPA/NO liposomes required >6 µg/mL NO to elicit cytotoxic action. These results agree with prior work that demonstrated that

Table 4.1. Properties of NO-releasing liposomes.

NO donor	Hydrodynamic size^a (nm)	Encapsulation efficiency^b (%)	Total NO^c (µg/mL)
PAPA/NO	377 ± 52	19.0 ± 3.5	125.7 ± 41.1
DETA/NO	246 ± 32	20.6 ± 3.2	133.2 ± 26.7

^aZ-average size measured using DLS. ^bRatio of µmol of NO inside liposomes to µmol used for synthesis, multiplied by 100. ^cTotal amount of NO release in acid normalized to the injected liposome volume.

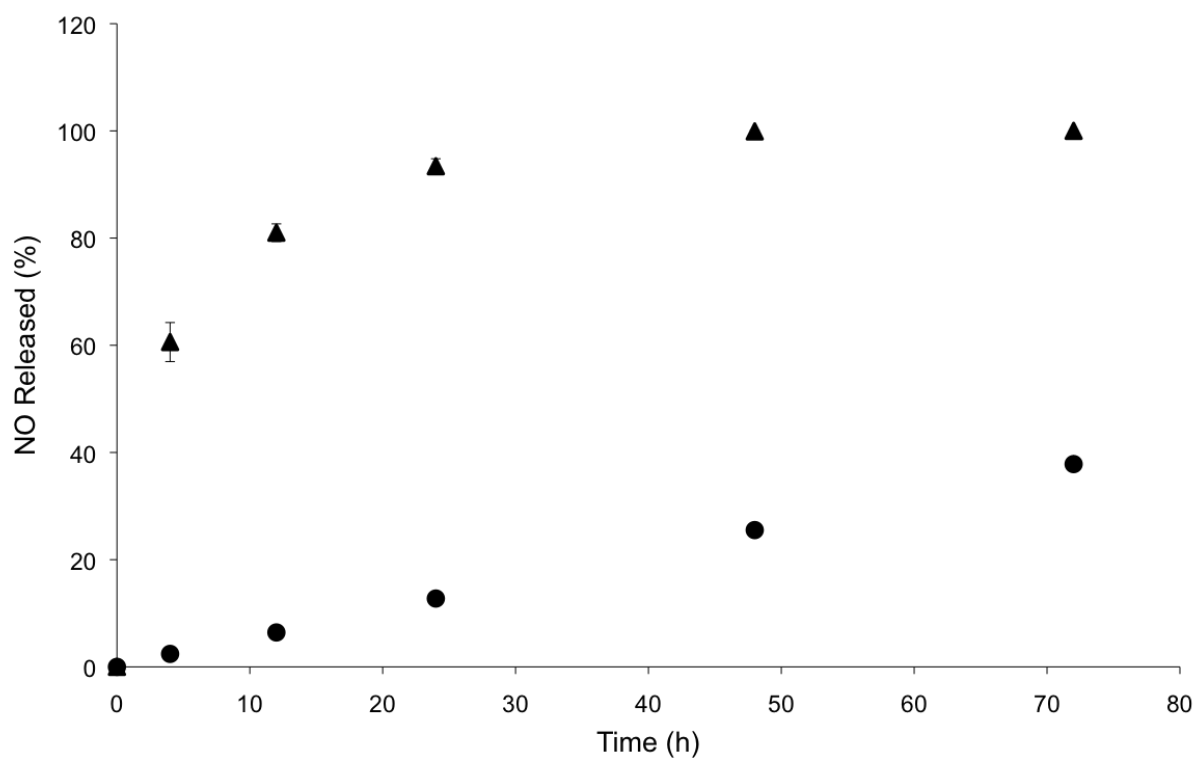


Figure 4.1. Nitric oxide-release profiles from liposomal (●) DETA/NO and (▲) PAPA/NO in 10 mM PBS (pH 7.4, 37 °C) over the first 72 h.

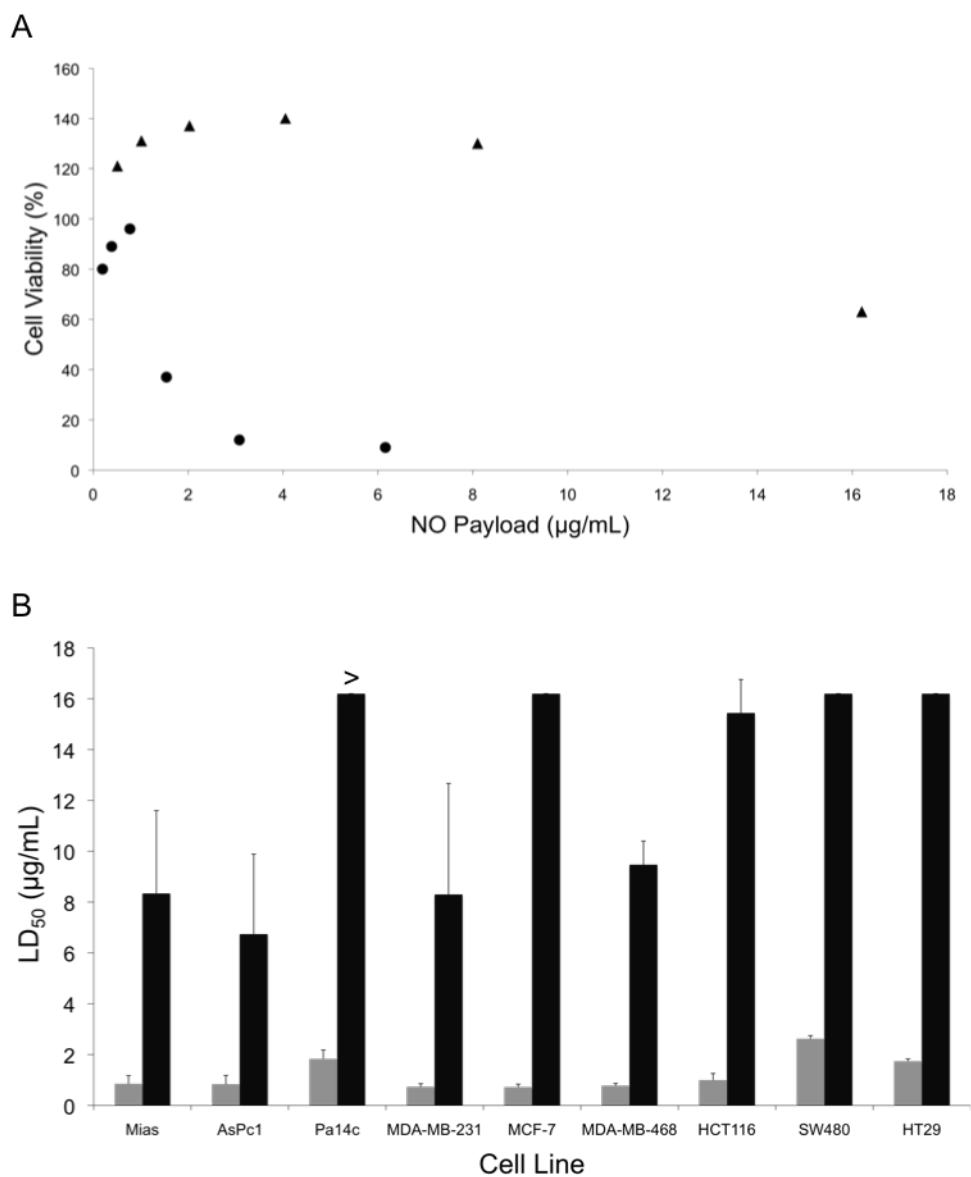


Figure 4.2. (A) Cytotoxicity of liposomal (●) DETA/NO and (▲) PAPA/NO as a function of NO payload against human Pa14c pancreatic cancer cells after 72 h of exposure. (B) Calculated LD₅₀ values for (grey bars) DETA/NO and (black bars) PAPA/NO liposomes against pancreatic, breast, and colorectal cancer cell lines. Of note, the LD₅₀ of PAPA/NO liposomes against Pa14c cells was >16.2 µg/mL. NO payloads were calculated based on the total amount of NO released from the liposomes over 72 h in PBS.

free NO donors exhibiting slow NO-release kinetics required lower anticancer payloads relative to their fast-releasing counterparts.^{29,33,45}

A human breast cancer cell line (MCF-7) was chosen as a representative model for further evaluation of the NO-release kinetics and associated cytotoxicity because of the stark differences in the LD₅₀ values for the PAPA/NO and DETA/NO liposomes. Our immediate goal was to determine if the PAPA/NO liposomes induced cytotoxicity earlier in the assay (i.e., before 72 h). Cells were exposed to the 72 h LD₅₀ concentrations of the DETA/NO and PAPA/NO liposomes (0.75 µg/mL and 16.2 µg/mL after 72 h exposure, respectively) for 8, 24, 48, and 72 h. As shown in Figure 3, neither the fast nor slow NO-releasing liposome system exhibited cytotoxic effects at early timepoints (8 h). Rather, mild cell proliferation was noted for both. After 24 h, cell viability diminished greatly (up to 60%) for cells exposed to the PAPA/NO system (16.2 µg/mL NO), with no further change through 72 h. PAPA/NO liposomes deliver ~90% of the NO payload by 24 h (Figure 1), correlating with this observed cytotoxicity. The NO liberated from the DETA/NO liposomes (0.75 µg/mL) displayed a more consistent cell viability profile with a steady drop over the 72 h period. Cytotoxicity for PAPA/NO liposomes at 0.75 µg/mL payloads was not induced at any time point (negligible toxicity relative to controls). Collectively, this data suggests that faster NO release (i.e., using shorter half-life NO donors) elicits cytotoxicity more rapidly than corresponding slower release, but necessitates larger NO payloads. The large levels of produced NO from the fast NO-releasing liposomes may be better at increasing the entropy of the cellular system through the denaturation of proteins than the slow NO-releasing liposomes.

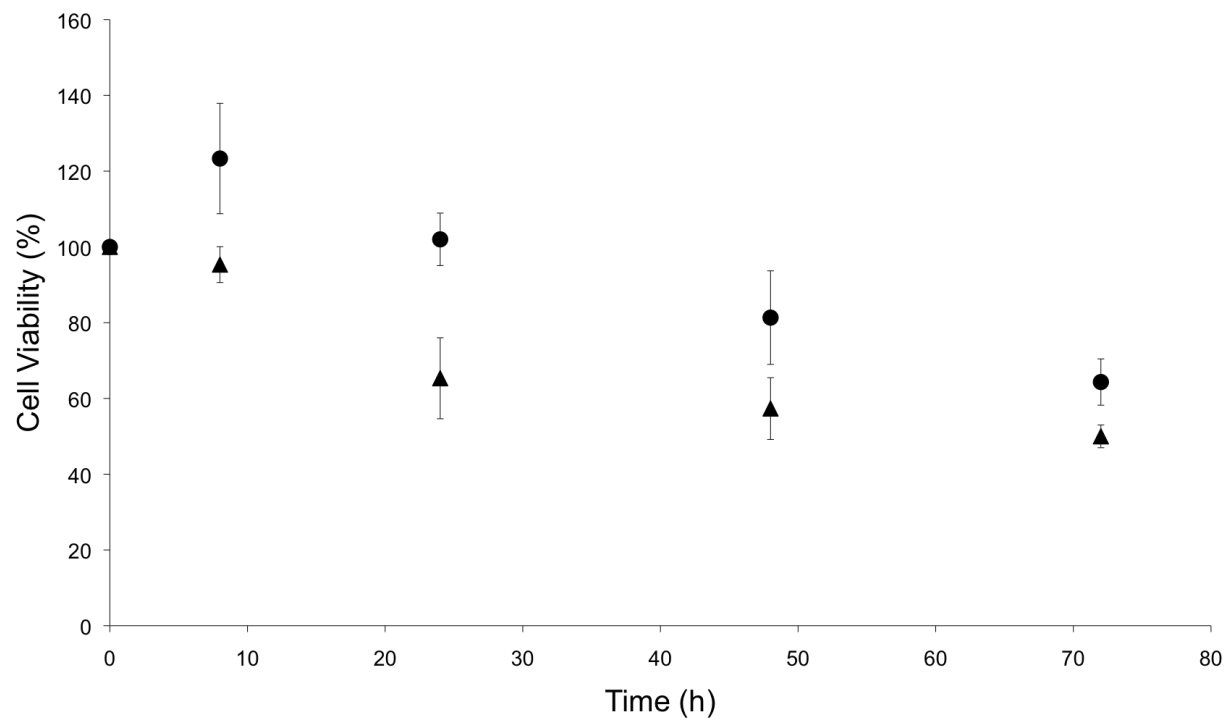


Figure 4.3. Time-course cytotoxicity study of liposomal (●) DETA/NO and (▲) PAPA/NO at their respective LD₅₀ values against human MCF-7 breast cancer cells.

4.3.2. Intracellular liposome uptake and NO delivery

The observed relationship between liposome NO-release kinetics and anticancer action was hypothesized to be the result of intracellular NO accumulation. Confocal fluorescence microscopy was employed to measure intracellular NO build-up over time for the two systems using DAF-FM, a molecular probe that selectively reacts with NO to form a fluorescent benotriazole compound.⁴⁶ Additionally, cellular uptake of the liposomes was visualized by incorporating a fluorescent phospholipid (Rh-PE) into the lipid bilayer.⁴⁷ A 2 h exposure period was initially selected for this study as cell have been shown to initiate liposomal uptake within this timeframe,⁴⁸⁻⁴⁹ allowing for visualization of delivered NO. The bright field and fluorescence images of MCF-7 cells after exposure to DETA/NO and PAPA/NO liposomes (at their LD₅₀ values) are provided in Figure 4A. Of note, the amount of NO released during the confocal experiment is significantly lower than the corresponding LD₅₀ values due to the shorter exposure time (2 vs. 72 h). Liposome uptake was clearly observed after 2 h, with z-stack images revealing intracellular localization of the NO-releasing liposomes (Figure 5). The rapid uptake of the liposomes results from their ability to adsorb to and then fuse with the cell membrane, a phenomena that does not readily occur with other delivery vehicles (e.g., nanoparticles).⁶ Relative to DETA/NO liposomes, cells exposed to PAPA/NO liposomes had substantially elevated levels of intracellular NO. Densitometry calculations were carried out to quantify intracellular NO levels for the two liposomes (Figure 4B). Treatment with PAPA/NO liposomes resulted in a 4-times larger fluorescence signal relative to DETA/NO after 2 h, supporting the results observed in the time-course study where the fast release system elicited more rapid cytotoxicity (at 24 h). The lack of cytotoxicity observed for the PAPA/NO liposomes at the same NO payloads as the DETA/NO liposomes (0.75 µg/mL) was supported by negligible intracellular

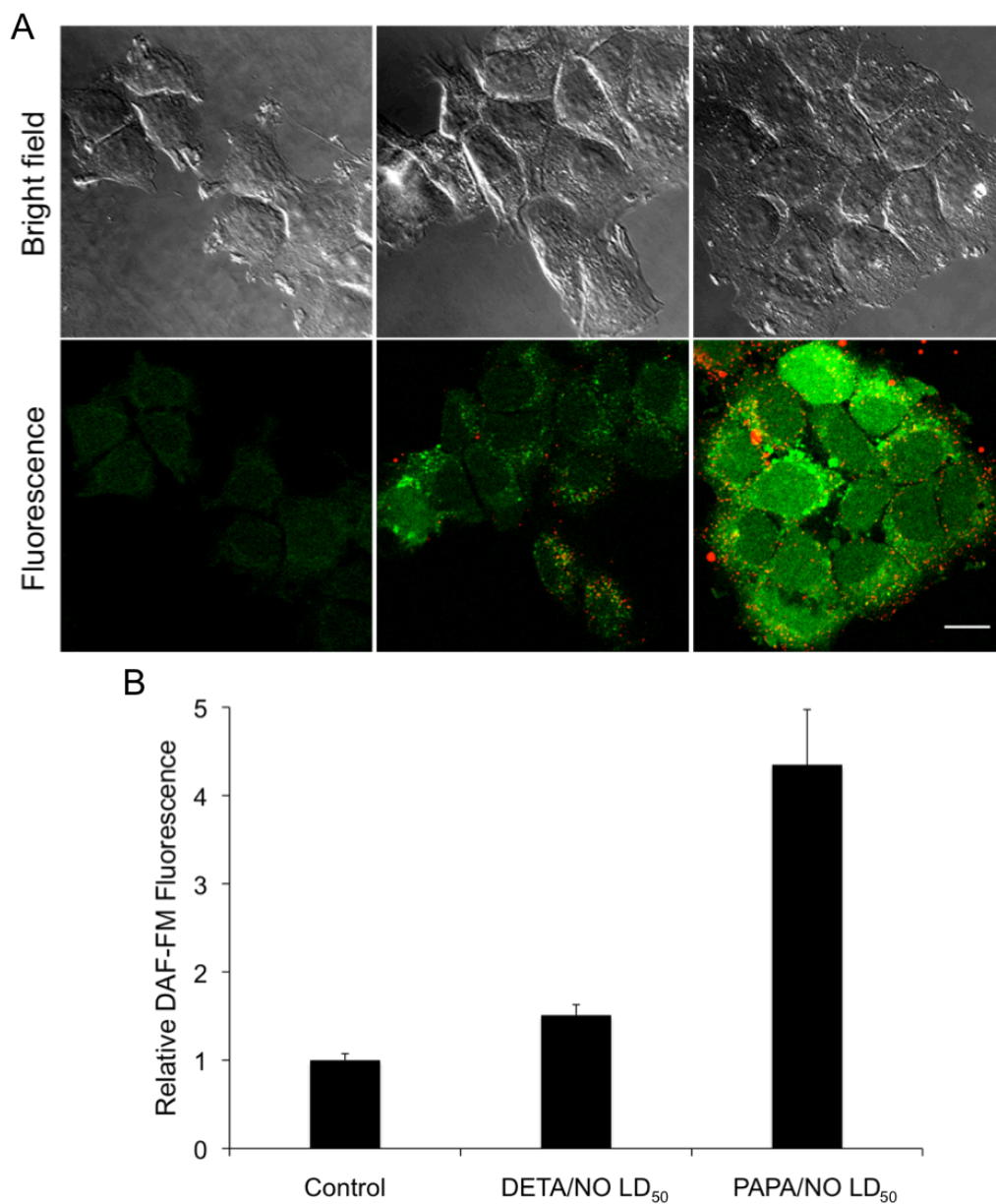


Figure 4.4. (A) Confocal fluorescence images of MCF-7 cells incubated with DAF-FM (green) and treated with NO-releasing liposomes (red) for 2 h. Scale bar represents 15 μm . Column 1 is controls. Column 2 and 3 are cells exposed to the LD₅₀ values of DETA/NO and PAPA/NO liposomes, respectively. By 2 h, DETA/NO and PAPA/NO liposomes released ~ 1 and 30% of their NO payloads, respectively. (B) Densitometric analysis of intracellular DAF-FM levels relative to untreated controls.

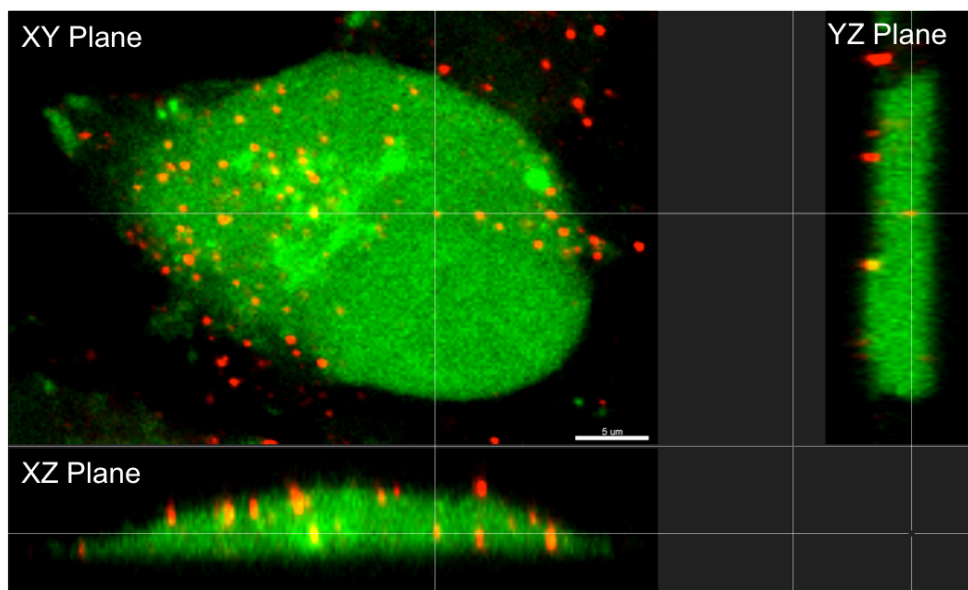


Figure 4.5. Orthogonal view of MCF-7 cells after treatment with PAPA/NO liposomes. Scale bar represents 5 μm .

NO accumulation at 2 h (data not shown). Collectively, the greater NO accumulation and NO exposure observed for the PAPA/NO liposomes leads to more rapid anticancer action.

4.3.3. *Kinetics of intracellular NO accumulation*

The rapid NO delivery from the PAPA/NO liposomes was hypothesized to be key in eliciting cytotoxicity at short time periods (i.e., 24 h). The more gradual cell killing observed using the DETA/NO liposomes would be expected to parallel the build-up of intracellular NO over time. Flow cytometry was utilized to quantify NO accumulation within the MCF-7 cells over a 72 h period using the same DAF-FM probe (Figure 6). A large increase in intracellular fluorescence was observed by 24 h for cells treated with PAPA/NO liposomes (16.2 $\mu\text{g/mL}$ NO). At 48 and 72 h, the fluorescence essentially remained at the same level, signaling that no more NO was delivered to the cell. In contrast, the fluorescence within cells treated with the slower NO-releasing DETA/NO liposomes (0.75 $\mu\text{g/mL}$ NO) continued to increase steadily over the entire 72 h period. The therapeutic action of both slow and fast NO-releasing liposomes followed the same trend observed in the cytotoxicity time-course study, where cytotoxicity was elicited more rapidly with PAPA/NO liposomes and the DETA/NO liposomes required the full 72 h before eliciting toxicity. At equal NO payloads (0.75 $\mu\text{g/mL}$), minimal intracellular NO accumulation was observed for the PAPA/NO liposomes due to premature NO loss prior to cellular uptake (Appendix C), which is in agreement with cytotoxicity findings.

A median fluorescence intensity comparison between free and liposomal NO donors was performed to highlight the benefits of using NO-releasing liposomes over the low molecular weight NO donors. Cells treated with NO-releasing liposomes exhibited greater intracellular NO accumulation (Figure 6), as a result of enhanced NO donor stability (within the liposomes) and

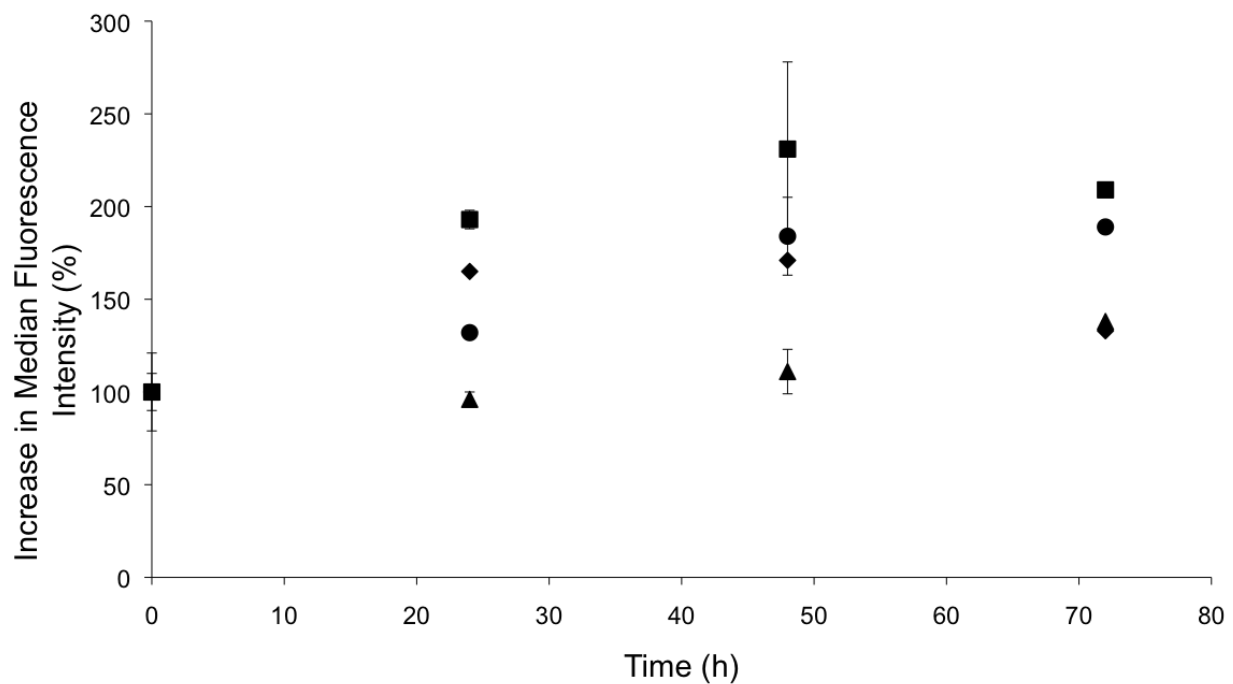


Figure 4.6. Change in median fluorescence intensity over time indicating intracellular NO accumulation, as determined by flow cytometry, after treating MCF-7 cells with 0.75 $\mu\text{g/mL}$ NO from (●) liposomal and (▲) free DETA/NO, and 16.2 $\mu\text{g/mL}$ NO from (■) liposomal and (□) free PAPA/NO.

targeted cellular uptake. Similar behavior has been observed for other small molecule drugs (e.g., gemcitabine and doxorubicin) encapsulated within liposomes.^{8,50}

4.3.4. *Effect of liposomes on intracellular signaling*

Western blot analysis was employed to evaluate if any differences existed in protein expression levels. Poly(ADP-ribose) polymerase (PARP) is a critical mediator of DNA repair and upon cleavage by caspase-3 initiates cellular breakdown and apoptosis.⁵¹ A measurement of increased PARP levels after treatment would indicate that cells underwent PARP-mediated apoptosis. Cyclin analysis would facilitate understanding the cell cycle and whether cells were arrested or ejected.⁵²⁻⁵³ The expressions of these regulator proteins in MCF-7 cells were measured after NO exposure at 24, 48, and 72 h (Figure 8A). Cleaved PARP levels were the greatest for cells treated with 16.2 $\mu\text{g}/\text{mL}$ NO from PAPA/NO liposomes, indicating apoptosis, especially at early timepoints (i.e., 24 and 48 h). This data correlates well with the rapid cytotoxicity observed from the fast NO-release system (Figure 3). Densitometric calculations were performed on the blots to more accurately compare protein levels between exposure conditions. Even though cells treated with DETA/NO liposomes exhibited reduced cyclin B1 levels relative to controls by 24 h (Figure 8B), the levels were still greater than cells treated with PAPA/NO liposomes. At 72 h, the two systems, at their respective LD_{50} values, had similar expressions of cyclin D1 (Figure 8C), suggesting an equivalent capacity to either inactivate transcription factors that drive cell proliferation (i.e., prevent cell growth) or initiate cyclin D1 destruction. Of note, minimal changes in protein expression were observed for cells exposed to PAPA/NO liposomes at NO payloads (0.75 $\mu\text{g}/\text{mL}$) equivalent to the DETA/NO liposomes, corroborating insufficient NO delivery and low toxicity. These results suggest that both types of

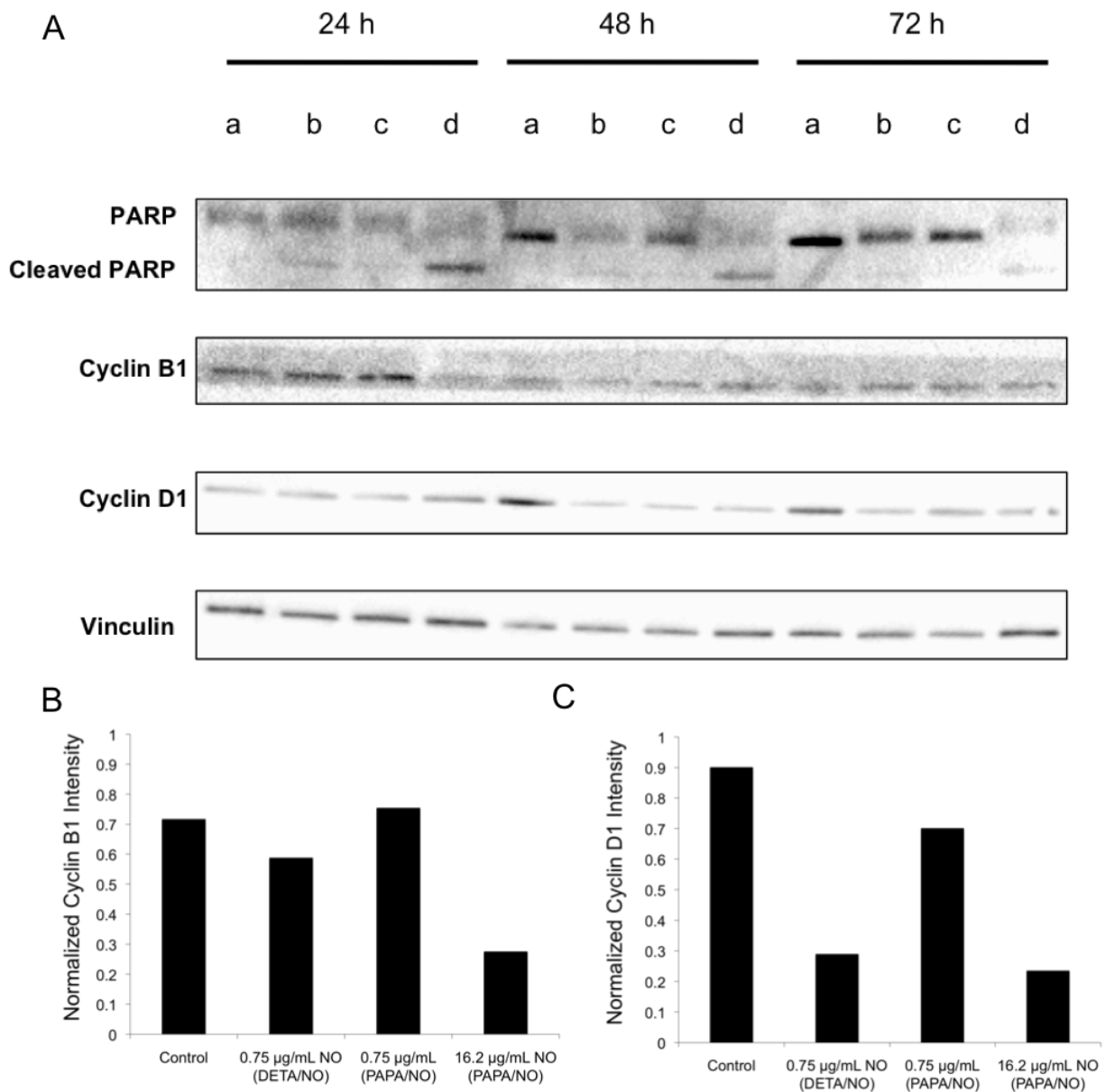


Figure 4.7. (A) Western blot of MCF-7 cells after no treatment (lane a), 0.75 µg/mL NO from DETA/NO liposomes (lane b), 0.75 µg/mL NO from PAPA/NO liposomes (lane c), and 16.2 µg/mL NO from PAPA/NO liposomes (lane d). (B) Densitometric analysis of cyclin B1 levels after 24 h exposure. (C) Densitometric analysis of cyclin D1 levels after 72 h exposure.

NO-releasing liposomes trigger the same anticancer pathways, but to different degrees depending on the exposure time and NO concentration. Slower NO release elicits a more gradual increase in cleaved PARP levels (i.e., apoptosis) and arrested cells in the cell cycle, while faster NO release promotes rapid PARP cleavage and prevention of mitosis.

4.4 Conclusions

The transition from low molecular weight NO donors to macromolecular NO-release systems for anticancer treatments may represent an important step in creating more effective chemotherapies. Two NO-releasing liposome systems with distinct NO-release kinetics were used to study cytotoxicity against pancreatic, colorectal, and breast cancer cell lines. Through the encapsulation of the low molecular weight NO donor within liposomes, greater intracellular NO accumulation was observed due to enhanced uptake. The preliminary cell studies herein suggest that NO-release kinetics play an important role in eliciting cell death, with a direct relationship to intracellular NO accumulation. Fast NO-releasing liposomes represent a less effective anticancer therapeutic as the NO is liberated too rapidly in advance of intracellular uptake. Further cytotoxicity studies using liposomes bearing cancer targeting ligands (e.g., folate) are the next steps in enhancing the selectivity of the NO-releasing liposomes. This work points towards the promise of using NO-releasing liposomes as anticancer agents, and the importance of controlling NO-release rates for other macromolecular delivery scaffolds. The ability of NO to further increase the number of oxidative/nitrosative species that cancer cells are already exposed to is a unique mechanism to specifically target cancer cells over healthy cells.

REFERENCES

- (1) Bender, A.; Schieber, J.; Glick, M.; Davies, J.W.; Azzaoui, K.; Hamon, J.; Urban, L.; Whitebread, S.; Jenkins, J.L. "Analysis of pharmacology data and the prediction of adverse drug reactions and off-target effects from chemical structure." *ChemMedChem* **2007**, *2*, 861-873.
- (2) Park, B.K.; Boobis, A.; Clarke, S.; Goldring, C.; Jones, D.; Kenna, J.G.; Lambert, C.; Lavery, H.G.; Naisbitt, D.J.; Nelson, S.; Nicoll-Griffith, D.A.; Obach, R.S.; Routledge, P.; Smith, D.A.; Tweedie, D.J.; Vermeulen, N.; Williams, D.P.; Wilson, I.D.; Baillie, T.A. "Managing the challenge of chemically reactive metabolites in drug development." *Nature Reviews Drug Discovery* **2011**, *10*, 292-306.
- (3) Widakowich, C.; De Castro, G.; De Azambuja, E.; Dinh, P.; Awada, A. "Review: Side effects of approved molecular targeted therapies in solid cancers." *The Oncologist* **2007**, *12*, 1443-1455.
- (4) Galluzzi, L.; Vitale, I.; Michels, J.; Brenner, C.; Szabadkai, G.; Harei-Bellan, A.; Castedo, M.; Kroemer, G. "Systems biology of cisplatin resistance: Past, present and future." *Cell Death and Disease* **2014**, *5*, 1-18.
- (5) De Angelis, A.; Urbanek, K.; Cappetta, D.; Piegari, E.; Ciuffreda, L.; Rivellino, A.; Russo, R.; Esposito, G.; Rossi, F.; Berrino, L. "Doxorubicin cardiotoxicity and target cells: A broader perspective." *Cardio-Oncology* **2016**, *2*, 1-8.
- (6) Torchilin, V.P. "Recent advances with liposomes as pharmaceutical carriers." *Nature Reviews Drug Discovery* **2005**, *4*, 145-160.
- (7) Allen, T.M.; Cullis, P.R. "Liposomal drug delivery systems: From concept to clinical applications." *Advanced Drug Delivery Reviews* **2013**, *65*, 36-48.
- (8) Barenholz, Y.C. "Doxil – The first FDA-approved nano-drug: Lessons learned." *Journal of Controlled Release* **2012**, *160*, 117-134.
- (9) Chen, H.; MacDonald, R.C.; Li, S.; Krett, N.L.; Rosen, S.T.; O'Halloran, T.V. "Lipid encapsulation of arsenic trioxide attenuates cytotoxicity and allows for controlled anticancer drug release." *Journal of the American Chemical Society* **2006**, *128*, 13348-13349.
- (10) Piccaluga, P.P.; Visani, G.; Martinelli, G.; Isidori, A.; Malagola, M.; Rondoni, M.; Baccarani, M.; Tura, S. "Liposomal daunorubicin (daunoXome) for treatment of relapsed meningeal acute myeloid leukemia." *Leukemia* **2002**, *16*, 1880-1881.
- (11) Taylor, E.L.; Megson, I.L.; Haslett, C.; Rossi, A.G. "Nitric oxide: A key regulator of myeloid inflammatory cell apoptosis." *Cell Death and Differentiation* **2003**, *10*, 418-430.

- (12) Wink, D.A.; Hines, H.B.; Cheng, R.S.; Switzer, C.H.; Flores-Santana, W.; Vitek, M.P.; Ridnour, L.A.; Colton, C.A. "Nitric oxide and redox mechanisms in the immune response." *Journal of Leukocyte Biology* **2011**, *89*, 873-891.
- (13) Sharma, J.N.; Al-Omran, A.; Parvathy, S.S. "Role of nitric oxide in inflammatory diseases." *Inflammopharmacology* **2007**, *15*, 252-259.
- (14) Thomas, D.D.; Ridnour, L.A.; Isenberg, J.S.; Flores-Santana, W.; Switzer, C.H.; Donzelli, S.; Hussain, P.; Vecoli, C.; Paolocci, N.; Ambs, S.; Colton, C.A.; Harris, C.C.; Roberts, D.D.; Wink, D.A. "The chemical biology of nitric oxide: Implications in cellular signaling." *Free Radical Biology & Medicine* **2008**, *45*, 18-31.
- (15) Moncada, S.; Palmer, R.; Higgs, E. "Nitric oxide: Physiology, pathophysiology, and pharmacology." *Pharmacological Reviews* **1991**, *43*, 109-142.
- (16) Carpenter, A.W.; Schoenfisch, M.H. "Nitric oxide release: Part II. Therapeutic applications." *Chemical Society Reviews* **2011**, *41*, 3742-3752.
- (17) Fang, F.C. "Perspective series: Host/pathogen interactions. Mechanisms of nitric oxide-related antimicrobial activity." *Journal of Clinical Investigation* **1997**, *99*, 2818-2825.
- (18) Fang, F.C. "Antimicrobial reactive oxygen and nitrogen species: Concepts and controversies." *Nature Reviews Microbiology* **2004**, *2*, 820-832.
- (19) Jones, S.P.; Bolli, R. "The ubiquitous role of nitric oxide in cardioprotection." *Journal of Molecular and Cellular Cardiology* **2006**, *40*, 16-23.
- (20) Calabrese, V.; Mancuso, C.; Calvani, M.; Rizzarelli, E.; Butterfield, D.A.; Stella, A.M. "Nitric oxide in the central nervous system: Neuroprotection versus neurotoxicity." *Nature Reviews Neuroscience* **2007**, *8*, 766-775.
- (21) Wink, D.A.; Vodovotz, Y.; Laval, J.; Laval, F.; Dewhirst, M.W.; Mitchell, J.B. "The multifaceted roles of nitric oxide in cancer." *Carcinogenesis* **1998**, *19*, 711-721.
- (22) Wang, L.; Xie, K. "Nitric oxide and pancreatic cancer pathogenesis, prevention, and treatment." *Current Pharmaceutical Design* **2010**, *16*, 421-427.
- (23) Sullivan, R.; Graham, C.H. "Chemosensitization of cancer by nitric oxide." *Current Pharmaceutical Design* **2008**, *14*, 1113-1123.
- (24) Miller, M.R.; Megson, I.L. "Recent developments in nitric oxide donor drugs." *British Journal of Pharmacology* **2007**, *151*, 305-321.
- (25) Hrabie, J.A.; Klose, J.R.; Wink, D.A.; Keefer, L.K. "New nitric oxide-releasing zwitterions derived from polyamines." *Journal of Organic Chemistry* **1993**, *58*, 1472-1476.

- (26) Keefer, L.K. "Fifty years of diazeniumdiolate research. From laboratory curiosity to broad-spectrum biomedical advances." *ACS Chemical Biology* **2011**, *6*, 1147-1155.
- (27) Shamim, U.; Hanif, S.; Albanyan, A.; Beck, F.; Bao, B.; Wang, Z.; Banerjee, S.; Sarkar, F. H.; Mohammad, R. M.; Hadi, S. M.; Azmi, A. S. "Resveratrol-induced apoptosis is enhanced in low pH environments associated with cancer." *Journal of Cellular Physiology* **2012**, *227*, 1493-1500.
- (28) Tannock, I. F.; Rotin, D. "Acid pH in tumors and its potential for therapeutic exploitation." *Cancer Research* **1989**, *49*, 4373-4384.
- (29) Maragos, C.M.; Wang, J.M.; Hrabie, J.A.; Oppenheim, J.J.; Keefer, L.K. "Nitric oxide/nucleophile complexes inhibit the *in vitro* proliferation of A375 melanoma cells via nitric oxide release." *Cancer Research* **1993**, *53*, 564-568.
- (30) Stuehr, D.J.; Nathan, C.F. "A macrophage product responsible for cytostasis and respiratory inhibition of tumor target cells." *Journal of Experimental Medicine* **1989**, *169*, 1543-1555.
- (31) Tamir, S.; Lewis, R.S.; Walker, T.; Deen, W.M.; Wishnok, J.S.; Tannenbaum, S.R. "The influence of delivery rate on the chemistry and biological effects of nitric oxide." *Chemical Research in Toxicology* **1993**, *6*, 895-899.
- (32) Mooradian, D.L.; Hutsell, T.C.; Keefer, L.K. "Nitric oxide (NO) donor molecules: Effect of NO release rate on vascular smooth muscle cell proliferation *in vitro*." *Journal of Cardiovascular Pharmacology* **1995**, *25*, 674-678.
- (33) Kielbik, M.; Klink, M.; Brzezinska, M.; Szulc, I.; Sulowska, Z. "Nitric oxide donors: Spermine/NO and diethylenetriamine induce ovarian cancer cell death and affect STAT3 and AKT signaling proteins." *Nitric Oxide* **2013**, *35*, 93-109.
- (34) Taylor, E.L.; Megson, I.L.; Haslett, C.; Rossi, A.G. "Dissociation of DNA fragmentation from other hallmarks of apoptosis in nitric oxide-treated neutrophils: Differences between individual nitric oxide donor drugs." *Biochemical and Biophysical Research Communications* **2001**, *289*, 1229-1236.
- (35) Meßmer, U.K.; Brüne, B. "Nitric oxide (NO) in apoptotic versus necrotic RAW 264.7 macrophage cell death: The role of NO-donor exposure, NAD⁺ content, and p53 accumulation." *Archives of Biochemistry and Biophysics* **1996**, *327*, 1-10.
- (36) Suchyta, D.J.; Schoenfisch, M.H. "Encapsulation of *N*-diazeniumdiolates within liposomes for enhanced nitric oxide donor stability and delivery." *Molecular Pharmaceutics* **2015**, *12*, 3569-3574.
- (37) Szoka, F. Jr.; Papahadjopoulos, D. "Procedure for preparation of liposomes with large internal aqueous space and high capture by reverse-phase evaporation." *Proceedings of the National Academy of Sciences* **1978**, *75*, 4194-4198.

- (38) Soto, R.J.; Yang, L.; Schoenfisch, M.H. "Functionalized mesoporous silica via an aminosilane surfactant ion exchange reaction: Controlled scaffold design and nitric oxide release." *ACS Applied Materials and Interfaces* **2016**, *8*, 2220-2231.
- (39) Worley, B.V.; Schilly, K.M.; Schoenfisch, M.H. "Anti-biofilm efficacy of dual-action nitric oxide-releasing alkyl chain modified poly(amidoamine) dendrimers." *Molecular Pharmaceutics* **2015**, *12*, 1573-1583.
- (40) Ganguly, S.; Bandyopadhyay, S.; Sarkar, A.; Chatterjee, M. "Development of a semi-automated colorimetric assay for screening of anti-leishmanial agents." *Journal of Microbiological Methods* **2006**, *66*, 79-86.
- (41) Elnaggar, M.A.; Subbiah, R.; Han, D.K.; Joung, Y.K. "Lipid-based carriers for controlled delivery of nitric oxide." *Expert Opinion on Drug Delivery* **2017**, 1-13.
- (42) Ong, S.; Ming, L.C.; Lee, K.S.; Yuen, K.H. "Influence of the encapsulation efficiency and size of liposomes on the oral bioavailability of griseofulvin-loaded liposomes." *Pharmaceutics* **2016**, *8*, 25.
- (43) Villalobo, A. "Nitric oxide and cell proliferation." *FEBS Journal* **2006**, *273*, 2329-2344.
- (44) Pelicano, H.; Carney, D.; Huang, P. "ROS stress in cancer cells and therapeutic implications." *Drug Resistance Updates* **2004**, *7*, 91-110.
- (45) Shami, P.J.; Sauls, D.L.; Weinberg, J.B. "Schedule and concentration-dependent induction of apoptosis in leukemia cells by nitric oxide." *Leukemia* **1998**, *12*, 1461-1466.
- (46) Sheng, J.; Wang, D.; Braun, A.P. "DAF-FM (4-amino-5-methylamino-2',7'-difluorescein) diacetate detects impairment of agonist-stimulated nitric oxide synthesis by elevated glucose in human vascular endothelial cells: Reversal by vitamin C and L-sepiapterin." *Journal of Pharmacology and Experimental Therapeutics* **2005**, *315*, 931-940.
- (47) Skalko, N.; Peschka, R.; Altenschmidt, U.; Lung, A.; Schubert, R. "pH-sensitive liposomes for receptor-mediated delivery to chicken hepatoma (LMH) cells." *FEBS Letters* **1998**, *434*, 351-356.
- (48) Mastrobattista, E.; Storm, G.; van Bloois, L.; Reszka, R.; Bloemen, P.; Crommelin, D.; P. "Cellular uptake of liposomes targeted to intercellular adhesion molecule-1 (ICAM-1) on bronchial epithelial cells." *Biochimica et Biophysica Acta* **1999**, *1419*, 353-363.
- (49) Thurston, G.; McLean, J.W.; Rizen, M.; Baluk, P.; Haskell, A.; Murphy, T.J.; Hanahan, D.; McDonald, D.M. "Cationic liposomes target angiogenic endothelial cells in tumors and chronic inflammation in mice." *Journal of Clinical Investigation* **1998**, *101*, 1401-1413.
- (50) Cosco, D.; Bulotta, A.; Ventura, M.; Celia, C.; Calimeri, T.; Perri, G.; Paolino, D.; Costa, N.; Veri, P.; Tagliaferri, P.; Tassonem P.; Fresta, M. "In vivo activity of gemcitabine-loaded

PEGylated small unilamellar liposomes against pancreatic cancer.” *Cancer Chemotherapy and Pharmacology* **2009**, *64*, 1009-1020.

(51) Javle, M.; Curtin, N.J. “The role of PARP in DNA repair and its therapeutic exploitation.” *British Journal of Cancer* **2011**, *105*, 1114-1122.

(52) Hwang, A.; Maity, A.; McKenna, W.G.; Muschel, R.J. “Cell cycle-dependent regulation of the cyclin B1 promoter.” *The Journal of Biological Chemistry* **1995**, *270*, 28419-28424.

(53) Stacey, D.W. “Cyclin D1 serves as a cell cycle regulatory switch in actively proliferating cells.” *Current Opinion in Cell Biology* **2003**, *15*, 158-163.

CHAPTER 5: SUMMARY AND FUTURE DIRECTIONS

5.1 Summary of dissertation research

The therapeutic potential of exogenous NO has been met with many obstacles that can be overcome using drug delivery vehicles. While macromolecular NO-release systems such as gold nanoparticles,¹⁻² silica nanoparticles,³⁻¹⁰ and dendrimers¹¹⁻¹⁵ have been developed, they often fall short in terms of *in vivo* delivery due to limitations in NO donor stability. My dissertation research focused on the use of liposomes for *N*-diazeniumdiolate delivery vehicles with the intent to encapsulate and protect the NO donor. Chapter 2 detailed the synthesis and characterization of NO-releasing liposomes. As prepared using dipalmitoylphosphatidylcholine, liposomes were ~275 nm in size (diameter) and capable of releasing NO up to 7-times longer than the free NO donor alone. At 4 °C in a basic solution, the vesicles retained ~80% of their encapsulated NO at 3 months of storage. To ascertain utility of NO-releasing liposomes as anticancer agents, the cytotoxicity of the liposomes against pancreatic cancer cells was compared to the free NO donor. The free NO donor required much greater NO concentrations (2.4 mM) to elicit anticancer effects relative to the NO-releasing liposomes (0.183 mM). Thus, liposomes were shown to both enhance stability of the *N*-diazeniumdiolate and increase anticancer activity, attributed to a more localized NO delivery.

Chapter 3 described a systematic evaluation of the parameters influencing liposomal NO release. A change in liposomal NO-release kinetics was readily achieved by altering the structure of the encapsulated *N*-diazeniumdiolate and/or the composition of the lipid bilayer (i.e., phospholipid identity). As evidenced by the data, the lipid headgroup surface area was the key

factor in regulating NO-release kinetics. A notable increase in NO release was observed upon decreasing the headgroup surface area, which was attributed to the tighter headgroup packing impeding proton diffusion into the core. Nitric oxide release was also measured in blood and serum to understand the role of protein binding to the bilayer and potential bilayer disruption. The NO-release kinetics in serum were equivalent to those in buffer, while those measured in blood were ~60% faster. The faster release was attributed to the presence of cells (e.g., erythrocytes) and other potent NO scavengers such as hemoglobin, shifting the equilibrium of NO diffusion. However, lipid bilayer decomposition may also have contributed to the faster NO-release kinetics.

The impact of NO-release kinetics on cancer cell killing was detailed in Chapter 4. Specifically, the effects of fast ($t_{1/2} \sim 2.5$ h) and slow ($t_{1/2} > 72$ h) NO release on cancer cell killing were evaluated using several cancer cell lines. Slow NO-releasing liposomes yielded consistently lower LD₅₀ values (<230 μ M NO) relative to the fast NO-releasing system (>230 μ M NO), regardless of the cancer cell (breast, colorectal, and pancreatic cancer). However, time course studies revealed that a more rapid decline in cell viability occurred for the fast NO-release system. Both confocal fluorescence microscopy and flow cytometry verified that the faster NO release led to an increased rate of intracellular NO accumulation. In contrast, slow NO release resulted in a more gradual intracellular NO build up. Western blotting analysis revealed that both the slow and fast NO-release systems induced apoptosis, albeit to different degrees. Overall, these studies suggest that faster NO-release kinetics elicit anticancer action at the expense of high NO donor concentrations, whereas lower concentrations of NO via slower NO-release kinetics necessitates longer exposures to elicit cell killing. The employment of slow NO-release

systems for anticancer action may therefore minimize adverse systemic effects due to the lower LD₅₀ values.

5.2 Future directions

5.2.1 Conjugation of targeting ligands to liposome surface

In order to achieve active targeting *in vivo*, ligands should be appended to the liposome exterior that selectively bind to membrane moieties located on cancer cells. Conjugation may be performed using two different methods: bilayer insertion using long alkyl chains or covalent attachment to the lipid headgroup. Bilayer insertion of the targeting ligand is a more general approach that allows for a greater variety of ligands to be created at the expense of low bilayer incorporation efficiencies and risk of removal during transport.¹⁶⁻¹⁷ Long alkyl chains (e.g., dodecyl) are attached to the ligand that then insert themselves into the hydrophobic domain of the lipid bilayer. However, the single alkyl tail may disrupt the order of the bilayer, thus reducing the ligand's stability and increasing the likelihood of its ejection in biological milieu. One advantage though is that many chemistries, including acid chloride and maleimide reactions, may be utilized to attach a large number of ligands (Table 5.1).¹⁷

In contrast, covalent attachment relies on the reaction of an existing phospholipid comprising the bilayer with the targeting ligand. Distearoylphosphatidylethanolamine (DSPE) is widely used as a phospholipid for covalent attachment due to its reactive headgroup (i.e., a primary amine).¹⁸⁻¹⁹ For example, carboxylic acid moieties on folic acid have been reacted with DSPE's primary amine to yield folate-modified phospholipids.²⁰ By using covalent attachment, the targeting ligands are less prone to dislodge from the bilayer during blood exposure because their hydrophobic tails are identical to those comprising the existing bilayer.

Table 5.1. Ligands used for active targeting. ^a

Targeting ligands and antibodies	Alternative names (trade name)	Target
RGD peptide		Cellular adhesion molecules such as $\alpha v\beta 3$ - integrin
NGR peptide		Aminopeptidase N (CD13)
GM-CSF glycoprotein		GM-CSF receptor
Folate		Folate receptor
Transferrin		Transferrin receptor
Galactosamine		Galactosamine receptors on hepatocytes
Anti-VEGFR	2C3	Vasculature endothelial growth-factor receptor (FLK1)
Anti-ERBB2	Trastuzumab (Herceptin)	ERBB2 receptor
Anti-CD20	Rituximab (Rituxan), ibritumomab tiuxetan (Zevalin)	CD20, a B-cell surface antigen
Anti-CD22	Epratuzumab, LL2, RFB4	CD22, a B-cell surface antigen
Anti-CD19	B4, HD37	CD19, a pan-B cell surface epitope
Anti-CD33	Gemtuzumab, ozogamicin (Mylotarg)	CD33, a sialo-adhesion molecule, leukocyte differentiation antigen
Anti-CD33	M195	CD33, a T-cell epitope
Anti-CD25	Anti-Tac, LMB2	CD25, α -subunit of the interleukin-2 receptor on activated T cells
Anti-CD25	Denileukin diftitox (Ontak)	Interleukin-2 receptor
Anti-HLA-DR10 β	Lym1	HLA-DR10 β subunit
Anti-tenascin	81C6	Extracellular-matrix protein overexpressed in many tumors
Anti-CEA	MN-14, F6, A5B7	CEA
Anti-MUC1	HMFG1, BrE3	MUC1, an aberrantly glycosylated epithelial mucin
Anti-TAG72	CC49, B72.3	TAG72, oncofetal antigen tumor-associated glycoprotein-72

^aAdapted with permission from Nature Reviews Cancer, 2002, 2, Allen, T.M. "Ligand-targeted therapeutics in anticancer therapy" pages 750–763, Copyright 2002 Nature Publishing Group.

Utilizing the above chemistries, many targeting ligands have been appended to the exterior of liposomes.¹⁸ Folic acid, a critical biomolecule required for DNA synthesis, has been conjugated to the surface of liposomes to enable binding to the overexpressed folate receptors on the surface of cancer cells.²¹⁻²² In order to compensate for the increased replication rates of cancer, folate receptors are more populated on their cell surface. Folate-appended arsenic trioxide liposomes were 9- and 28-times more toxic towards HeLa and KB cells, respectively, than the same liposomes without the folate groups. Transferrin, a beta globulin protein that functions to transport iron in biological fluids, represents another ligand that has been attached to liposomes. Like folate, the transferrin receptor is overexpressed on the surface of cancer cells.²³⁻²⁴ As DNA polymerase requires iron for DNA replication, increased transferrin uptake helps maintain iron homeostasis.²⁵ Liposomes bearing transferrin ligands have exhibited improved cellular uptake (~10-times greater) relative to controls as measured via confocal fluorescence microscopy.²⁶

The large nutrient requirement for tumors and cancer cells has lead to an emerging area of research whereby sugar units (e.g., glucose) are attached to the exterior of drugs, with the intent of facilitating more rapid uptake resulting from the high activity of the glucose transport receptors (e.g., GLUT-1) on cancer cells.²⁷⁻²⁸ Upon glucose conjugation to polymeric vesicles, for example, greater intracellular accumulation was observed as measured by transmission electron microscopy and flow cytometry.²⁹ The attachment of similar ligands to the surface of NO-releasing liposomes may lead to greater accumulation at cancer sites. For any modification, it will be necessary to examine any influence on the NO release. Future work should include a multi-pronged study using cytotoxicity assays, confocal fluorescence microscopy, and flow

cytometry to elucidate if NO-releasing liposomes would benefit from the conjugation of targeting ligands.

5.2.2 *Dual-encapsulation to enhance anticancer action*

While evidence of the chemotherapeutic effects of NO-releasing liposomes was provided in Chapter 4, reducing the cytotoxic concentrations into the nanomolar range would improve the therapeutic potential of our system. Our lab has previously reported on the synthesis of dual-action scaffolds that are capable of inducing cell death via multiple mechanisms.³⁰⁻³³ Similarly, it is possible to encapsulate NO with other therapeutics within the liposomes to potentially improve anticancer activity. Molecules of varying charges, molecular weights, and solubilities, have all been encapsulated within liposomes. Indeed, the hydrophilic (i.e., aqueous core) and hydrophobic (i.e., lipid bilayer) domains located within liposomes facilitate encapsulation of molecules exhibiting differing properties (e.g., doxorubicin and DNA).

The constricted vasculature of tumor sites inhibits extravasation of many drug delivery systems.³⁴ Pretreatment with NO has been shown to increase the efficacy of current chemotherapeutics due to NO's vasodilatory properties.³⁵⁻³⁶ The enlargement of tumor blood vasculature allows for improved delivery and accumulation of the drug delivery system at the malignant site. Unlike current methods, multi-drug encapsulation within liposomes would remove the need for pretreatment because the liposomes could be engineered to have NO released simultaneously with the drug of interest.

Future studies should focus on the combination of doxorubicin and *N*-diazoniumdiolates. Due to poor water solubility, doxorubicin is a difficult drug to deliver in the body. Barenholz described the benefit of encapsulating doxorubicin within liposomes.³⁷ In this manner, large amounts of doxorubicin were loaded into liposomes using a unique transmembrane ammonium

sulfate gradient.³⁸ Although showing some efficacy *in vivo*, rather large doses were required due in part to the constricted vasculature system. A number of adverse side effects were reported, including mouth sores and acral erythema (i.e., hand-foot syndrome). While Pedrini et al. combined liposomal doxorubicin with NO using nitrate-modified doxorubicin, this derivative, as with most organic nitrates, required enzymatic cleavage for the NO to be released.³⁹ In contrast, encapsulated *N*-diazoniumdiolates would offer spontaneous release of NO under biological conditions. Incorporation of both *N*-diazoniumdiolates and doxorubicin into the liposome system may enable a practical chemosensitization scaffold with dual-action efficacy.

Gemcitabine represents an equally attractive co-encapsulant with NO donors. Known as the gold standard for treating pancreatic cancer, gemcitabine is utilized for its ability to replace essential building blocks in the synthesis of DNA.⁴⁰ In contrast to NO, which would initiate cell membrane disruption, gemcitabine necessitates cellular uptake and replication in order to exert its therapeutic activity. Liposomes have long been investigated as delivery agents for gemcitabine due to the potential for enhanced cellular uptake relative to free molecules. *In vivo* studies demonstrated that liposomal gemcitabine showed greater reduction in tumor size at 3-times lower concentrations (relative to free gemcitabine).⁴⁰ Introducing NO into the liposomal system may increase accumulation of the vesicles at the cancer site and increase anticancer action to an even greater extent due to chemosensitization, as well as exerting nitrosative/oxidative stress from both inside and outside the cell.

5.2.3 *Antibacterial properties of NO-releasing liposomes*

Liposomes have been utilized as antibacterial agents for the same reason they are attractive as chemotherapeutics. Efficient delivery and cellular uptake of small molecule antibiotics have been major obstacles for treating both chronic and acute infections. Through the

encapsulation of tobramycin and gentamicin, liposomes have shown to improve biocidal action against *Pseudomonas aeruginosa* relative to the free antibiotics.⁴¹ Depending on the bacterial strain, minimum inhibitory concentrations (MIC) were nearly 128-times lower when the antibiotic was encapsulated versus in free form, highlighting the potential of liposomes as vehicles for antibacterials.⁴¹ Association with bacteria is often a decisive factor in determining the biocidal role of a therapeutic.^{7,9} As liposomes can be designed to have distinct exterior charge (i.e., electrostatic attraction to bacteria) and facilitate fusion into the bacteria, key targeting advantages over other drug delivery scaffolds (e.g., silica nanoparticles) become apparent.

Our lab has previously synthesized macromolecular NO-release scaffolds having strong biocidal action. To date, the two most potent include NO-releasing dendritic polymers and polysaccharides.^{11-15,42-45} The large NO payloads and bacteria-scaffold association of these delivery systems affords excellent bacteria eradication properties. While both scaffolds have demonstrated success, premature release of NO before localization at the bacterial membrane remains a potential concern. As demonstrated in Chapter 4, liposomes mitigate premature NO release via encapsulation of the NO donor. Encapsulation of macromolecular NO-release scaffolds thus might prove useful in further improving biocidal activity.

Khopade et al. have reported successful encapsulation of dendrimers within liposomes, resulting in final vesicle sizes ranging from 100 nm to 1 μm .⁴⁶ Both dendrimer loading efficiency and release kinetics were tuned by varying the dendrimer structure or the lipid bilayer composition. Unfortunately, the use of dendrimers has been linked to liposome leakage and stability shortcomings due to the dendritic chains intercalating into the bilayer.⁴⁷ It is therefore important to study the interaction of the dendrimer with the liposome membrane after encapsulation to ensure the formation of a structurally stable system. Dynamic light scattering,

fluorophore co-encapsulation, and nuclear magnetic resonance spectroscopy could each be utilized to examine liposome rupture and encapsulant retention.

Likewise, polysaccharides could be encapsulated within liposomes. For example, Liu et al. coencapsulated a polysaccharide derived from the *Ganoderma lucidum* fungus (molecular weight=37 kDa) with ovalbumin (molecular weight=43 kDa) to create a potent vaccine.⁴⁸ Although polysaccharides are less likely to damage the liposome membrane due to their hydrophilic nature, lower encapsulation efficiencies may be observed as a result of their high molecular weight. Encapsulation studies should be performed as a function of the polysaccharides molecular weight to understand loading and the resulting antibacterial action.

5.3 Conclusions

Current macromolecular NO-release scaffolds may have limited efficacy in delivering NO intravenously (i.e., bloodstream administration) to a target of interest due to premature NO release. Liposomes represent a unique alternative for *in vivo* NO delivery. The biodegradability and biocompatibility of liposomes mitigates potential immune response and cytotoxicity, while the lipid bilayer impedes proton diffusion into the aqueous core, thus protecting the NO donor from degradation and preserving its therapeutic payload. The studies provided in this dissertation support that liposomes can both encapsulate *N*-diazoniumdiolates and enhance their stability, and exhibit potent tumoricidal activity against representative aggressive cancer cells. In order to further increase the potential *in vivo* chemotherapeutic effects of the NO-releasing system, studies should be performed that evaluate the specificity of the liposomes for cancer cells. Additionally, a direct comparison to current chemotherapeutics (e.g., doxorubicin) in regards to anticancer action, specificity, and *in vivo* stability would highlight the benefits of NO-releasing liposomes as an alternative treatment strategy. Understanding the obstacles that limit the use of

NO as a systemic therapeutic is critical in order to design more effective *in vivo* delivery vehicles.

REFERENCES

- (1) Rothrock, A.R.; Donkers, R.L.; Schoenfish, M.H. "Synthesis of nitric oxide-releasing gold nanoparticles" *Journal of the American Chemical Society* **2005**, *127*, 9362-9363.
- (2) Polizzi, M.A.; Stasko, N.A.; Schoenfish, M.H. "Water-soluble nitric oxide-releasing gold nanoparticles" *Langmuir* **2007**, *23*, 4938-4943.
- (3) Shin, J.H.; Metzger, S.K.; Schoenfish, M.H. "Synthesis of nitric oxide-releasing silica nanoparticles" *Journal of the American Chemical Society* **2007**, *129*, 4612-4619.
- (4) Shin, J.H.; Schoenfish, M.H. "Inorganic/organic hybrid silica nanoparticles as a nitric oxide delivery scaffold" *Chemistry of Materials* **2008**, *20*, 239-249.
- (5) Hetrick, E.M.; Shin, J.H.; Stasko, N.A.; Johnson, C.B.; Wespe, D.A.; Holmuhamedov, E.; Schoenfish, M.H. "Bactericidal efficacy of nitric oxide-releasing silica nanoparticles" *ACS Nano* **2008**, *2*, 235-246.
- (6) Soto, R.J.; Yang, L.; Schoenfish, M.H. "Functionalized mesoporous silica via an aminosilane surfactant ion exchange reaction: Controlled scaffold design and nitric oxide release" *ACS Applied Materials & Interfaces* **2016**, *8*, 2220-2231.
- (7) Carpenter, A.W.; Slomberg, D.L.; Rao, K.S.; Schoenfish, M.H. "Influence of scaffold size on bactericidal activity of nitric oxide-releasing silica nanoparticles" *ACS Nano* **2011**, *5*, 7235-7244.
- (8) Hetrick, E.M.; Shin, J.H.; Paul, H.S.; Schoenfish, M.H. "Anti-biofilm efficacy of nitric oxide-releasing silica nanoparticles" *Biomaterials* **2009**, *30*, 2782-2789.
- (9) Slomberg, D.L.; Lu, Y.; Broadnax, A.D.; Hunter, R.A.; Carpenter, A.W.; Schoenfish, M.H. "Role of size and shape on biofilm eradication for nitric oxide-releasing silica nanoparticles" *ACS Applied Materials & Interfaces* **2013**, *5*, 9322-9329.
- (10) Stevens, E.V.; Carpenter, A.W.; Shin, J.H.; Liu, J.; Der, C.J.; Schoenfish, M.H. "Nitric oxide-releasing silica nanoparticle inhibition of ovarian cancer cell growth" *Molecular Pharmaceutics* **2010**, *7*, 775-785.
- (11) Stasko, N.A.; Schoenfish, M.H. "Dendrimers as a scaffold for nitric oxide release" *Journal of the American Chemical Society* **2006**, *128*, 8265-8271.
- (12) Lu, Y.; Sun, B.; Li, C.; Schoenfish, M.H. "Structurally diverse nitric oxide-releasing poly(propylene imine) dendrimers" *Chemistry of Materials* **2011**, *23*, 4227-4233.
- (13) Sun, B.; Slomberg, D.L.; Chudasama, S.L.; Lu, Y.; Schoenfish, M.H. "Nitric oxide-releasing dendrimers as antibacterial agents" *Biomacromolecules* **2012**, *13*, 3343-3354.

- (14) Worley, B.V.; Schilly, K.M.; Schoenfisch, M.H. "Anti-biofilm efficacy of dual-action nitric oxide-releasing alkyl chain modified poly(amidoamine) dendrimers" *Molecular Pharmaceutics* **2015**, *12*, 1573-1583.
- (15) Backlund, C.J.; Worley, B.V.; Schoenfisch, M.H. "Anti-biofilm action of nitric oxide-releasing alkyl-modified poly(amidoamine) dendrimers against *Streptococcus mutans*" *Acta Biomaterialia* **2016**, *29*, 198-205.
- (16) Fang, R.H.; Hu, C.; Chen, K.; Luk, B.T.; Carpenter, C.W.; Gao, W.; Li, S.; Zhang, D.; Lu, W.; Zhang, L. "Lipid-insertion enables targeting functionalization of erythrocyte membrane-clocked nanoparticles" *Nanoscale* **2013**, *5*, 8884-8888.
- (17) Nie, Y.; Ding, H.; Xie, L.; Li, L.; He, B.; Wu, Y.; Gu, Z. "Cholesterol derivatives based charged liposomes for doxorubicin delivery: Preparation, *in vitro*, and *in vivo* characterization" *Theranostics* **2012**, *2*, 1092-1103.
- (18) Allen, T.M. "Ligand-targeted therapeutics in anticancer therapy" *Nature Reviews Cancer* **2002**, *2*, 750-763.
- (19) Wang, R.; Xiao, R. Zeng, Z.; Xu, L.; Wang, J. "Applications of poly(ethylene glycol)-distearoylphosphatidylethanolamine (PEG-DSPE) block copolymers and their derivatives as nanomaterials in drug delivery" *International Journal of Nanomedicine* **2012**, *7*, 4185-4198.
- (20) Gabizon, A.; Horowitz, A.T.; Goren, D.; Tzemach, D.; Mandelbaum-Shavit, F.; Qazen, M.M.; Zalipsky, S. "Targeting folate receptor with folate linked to extremities of poly(ethylene glycol)-grafted liposomes: In vitro studies" *Bioconjugate Chemistry* **1999**, *10*, 289-298.
- (21) Zwicke, G.L.; Mansoori, G.A.; Jeffery, C.J. "Utilizing the folate receptor for active targeting of cancer nanotherapeutics" *Nano Reviews* **2012**, *3*, 18496.
- (22) Chen, H.; Ahn, R.; Van der Bossche, J.; Thompson, D.H.; O'Halloran, T.V. "Folate-mediated intracellular drug delivery increases the anticancer efficacy of nanoparticulate formulation of arsenic trioxide" *Molecular Cancer Therapeutics* **2009**, *8*, 1955-1963.
- (23) Zhai, G.; Wu, J.; Yu, B.; Guo, C.; Yang, X.; Lee, R.J. "A transferring receptor-targeted liposomal formulation for docetaxel" *Journal of Nanoscience and Nanotechnology* **2010**, *10*, 5129-5136.
- (24) Daniels, T.R.; Bernabeu, E.; Rodriguez, J.A.; Patel, S.; Kozman, M.; Chiappetta, D.A.; Holler, E.; Ljubimova, J.Y.; Helguera, G.; Penichet, M.L. "Transferrin receptors and the targeted delivery of therapeutic agents against cancer" *Biochimica et Biophysica Acta* **2012**, *1820*, 291-317.
- (25) Zhang, C. "Essential functions of iron-requiring proteins in DNA replication, repair and cell cycle control" *Protein and Cell* **2014**, *5*, 750-760.

- (26) Voinea, M.; Dragomir, E.; Manduteanu, I.; Simionescu, A. "Binding and uptake of transferrin-bound liposomes targeted to transferrin receptors of endothelial cells" *Vascular Pharmacology* **2002**, *39*, 13-20.
- (27) Higashi, T.; Tamaki, N.; Honda, T.; Torizuka, T.; Kimura, T.; Inokuma, T.; Ohshio, G.; Hosotani, R.; Imamura, M.; Konishi, J. "Expression of glucose transporters in human pancreatic tumors compared with increased FDG accumulation in PET study" *Journal of Nuclear Medicine* **1997**, *38*, 1337-1344.
- (28) Smith, T. "Facilitative glucose transport expression in human cancer tissue" *British Journal of Biomedical Science* **1999**, *56*, 285-292.
- (29) Dufes, C.; Schatzlein, A.G.; Tetley, L.; Gray, A.I.; Watson, D.G.; Olivier, J.; Couet, W.; Uchegbu, I. "Niosomes and polymeric chitosan based vesicles bearing transferrin and glucose ligands for drug targeting" *Pharmaceutical Research* **2000** *17*, 1250-1258.
- (30) Worley, B.V.; Schilly, K.M.; Schoenfisch, M.H. "Anti-biofilm efficacy of dual-action nitric oxide-releasing alkyl chain modified poly(amidoamine) dendrimers" *Molecular Pharmaceutics* **2015**, *12*, 1573-1583.
- (31) Storm, W.L.; Johnson, J.A.; Worley, B.V.; Slomberg, D.L.; Schoenfisch, M.H. "Dual action antimicrobial surfaces via combined nitric oxide and silver release" *Journal of Biomedical Materials Research Part A* **2015**, *103*, 1974-1984.
- (32) Carpenter, A.W.; Worley, B.V.; Slomberg, D.L.; Schoenfisch, M.H. "Dual action antimicrobials: Nitric oxide release from quaternary ammonium-functionalized silica nanoparticles" *Biomacromolecules* **2012**, *13*, 3334-3342
- (33) Worley, B.V.; Slomberg, D.L.; Schoenfisch, M.H. "Nitric oxide-releasing, quaternary ammonium-modified poly(amidoamine) dendrimers as dual action antibacterial agents" *Bioconjugate Chemistry* **2014**, *25*, 918-927.
- (34) Jang, S.H.; Wientjes, M.G.; Lu, D.; Au, J. "Drug delivery and transport to solid tumors" *Pharmaceutical Research* **2003**, *20*, 1337-1350.
- (35) Sullivan, R.; Graham, C.H. "Chemosensitization of cancer by nitric oxide" *Current Pharmaceutical Design* **2008**, *14*, 1113-1123.
- (36) Matthews, N.E.; Adams, M.A.; Maxwell, L.R.; Gofton, T.E.; Graham, C.H. "Nitric oxide-mediated regulation of chemosensitivity in cancer cells" *Journal of the National Cancer Institute* **2001**, *93*, 1879-1885.
- (37) Barenholz, Y.C. "Doxil – The first FDA-approved nano-drug: Lessons learned" *Journal of Controlled Release* **2012**, *160*, 117-134.

- (38) Haran, G.; Cohen, R.; Bar, L.K.; Barenholz, Y. "Transmembrane ammonium sulfate gradients in liposomes produce efficient and stable entrapment of amphipathic weak bases" *Biochimica et Biophysica Acta* **1993**, *1151*, 201-215.
- (39) Pedrini, I.; Gazzano, E.; Chegaev, K.; Rolando, B.; Marengo, A.; Kopecka, J.; Fruttero, R.; Ghigo, D.; Arpicco, S.; Riganti, C. "Liposomal nitrooxy-doxorubicin: One step over caelyx in drug-resistant human cancer cells" *Molecular Pharmaceutics* **2014**, *11*, 3068-3079.
- (40) Cosco, D.; Bulotta, A.; Ventura, M.; Celia, C.; Calimeri, T.; Perri, G.; Paolino, D.; Costa, N.; Neri, P.; Tagliaferri, P.; Tassone, P.; Fresta, M. "In vivo activity of gemcitabine-loaded PEGylated small unilamellar liposomes against pancreatic cancer" *Cancer Chemotherapy and Pharmacology* **2009**, *64*, 1009-1020.
- (41) Mugabe, C.; Halwani, M.; Azghani, A.O.; Lafrenie, R.M.; Omri, A. "Mechanism of enhanced activity of liposome-entrapped aminoglycosides against resistant strains of *Pseudomonas aeruginosa*" *Antimicrobial Agents and Chemotherapy* **2006**, *50*, 2016-2022.
- (42) Reighard, K.P.; Hill, D.B.; Dixon, G.A.; Schoenfisch, M.H. "Disruption and eradication of *P. aeruginosa* biofilms using nitric oxide-releasing chitosan oligosaccharides" *Biofouling* **2015**, *31*, 775-787.
- (43) Reighard, K.P.; Schoenfisch, M.H. "Antibacterial action of nitric oxide-releasing chitosan oligosaccharides against *Pseudomonas aeruginosa* under aerobic and anaerobic conditions" *Antimicrobial Agents and Chemotherapy* **2015**, *59*, 6506-6513.
- (44) Lu, Y.; Sha, A.; Hunter, R.A.; Soto, R.J.; Schoenfisch, M.H. "S-nitrosothiol-modified nitric oxide-releasing chitosan oligosaccharides as antibacterial agents" *Acta Biomaterialia* **2015**, *12*, 62-69.
- (45) Lu, Y.; Slomberg, D.L.; Schoenfisch, M.H. "Nitric oxide-releasing chitosan oligosaccharides as antibacterial agents" *Biomaterials* **2014**, *35*, 1716-1724.
- (46) Khopade, A.J.; Caruso, F.; Tripathi, P.; Nagaich, S.; Jain, N.K. "Effect of dendrimers on entrapment and release of bioactive from liposomes" *International Journal of Pharmaceutics* **2002**, *232*, 157-162.
- (47) Evans, K.O.; Laszlo, J.A.; Compton, D.L. "Carboxyl-terminated PAMAM dendrimer interaction with 1-palmitoyl-2-oleoyl phosphocholine bilayers" *Biochimica et Biophysica Acta* **2014**, *1838*, 445-455.
- (48) Liu, Z.; Xing, J.; Zheng, S.; Bo, R.; Luo, L.; Huang, Y.; Niu, Y.; Li, Z.; Wang, D.; Hu, Y.; Liu, J.; Wu, Y. "*Ganoderma lucidum* polysaccharides encapsulated in liposomes as an adjuvant to promote Th1-bias immune response" *Carbohydrate Polymers* **2016**, *142*, 141-148.

Appendix A: Supplemental Information of Chapter 2

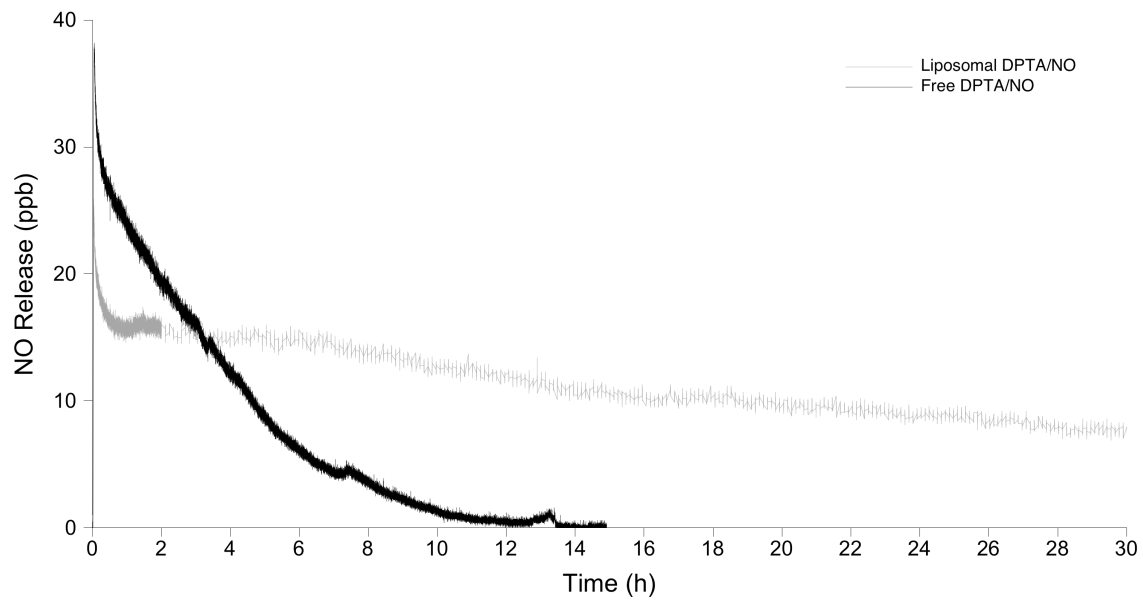


Figure A1. Nitric oxide release profile measured in real-time of free DPTA/NO versus liposomal DPTA/NO in 10 mM PBS (pH 7.4, 37 °C).

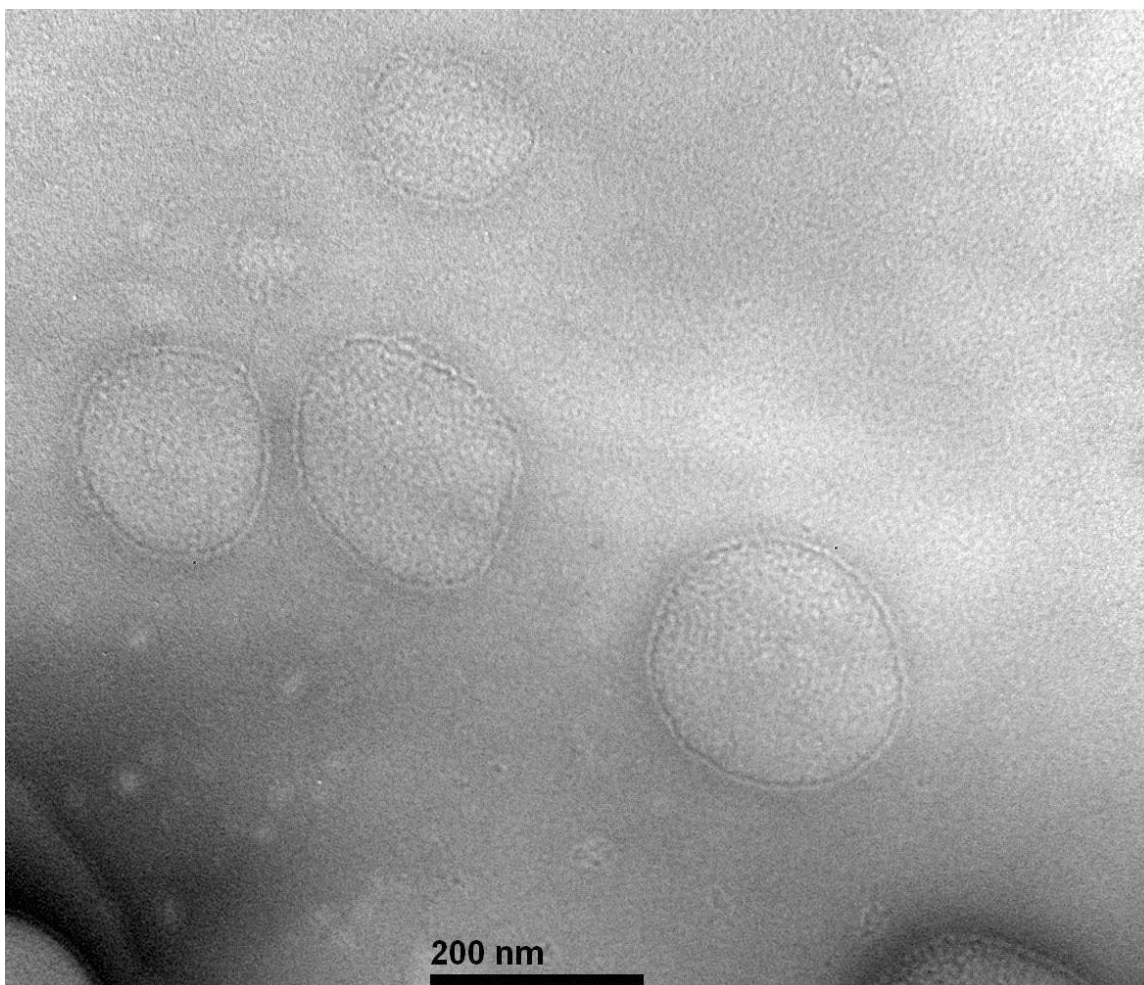


Figure A2. Transmission electron micrograph of DPTA/NO loaded liposomes after a 1:1 dilution and negative-staining with 2% uranyl acetate. Any shape deformation is most likely attributed to the liposomes flattening on the grid's surface.

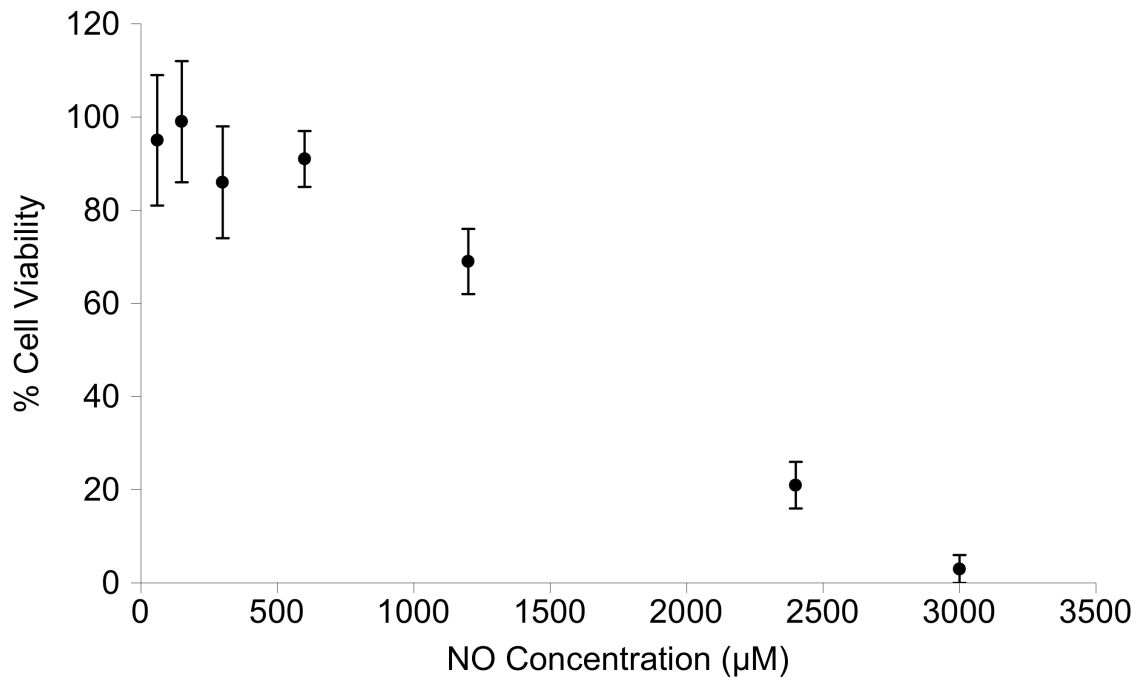


Figure A3. Cytotoxicity on human PANC-1 cells after a 24 h incubation using varying concentrations of free DPTA/NO. Error bars indicated standard deviation from ≥ 3 separate experiments.

Appendix B: Supplemental Information of Chapter 3

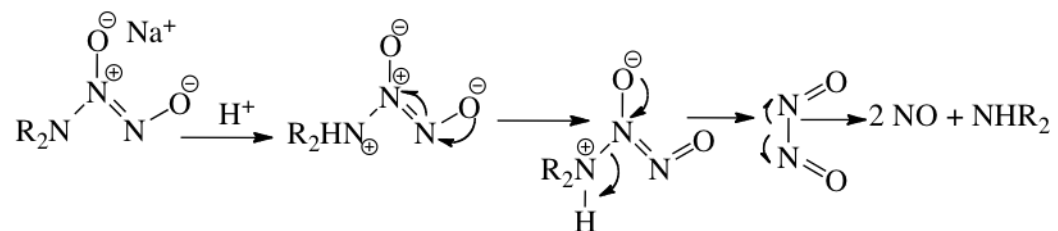


Figure B1. Proton-initiated decomposition mechanism of *N*-diazeniumdiolates to liberate NO.

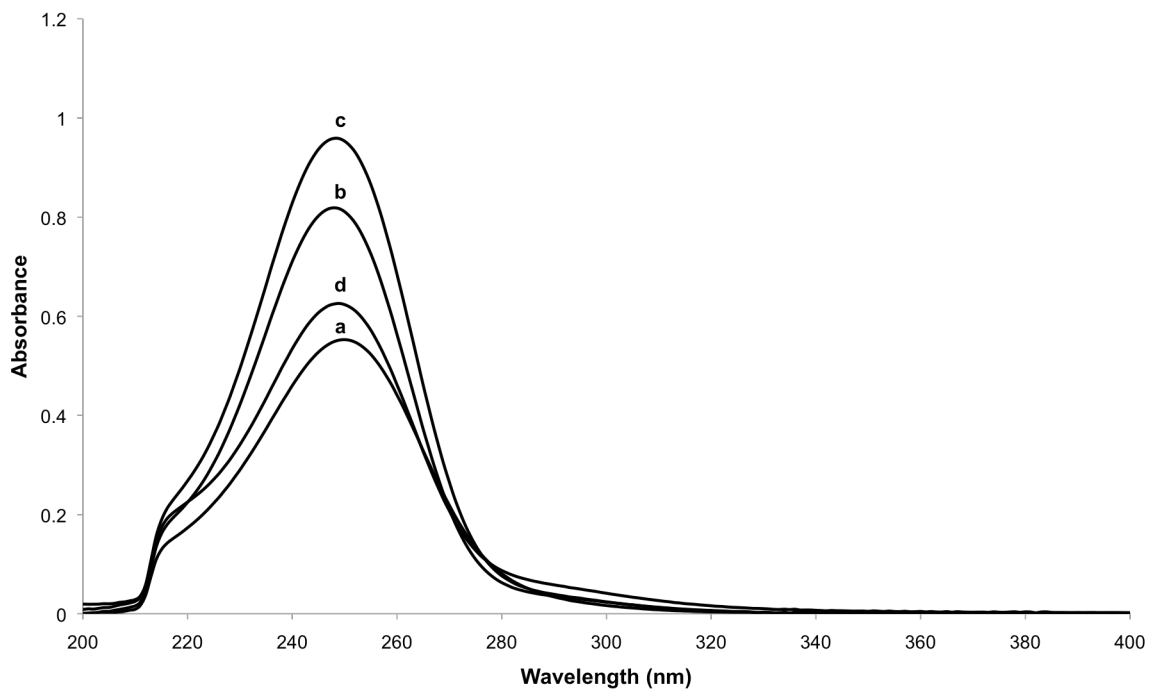
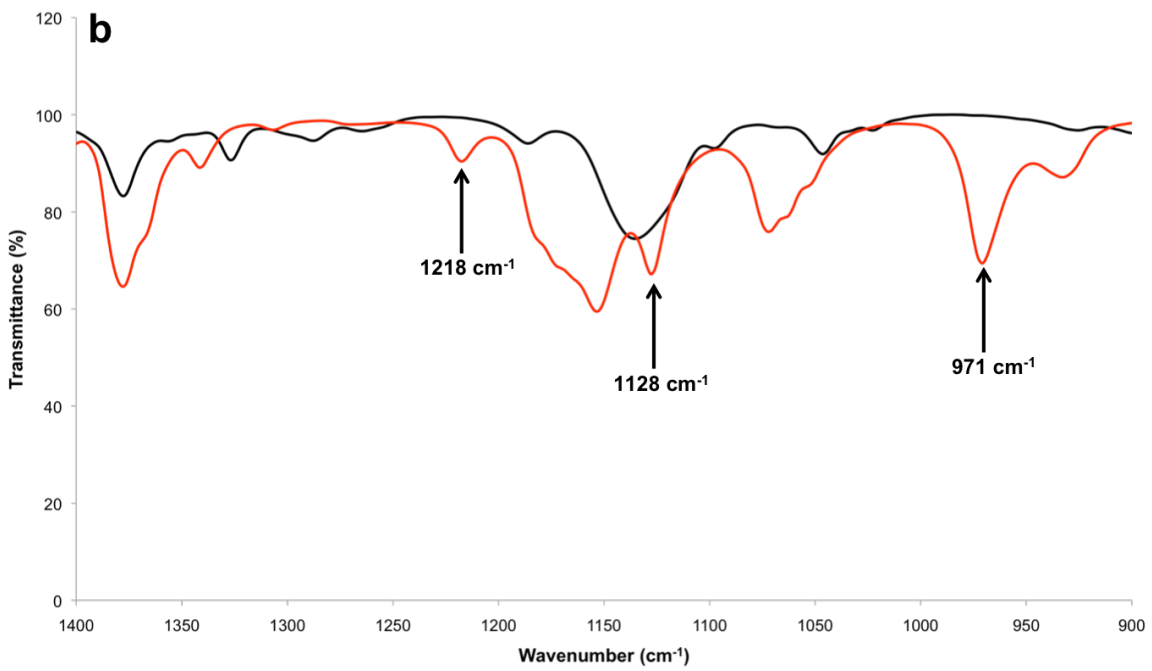
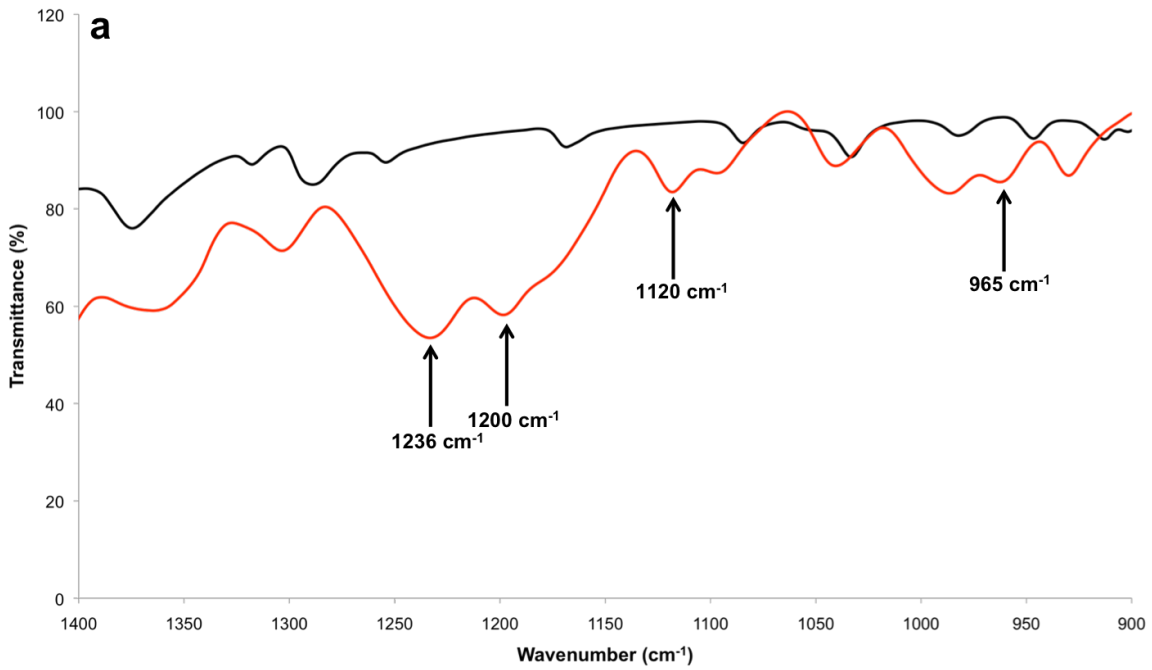


Figure B2. UV-vis spectra of 0.020 mg/mL (a) PROLI/NO, (b) DEA/NO, (c) PAPA/NO, and (d) SPER/NO in 50 mM NaOH. Typical 252 nm absorbance peak associated with the diazeniumdiolate group is observed.¹



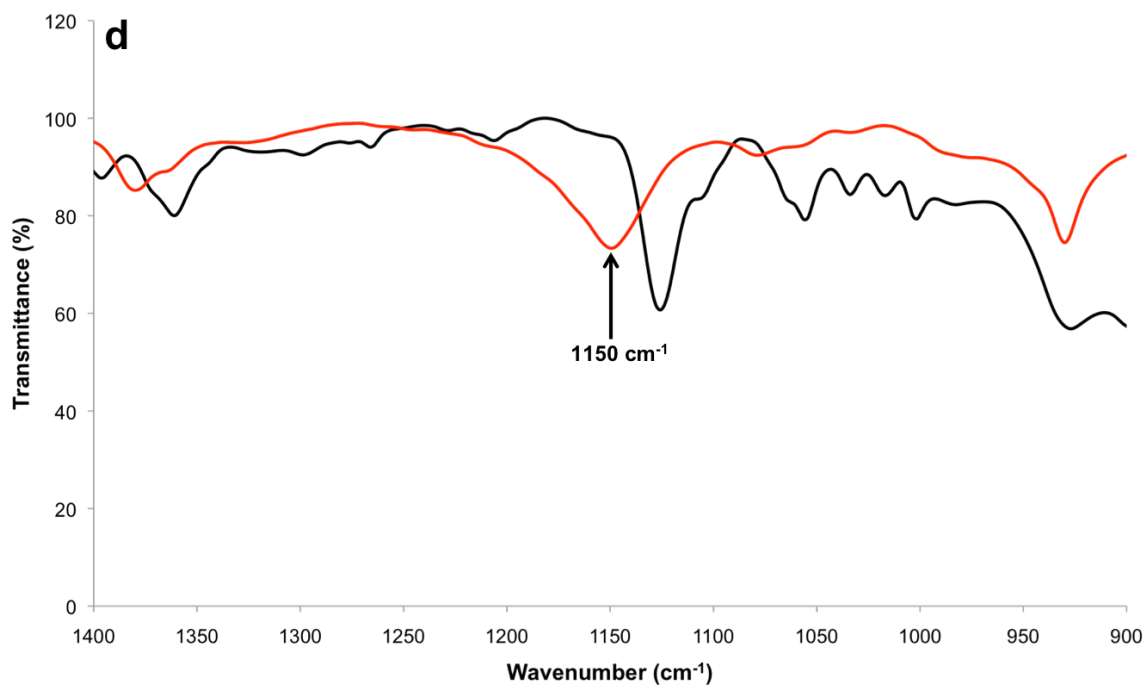
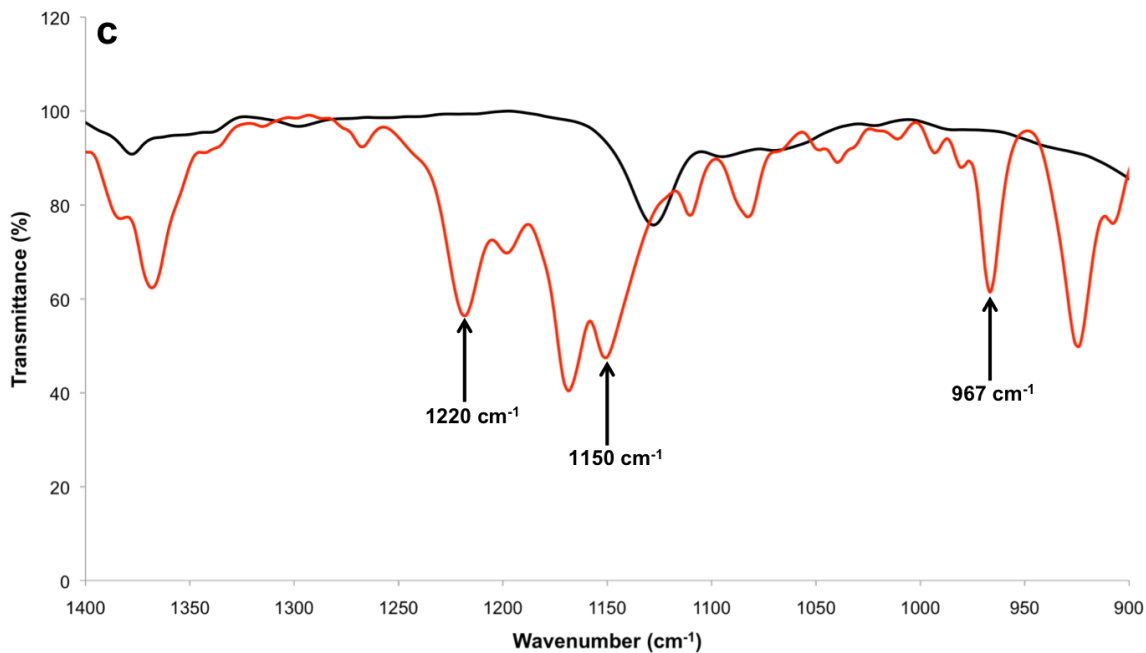


Figure B3. FTIR spectra of (a) PROLI/NO, (b) DEA/NO, (c) PAPA/NO, and (d) SPER/NO. Precursor amine spectra are in black and NO donors are in red. N-O stretches ($1236\text{-}1210\text{ cm}^{-1}$), in-plane N_2 symmetric stretches ($1200\text{-}1150\text{ cm}^{-1}$ and $965\text{-}975\text{ cm}^{-1}$), and N-N stretches ($1128\text{-}1120\text{ cm}^{-1}$) can be observed due to the presence of the diazeniumdiolate group.¹⁻²

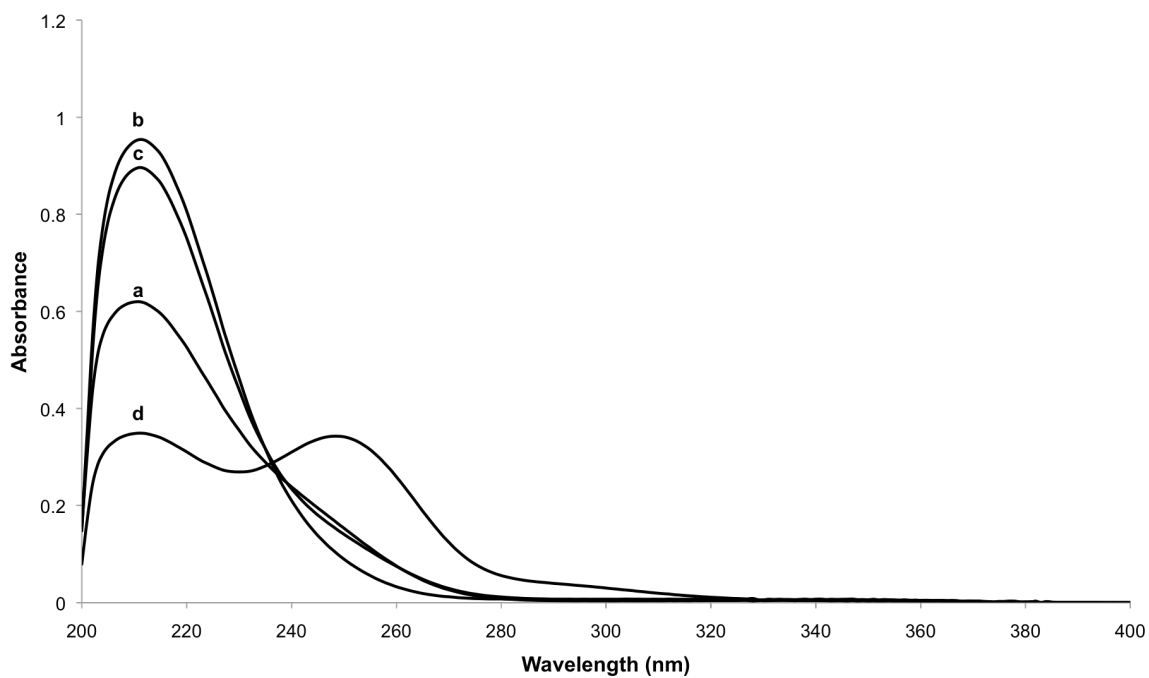


Figure B4. UV-vis spectra of 0.020 mg/mL (a) PROLI/NO, (b) DEA/NO, (c) PAPA/NO, and (d) SPER/NO in 10 mM PBS (pH 7.4) after incubation at 37 °C for 2 h. Absorbance peak at 210 nm is associated with nitrite/nitrate formation.

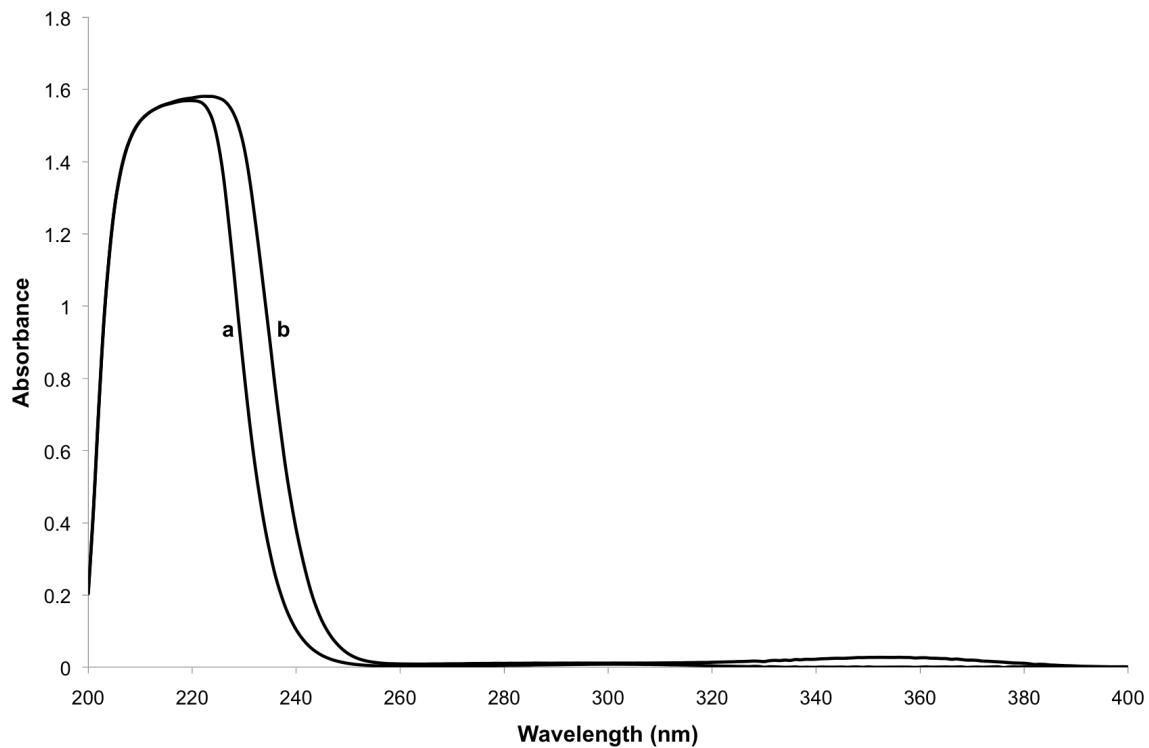


Figure B5. UV-vis spectra of 0.010 mg/mL (a) sodium nitrate and (b) sodium nitrite in 10 mM PBS (pH 7.4, 37 °C). Peak at ~350 nm is from sodium nitrite.

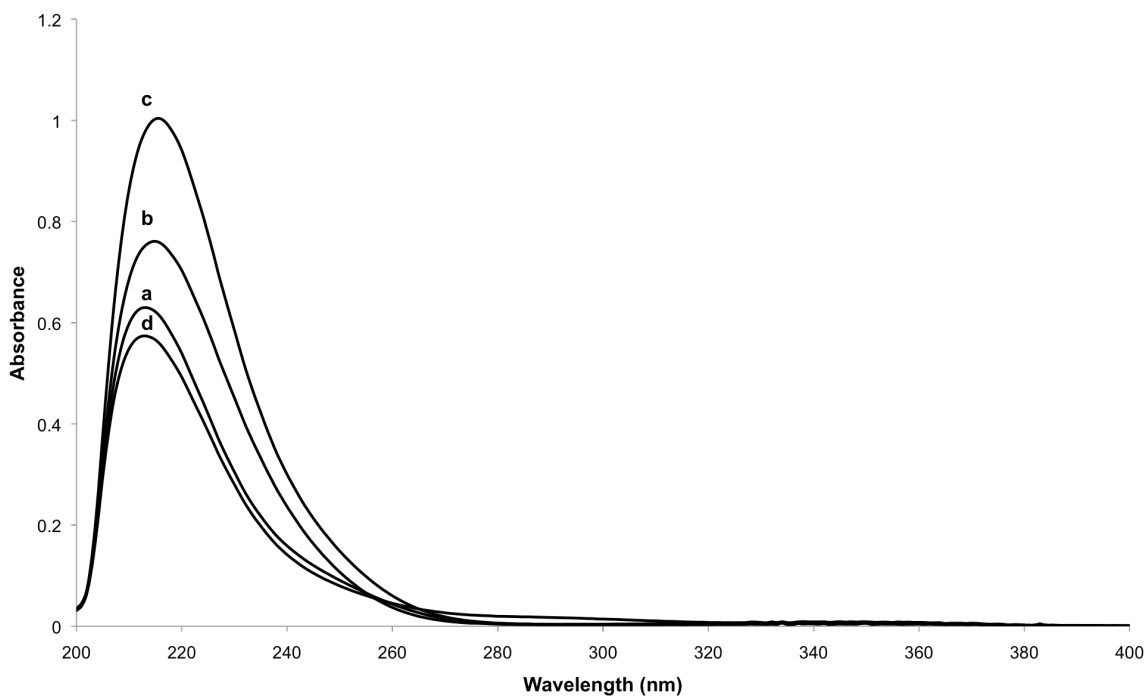
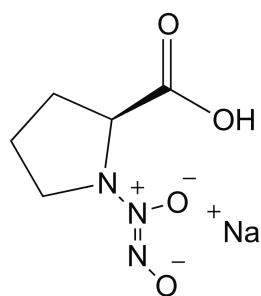
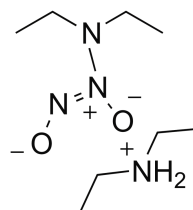


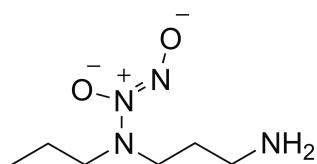
Figure B6. UV-vis spectra of 0.020 mg/mL (a) PROLI/NO, (b) DEA/NO, (c) PAPA/NO, and (d) SPER/NO in 10 mM MES buffer (pH 5.4) after incubation at 37 °C for 2 h.



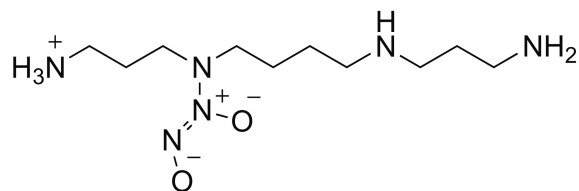
PROLI/NO ($t_{1/2} = 2$ s)



DEA/NO ($t_{1/2} = 2$ min)



PAPA/NO ($t_{1/2} = 15$ min)



SPER/NO ($t_{1/2} = 37$ min)

Figure B7. *N*-diazeniumdiolate NO donors with their reported NO-release half-lives in 10 mM PBS (pH 7.4, 37 °C).³

Table B1. Nitric oxide-release properties of DPPC liposomes as a function of encapsulated *N*-diazeniumdiolate NO donor in MES (pH = 5.4) at 37 °C. ^a

NO donor	$t_{1/2}^b$ (h)	t_d^c (h)	[NO] _{total} ^d (μmol/mL)
PROLI/NO	0.06 ± 0.02	1.7 ± 0.9	4.71 ± 0.80
DEA/NO	0.12 ± 0.04	5.5 ± 1.6	8.37 ± 0.62
PAPA/NO	0.84 ± 0.24	20.7 ± 4.6	7.75 ± 1.09
SPER/NO	10.4 ± 1.9	44 ± 9.0	6.81 ± 0.78

^aError indicates standard deviation from at least 3 separate liposome preparations. ^bHalf-life of NO release. ^cDuration of NO release until the measured NO reached 10 ppb per 300 μL of liposomes (three-times the detection limit of the instrument). ^dTotal amount of NO released normalized to the injected volume from the liposome stock solution.

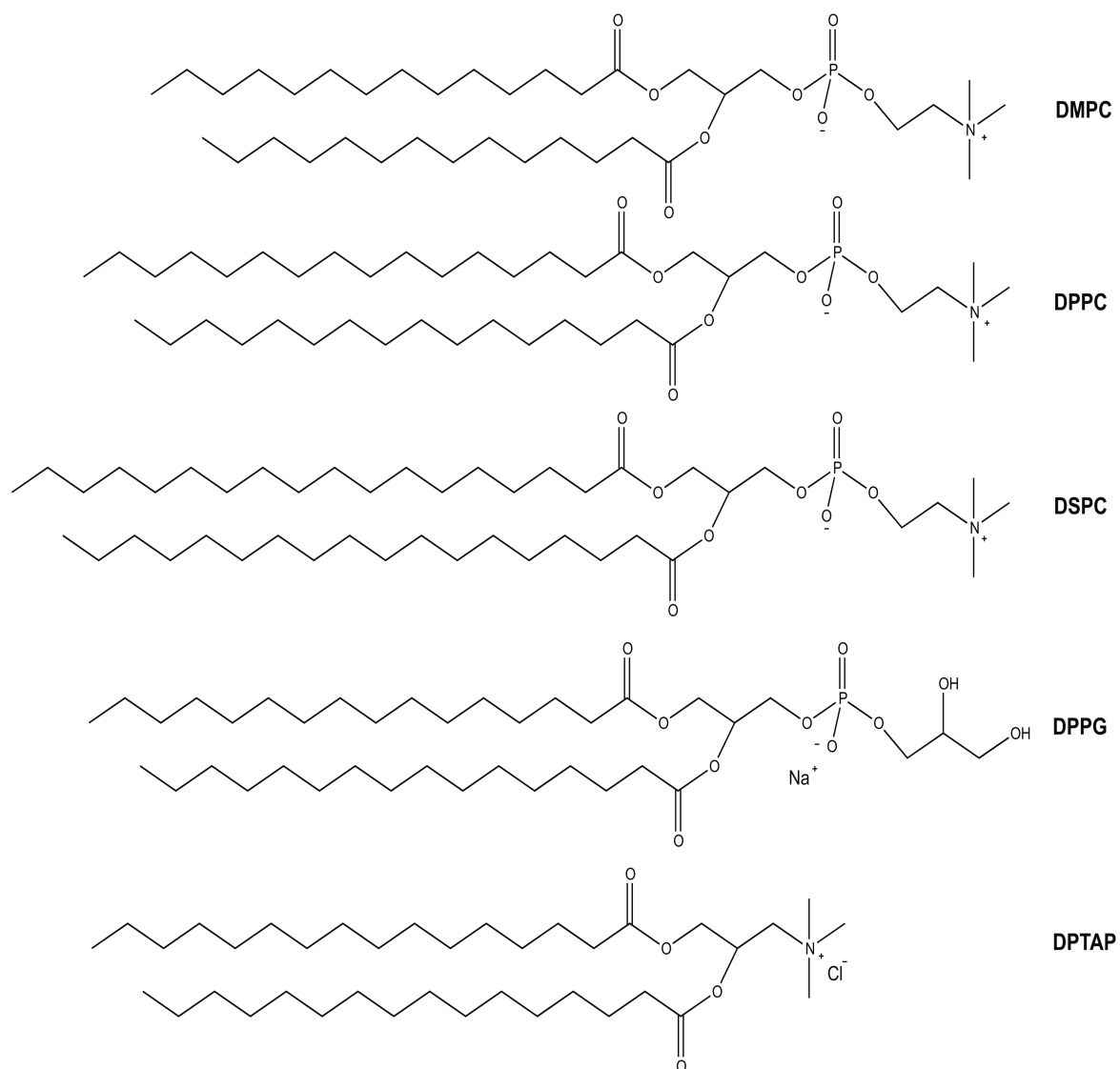


Figure B8. Structures of lipids used to make the liposomes from Table 3.

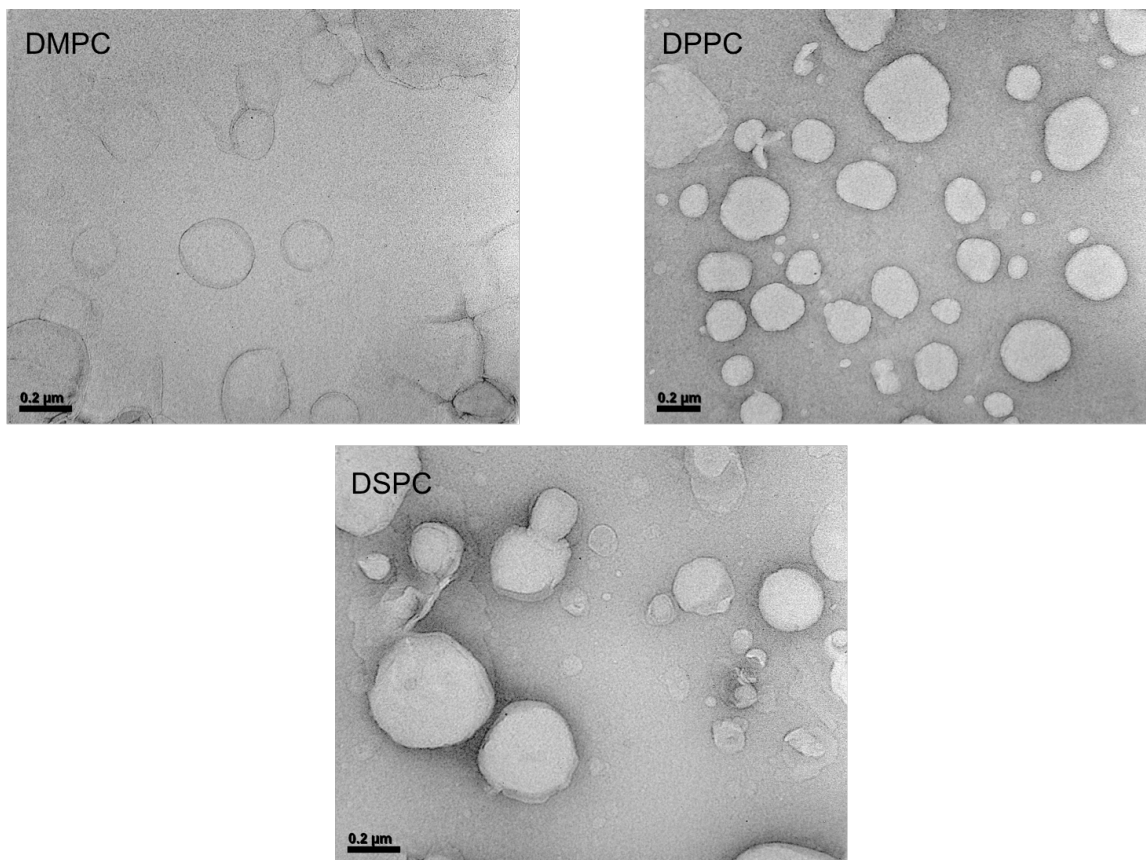


Figure B9. Transmission electron micrographs of DMPC (C_{14}), DPPC (C_{16}), and DSPC (C_{18})-based PAPA/NO liposomes. Scale bar represents 0.2 μm .

Table B2. Fluorophore encapsulation efficiency for DPPC and DPPG liposomes.^a

Molecule	DPPC (C₁₆) EE (%)	DPPG (- C₁₆) EE (%)
Coumarin ^b	25.6	26.1
5(6)-carboxyfluorescein ^c	21.7	11.3

^aEncapsulation efficiency was calculated as the ratio of mol of fluorophore inside liposomes to mol used for synthesis multiplied by 100. A calibration curve was created using each fluorophore for quantification. ^bExcitation at 355 nm and emission measured at 510 nm. ^cExcitation at 495 nm and emission measured at 517 nm.

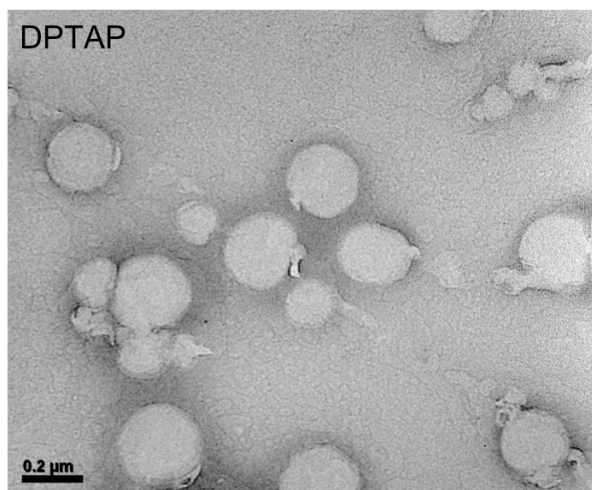
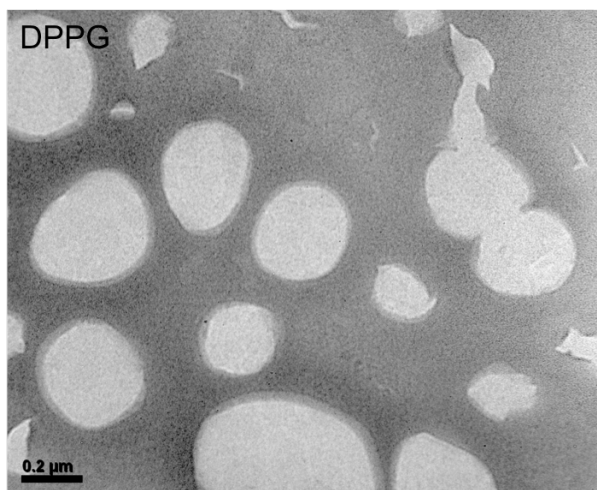


Figure B10. Transmission electron micrographs of DPPG (- C₁₆) and DPTAP (+ C₁₆) PAPA/NO liposomes. Scale bar represents 0.2 μm .

Table B3. Nitric oxide-release properties of PAPA/NO liposomes as a function of bilayer hydrophobicity and charge in MES (pH = 5.4) at 37 °C.

Lipid	$t_{1/2}^a$ (h)	t_d^b (h)	[NO]_{total}^c (μmol/mL)
DMPC (C ₁₄)	1.6 ± 1.2	22.3 ± 2.6	7.90 ± 0.29
DPPC (C ₁₆)	0.84 ± 0.24	20.7 ± 4.6	7.75 ± 1.09
DSPC (C ₁₈)	12.3 ± 1.3	59.4 ± 7.7	8.91 ± 0.62
DPPG (- C ₁₆)	1.2 ± 0.3	19.9 ± 6.5	6.13 ± 0.97
DPTAP (+ C ₁₆)	0.09 ± 0.01	6.5 ± 2.1	7.94 ± 0.96

^aHalf-life of NO release. ^bDuration of NO release until the measured NO reached 10 ppb per 300 μL of liposomes (three-times the detection limit of the instrument). ^cTotal amount of NO released normalized to the injected volume from the liposome stock solution.

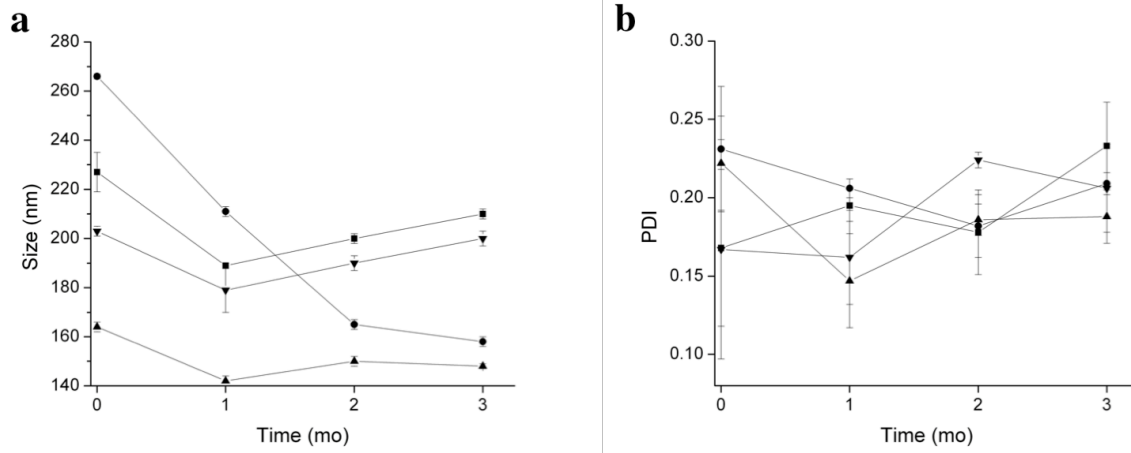


Figure B11. (a) Z-average size and (b) polydispersity index values of PAPA/NO-encapsulated (▼) DPPC, (▲) DPPG, (■) 50:50 DPPC:DPTAP, and (●) 10:90 DPPE-PEG/DPPC liposomes over time as measured by dynamic light scattering. Liposomes were stored at 4 °C between measurements.

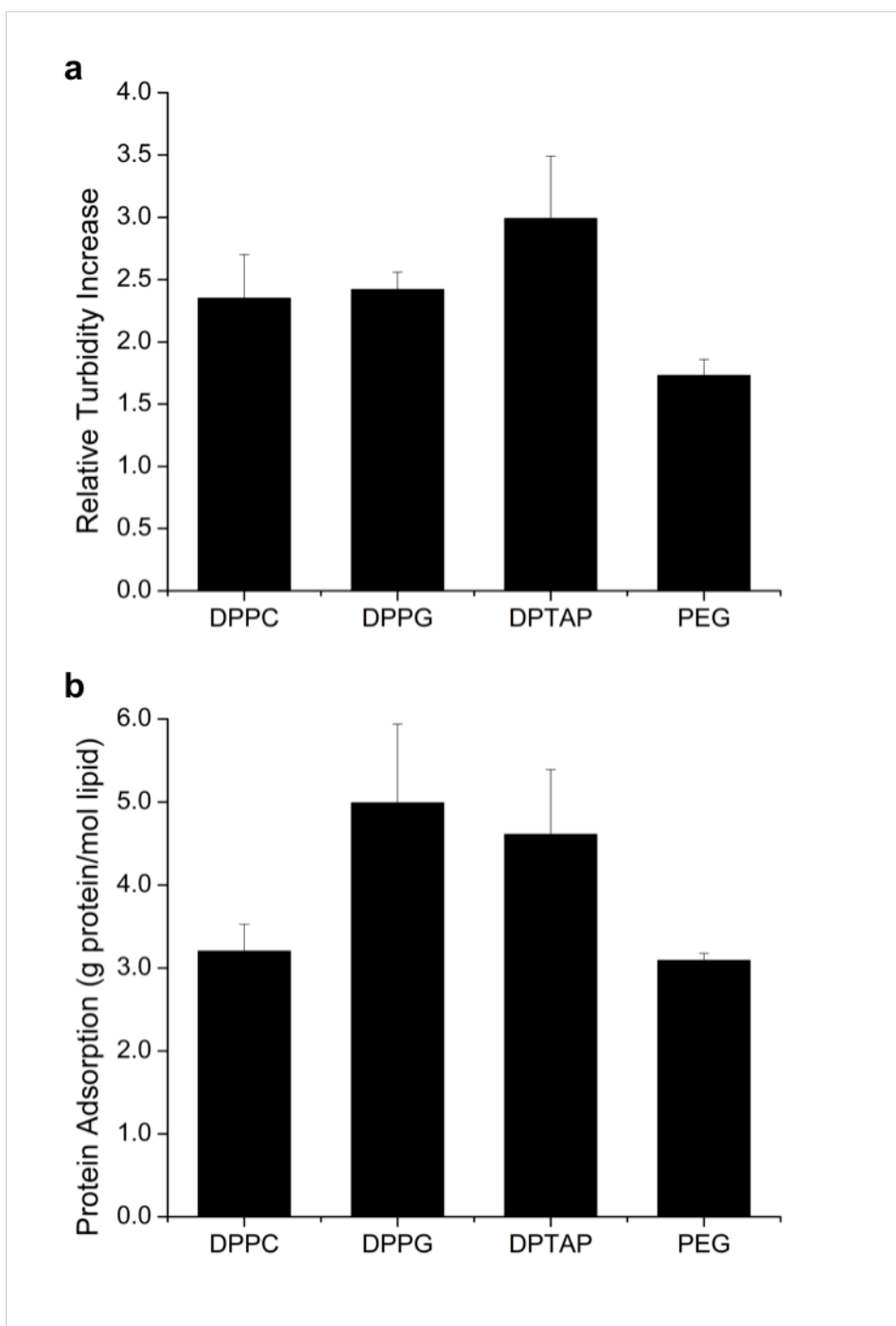


Figure B12. (a) Normalized absorbance measured at 450 nm for 5% (v/v) liposome solutions in serum. (b) Amount of protein adsorbed to the liposomes, normalized to moles of lipid, as measured by the Bradford assay. The DPTAP and PEG liposomes were composed of a 50:50 DPTAP:DPPC and 10:90 DPPE-PEG:DPPC molar ratios, respectively.

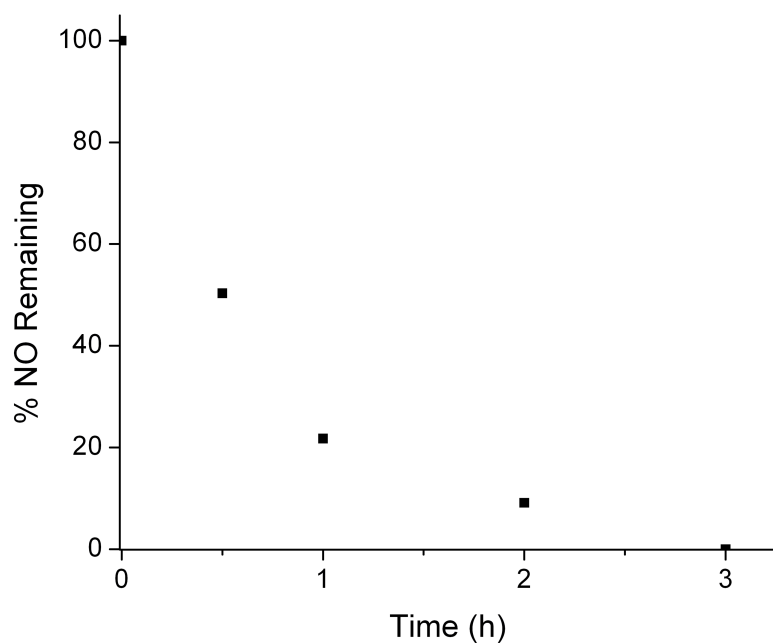


Figure B13. Nitric oxide release from neutral DPPC PAPA/NO liposomes suspended in 10 mM PBS (pH 7.4, 37 °C) containing 157 mg/mL hemoglobin. The amount of NO remaining within the liposomes was determined by injecting the liposomes into an acidic solution at discrete timepoints.

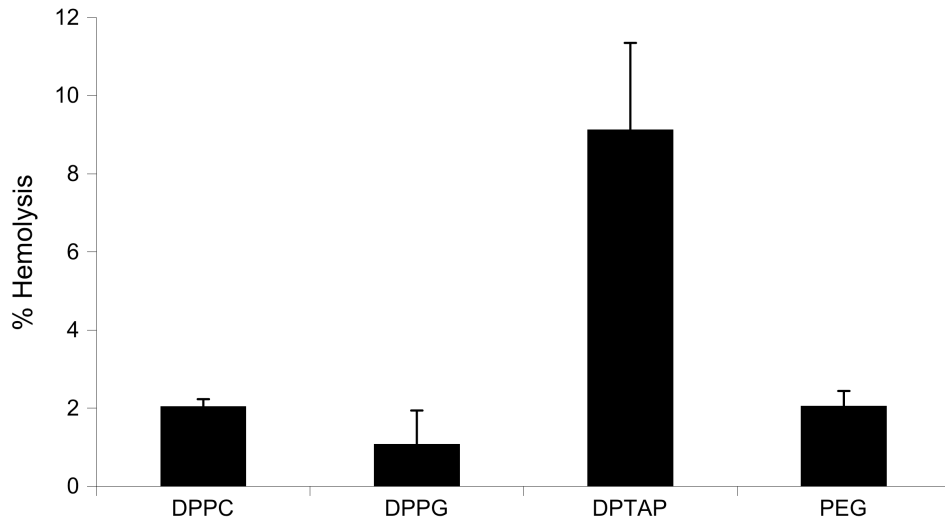


Figure B14. Hemolytic activity of various PAPA/NO-encapsulated liposome systems. The DPTAP liposomes are composed of a 50:50 DPTAP:DPPC molar ratio and PEG liposomes are composed of a 10:90 DPPE-PEG:DPPC molar ratio.

B.1 Experimental section

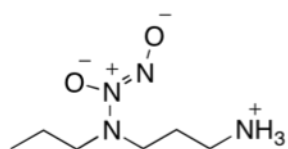
B.1.1. Protocol for hemolysis assay

A standard hemolysis assay was employed for determining the hemolytic activity of the NO-releasing liposomes.⁴⁻⁶ Red blood cells (RBCs) are harvested from freshly-obtained citrated canine blood and resuspended in 0.9% isotonic saline to a 10% (v/v) concentration. The RBCs (300 μ L) are mixed with the stock liposome solution (15 μ L) and incubated at 37 °C for 30 min with slight agitation. Afterwards, the RBCs are separated from free hemoglobin by centrifugation at $1,000 \times g$ for 10 min. The supernatant (80 μ L) was added to a 96-well plate and the absorbance was measured at 405 nm using a ThermoScientific Multiskan EX plate reader (Waltham, MA). Absorbance values from negative controls (300 μ L blood mixed with 15 μ L 0.9% saline) were subtracted from all absorbance values. The % hemolysis was determined by dividing the sample absorbance with that of RBCs incubated with 1% triton in saline.

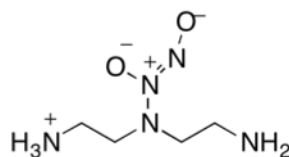
REFERENCES

1. Hrabie, J.A.; Keefer, L.K. "Chemistry of the nitric-oxide releasing diazeniumdiolate ("Nitrosohydroxylamine") functional group and its oxygen-substituted derivatives." *Chemical Reviews* **2002**, *102*, 1135-1154.
2. Keefer, L.K.; Flippen-Anderson, J. L.; George, C.; Shanklin, A.P.; Dunams, T.M.; Christodoulou, Saavedra, J.E.; Sagan, E.S.; Bohle, D.S. "Chemistry of the diazeniumdiolates. I. Structural and spectral characteristics of the [N(O)NO]-functional group." *Nitric Oxide* **2001**, *5*, 377-394.
3. Keefer, L.K. "Fifty years of diazeniumdiolate research. From laboratory curiosity to broad-spectrum biomedical advances." *ACS Chemical Biology* **2011**, *6*, 1147-1155.
4. Nie, Y.; Ji, L.; Ding, H.; Xie, L.; Li, L.; He, B.; Wu, Y.; Gu, Z. "Cholesterol derivatives based charged liposomes for doxorubicin delivery: Preparation, *in vitro*, and *in vivo* characterization." *Theranostics* **2012**, *2*, 1092-1103.
5. Bock, T.K.; Müller, B.W. "A novel assay to determine the hemolytic activity of drugs incorporated in colloidal carrier systems." *Pharmaceutical Research* **1994**, *11*, 589-591.
6. Senior, J.H.; Trimble, K.R.; Maskiewicz, R. "Interaction of positively-charged liposomes with blood: Implications for their application *in vivo*." *Biochimica et Biophysica Acta* **1991**, *1070*, 173-179.

Appendix C: Supplemental Information of Chapter 4



PAPA/NO



DETA/NO

Figure C1. Molecular structures of the *N*-diazoniumdiolate NO donors.

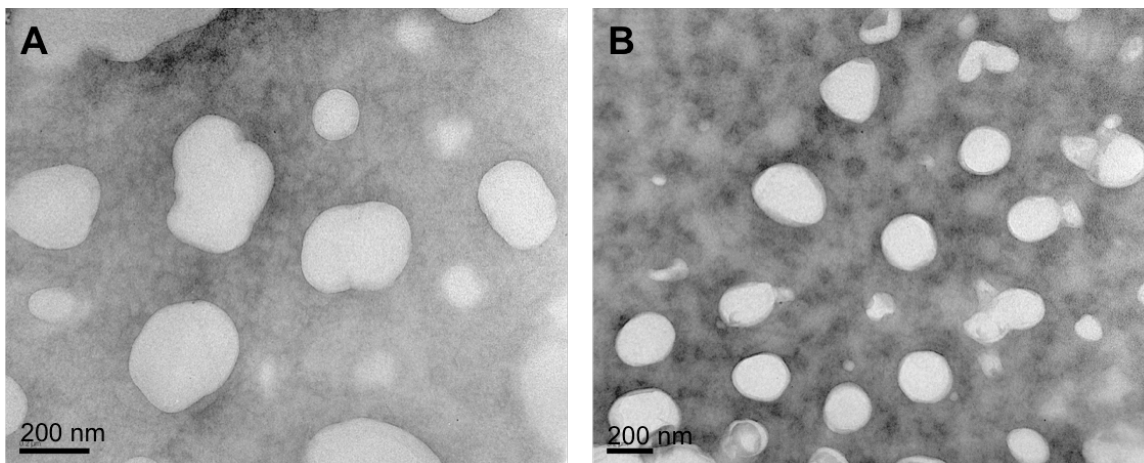


Figure C2. Transmission electron micrographs of (A) PAPA/NO and (B) DETA/NO liposomes.

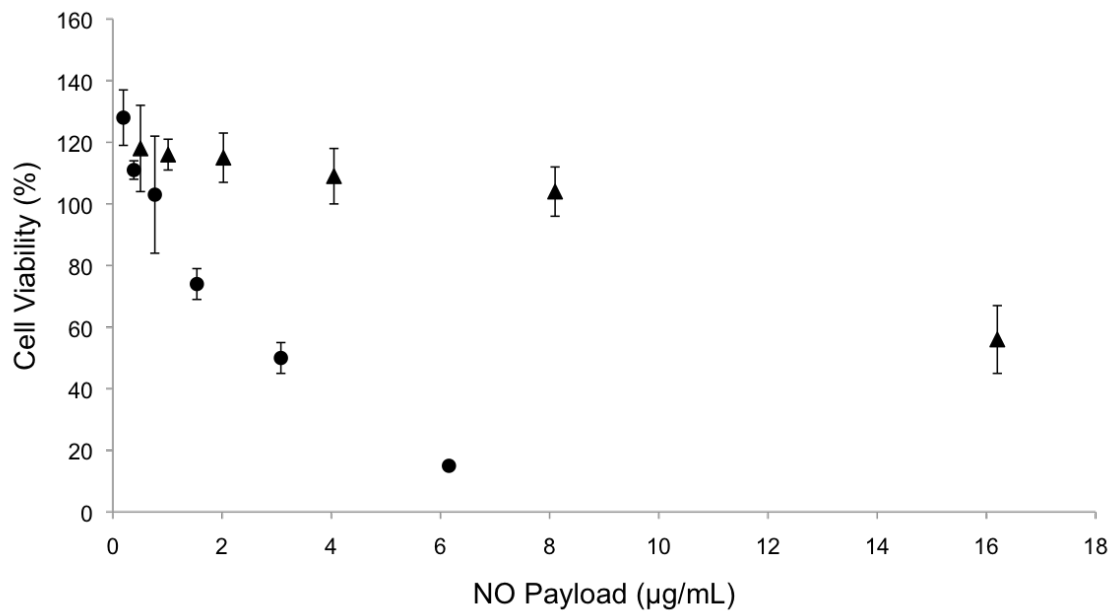


Figure C3. Cytotoxicity plot of liposomal (▲) PAPA/NO and (●) DETA/NO as a function of NO concentration against human HPNE epithelial pancreatic cells.

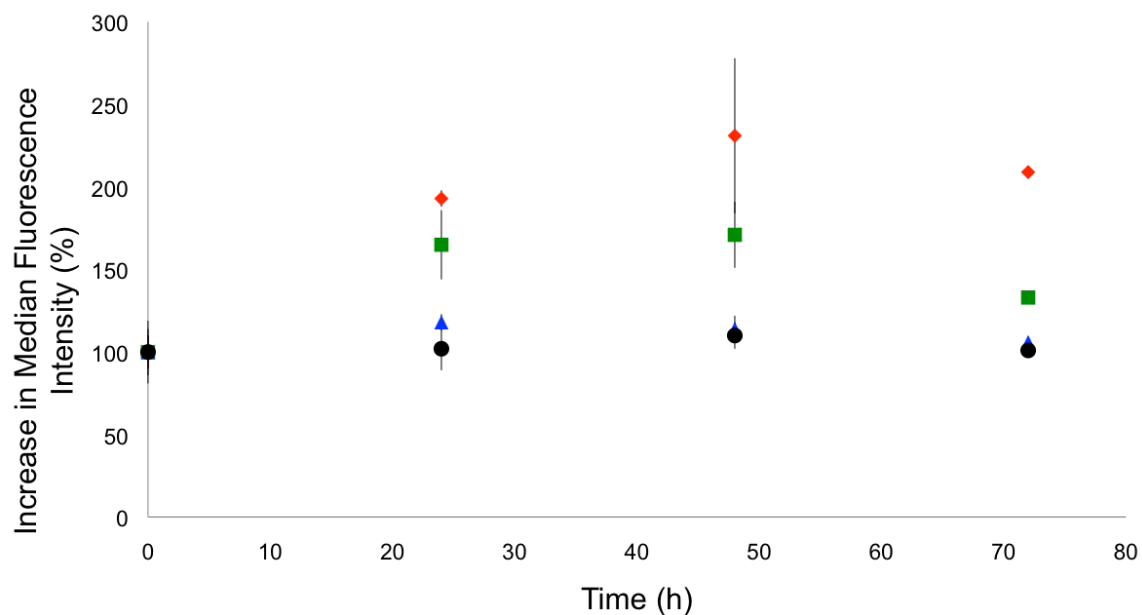


Figure C4. Change in median fluorescence intensity over time, as determined by flow cytometry, after treating MCF-7 cells with free PAPA/NO at 16.2 µg NO/mL (green squares) and 0.75 µg NO/mL (black circles), and liposomal PAPA/NO at 16.2 µg NO /mL (red diamonds) and 0.75 µg NO/mL (blue triangles).

APPENDIX D: SELECTIVE MONOPHOSPHORYLATION OF CHITOSAN VIA PHOSPHORUS OXYCHLORIDE⁴

D.1 Introduction

The medical field is increasingly turning to renewable biopolymers, such as cellulose,¹⁻² collagen,³⁻⁴ alginate,⁵⁻⁷ and chitosan,⁸⁻¹⁰ for tissue engineering and drug delivery applications due to their favorable *in vivo* properties.¹¹ For tissue reconstruction, such polymers tend to elicit a reduced immune response, lower implant rejection rates, and decreased toxicity as a result of biomimicry (i.e., the ability to mimic the natural tissue environment).¹²⁻¹⁴ The glycosidic linkages of biopolymers also promote facile biodegradation via enzymatic hydrolysis.¹³⁻¹⁵

Chitosan, a polysaccharide derived from crustacean shells, consists of repeating units of *N*-acetylglucosamine and *D*-glucosamine. The primary alcohols and amines of these units are readily accessible and enable a diverse range of chemical modifications.⁸ As such, researchers have engineered chitosan-based materials for wound dressing,¹⁶ metal and dye chelation,¹⁶ drug delivery,¹⁷ sensing,¹⁸ fuel cell,¹⁹ and antibacterial²⁰⁻²¹ applications. For example, Ishiara²² reported the modification of chitosan with azides to enhance the mechanical properties of the biopolymer for wound-healing applications. Sashiwa *et al.* added α -galactosyl pendants to chitosan to inhibit binding of human antibodies and evade the host immune response.²³ The authors demonstrated the benefits of the α -galactosyl pendants in a pig liver xenotransplant model.

Chitosan's poor solubility in physiological media represents a critical shortcoming that limits therapeutic utility. In general, chitosan of >20 kDa molecular weight is soluble only in

⁴ This appendix was adapted from an article that previously appeared in *Polymer Chemistry*. The original citation is as follows: Suchyta, D.J.; Soto, R.J.; Schoenfisch, M.H. "Selective monophosphorylation of chitosan via phosphorus oxychloride" *Polymer Chemistry* **2017**, *12*, 3569-3574.

acidic aqueous solutions.⁹ Though certain chemical modifications may alter functional aspects of chitosan for a given application, often the modification does not influence the solubility since many of these entities are electrically neutral (e.g., sugars) at pH 7.4. A satisfactory alternative to chemical modifications is to work with lower molecular weight oligosaccharides (~10 kDa) that are water-soluble.²¹ However, a large molecular weight scaffold is preferred for many biomedical applications (e.g., wound dressings and polymeric membranes).

Phosphorylation is a popular chemical modification strategy for improving the water solubility of chitosan and maintaining its molecular weight.^{22,24} At pH >6.5, phosphorylated chitosan (P-chitosan) consists of deprotonated phosphate groups that enables high water solubility for biological and industrial applications. For example, P-chitosan solutions have been used to enhance Ca^{2+} remineralization of dentine resulting from the high surface adsorption/interaction that P-chitosan promotes with enamel.²⁵⁻²⁷ Of note, the efficacy of P-chitosan for dentine remineralization would be limited by poor water solubility and, likely, molecular weight.

Many researchers have phosphorylated chitosan predominantly by reaction with solutions of phosphoric acid, triethyl phosphate, and phosphorus pentoxide (P_2O_5).²⁸⁻³⁰ Unfortunately, chitosan is insoluble in many solvents, thus the ensuing heterogeneous reaction conditions result in poor phosphorylation and irreproducibility.²⁹⁻³⁰ To address this, Nishi *et al.*²⁸ reported an alternative phosphorylation reaction that employs methanesulfonic acid to solubilize the chitosan. Insoluble P_2O_5 was employed as the phosphorylating reagent, a chemical compound that results in the undesirable formation of polyphosphoric acids/ions.³¹ These polyphosphate byproducts are either free or bound to the chitosan through inter- and intramolecular bridging, making their removal difficult, and complicating adequate characterization of the resulting P-

chitosan's structure. In general, previous reports on chitosan phosphorylation have not adequately characterized the resulting product. Indeed, ^{31}P NMR data is rarely provided resulting in questionable or even outright neglected phosphorylation conversion efficiencies.

The shortcomings of P_2O_5 -based phosphorylation warrant further exploration into alternative phosphorylating reagents. Reactants that facilitate monophosphorylation (i.e., polyphosphate formation does not occur) are essential to both prevent intra- and intermolecular polyphosphate bridging and enable more accurate characterization. To this end, we explored the use of phosphorus oxychloride (POCl_3) to generate P-chitosan. Phosphorus oxychloride is a liquid phosphorylating reagent utilized in the synthesis of phosphate esters and cross-linked starch and cellulose because of its high solubility in organic solvents.³²⁻³⁶ Furthermore, negligible self-reaction should prevent the formation of polyphosphates, making it a promising alternative to P_2O_5 . Herein, we report the selective monophosphorylation of chitosan using POCl_3 in methanesulfonic acid to produce a water-soluble product of high molecular weight.

D.2 Experimental section

D.2.1. Materials

Low molecular weight chitosan (degree of acetylation: 27%), phosphorus pentoxide (P_2O_5), phosphorus oxychloride (POCl_3), low viscosity alginic acid sodium salt, methanesulfonic acid (MSA), cellulose, deuterium oxide (D_2O), D-glucosamine, D-glucosamine 1-phosphate, D-glucosamine 6-phosphate, and *N*-acetylglucosamine were purchased from Sigma (St. Louis, MO). Tetrahydrofuran (THF), sodium hydroxide (NaOH), nitric acid (HNO_3), orthophosphoric acid (H_3PO_4), diethyl ether, and calcium chloride (CaCl_2) dihydrate were purchased from Fisher Scientific (Fair Lawn, NJ). Water was purified to a resistivity of $18.2 \text{ M}\Omega\cdot\text{cm}$ and a total organic content ≤ 6 ppb using a Millipore Milli-Q UV Gradient A10 System (Bedford, MA).

D.2.2. Synthesis of phosphorylated chitosan

Chitosan (200 mg) was added to a round-bottomed flask and dissolved in 10 mL methanesulfonic acid. After complete dissolution, 2.060 mL POCl₃ were injected into this stirring solution. The reaction was allowed to proceed at room temperature for up to 72 h. To end the reaction, 1.40 mL of water were added to the flask and stirred for another 15 min. The solution was then transferred to centrifuge tubes, precipitated with diethyl ether, and centrifuged (4000 × g for 3 min) to pellet the P-chitosan. The P-chitosan was washed twice with THF, once with ethanol, dried under vacuum overnight, and stored at -20 °C until use.

D.2.3. ¹H and ³¹P nuclear magnetic resonance (NMR) spectroscopy

All NMR spectra were collected at 23 °C in 5 mm NMR tubes using a Bruker AVIII 600 MHz spectrometer equipped with a Quattro Nucleus Probe (QNP) C-P-N cryoprobe. Samples were prepared at ~2 mg/mL in D₂O (¹H NMR) or a 1:3 volumetric ratio of D₂O to 50 mM NaOH (³¹P NMR). Proton spectra were acquired using a conventional 1-D pulse sequence with 16 scans. Phosphorus spectra were collected using a standard proton decoupled pulse sequence with 800 scans. Data was processed using Bruker's TopSpin software. Relevant ¹H NMR data of P-chitosan (600 MHz, D₂O, δ): 1.9 (C₇: CHNHCOCH₃), 2.67 (SO₃CH₃), 3.1 (C₂: CHCHNH₃⁺), 3.4-3.9 (C₃, C₄, C₅, C₆: OHCH, OCHCH(OH)CH(NH₂), OHCH₂CH, OHCH₂CH).

D.2.4. X-ray photoelectron spectroscopy (XPS)

Samples for XPS analysis were prepared by casting 20 μL of 1 mg/mL P-chitosan in water onto gold-sputtered glass slides and evaporating the water under vacuum overnight. The sample-coated gold substrates were analyzed using a Kratos Axis Ultra DLD X-ray photoelectron spectrometer equipped with a monochromatic Al Kα X-ray excitation source (base pressure = 6 × 10⁻⁹ torr). Emitted photoelectrons were measured at a 90° take-off angle. A pass

energy of 20 eV was utilized for all high-resolution scans. A standard Shirley baseline correction algorithm was employed after data collection with relative sensitivity factors from the Kratos Vision software to calculate atomic concentrations.

D.2.5. Molecular weight determination

The average molecular weight and polydispersity of the polymers were determined using gel permeation chromatography (GPC). Low molecular weight chitosan (1 mg/mL in 2 vol % acetic acid) and P-chitosan (1 mg/mL in water) solutions were passed through a 0.22 μm diameter syringe filter and injected (100 μL) onto a Waters 2695 GPC column (flow rate = 0.925 mL/min) equipped with a Waters 2414 refractometric detector. Three Ultrahydrogel 1000, 7.8x300 mm columns were connected in series with an Ultrahydrogel guard column. Molecular weight calibration curves were created using polyethylene oxide standards in a range from 25–881 kDa.

D.2.6. Calcium chelation

P-chitosan (10.0 mg) was dissolved in a 10 mM CaCl_2 solution (2.5 mL) at 37 °C. The mixture was stirred in a 37 °C incubator for 2 min. The solution was then transferred to a centrifuge tube, diluted with 10.0 mL THF, and centrifuged at $4000 \times g$ for 2 min. After decanting the liquid into a glass vial, the solvent was evaporated under vacuum. The remaining calcium chloride was digested in a known volume of 2 vol % HNO_3 prior to calcium content analysis by inductively coupled plasma-optical emission spectrometry (ICP-OES). The ICP-OES was first calibrated using calcium standards (0.1–25 ppm) prepared in 2 vol % HNO_3 . The calcium emission intensity at 317.93 nm was used for quantification.

D.3 Results and discussion

The use of anhydrous liquid organic acids during the synthesis of P-chitosan is critical to prevent undesirable hydrolysis of the phosphorylating reagent. While other organic acids are available, methanesulfonic acid (MSA) is one of the few liquid organic acids that is sufficiently acidic enough to fully solubilize chitosan. Phosphorylating reagents such as P_2O_5 are insoluble in organic acids like MSA, but this issue can be resolved by employing $POCl_3$.

Chitosan's reactivity with $POCl_3$ was initially examined using 1H NMR spectroscopy (Figure D.1). The protonation of chitosan's primary amine was followed throughout the reaction and washing steps by monitoring the associated alpha-carbon (C_2) proton peak. When protonated, the peak appears at 3.1 ppm. Washing P-chitosan with 50 mM NaOH, which deprotonates the amine, shifts the peak at 3.1 ppm upfield to 2.6 ppm. In addition to the protonation state of the amine, 1H NMR may be used to confirm the presence of ionically-bound MSA. Following extensive washing of P-chitosan to remove free acid, the peak near 2.7 ppm from the methyl hydrogens of MSA revealed that the methanesulfonate anion serves as a counterion to chitosan's protonated amine. Subsequential washings with 2 M HCl replaces the methanesulfonate with a chloride counterion (Figure D.2). Unfortunately, actual phosphorylation is not directly observed using 1H NMR.

^{31}P NMR spectroscopy may be employed to directly examine P-chitosan phosphorylation. Sample preparation under basic conditions was essential to differentiate ^{31}P NMR phosphate peaks from one another. When samples are prepared solely in neutral D_2O (Figure D.3a), a broad peak appears near 0.5 ppm, similar in location to that of phosphoric acid. Under basic conditions (13 mM NaOH in D_2O) the appended phosphate groups are deprotonated, resulting in adequate

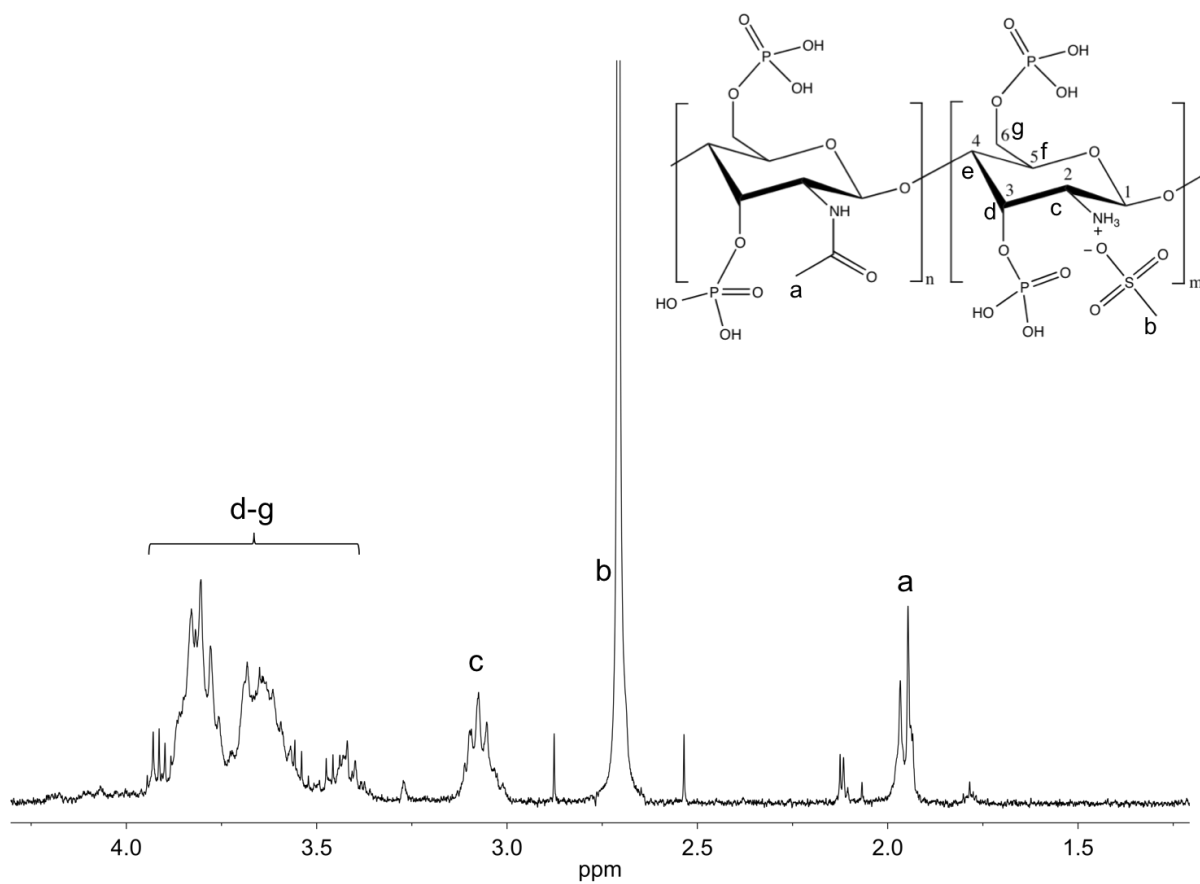


Figure D.1. ^1H NMR spectrum of phosphorylated chitosan (molecular structure shown above).

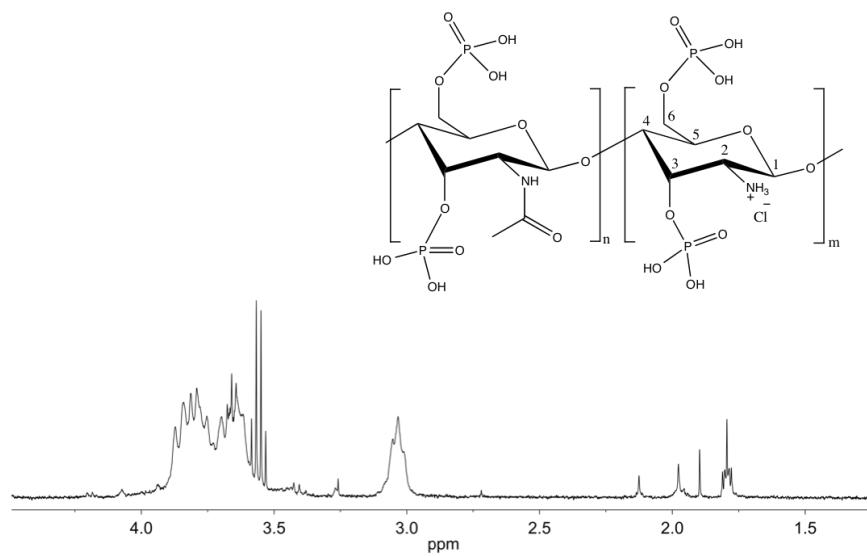


Figure D.2. ^1H NMR spectrum in D_2O of P-chitosan after washing with 2 M HCl.

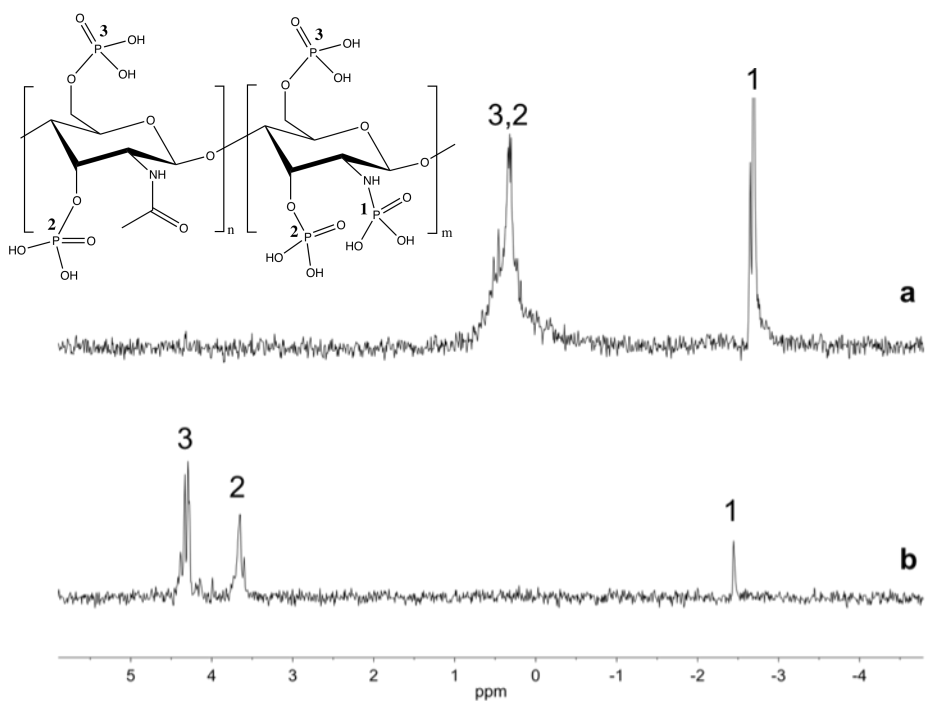


Figure D.3. ^{31}P NMR spectra of phosphorylated chitosan (molecular structure shown above) prepared in (a) D_2O and (b) 1:3 volumetric ratio of D_2O to 50 mM NaOH. Numeric labels (1, 2, 3) indicate the associated phosphate group.

peak separation due to a downfield shift (Figure D.3b). The separated peaks at 4.30 and 3.65 ppm are assignable to the phosphates attached to the primary and secondary alcohols of chitosan, respectively. Spectra acquired from solutions of D-glucosamine 1-phosphate and D-glucosamine 6-phosphate corroborate these peak transitions and assignments (Figures D.4 and D.5).

The ^{31}P NMR peak near -2.5 ppm (Figure D.3) is assigned to the monophosphorylation of chitosan's primary amine. While Wang et al. implied phosphorylation of the amine, clear evidence (^{31}P NMR characterization) was not provided as to support primary amine phosphorylation.³⁰ We sought to confirm amine phosphorylation by reacting other biopolymers (i.e., alginate, cellulose) lacking primary amines with POCl_3 as well. ^{31}P NMR analysis of both phosphorylated alginate and cellulose revealed no peaks near -2.5 ppm (Figures D.6 and D.7), confirming the identity of the -2.5 ppm peak as an amine-bound phosphate (both spectra contained peaks at ~4 ppm indicating phosphorylation of their alcohol groups). In contrast to prior work,³⁰ we believe that only the primary amines and not the acetylated amines (i.e., amides) are participating in the reaction. The electron-withdrawing properties of the carbonyl group, in conjunction with resonance, likely reduce the nucleophilicity of the nitrogen atom, preventing the amide from attacking POCl_3 . To verify this hypothesis, we synthesized both phosphorylated D-glucosamine containing no amide groups and *N*-acetylglucosamine with amide groups under identical conditions that were used to prepare P-chitosan. As predicted, the ^{31}P NMR spectrum of phosphorylated D-glucosamine revealed a peak at -2.5 ppm, while that of *N*-acetylglucosamine lacked the -2.5 ppm peak (Figures D.8 and D.9). These results confirm that POCl_3 phosphorylation only occurs at the alcohols and primary amines of chitosan.

The POCl_3 reaction was also compared to the P_2O_5 reaction following a published protocol.²⁸ While both phosphorylated amine and alcohol peaks were clearly apparent in the ^{31}P

NMR spectra (Figure D.10) after chitosan phosphorylation with P_2O_5 , several additional peaks appeared at more negative chemical shifts that were indicative of polyphosphate formation. In fact, the NMR data reveals the presence of both pyrophosphates³⁷ (-6 to -11 ppm) and tripolyphosphates³⁷ (-21 to -25 ppm). In contrast to the P_2O_5 reaction, the $POCl_3$ reaction generates no polyphosphates, allowing for more reliable characterization and inherent P-chitosan homogeneity.

D.3.1. Controlling phosphorylation efficiency

The extent of phosphorylation as a function of $POCl_3$ and the chitosan concentration was characterized using X-ray photoelectron spectroscopy (XPS). The nitrogen atomic percent (N 1s peak) was used as a normalization factor across syntheses as changes in nitrogen content are unlikely to occur during phosphorylation. The molar ratio of $POCl_3$ relative to chitosan alcohol groups was varied from 1 to 10, while the overall reaction time (48 h) and chitosan concentration (20 mg/mL) were kept constant. At molar ratios of $POCl_3 < 10$, phosphorylation was not observed at any appreciable level (i.e., below the XPS limit of detection). An increase in the P/N ratio to 0.232 was measured after reaction with a 10-molar excess of $POCl_3$. The large excess of $POCl_3$ required is attributed to the slower and less favorable reaction kinetics under strongly acidic conditions.

Tuning the phosphorylation efficiency through simple changes in the reaction conditions (e.g., chitosan concentration) is highly desirable for chemical versatility. As shown in Table D.1, the P/N ratio correlated well with the concentration of chitosan from 5 to 80 mg/mL. We also monitored the Cl/N atomic ratio (zero for all concentrations) to ensure post-synthetic removal of unreacted $POCl_3$ and appended chlorine groups. Likewise, the P/N ratio was measured as a

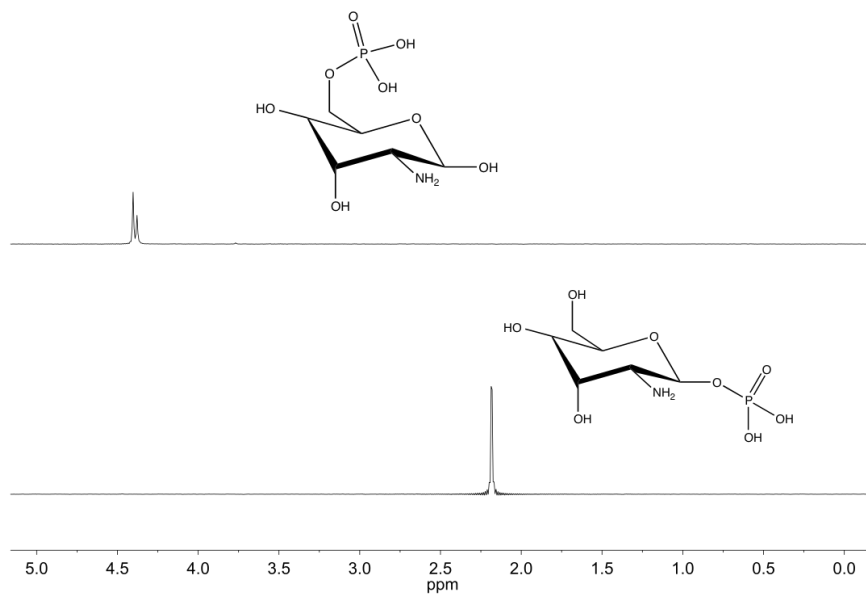


Figure D.4. ^{31}P NMR spectrum of (top) D-glucosamine 6-phosphate and (bottom) D-glucosamine 1-phosphate. Samples were prepared in 1:3 volumetric ratio of D_2O to 50 mM NaOH.

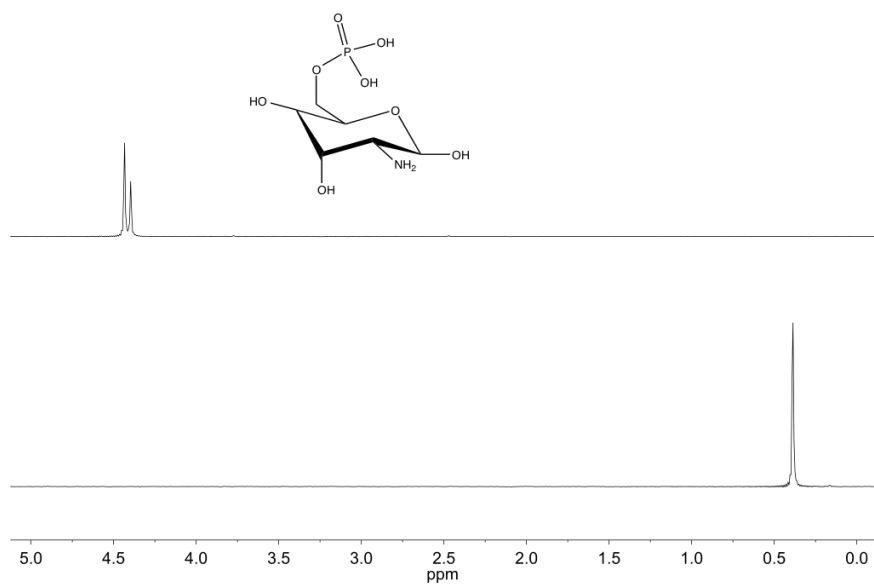


Figure D.5. ^{31}P NMR spectrum of D-glucosamine 6-phosphate prepared in (top) 1:3 volumetric ratio of D_2O to 50 mM NaOH and (bottom) 1:3 volumetric ratio of D_2O to 50 mM HCl.

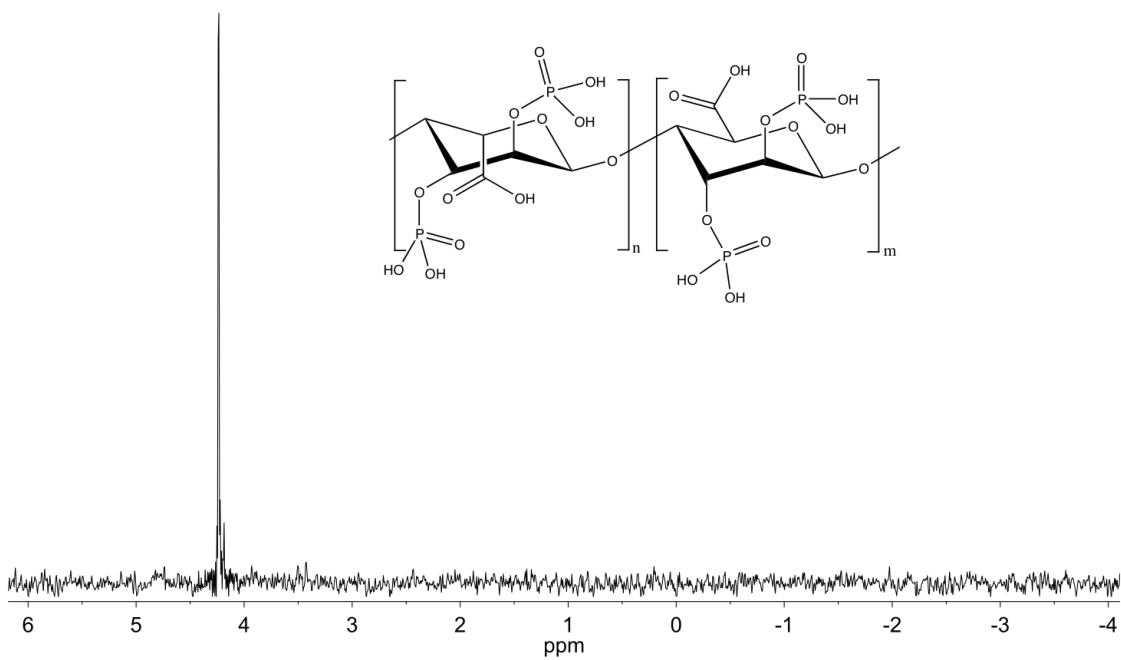


Figure D.6. ^{31}P NMR spectrum of phosphorylated alginate. Sample was prepared in 1:3 volumetric ratio of D_2O to 50 mM NaOH.

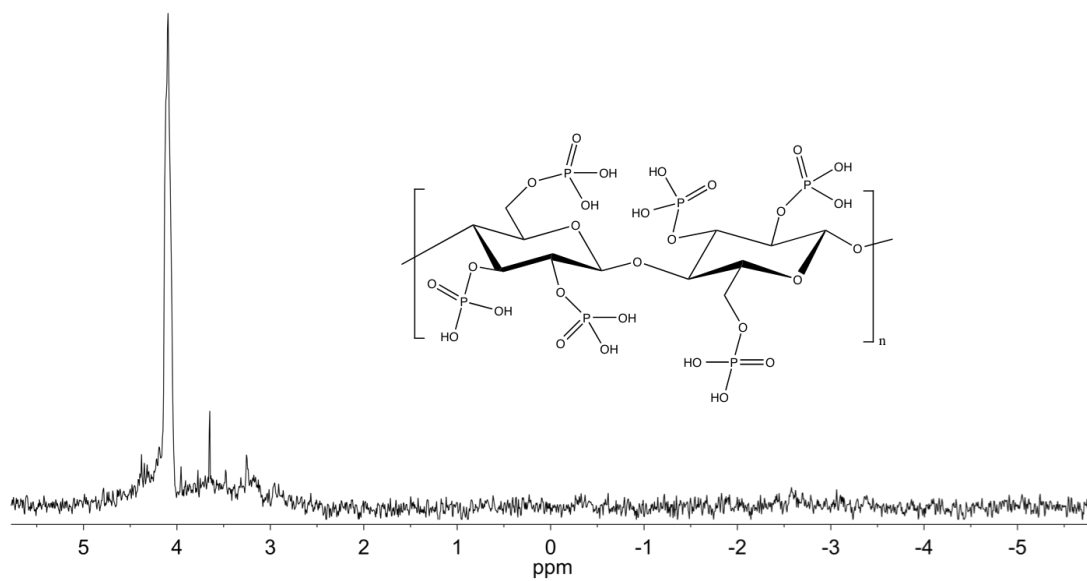


Figure D.7. ^{31}P NMR spectrum of phosphorylated cellulose. Sample was prepared in 1:3 volumetric ratio of D_2O to 50 mM NaOH.

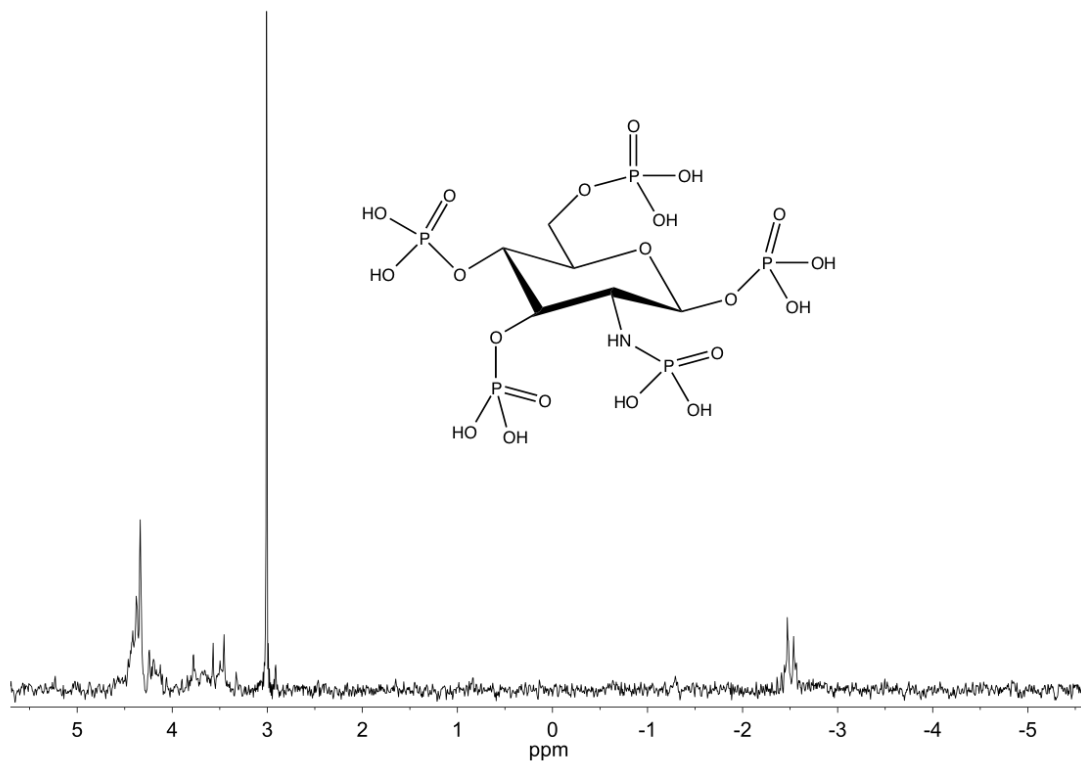


Figure D.8. ^{31}P NMR spectrum of phosphorylated D-glucosamine. Sample was prepared in 1:3 volumetric ratio of D_2O to 50 mM NaOH.

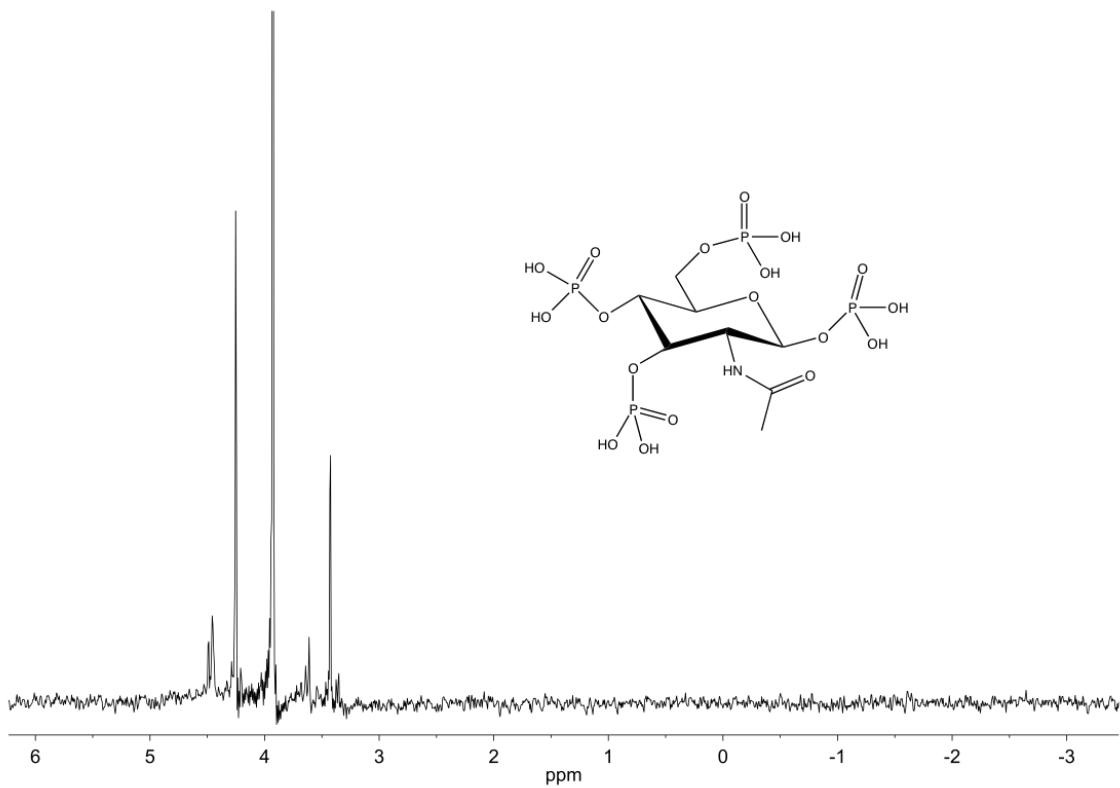


Figure D.9. ^{31}P NMR spectrum of phosphorylated *N*-acetylglucosamine. Sample was prepared in 1:3 volumetric ratio of D_2O to 50 mM NaOH.

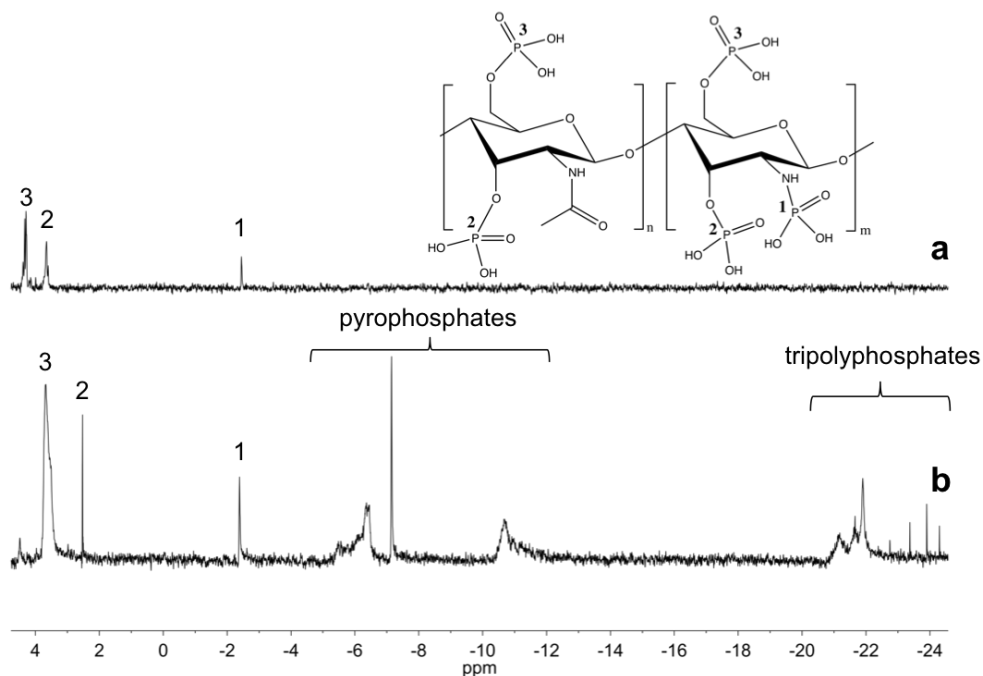


Figure D.10. ^{31}P NMR spectra of phosphorylated chitosan synthesized by the (a) POCl_3 method and (b) P_2O_5 method. Peaks located between -6 and -11 are assigned as pyrophosphates, while those located between -20 and -25 are tripolyphosphates.

Table D.1. Chitosan concentration effect on phosphorylation P/N atomic ratio.^a

Chitosan concentration (mg/mL)	P/N atomic ratio
5	n/a
20	0.232 ± 0.029
40	0.279 ± 0.038
80	0.436 ± 0.066

^aError bars represent the standard deviation from $n \geq 3$ separate preparations using a 48 h reaction time. The chlorine-to-nitrogen atomic ratio was zero for all concentrations.

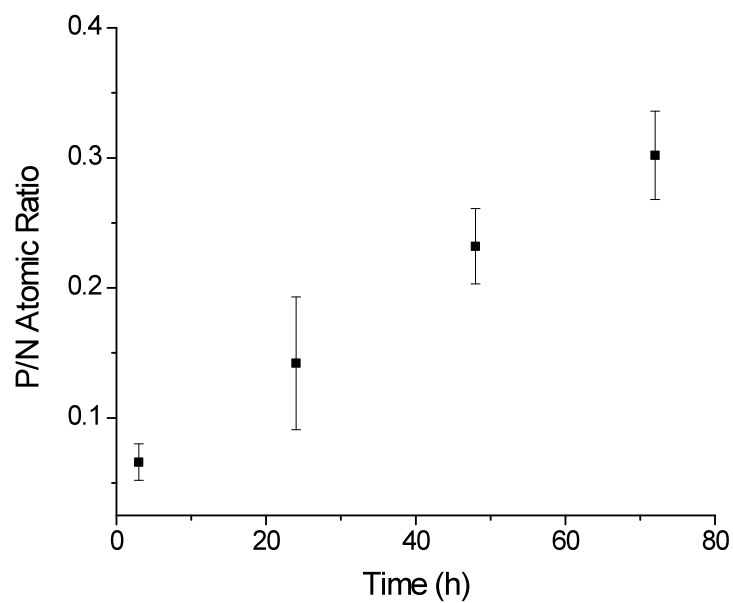


Figure D.11. Atomic P/N ratio as a function of reaction time for reactions with 20 mg/mL chitosan (10 molar ratio of POCl_3).

function of reaction time for a 20 mg/mL chitosan solution and 10-molar excess of POCl₃ (Figure D.11). The phosphorus content increased steadily over the course of 3 d, allowing for precise tunability (up to 72 h) of the phosphate content. An ability to decrease the reaction time while maintaining high P/N ratios was also observed by heating the reaction. For example, increasing the temperature of the 3 h reaction to 37 °C resulted in atomic ratios (P/N = 0.162) near those obtained at 25 °C for 24 h (P/N = 0.142).

D.3.2. *Molecular weight*

Degradation of P-chitosan is a concern given that the phosphorylation reaction occurs in a strong organic acid. The *O*-glycosidic bonds that link monomers of chitosan together are prone to cleavage in acidic environments.³⁸⁻³⁹ The change in P-chitosan molecular weight versus reaction time was investigated using gel permeation chromatography (GPC). Of note, the molecular weight of unmodified chitosan was ~85,000 g/mol (experimentally determined), a value within the range of typical chitosan materials (20,000–130,000 g/mol).⁴⁰ As shown in Table D.2, only a slight reduction in molecular weight was observed over a 72 h reaction period. In the absence of phosphorylation (i.e., without the addition of POCl₃), the molecular weight was ~85,000 g/mol, indicating negligible acid degradation. The anhydrous nature of the reaction likely mitigates degradation due to minimal hydrolysis (the primary mechanism of breaking glycosidic bonds). The consistent molecular weight also suggests that the water solubility of P-chitosan largely results from the addition of anionic phosphate groups.

D.3.3. *Calcium chelation efficiency*

A practical application for phosphorylated biopolymers is metal ion chelation. For example, phosphorylated chitosan effectively complexes Ca²⁺ to enhance tooth enamel remineralization and prevent future acid-catalyzed demineralization.^{26,41} We examined the Ca²⁺

Table D.2. Molecular weight and dispersity (\mathbb{D}) of P-chitosan as a function of POCl_3 reaction time.^a

Reaction time (h)	Molecular weight (M_n)	\mathbb{D}
0	85,100 \pm 200	1.72 \pm 0.05
24	78,700 \pm 400	1.98 \pm 0.05
48	84,300 \pm 350	1.60 \pm 0.05
72	83,800 \pm 250	1.41 \pm 0.09

^aError bars represent the standard deviation from $n \geq 3$ separate preparations.

chelation properties of P-chitosan by measuring total calcium chelation as a function of phosphorylation degree (Table D.3). P-chitosan chelation was compared to that observed from control chitosan (i.e., no phosphorylation). After brief exposure to a CaCl_2 solution, and removal of the polymer, the supernatant was analyzed for Ca^{2+} as an indication of P-chitosan chelation efficiency. Chitosan lacking phosphorylation chelated approximately $24.9 \mu\text{g Ca}^{2+}$ per mg chitosan, an unsurprising result given previous research demonstrating chitosan's native ability to bind divalent metal cations.⁴² The total amount of chelated calcium increased predictably with the P/N atomic ratio, with $46.2 \mu\text{g Ca}^{2+}$ per mg chitosan achieved at the greatest P/N atomic ratio (0.30). The data collected here supports the employment of P-chitosan into applications where calcium chelation is desired (e.g., oral care).

D.4 Conclusions

The reaction of chitosan with POCl_3 is a simple and reliable strategy for achieving monophosphorylation of chitosan's amine and alcohols. Precise tuning of the extent of phosphorylation is possible by adjusting specific reaction conditions (e.g., chitosan concentration, reaction time). Although alginate and cellulose were not extensively studied herein, similar monophosphorylation using POCl_3 should be expected. Lastly, a range of P-chitosan architectures (e.g., particles, hydrogels) could be expected given the preservation of high molecular weight throughout the reaction.

Table D.3. Calcium chelation amount of P-chitosan as a function of phosphorylation degree.

P/N atomic ratio	Chelated calcium ($\mu\text{g Ca}^{2+}/\text{mg chitosan}$)
0	24.9 ± 0.6^a
0.066	25.1 ± 1.8
0.142	41.9 ± 0.8
0.232	43.5 ± 1.0
0.302	46.2 ± 0.7

^aDetermined using a water-soluble 5 kDa chitosan without any phosphorylation.

REFERENCES

- (1) Klemm, D.; Heublein, B.; Fink, H.; Bohn, A. "Cellulose: Fascinating biopolymer and sustainable raw material." *Angewandte Chemie International Edition* **2005**, *44*, 3358-3393.
- (2) Ummartyotin, S.; Manuspiya, H. "A critical review on cellulose: From fundamental to an approach on sensor technology." *Renewable and Sustainable Energy Reviews* **2015**, *41*, 402-412.
- (3) Chattopadhyay, S.; Raines, R.T. "Collagen-based biomaterials for wound healing." *Biopolymers* **2014**, *101*, 821-833.
- (4) Sell, S.A.; McClure, M.J.; Garg, K.; Wolfe, P.S.; Bowlin, G.L. "Electrospinning of collagen/biopolymers for regenerative medicine and cardiovascular tissue engineering." *Advanced Drug Delivery Reviews* **2009**, *61*, 1007-1019.
- (5) Lee, K.Y.; Mooney, D.J. "Alginate: Properties and biomedical applications." *Progress in Polymer Science* **2012**, *37*, 106-126.
- (6) Venkatesan, J.; Bhatnager, I.; Manivasag, P.; Kang, K.; Kim, S. "Alginate composites for bone tissue engineering: A review." *International Journal of Biological Macromolecules* **2015**, *72*, 269-281.
- (7) Zia, K.; Zia, F.; Zuber, M.; Rehman, S.; Ahmad, M. "Alginate based polyurethanes: A review of recent advances and perspective." *International Journal of Biological Macromolecules* **2015**, *79*, 377-387.
- (8) Prabharan, M. "Review paper: Chitosan derivatives as promising materials for controlled drug delivery." *Journal of Biomaterials Applications* **2008**, *23*, 5-36.
- (9) Kumar, M.; Muzzarelli, R.; Muzzarelli, C.; Sashiwa, H.; Domb, A. "Chitosan chemistry and pharmaceutical perspectives." *Chemical Reviews* **2004**, *104*, 6017-6084.
- (10) Thakur, V.K.; Thakur, M. K. "Recent advances in graft copolymerization and applications of chitosan: A review." *ACS Sustainable Chemistry and Engineering* **2014**, *2*, 2637-2652.
- (11) Yates, M.R.; Barlow, C.Y. "Life cycle assessments of biodegradable, commercial biopolymers—A critical review." *Resources, Conservation and Recycling* **2013**, *78*, 54-66.
- (12) Balakrishnan, B.; Banerjee, R. "Biopolymer-based hydrogels for cartilage tissue engineering." *Chemical Reviews* **2011**, *111*, 4453-4474.
- (13) Dang, J.M.; Leong, K.W. "Natural polymers for gene delivery and tissue engineering." *Advanced Drug Delivery Reviews* **2006**, *58*, 487-499.
- (14) Vieira, M.; da Silva, M.; dos Santos, L.; Beppu, M. "Natural-based plasticizers and biopolymer films: A review." *European Polymer Journal* **2011**, *47*, 254-263.
- (15) Franková, L.; Fry, S.C. "Biochemistry and physiological roles of enzymes that 'cut and paste' plant cell-wall polysaccharides." *Journal of Experimental Botany* **2013**, *64*, 3519-3550.

- (16) Ravi Kumar, M. "A review of chitin and chitosan applications." *Reactive and Functional Polymers* **2000**, *46*, 1-27.
- (17) Sinha, V.R.; Singla, A.K.; Wadhawan, S.; Kaushik, R.; Kumria, R.; Bansal, K.; Dhawan, S. "Chitosan microspheres as a potential carrier for drugs." *International Journal of Pharmaceutics* **2004**, *274*, 1-33.
- (18) Karra, S.; Gorski, W.; "Signal amplification in enzyme-based amperometric biosensors." *Analytical Chemistry* **2013**, *85*, 10573-10580.
- (19) Ma, J.; Sahai, Y. "Chitosan biopolymer for fuel cell applications." *Carbohydrate Polymers* **2013**, *92*, 955-975.
- (20) Reighard, K.P.; Hill, D.B.; Dixon, G.A.; Schoenfisch, M.H. "Disruption and eradication of *P. aeruginosa* biofilms using nitric oxide-releasing chitosan oligosaccharides." *Biofouling* **2015**, *31*, 775-787.
- (21) Lu, Y.; Slomberg, D.L.; Schoenfisch, M.H. "Nitric oxide-releasing chitosan oligosaccharides as antibacterial agents." *Biomaterials* **2014**, *35*, 1716-1724.
- (22) Ishiara, M. "Photocrosslinkable chitosan hydrogel as a wound dressing and biological adhesive." *Trends Glycoscience and Glycotechnology* **2002**, *14*, 331-341.
- (23) Sashiwa, H.; Thompson, J.M.; Das, S.K.; Shigemasa, Y.; Tripathy, S.; Roy, R. "Chemical modification of chitosan: Preparation and lectin binding properties of α -galactosyl-chitosan conjugates. Potential inhibitors in acute rejection following xenotransplantation." *Biomacromolecules* **2000**, *1*, 303-305.
- (24) Madihally, S.V.; Matthew, H. "Porous chitosan scaffolds for tissue engineering." *Biomaterials* **1999**, *20*, 1133-1142.
- (25) Zhang, X.; Li, Y.; Sun, X.; Kishen, A.; Deng, X.; Yang, X.; Wang, H.; Cong, C.; Wang, Y.; Wu, M. "Biomimetic remineralization of demineralized enamel with nanocomplexes of phosphorylated chitosan and amorphous calcium phosphate." *Journal of Materials Science: Materials in Medicine* **2014**, *25*, 2619-2628.
- (26) Yokogawa, Y.; Reyes, J.P.; Mucalo, M.R.; Toriyama, M.; Kawamoto, Y.; Suzuki, T.; Nishizawa, K.; Nagata, F.; Kamayama, T. "Growth of calcium phosphate on phosphorylated chitin fibres." *Journal of Materials Science: Materials in Medicine* **1997**, *8*, 407-412.
- (27) Chesnutt, B.M.; Yuan, Y.; Brahmandam, N.; Yang, Y.; Ong, J.L.; Haggard, W.O.; Bumgardner, J.D. "Characterization of biomimetic calcium phosphate on phosphorylated chitosan films." *Journal of Biomedical Materials Research Part A* **2007**, *82*, 343-353.
- (28) Nishi, N.; Ebina, A.; Nishimura, S.; Tsutsumi, A.; Hasegawa, O.; Tokura, S. "Highly phosphorylated derivatives of chitin, partially deacetylated chitin and chitosan as new functional polymers: preparation and characterization." *International Journal of Biological Macromolecules* **1986**, *8*, 311-317.

- (29) Lee, Y.M.; Shin, E.M. "Pervaporation separation of water-ethanol through modified chitosan membranes. IV. Phosphorylated chitosan membranes." *Journal of Membrane Science* **1991**, *64*, 145-152.
- (30) Wang, K.; Liu, Q. "Chemical structure analyses of phosphorylated chitosan." *Carbohydrate Research* **2014**, *386*, 48-56.
- (31) Masson, J-F. "Brief review of the chemistry of polyphosphoric acid (PPA) and bitumen." *Energy Fuels* **2008**, *22*, 2637-2640.
- (32) Miao, Z.; Zhang, J.; You, L.; Wang, J.; Sheng, C.; Yao, J.; Zhang, W.; Feng, H.; Guo, W.; Zhou, L.; Zhu, L.; Cheng, P.; Che, X.; Wang, W.; Luo, C.; Xu, Y.; Dong, G. "Phosphate ester derivatives of homocamptothecin: Synthesis, solution stabilities and antitumor activities." *Bioorganic and Medicinal Chemistry* **2010**, *18*, 3140-3146.
- (33) Illy, N.; Fache, M.; Ménard, R.; Negrell, C.; Caillol, S.; David, G. "Phosphorylation of bio-based compounds: The state of the art." *Polymer Chemistry* **2015**, *6*, 6257-6291.
- (34) Jayakumar, R.; Selvamurugan, N.; Nair, S.V.; Tokura, S.; Tamura, H. "Preparative methods of phosphorylated chitin and chitosan-an overview." *International Journal of Biological Macromolecules* **2008**, *43*, 221-225.
- (35) Lohmar, R.; Sloan, J.W.; Rist, C.E. "Phosphorylation of starch." *Journal of the American Chemical Society* **1950**, *72*, 5717-5720.
- (36) Reid, J.D.; Mazzeno, L.W. "Preparation and properties of cellulose phosphates." *Industrial and Engineering Chemistry* **1949**, *41*, 2828-2831.
- (37) Manoi, K.; Rizvi, S.S. "Physicochemical characteristics of phosphorylated cross-linked starch produced by reactive supercritical fluid extrusion." *Carbohydrate Polymers* **2010**, *81*, 687-694.
- (38) Einbu, A.; Grasdalen, H.; Vårum, K.M. "Kinetics of hydrolysis of chitin/chitosan oligomers in concentrated hydrochloric acid." *Carbohydrate Research* **2007**, *342*, 1055-1062.
- (39) Einbu, A.; Vårum, K.M. "Depolymerization and De-N-acetylation of chitin oligomers in hydrochloric acid." *Biomacromolecules* **2007**, *8*, 309-314.
- (40) Sumiyoshi, M.; Kimura, Y. "Low molecular weight chitosan inhibits obesity induced by feeding a high-fat diet long-term in mice." *Journal of Pharmacy and Pharmacology* **2010**, *58*, 201-207.
- (41) Cao, C.; Mei, M.; Li, Q.; Lo, E.; Chu, C. "Methods for biomimetic remineralization of human dentine: A systematic review." *International Journal of Molecular Sciences* **2015**, *16*, 4615-4627.
- (42) Gamage, A.; Shahidi, F. "Use of chitosan for the removal of metal ion contaminants and proteins from water." *Food Chemistry* **2007**, *104*, 989-996.